Evidence-Based Complementary and Alternative Medicine

Application of Natural Products in Experimental, and Cheminformatics-based Therapy for Neurological Disorders

Lead Guest Editor: Rajeev K Singla
Guest Editors: Ghulam Ashraf and George E. Barreto

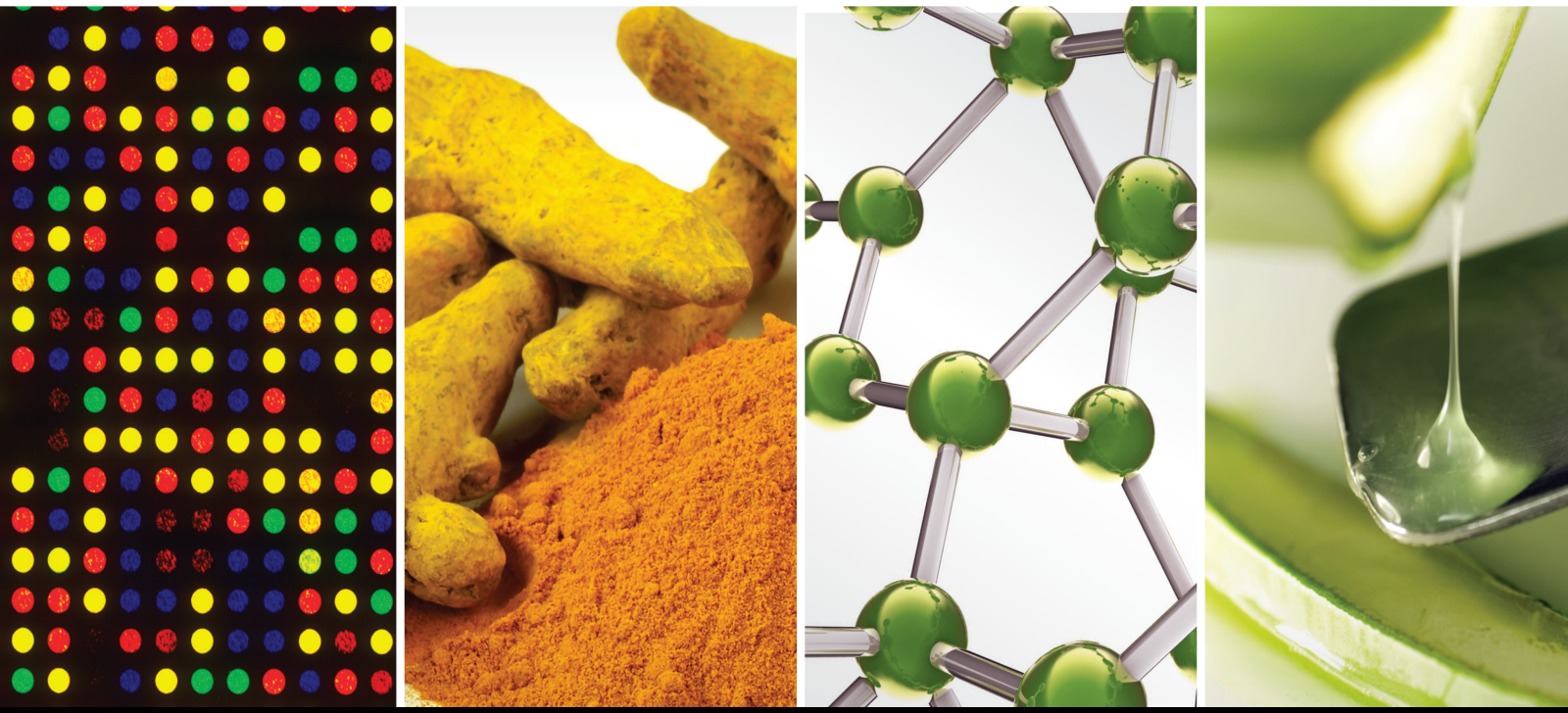

Application of Natural Products in Experimental, and Cheminformatics-based Therapy for Neurological Disorders

Evidence-Based Complementary and Alternative Medicine

Application of Natural Products in Experimental, and Cheminformatics-based Therapy for Neurological Disorders

Lead Guest Editor: Rajeev K Singla
Guest Editors: Ghulam Ashraf and George E. Barreto

Copyright © 2021 Hindawi Limited. All rights reserved.

This is a special issue published in “Evidence-Based Complementary and Alternative Medicine.” All articles are open access articles distributed under the Creative Commons Attribution License, which permits unrestricted use, distribution, and reproduction in any medium, provided the original work is properly cited.

Chief Editor

Jian-Li Gao, China

Associate Editors

Hyunsu Bae, Republic of Korea
Raffaele Capasso, Italy
Jae Youl Cho, Republic of Korea
Caigan Du, Canada
Yuewen Gong, Canada
Hai-dong Guo, China
Kuzhuvelil B. Harikumar, India
Ching-Liang Hsieh, Taiwan
Cheorl-Ho Kim, Republic of Korea
Victor Kuete, Cameroon
Hajime Nakae, Japan
Yoshiji Ohta, Japan
Olumayokun A. Olajide, United Kingdom
Chang G. Son, Republic of Korea
Shan-Yu Su, Taiwan
Michał Tomczyk, Poland
Jenny M. Wilkinson, Australia

Academic Editors

Eman A. Mahmoud, Egypt
Ammar AL-Farga, Saudi Arabia
Smail Aazza, Morocco
Nahla S. Abdel-Azim, Egypt
Ana Lúcia Abreu-Silva, Brazil
Gustavo J. Acevedo-Hernández, Mexico
Mohd Adnan, Saudi Arabia
Jose C Adsuar, Spain
Sayeed Ahmad, India
Touqeer Ahmed, Pakistan
Basiru Ajiboye, Nigeria
Bushra Akhtar, Pakistan
Fahmida Alam, Malaysia
Mohammad Jahoor Alam, Saudi Arabia
Clara Albani, Argentina
Ulysses Paulino Albuquerque, Brazil
Mohammed S. Ali-Shtayeh, Palestinian Authority
Ekram Alias, Malaysia
Terje Alraek, Norway
Adolfo Andrade-Cetto, Mexico
Letizia Angiolella, Italy
Makoto Arai, Japan
Daniel Dias Rufino Arcanjo, Brazil
Duygu AĞAGÜNDÜZ, Turkey
Neda Baghban, Iran
Samra Bashir, Pakistan
Rusliza Basir, Malaysia
Jairo Kenupp Bastos, Brazil
Arpita Basu, USA
Mateus R. Beguelini, Brazil
Juana Benedí, Spain
Samira Boulbaroud, Morocco
Mohammed Bourhia, Morocco
Abdelhakim Bouyahya, Morocco
Nunzio Antonio Cacciola, Italy
Francesco Cardini, Italy
María C. Carpinella, Argentina
Harish Chandra, India
Guang Chen, China
Jianping Chen, China
Kevin Chen, USA
Mei-Chih Chen, Taiwan
Xiaojia Chen, Macau
Evan P. Cherniack, USA
Giuseppina Chianese, Italy
Kok-Yong Chin, Malaysia
Lin China, China
Salvatore Chirumbolo, Italy
Hwi-Young Cho, Republic of Korea
Jeong June Choi, Republic of Korea
Jun-Yong Choi, Republic of Korea
Kathrine Bisgaard Christensen, Denmark
Shuang-En Chuang, Taiwan
Ying-Chien Chung, Taiwan
Francisco José Cidral-Filho, Brazil
Daniel Collado-Mateo, Spain
Lisa A. Conboy, USA
Kieran Cooley, Canada
Edwin L. Cooper, USA
José Otávio do Amaral Corrêa, Brazil
Maria T. Cruz, Portugal
Huantian Cui, China
Giuseppe D'Antona, Italy
Ademar A. Da Silva Filho, Brazil
Chongshan Dai, China
Laura De Martino, Italy
Josué De Moraes, Brazil

Arthur De Sá Ferreira, Brazil
Nunziatina De Tommasi, Italy
Marinella De leo, Italy
Gourav Dey, India
Dinesh Dhamecha, USA
Claudia Di Giacomo, Italy
Antonella Di Sotto, Italy
Mario Dioguardi, Italy
Jeng-Ren Duann, USA
Thomas Efferth, Germany
Abir El-Alfy, USA
Mohamed Ahmed El-Esawi, Egypt
Mohd Ramli Elvy Suhana, Malaysia
Talha Bin Emran, Japan
Roger Engel, Australia
Karim Ennouri, Tunisia
Giuseppe Esposito, Italy
Tahereh Eteraf-Oskouei, Iran
Robson Xavier Faria, Brazil
Mohammad Fattahi, Iran
Keturah R. Faurot, USA
Piergiorgio Fedeli, Italy
Laura Ferraro, Italy
Antonella Fioravanti, Italy
Carmen Formisano, Italy
Hua-Lin Fu, China
Liz G Müller, Brazil
Gabino Garrido, Chile
Safoora Gharibzadeh, Iran
Muhammad N. Ghayur, USA
Angelica Gomes, Brazil
Elena González-Burgos, Spain
Susana Gorzalczany, Argentina
Jiangyong Gu, China
Maruti Ram Gudavalli, USA
Jian-You Guo, China
Shanshan Guo, China
Narcís Gusi, Spain
Svein Haavik, Norway
Fernando Hallwass, Brazil
Gajin Han, Republic of Korea
Ihsan Ul Haq, Pakistan
Hicham Harhar, Morocco
Mohammad Hashem Hashempur, Iran
Muhammad Ali Hashmi, Pakistan
Waseem Hassan, Pakistan
Sandrina A. Heleno, Portugal
Pablo Herrero, Spain
Soon S. Hong, Republic of Korea
Md. Akil Hossain, Republic of Korea
Muhammad Jahangir Hossen, Bangladesh
Shih-Min Hsia, Taiwan
Changmin Hu, China
Tao Hu, China
Weicheng Hu, China
Wen-Long Hu, Taiwan
Xiao-Yang (Mio) Hu, United Kingdom
Sheng-Teng Huang, Taiwan
Ciara Hughes, Ireland
Attila Hunyadi, Hungary
Liaqat Hussain, Pakistan
Maria-Carmen Iglesias-Osma, Spain
Amjad Iqbal, Pakistan
Chie Ishikawa, Japan
Angelo A. Izzo, Italy
Satveer Jagwani, USA
Rana Jamous, Palestinian Authority
Muhammad Saeed Jan, Pakistan
G. K. Jayaprakasha, USA
Kyu Shik Jeong, Republic of Korea
Leopold Jirovetz, Austria
Jeeyoun Jung, Republic of Korea
Nurkhalida Kamal, Saint Vincent and the Grenadines
Atsushi Kameyama, Japan
Kyungsu Kang, Republic of Korea
Wenyi Kang, China
Shao-Hsuan Kao, Taiwan
Nasiara Karim, Pakistan
Morimasa Kato, Japan
Kumar Katragunta, USA
Deborah A. Kennedy, Canada
Washim Khan, USA
Bonglee Kim, Republic of Korea
Dong Hyun Kim, Republic of Korea
Junghyun Kim, Republic of Korea
Kyungho Kim, Republic of Korea
Yun Jin Kim, Malaysia
Yoshiyuki Kimura, Japan

Nebojša Kladar, Serbia
Mi Mi Ko, Republic of Korea
Toshiaki Kogure, Japan
Malcolm Koo, Taiwan
Yu-Hsiang Kuan, Taiwan
Robert Kubina, Poland
Chan-Yen Kuo, Taiwan
Kuang C. Lai, Taiwan
King Hei Stanley Lam, Hong Kong
Fanuel Lampiao, Malawi
Ilaria Lampronti, Italy
Mario Ledda, Italy
Harry Lee, China
Jeong-Sang Lee, Republic of Korea
Ju Ah Lee, Republic of Korea
Kyu Pil Lee, Republic of Korea
Namhun Lee, Republic of Korea
Sang Yeoup Lee, Republic of Korea
Ankita Leekha, USA
Christian Lehmann, Canada
George B. Lenon, Australia
Marco Leonti, Italy
Hua Li, China
Min Li, China
Xing Li, China
Xuqi Li, China
Yi-Rong Li, Taiwan
Vuanghao Lim, Malaysia
Bi-Fong Lin, Taiwan
Ho Lin, Taiwan
Shuibin Lin, China
Kuo-Tong Liou, Taiwan
I-Min Liu, Taiwan
Suhuan Liu, China
Xiaosong Liu, Australia
Yujun Liu, China
Emilio Lizarraga, Argentina
Monica Loizzo, Italy
Nguyen Phuoc Long, Republic of Korea
Zaira López , Mexico
Chunhua Lu, China
Ângelo Luís, Portugal
Anderson Luiz-Ferreira, Brazil
Ivan Luzardo Luzardo-Ocampo, Mexico
Michel Mansur Machado, Brazil
Filippo Maggi, Italy
Juraj Majtan, Slovakia
Toshiaki Makino, Japan
Nicola Malafronte, Italy
Giuseppe Malfa, Italy
Francesca Mancianti, Italy
Carmen Mannucci, Italy
Juan M. Manzaneque, Spain
Fatima Martel, Portugal
Carlos H. G. Martins, Brazil
Maulidiani Maulidiani, Malaysia
Andrea Maxia, Italy
Avijit Mazumder, India
Isac Medeiros, Brazil
Ahmed Mediani, Malaysia
Lewis Mehl-Madrona, USA
Ayikoé Guy Mensah-Nyagan, France
Oliver Micke, Germany
Maria G. Miguel, Portugal
Luigi Milella, Italy
Roberto Miniero, Italy
Letteria Minutoli, Italy
Prashant Modi, India
Daniel Kam-Wah Mok, Hong Kong
Changjong Moon, Republic of Korea
Albert Moraska, USA
Mark Moss, United Kingdom
Yoshiharu Motoo, Japan
Yoshiki Mukudai, Japan
Sakthivel Muniyan, USA
Saima Muzammil, Pakistan
Benoit Banga N'guessan, Ghana
Massimo Nabissi, Italy
Siddavaram Nagini, India
Takao Namiki, Japan
Srinivas Nammi, Australia
Krishnadas Nandakumar, India
Vitaly Napadow, USA
Edoardo Napoli, Italy
Jorddy Neves Cruz, Brazil
Marcello Nicoletti, Italy
Eliud Nyaga Mwaniki Njagi, Kenya
Cristina Nogueira, Brazil

Sakineh Kazemi Noureini, Iran
Rômulo Dias Novaes, Brazil
Martin Offenbaecher, Germany
Oluwafemi Adeleke Ojo, Nigeria
Olufunmiso Olusola Olajuyigbe, Nigeria
Luís Flávio Oliveira, Brazil
Mozaniel Oliveira, Brazil
Atolani Olubunmi, Nigeria
Abimbola Peter Oluyori, Nigeria
Timothy Omara, Austria
Chiagoziem Anariochi Otuechere, Nigeria
Sokcheon Pak, Australia
Antônio Palumbo Jr, Brazil
Zongfu Pan, China
Siyaram Pandey, Canada
Niranjan Parajuli, Nepal
Gunhyuk Park, Republic of Korea
Wansu Park, Republic of Korea
Rodolfo Parreira, Brazil
Mohammad Mahdi Parvizi, Iran
Luiz Felipe Passero, Brazil
Mitesh Patel, India
Claudia Helena Pellizzon, Brazil
Cheng Peng, Australia
Weijun Peng, China
Sonia Piacente, Italy
Andrea Pieroni, Italy
Haifa Qiao, USA
Cláudia Quintino Rocha, Brazil
DANIELA RUSSO, Italy
Muralidharan Arumugam Ramachandran, Singapore
Manzoor Rather, India
Miguel Rebollo-Hernanz, Spain
Gauhar Rehman, Pakistan
Daniela Rigano, Italy
José L. Rios, Spain
Francisca Rius Diaz, Spain
Eliana Rodrigues, Brazil
Maan Bahadur Rokaya, Czech Republic
Mariangela Rondanelli, Italy
Antonietta Rossi, Italy
Mi Heon Ryu, Republic of Korea
Bashar Saad, Palestinian Authority
Sabiu Saheed, South Africa
Mohamed Z.M. Salem, Egypt
Avni Sali, Australia
Andreas Sandner-Kiesling, Austria
Manel Santafe, Spain
José Roberto Santin, Brazil
Tadaaki Satou, Japan
Roland Schoop, Switzerland
Sindy Seara-Paz, Spain
Veronique Seidel, United Kingdom
Vijayakumar Sekar, China
Terry Selfe, USA
Arham Shabbir, Pakistan
Suzana Shahar, Malaysia
Wen-Bin Shang, China
Xiaofei Shang, China
Ali Sharif, Pakistan
Karen J. Sherman, USA
San-Jun Shi, China
Insop Shim, Republic of Korea
Maria Im Hee Shin, China
Yukihiro Shoyama, Japan
Morry Silberstein, Australia
Samuel Martins Silvestre, Portugal
Preet Amol Singh, India
Rajeev K Singla, China
Kuttulebbai N. S. Sirajudeen, Malaysia
Slim Smaoui, Tunisia
Eun Jung Sohn, Republic of Korea
Maxim A. Solovchuk, Taiwan
Young-Jin Son, Republic of Korea
Chengwu Song, China
Vanessa Steenkamp, South Africa
Annarita Stringaro, Italy
Keiichiro Sugimoto, Japan
Valeria Sulsen, Argentina
Zewei Sun, China
Sharifah S. Syed Alwi, United Kingdom
Orazio Taglialatela-Scafati, Italy
Takashi Takeda, Japan
Gianluca Tamagno, Ireland
Hongxun Tao, China
Jun-Yan Tao, China
Lay Kek Teh, Malaysia
Norman Temple, Canada

Kamani H. Tennekoon, Sri Lanka
Seong Lin Teoh, Malaysia
Menaka Thounaojam, USA
Jinhui Tian, China
Zipora Tietel, Israel
Loren Toussaint, USA
Riaz Ullah, Saudi Arabia
Philip F. Uzor, Nigeria
Luca Vanella, Italy
Antonio Vassallo, Italy
Cristian Vergallo, Italy
Miguel Vilas-Boas, Portugal
Aristo Vojdani, USA
Yun WANG, China
QIBIAO WU, Macau
Abraham Wall-Medrano, Mexico
Chong-Zhi Wang, USA
Guang-Jun Wang, China
Jinan Wang, China
Qi-Rui Wang, China
Ru-Feng Wang, China
Shu-Ming Wang, USA
Ting-Yu Wang, China
Xue-Rui Wang, China
Youhua Wang, China
Kenji Watanabe, Japan
Jintanaporn Wattanathorn, Thailand
Silvia Wein, Germany
Katarzyna Winska, Poland
Sok Kuan Wong, Malaysia
Christopher Worsnop, Australia
Jih-Huah Wu, Taiwan
Sijin Wu, China
Xian Wu, USA
Zuoqi Xiao, China
Rafael M. Ximenes, Brazil
Guoqiang Xing, USA
JiaTuo Xu, China
Mei Xue, China
Yong-Bo Xue, China
Haruki Yamada, Japan
Nobuo Yamaguchi, Japan
Junqing Yang, China
Longfei Yang, China
Mingxiao Yang, Hong Kong
Qin Yang, China
Wei-Hsiung Yang, USA
Swee Keong Yeap, Malaysia
Albert S. Yeung, USA
Ebrahim M. Yimer, Ethiopia
Yoke Keong Yong, Malaysia
Fadia S. Youssef, Egypt
Zhilong Yu, Canada
RONGJIE ZHAO, China
Sultan Zahiruddin, USA
Armando Zarrelli, Italy
Xiaobin Zeng, China
Y Zeng, China
Fangbo Zhang, China
Jianliang Zhang, China
Jiu-Liang Zhang, China
Mingbo Zhang, China
Jing Zhao, China
Zhangfeng Zhong, Macau
Guoqi Zhu, China
Yan Zhu, USA
Suzanna M. Zick, USA
Stephane Zingue, Cameroon

Contents

Hindawi
Evidence-Based Complementary and Alternative Medicine
Volume 2021, Article ID 5528403, 12 pages
https://doi.org/10.1155/2021/5528403

Research Article

Study on Mechanism of Jiawei Chaiqin Wendan Decoction in Treatment of Vestibular Migraine Based on Network Pharmacology and Molecular Docking Technology

Menglin Liu,[1,2] **Genhao Fan**,[2] **Daopei Zhang**,[3] **Mingjun Zhu**,[3] **and Huailiang Zhang**[3]

[1]*Henan University of Traditional Chinese Medicine, Zhengzhou 450000, China*
[2]*Tianjin University of Traditional Chinese Medicine, Tianjin 301617, China*
[3]*The First Affiliated Hospital of Henan University of Chinese Medicine, Zhengzhou 450000, China*

Correspondence should be addressed to Huailiang Zhang; woshiwo20182021@126.com

Received 1 February 2021; Revised 10 July 2021; Accepted 22 September 2021; Published 31 October 2021

Academic Editor: Ghulam Ashraf

Copyright © 2021 Menglin Liu et al. This is an open access article distributed under the Creative Commons Attribution License, which permits unrestricted use, distribution, and reproduction in any medium, provided the original work is properly cited.

Objective. To predict the main active ingredients, potential targets, and key pathways of Jiawei Chaiqin Wendan decoction treatment in vestibular migraine and explore possible mechanisms by network pharmacology and molecular docking technology. *Methods*. The active ingredients and related targets of Jiawei Chaiqin Wendan decoction were obtained from the Traditional Chinese Medicine Systems Pharmacology Database and Analysis Platform (TCMSP). The corresponding genes of the target were queried by UniProt database, and the "drug-compound-target-disease" network was constructed by Cytoscape 3.7.2 software. GO functional enrichment analysis and KEGG pathway enrichment analysis were carried out by R software and Bioconductor, and column chart and bubble chart were drawn by Prism software and OmicShare database for visualization. Finally, the mechanism and potential targets of Jiawei Chaiqin Wendan decoction in the treatment of vestibular migraine were predicted. *Results*. The "drug-compound-target-disease" network contains 154 active ingredients and 85 intersection targets. The key targets include AKT1, IL6, MAPK3, VEGFA, EGFR, CASP3, EGF, MAPK1, PTGS2, and ESR1. A total of 1939 items were obtained by GO functional enrichment analysis ($P < 0.05$). KEGG pathway enrichment analysis screened 156 signal pathways ($P < 0.05$), involving PI3K-Akt signal pathway, AGE-RAGE signal pathway in diabetes complications, MAPK signal pathway, HIF-1 signal pathway, IL-17 signal pathway, etc. Molecular docking results showed that quercetin, luteolin, kaempferol, tanshinone IIa, wogonin, naringenin, nobiletin, dihydrotanshinlactone, beta-sitosterol, and salviolone have good affinity with core target proteins IL6, PTGS2, MAPK1, MAPK3, and CGRP1. *Conclusion*. The active ingredients in Jiawei Chaiqin Wendan decoction may regulate the levels of inflammatory factors and neurotransmitters by acting on multiple targets such as IL6, MAPK3, MAPK1, and PTGS2, so as to play a therapeutic role in vestibular migraine.

1. Introduction

Vestibular migraine (VM) is a chronic and disabling disease that is common and has a genetic tendency; the main symptoms are recurrent dizziness/vertigo, which may be accompanied by nausea and vomiting with or without headache [1]. Studies have shown that VM is one of the common causes of recurrent dizziness or vertigo [1,2]. VM can occur at any age, and the ratio of male to female is 1 : 1.5–1 : 5, and it is more common in women [3]. VM is generally regarded as a subtype of migraine. Since a new hypothesis was published in the Lancet in 1979, it has been proposed that trigeminal neurovascular system containing neuropeptides plays an indispensable role in migraine. Up to now, trigeminal neurovascular system has been widely regarded as the basis of this highly complex nervous system disease for 40 years [4]. At present, the pathogenesis of VM is still not completely clear at home and abroad, and the basis of pathogenesis may be associated with ion channel defect and cortical spreading depression (CSD). CSD activates the trigeminal neurovascular system, and the trigeminal ganglion releases calcitonin gene-related peptides (CGRP),

substance P, and other neuropeptides, causing meningeal vascular inflammation, and thus leading to migraine symptoms. In addition, the overlap of the pathways responsible for pain and balance in the central nervous system, the fibrous connection between the trigeminal nucleus and the vestibular nucleus, and the trigeminal nerve innervating the inner ear eventually lead to vestibular symptoms [5].

The diagnosis of VM is mainly based on the characteristics of the patient's clinical onset and lacks specific signs and objective diagnostic basis. In the past few decades, uncertainty about the diagnosis of VM has limited the progress of treatment [6]. There is insufficient evidence to support the use of drugs for VM treatment. Sometimes, western drugs are effective in preventing migraine, but their role in VM treatment is not clear, and the effect of these drugs on VM prevention cannot be verified [7]. Recurrent dizziness or vertigo has a significant impact on patients' quality of life and their psychology. Extensive examinations and long-term treatment impose a huge economic burden on patients' families and society. It is obvious that further research on potential new treatments for VM therapy is needed. Vestibular migraine is characterized by dizziness or vertigo, visual rotation, instability, and current or previous migraine, which can be classified as "xuan yun" in traditional Chinese medicine. The earliest description of "xuan yun" in traditional Chinese medicine can be mentioned in the "Canon of Medicine." Doctors of various dynasties had different understandings of "xuan yun," with different emphasis on syndrome differentiation and treatment. And to sum up, there are five aspects: wind, fire, phlegm, deficiency, and blood stasis. In the treatment of vertigo, traditional Chinese medicine has unique advantages. A study has compared the curative effect of TCM syndrome differentiation treatment and conventional western medicine treatment on patients with vertigo and found that, compared with conventional western medicine treatment, TCM syndrome differentiation treatment of vertigo can more effectively improve the clinical symptoms of patients [8].

Chaiqin Wendan decoction is made of Wendan decoction from Yao Sengyuan in the Southern and Northern dynasties. The modified Chaiqin Wendan decoction (JCWD) is an effective empirical prescription for the treatment of vertigo in clinic. This prescription is composed of Radix Bupleuri (Chaihu), Radix Scutellariae (Huangqin), Pinellia tuber (Banxia), Dried tangerine Peel (Chenpi), Fructus Aurantii Immaturus (Zhishi), Poria cocos (Fuling), Radix Paeoniae Alba (Baishao), Angelica sinensis (Danggui), Salvia miltiorrhiza (Danshen), Gastrodia elata (Tianma), Uncariae Ramulus Cumuncis (Gouteng), and Shi Cassia (Shijueming). At present, clinical observation indicates that Chaiqin Wendan decoction has a significant effect on the treatment of patients with dizziness and headache caused by Triple Burner Congestion [9–11]. There have been some studies based on network pharmacology to reveal the molecular mechanism of TCM treatment of diseases. This study aims to predict the potential target and mechanism of JCWD in treating VM through network pharmacology and molecular docking methods.

2. Materials and Method

2.1. Acquisition of Active Ingredients and Targets of TCM. The TCMSP (http://tcmspw.com/tcmsp.php) [12] database was used to search the TCM in JCWD formulae (Radix Bupleuri, Radix Scutellariae, Pinellia tuber, Dried tangerine Peel, Fructus Aurantii Immaturus, Poria cocos, Radix Paeoniae Alba, Angelica sinensis, Salvia miltiorrhiza, Gastrodia elata, Uncariae Ramulus Cumuncis, and Shi Cassia), with two parameters related to ADME (absorption, distribution, metabolism, and excretion), namely, oral bioavailability (OB greater than or equal to 30%) and class medicinal (DL greater than or equal to 0.18) for screening of TCM active ingredients. Based on TCMSP and DrugBank databases, the targets of active ingredients were retrieved by Perl software and UniProt KB (http://www.uniprot.org/), and gene annotation was performed.

2.2. Obtain the Intersection Genes of TCM and Diseases. Using GeneCards (https://www.genecards.org/) and OMIM database (https://omim.org/) by retrieving "vestibular migraine" look up vestibular migraine related genes and remove duplicates. Through Venny2.1 software, the target of active ingredients of traditional Chinese medicine obtained above was intersected with disease-related genes.

2.3. Draw "Drug-Compound-Target" Network. The information of drug name, drug active ingredient, gene target of intersection between drug and disease, and the relationship network among them were imported into Cytoscape3.7.2 software to construct the network diagram of "drug-compound-target" for visual analysis.

2.4. Protein-Protein interaction (PPI) Network and Core Gene Network. Multiple proteins were introduced into String11.0 (https://string-db.org/), and the species was selected as "*Homo sapiens*," with a medium confidence of 0.400 to predict the associated PPI network. Download protein-protein interaction TSV file, import Cytoscape3.7.2 software, and use CytoHubba plug-in to screen core target proteins.

2.5. GO and KEGG Enrichment Analysis. There is the core target gene ID through the R software and Bioconductor (http://www.bioconductor.org) to GO functional annotations and KEGG pathway enrichment analysis. $P < 0.05$ was selected for functional annotation clustering. In order to study the biological effects of VM targets of drug therapy by regulating specific pathways, the top 10 items were screened according to the enrichment degree and a bar chart was drawn. Similarly, $P < 0.05$ was selected as the significant pathway for cluster analysis, and the top 20 items were screened according to the enrichment degree to draw a bubble plot.

2.6. Molecular Docking. The 2D structures of key compounds were downloaded in PubMed (https://www.ncbi.nlm.nih.gov/pubmed). The 3D structures of ligands were

generated by Chem3D software, and their energy was minimized and exported to mol2 format. All compounds were saved as ligand parameter files in pdbqt format by AutodockTools-1.5.6 software. The 3D structure of the core target protein was downloaded from PDB database (https://www.rcsb.org/) and saved in PDB format. The solvent and water molecules in the target protein receptor molecules were removed by pymol software. Then, the protein receptor molecules were hydrogenated and calculated by AutodockTools software and saved in pdbqt format. After the ligand and protein receptor molecular preprocessing is completed, the appropriate box center and box lattice parameters are set by AutodockTools-1.5.6 software, the active pocket sites that small molecular ligands may bind to are included, and the parameter text file is set, and the other parameters remain default. Molecular docking was carried out by Autodock Vina, and 3D diagrams were drawn by PyMol software for the docking results with the strongest binding activity of each target protein to show the hydrogen bond and hydrophobic effect formed by it.

3. Results

3.1. Collection of Active Components and Targets of JCWD. A total of 221 active components of TCM, which were OB ≥ 30% and DL ≥ 0.18 in JCWD formulae, were retrieved by TCMSP database. The basic information of some active components of JCWD is shown in Table 1. Based on TCMSP and DrugBank database, a total of 3376 protein targets related to the above active ingredients were obtained by Perl software, and 1531 gene symbols were obtained after gene annotation using UniProt KB.

3.2. Intersection Targets of JCWD and VM. In GeneCards (https://www.genecards.org/) and OMIM database (https://omim.org/) by retrieving "vestibular migraine" search related genes, a total of 826 were extracted after duplication. Through Venny2.1 software, the intersection of traditional Chinese medicine target and disease genes was obtained, and 85 genes related to JCWD treatment of VM were obtained, as shown in Figure 1.

3.3. Construction of "Drug-Ingredient-Target" Network. First, the intersection between drug targets and disease genes is obtained, and then the information such as VM related genes, active ingredient targets of traditional Chinese medicine, and their interrelation network are imported into Cytoscape3.7.2 software for visual analysis, and the "drug-active ingredient-target" network diagram is constructed. The network consists of 249 nodes (10 TCM name nodes, 154active ingredient nodes, and 85 gene target nodes) and 915 edges, as shown in Figure 2. The average degree value of this network is 7.66, and the top 10 active ingredients were screened according to the degree value, as shown in Table 2, among which the degree values of quercetin, luteolin, kaempferol, tanshinone IIa, and wogonin are greater than or equal to 16 (more than 2 times the average value). In addition, quercetin, luteolin, kaempferol, naringenin, nobiletin, and β-sitosterol are the common active components in many TCMin JCWD, which can interact with 53, 21, 19, 13, 13, and 12 target proteins, respectively. The top 10 target genes in screening value were PTGS2, HSP90AA1, SCN5A, AR, ADRB2, ACHE, ESR1, NOS2, PPARG, and GABRA1, which could interact with 136, 91, 84, 70,62, 53, 43, 41, 35, and 28 active components, respectively.

3.4. Protein-Protein Interaction Network (PPI) and Core Gene Network Were Constructed. Eighty-five JCWD gene targets for VM treatment were introduced into String11.0 to construct a Protein-protein interaction network (PPI), and isolated nodes were removed, as shown in Figure 3. Then, the top 20 key genes were screened out according to the Degree value, as shown in Figure 4. The CytoHubba plug-in in Cytoscape3.7.2 software was used to screen the 10 core genes, as shown in Figure 5.

3.5. GO Functional Enrichment Analysis and KEGG Pathway Enrichment Analysis. GO function enrichment analysis and KEGG pathway enrichment analysis were carried out by R software and Bioconductor database installation packages such as clusterProfiler and enrichplot. 1939 GO enrichment results were obtained ($P < 0.05$), among which 1731 items of biological processes (BP) were closely related to the reactions of metal ions, blood circulation, reactive oxygen species, and oxidative stress, lipopolysaccharide, steroids, and bacterial origin molecules. The 141 items of molecular function (MF) are mainly related to protein phosphatase binding, nuclear receptor activity, and steroid receptor activity, transcription factor activity, cytokine activity, and receptor binding, NO synthase regulator activity, etc. 67 results of cell composition (CC) are mainly related to membrane microdomain, receptor complex, components, and inherent components of synaptic membrane and vesicle cavity, as shown in Figure 6.

In order to comprehensively study the role of JCWD in the prevention and treatment of VM, 156 pathways were screened by KEGG pathway enrichment analysis. It involves PI3K-Akt signal pathway, AGE-RAGE signal pathway, MAPK signal pathway, HIF-1 signal pathway, IL-17 signal pathway in diabetic complications, and signal pathways closely related to fluid shear stress and atherosclerosis, endocrine resistance, endometrial cancer, prostate cancer, etc., which mainly play an important role in inhibiting inflammatory reaction, hormone, and endocrine regulation. 20 pathways were selected for visualization, and the diagram is shown in Figure 7. In order to explore the role of JCWD in the signal pathway, a gene target-signal pathway network is constructed to identify the interaction between protein targets and signal pathways. Figure 8 shows a target and pathway network composed of 55 target genes and 20 key pathways. The results of network analysis show that there are 17 targets whose values are greater than the average value of 8.67, which may appear in multiple pathways. Nine pathways had degrees greater than 2 times the mean degrees, which may also be regulated by multiple targets. In addition, there are synergies between the pathways.

Table 1: Basic information of some active components of JCWD.

TCM	MOL ID	Molecule name	OB (%)	DL
Radix bupleuri	MOL002776	Baicalin	40.12	0.75
Radix bupleuri	MOL000449	Stigmasterol	43.83	0.76
Radix bupleuri	MOL000354	Isorhamnetin	49.6	0.31
Radix bupleuri	MOL000422	kaempferol	41.88	0.24
Radix scutellariae	MOL001689	Acacetin	34.97	0.24
Radix scutellariae	MOL000173	Wogonin	30.68	0.23
Radix scutellariae	MOL002714	Baicalein	33.52	0.21
Radix scutellariae	MOL002910	Carthamidin	41.15	0.24
Radix scutellariae	MOL002914	Eriodyctiol (flavanone)	41.35	0.24
Pinellia tuber	MOL002776	Baicalin	40.12	0.75
Pinellia tuber	MOL000358	Beta-sitosterol	36.91	0.75
Pinellia tuber	MOL000449	Stigmasterol	43.83	0.76
Pinellia tuber	MOL005030	Gondoic acid	30.7	0.2
Dried tangerine peel	MOL000359	Sitosterol	36.91	0.75
Dried tangerine peel	MOL004328	Naringenin	59.29	0.21
Dried tangerine peel	MOL005815	Citromitin	86.9	0.51
Dried tangerine peel	MOL005828	Nobiletin	61.67	0.52
Poria cocos	MOL000275	Trametenolic acid	38.71	0.8
Poria cocos	MOL000279	Cerevisterol	37.96	0.77
Poria cocos	MOL000283	Ergosterol peroxide	40.36	0.81
Poria cocos	MOL000289	Pachymic acid	33.63	0.81
Radix paeoniae alba	MOL001928	Albiflorin_qt	66.64	0.33
Radix paeoniae alba	MOL001930	Benzoyl paeoniflorin	31.27	0.75
Radix paeoniae alba	MOL000358	Beta-sitosterol	36.91	0.75
Radix paeoniae alba	MOL000359	Sitosterol	36.91	0.75
Fructus aurantii immaturus	MOL013276	Poncirin	36.55	0.74
Fructus aurantii immaturus	MOL013277	Isosinensetin	51.15	0.44
Fructus aurantii immaturus	MOL013279	5,7,4′-Trimethylapigenin	39.83	0.3
Fructus aurantii immaturus	MOL013428	Isosakuranetin-7-rutinoside	41.24	0.72
Fructus aurantii immaturus	MOL013430	Prangenin	43.6	0.29
Salvia miltiorrhiza	MOL001659	Poriferasterol	43.83	0.76
Salvia miltiorrhiza	MOL001771	Poriferast-5-en-3beta-ol	36.91	0.75
Salvia miltiorrhiza	MOL001942	Isoimperatorin	45.46	0.23
Salvia miltiorrhiza	MOL002651	Dehydrotanshinone II A	43.76	0.4
Angelica sinensis	MOL000358	Beta-sitosterol	36.91	0.75
Angelica sinensis	MOL000449	Stigmasterol	43.83	0.76
Uncariae ramulus cumuncis	MOL000358	Beta-sitosterol	36.91	0.75
Uncariae ramulus cumuncis	MOL000073	Ent-epicatechin	48.96	0.24
Uncariae ramulus cumuncis	MOL008457	Tetrahydroalstonine	32.42	0.81
Uncariae ramulus cumuncis	MOL008458	Angustidine	51.85	0.66

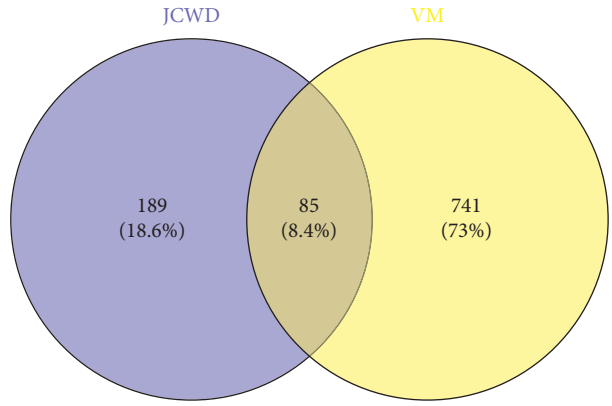

Figure 1: Venn diagram of the intersection target of JCWD and VM.

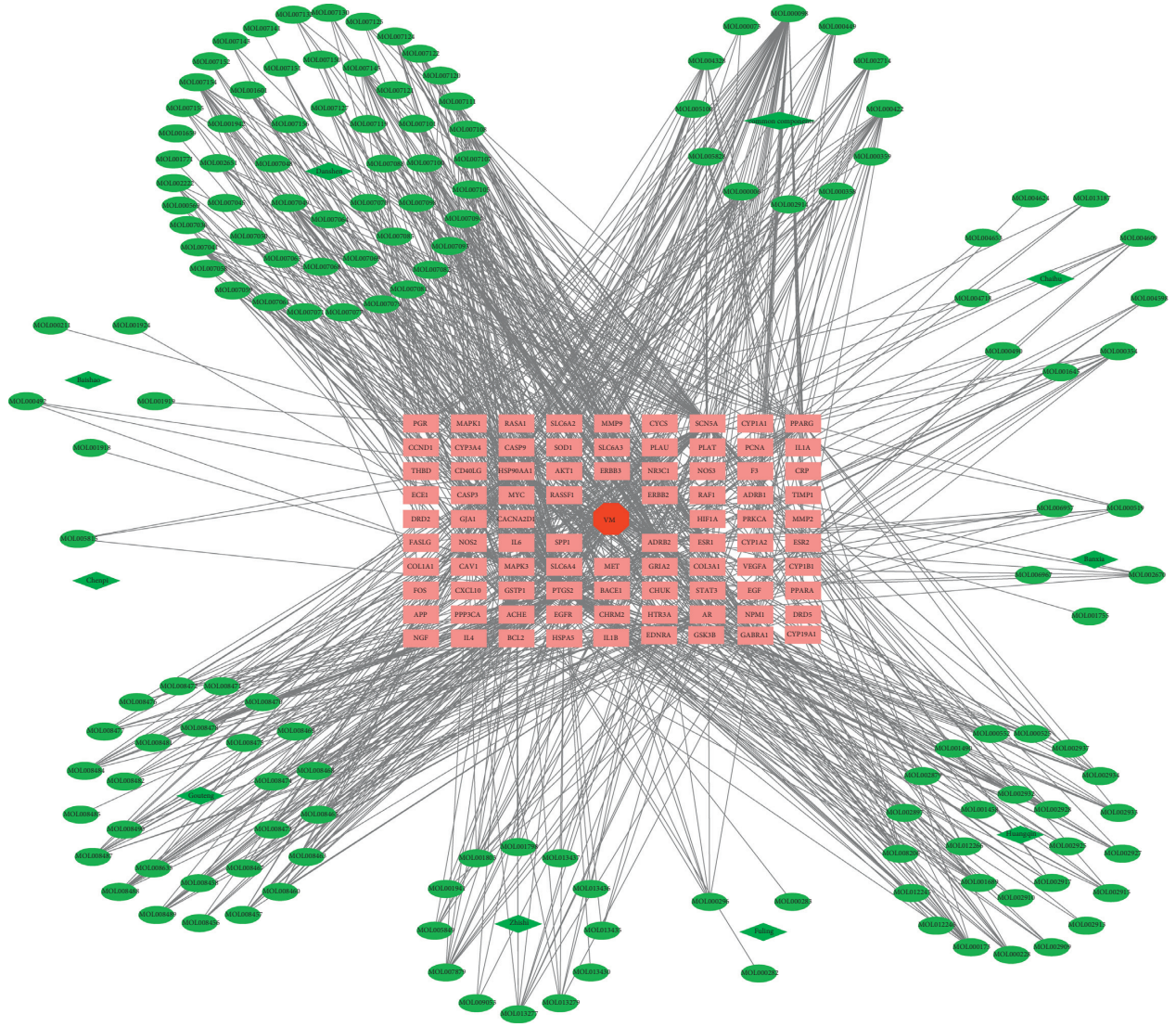

Figure 2: JCWD "drug-active compound-Gene Target" network diagram (where dark green represents the name of TCM, light green represents active ingredients, pink substitutes gene targets, and red color represents the name of the disease).

Table 2: Top 10 active ingredients by degree value.

MolID	Molecule name	Degree	Source
MOL000098	Quercetin	53	Radix bupleuri, uncariae ramulus cumuncis
MOL000006	Luteolin	21	Salvia miltiorrhiza, fructus aurantii immaturus
MOL000422	Kaempferol	19	Radix bupleuri, uncariae ramulus cumuncis, radix paeoniae alba
MOL007154	Tanshinone iia	16	Salvia miltiorrhiza
MOL000173	Wogonin	16	Radix scutellariae
MOL004328	Naringenin	13	Dried tangerine peel, fructus aurantii immaturus
MOL005828	Nobiletin	13	Fructus aurantii immaturus, dried tangerine peel
MOL007100	Dihydrotanshinlactone	13	Salvia miltiorrhiza
MOL000358	Beta-sitosterol	12	Radix paeoniae alba, pinellia tuber, radix scutellariae, angelica sinensis, uncariae ramulus cumuncis
MOL007145	Salviolone	12	Salvia miltiorrhiza

3.6. Molecular Docking between Active Ingredients and Potential Targets. It is generally believed that the lower the binding energy of the molecular docking process, the better the affinity between the receptor and the ligand. Molecular docking results showed that the molecular docking affinity of quercetin, luteolin, kaempferol, tanshinone Iia, wogonin, naringenin, nobiletin, dihydrotanshinlactone, beta-sitosterol, and salviolone with core target proteins IL6, PTGS2,

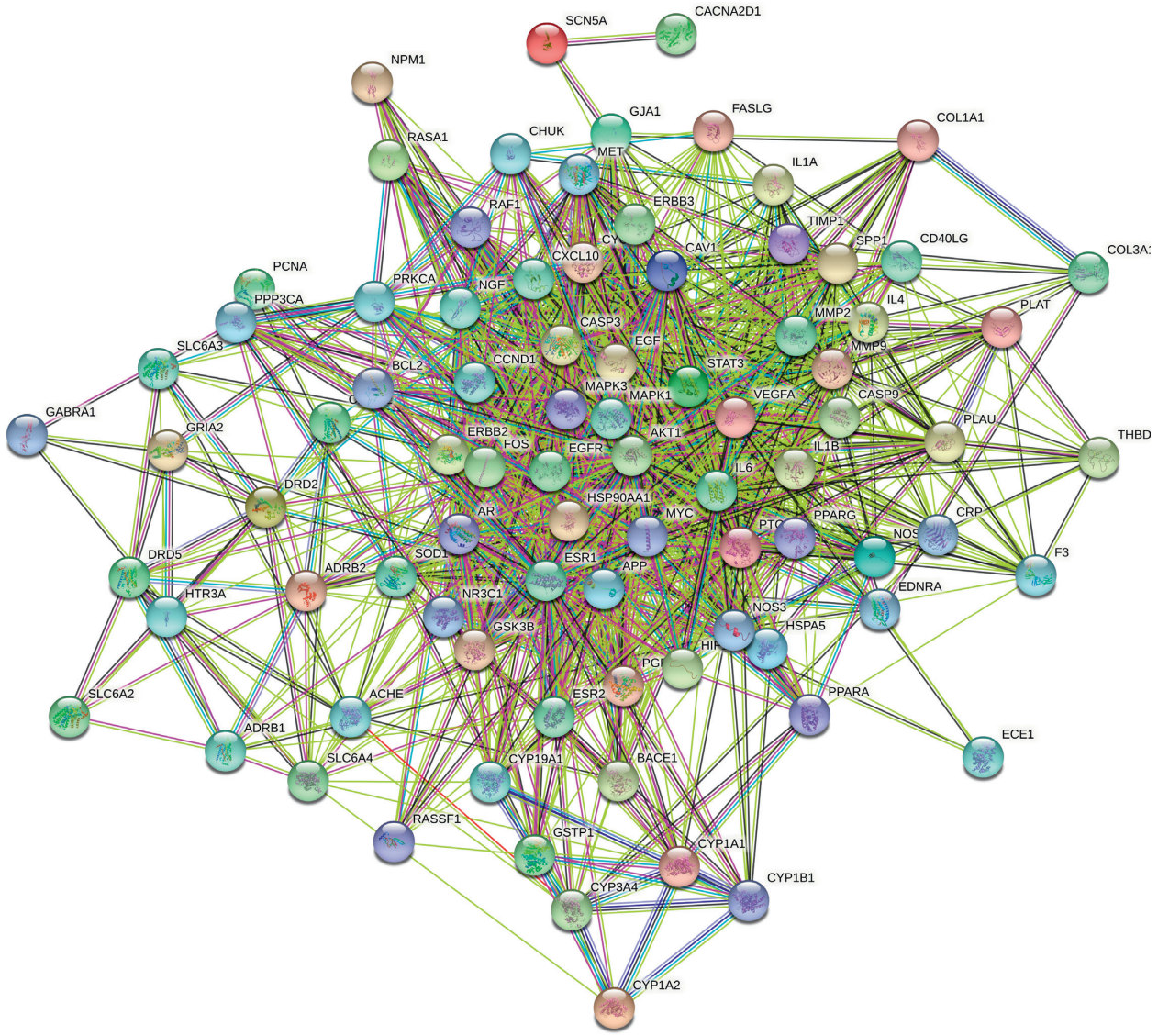

Figure 3: Protein-protein interaction network.

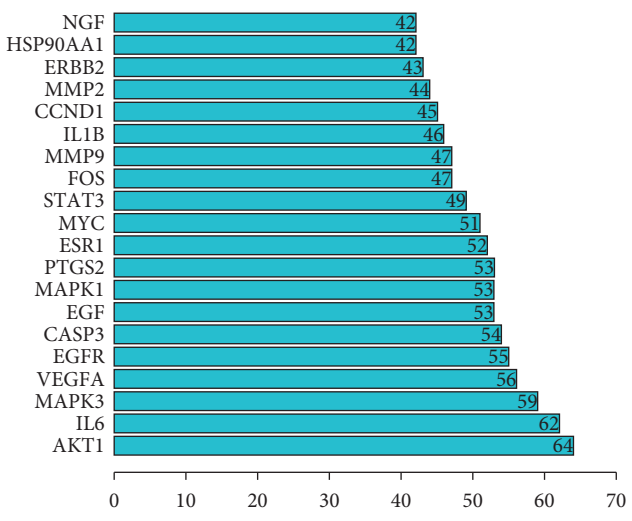

Figure 4: Degree ranking of top 20 target proteins.

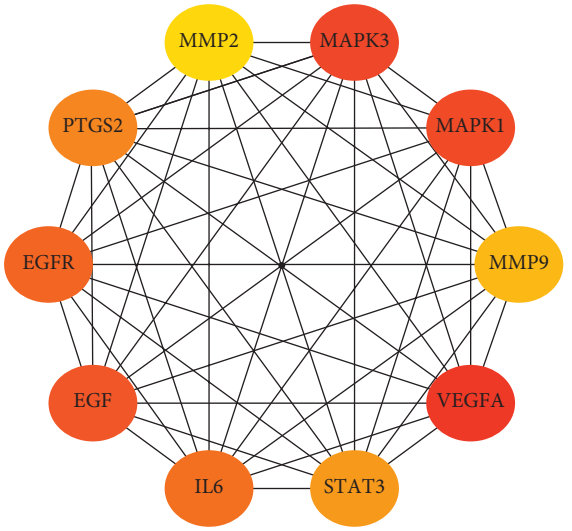

Figure 5: Core genes of JCWD potential therapeutic targets.

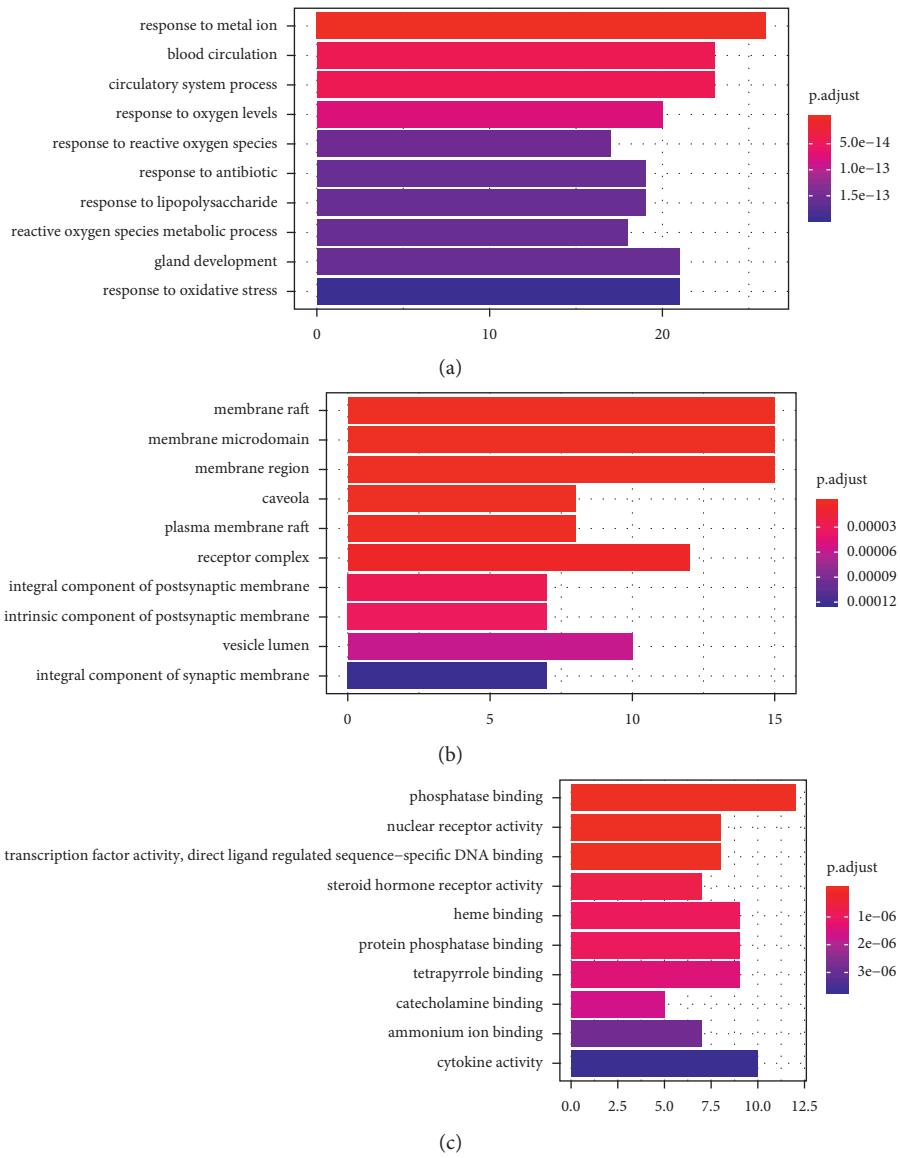

Figure 6: GO enrichment analysis of 85 target genes. (a) Biological process enrichment analysis. (b) Cellular component enrichment analysis. (c) Molecular function enrichment analysis.

MAPK1, MAPK3, and CGRP1 were all less than −5.0 kcal/mol, and the results are shown in Table 3 and the docking results of the interaction between target proteins and the active components with the strongest binding activity, as shown in Figure 9.

4. Discussion

According to the universally recognized pathogenesis of VM, namely, the trigeminal neurovascular reflex theory, VM can be considered as a proinflammatory disease. It has been found that there is a close connection between the nervous system and the immune system, and inhibiting the expression level of inflammatory factors can reduce the symptoms of VM or the occurrence of VM [13].

Modern pharmacological studies have shown that Wendan decoction has the effects of anti-inflammation and regulating immune function [14]. Lin Huangguo et al. [15] found that Wendan decoction could reduce the levels of NF-κB, TNF-α, and IL-6 in metabolic syndrome rats, indicating that Wendan decoction could inhibit the expression of inflammatory factors. Liu et al. [16] proved that Huanglian Wendan decoction could inhibit inflammatory reaction and reduce the levels of serum TNF-α and IL-6 in rats with metabolic syndrome. The research of Yu et al. [17] shows that Wendan decoction can effectively regulate the expression of TNF-α, IL-6, IL-17, and IL-22 and other related inflammatory cytokines in obese rats and improve the state of inflammatory reaction in obese rats. Dou et al. [18] found through experiments that modified Huanglian Wendan decoction could significantly improve the impairment of learning and memory and the pathological changes of hippocampus in rats with vascular dementia, reduce the expression of TNF-α and COX-2 in hippocampus, and play

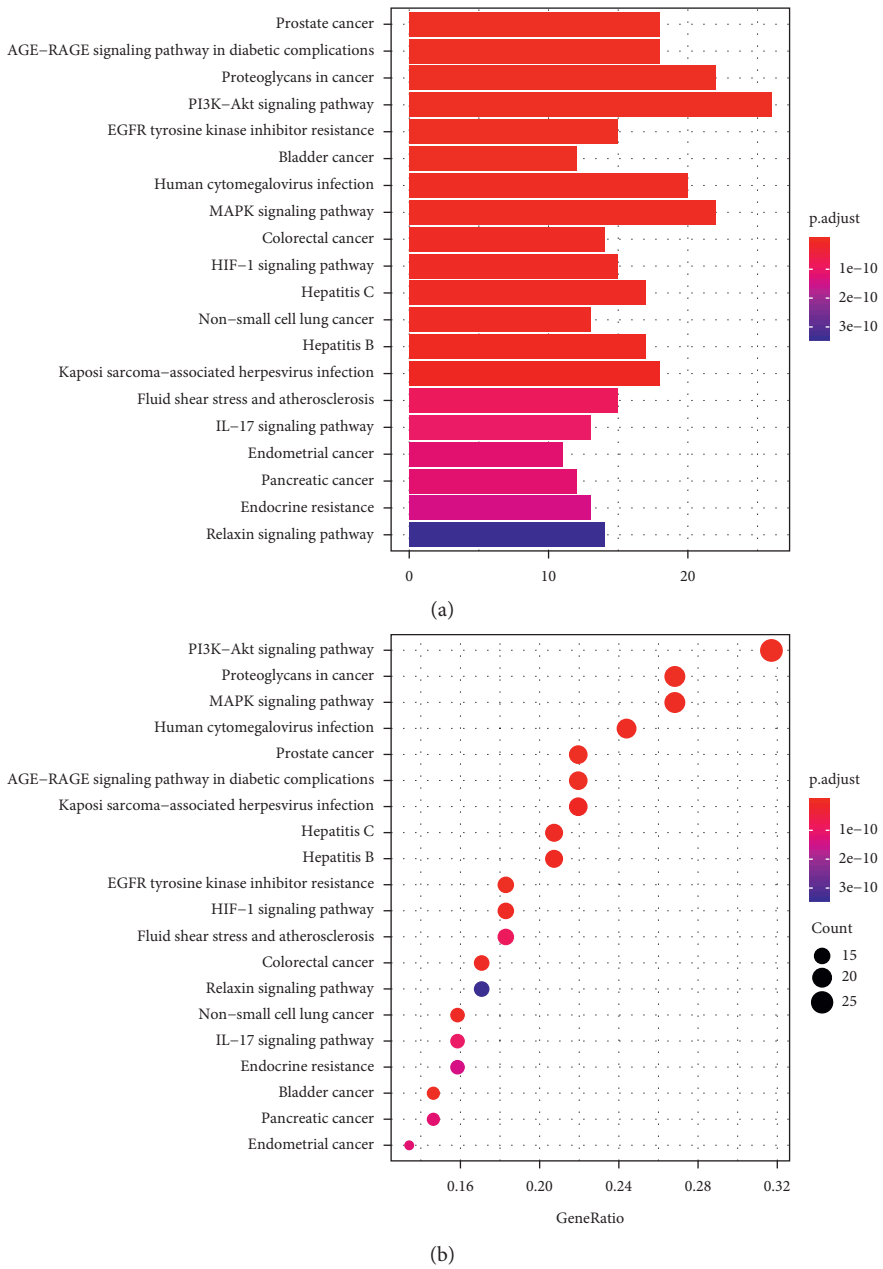

Figure 7: KEGG enrichment analysis of 85 target genes. (a) Barplot of KEGG analysis. (b) Dotplot of KEGG analysis: the size of dots indicates the number of target genes; the different color of dots indicates different P value ranges.

an inhibitory role in inflammatory response. Liu et al. [19] found that, in a certain glutamic acid environment, the drug-containing serum prepared with different doses of Wendan decoction could increase the survival rate of primary astrocytes P38MAPK extracted from the cerebral cortex of SD rats and upregulate the expression of P38MAPK phosphorylation and nonphosphorylation.

From the point of view of the active components of the drug, quercetin can exert its anti-inflammatory effect by inhibiting the production of IL-6, TNF-α and VEGF [20]. In addition, quercetin can exert its anti-inflammatory effect by inhibiting NF-κB and MAPK signal pathways [21]. Kaempferol is a flavanol compound, which has many pharmacological effects, such as antioxidation and anti-inflammation. It can regulate the levels of NO and NOS and protect endothelial cells from oxidative damage by inhibiting the degradation of NO [22]. Luteolin mainly acts on transcription factors such as Src in the nuclear transcription factor-κB (NF-κB) pathway, MAPK in the activator protein-1 pathway, and cytokine signal inhibitors in the signal transduction and transcriptional activator 3 pathway, regulating inflammatory mediators and playing an anti-inflammatory role. Luteolin can inhibit all proinflammatory cytokines, such as interleukin-1β, IL-2, IL-6, IL-8, IL-12, IL-17, TNF-α, interferon-β(IFN-β), and granulocyte-macrophage colony stimulating factor and upregulate anti-

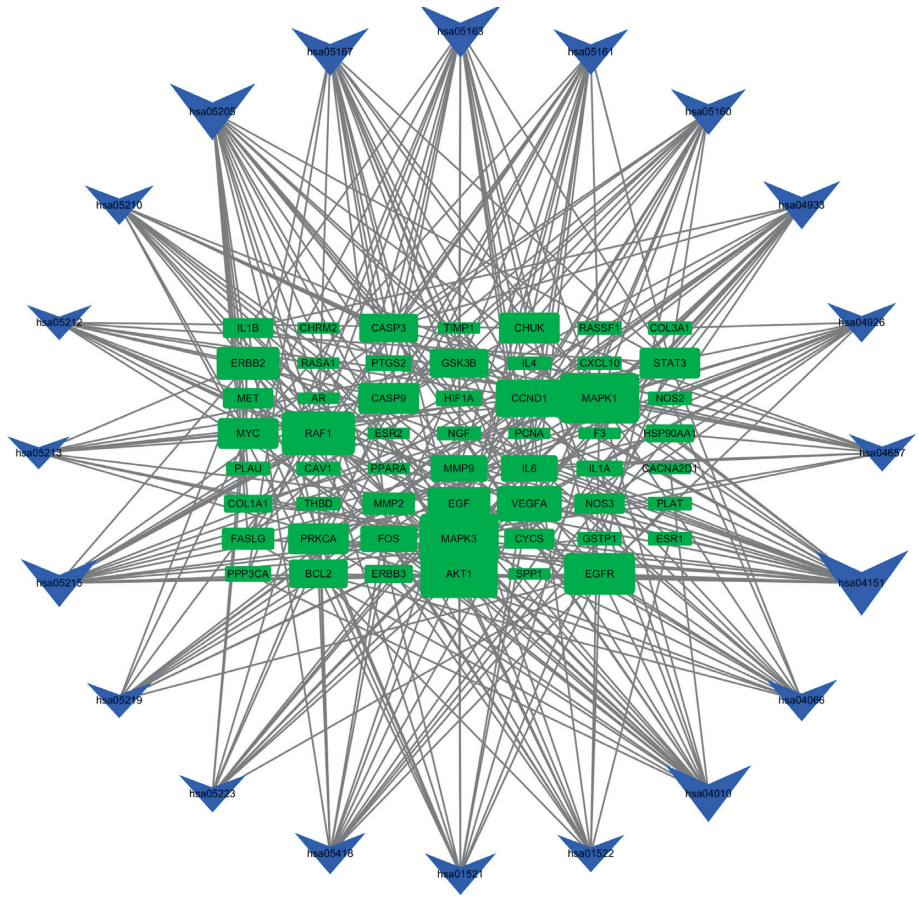

FIGURE 8: Targets-pathway network (the size of the icon represents the size of the degree value, the green rectangle represents the target gene, and the blue arrow represents the pathway.).

TABLE 3: The binding free energy of 10 small molecules with top 5 genes.

Molecule name	Affinity (kcal/mol)				
	IL6	PTGS2	MAPK1	MAPK3	CGRP
Beta-sitosterol	−5.9	−9.2	−7.5	−8.7	−6.7
Dihydrotanshinlactone	−7.8	−9.5	−8.9	−10.8	−8.2
Kaempferol	−7.6	−9.2	−7.7	−9.3	−9.0
Luteolin	−7.5	−10.0	−8.1	−9.4	−8.8
Naringenin	−7.2	−9.3	−8.0	−9.3	−8.5
Nobiletin	−6.2	−8.7	−6.9	−8.5	−7.9
Quercetin	−7.7	−9.6	−7.5	−9.3	−9.2
Salviolone	−7.2	−8.6	−9.1	−10.6	−7.7
Tanshinone iia	−7.6	−9.9	−8.6	−11.5	−7.9
Wogonin	−7.1	−9.4	−7.7	−9.3	−7.4

inflammatory cytokine IL-10 [23]. Wogonin can inhibit the activation of both MAPK pathway and NF-κB pathway, inhibit the expression of inducible nitric oxide synthase (iNOS), cyclooxygenase-2 (COX-2), TNF-α, IL-1β and IL-6, and reduce the inflammatory response of spinal dorsal root neurons induced by lipopolysaccharide [24,25]. Tanshinone IIA can inhibit the degradation of IκB-α and the activation of NF-κB induced by LPS by inhibiting the activation of NIK-IKK and MAPKs (p38, ERK1/2, JNK) signal pathways, so as to exert its anti-inflammatory activity [26].

Protein-protein interaction (PPI) network was used to screen out 10 core genes by Matthews correlation coefficient (MCC) algorithm. They are VEGFA (vascular endothelial growth factor A), MAPK3 (mitogen-activated protein kinase 3), MAPK1 (mitogen-activated protein kinase 1), EGF (epidermal growth factor), EGFR (epidermal growth factor receptor), IL-6 (interleukin-6), PTGS2 (prostaglandin endoperoxide synthase 2), STAT3 (signal transducer and activator of transcription 3), MMP9 (matrix metalloproteinase 9), and MMP2 (matrix metalloproteinase 2). Vascular endothelial growth factor (VEGF) has heparin active growth factor, which can play a role in vascular endothelial cells to cause the division and proliferation of vascular endothelial cells, thus forming new blood vessels and improving vascular permeability. The main causes of migraine include vasodilation and protein exudation. In the onset stage of migraine, patients' serum VEGF level is abnormally elevated, blood vessels dilate, and their permeability increases, eventually leading to extravasation of plasma protein [27]. Epidermal growth factor receptor (EGFR), widely expressed in the brain and aggregate distribution, is a functional receptor tyrosine kinase and, combined with neural regulatory proteins, can be changed after the epidermal growth factor receptor protein conformation, make its form dimers, and activate the downstream phosphatidyl inositol kinase/protein kinase B signaling pathway, which mediated

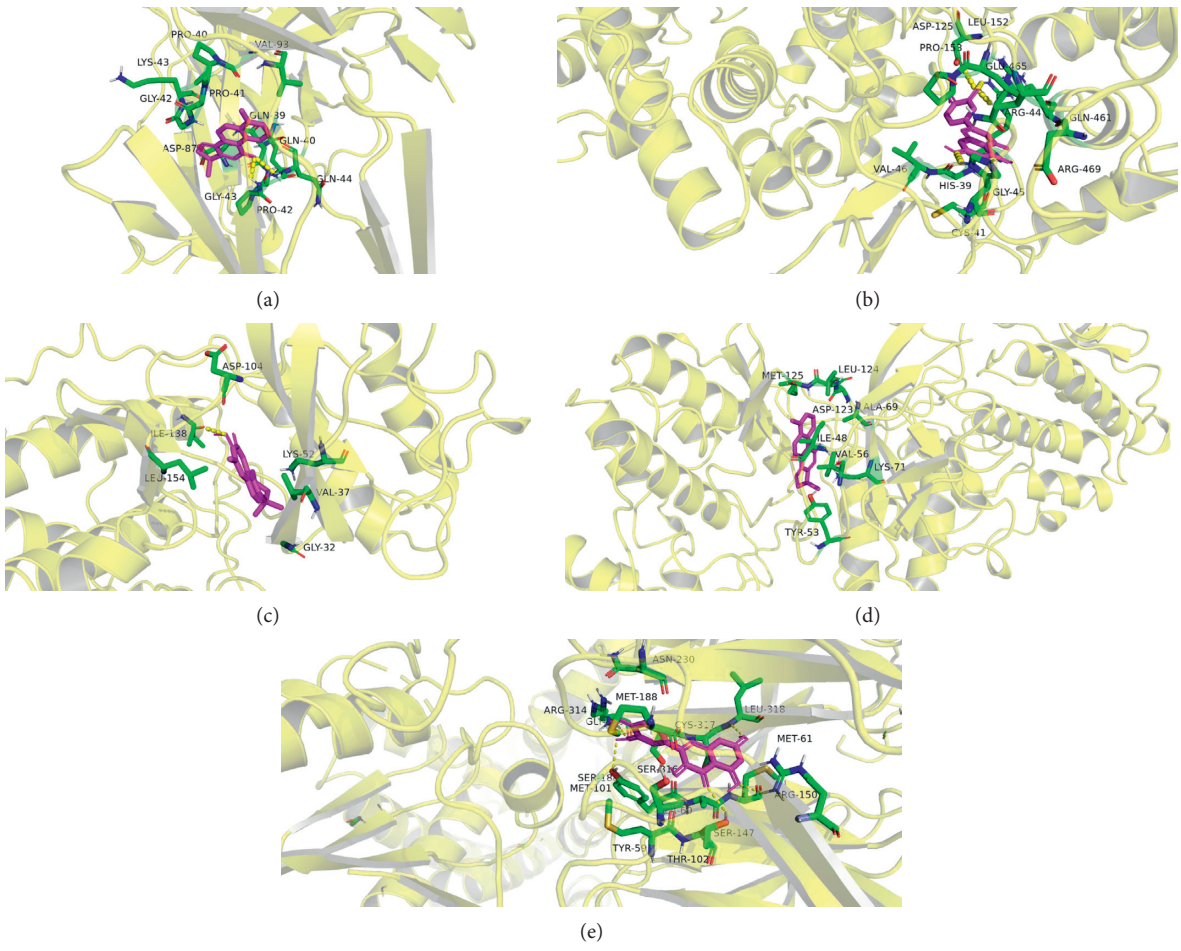

Figure 9: The molecular docking results of the interaction of active ingredients with the protein. (a) Binding pattern between IL-6 and dihydrotanshinlactone. (b) Binding pattern between PTGS2 and luteolin. (c) Binding pattern between MAPK1 and salviolone. (d) Binding pattern between MAPK3 and dihydrotanshinlactone. (e) Binding pattern between CGRP1 and quercetin.

inflammatory response [28]. MAPK is a class of intracellular serine/threonine protein kinases, an important signaling system that mediates extracellular signals to intracellular responses, and plays a key role in cell proliferation, apoptosis, inflammation, immunity, and angiogenesis [29]. Studies have observed changes in serum MMP9 levels in patients with migraine in different periods and subtypes and found that serum MMP9 was upregulated during the onset of migraine, which may be one of the potential related mechanisms of migraine [30]. IL-6 is a multipotent cytokine with a wide range of functions; it can regulate the growth and differentiation of many kinds of cells, regulate immune response, acute phase response and hematopoiesis, and play an important role in anti-infective immune response. PTGS2, also known as cyclooxygenase-2 (COX-2), is an enzyme that converts arachidonic acid into prostaglandins. It is overexpressed in response to mechanical, chemical, and physical stimuli and plays a key role in the promotion and development of inflammatory response [31,32]. Some studies have shown that COX-2 is involved in the pathogenesis of migraine, and the presence of aura has no effect on the level of serum COX-2, and some studies have suggested that exercise may improve the symptoms of vestibular migraine patients by inhibiting the COX-2 proinflammatory pathway and reducing the levels of TNF-α, IL-2, IL-6, and other proinflammatory factors [13].

Through the analysis of KEGG pathway, it is found that MAPK signal pathway, HIF-1 signal pathway, and IL-17 signal pathway are the main treatment pathways, which play a synergistic anti-inflammatory effect. MAPK signaling cascades include three different regulatory pathways: extracellular signal-regulated kinase (ERK1/2), c-jun N-terminal kinase (JNK) and p38 protein (P38), which are responsible for mitosis, proliferation, differentiation, and survival of cells during development [33], as well as neuronal plasticity and inflammation in adults [34]; in addition, these pathways contribute to the onset and maintenance of inflammation and pain [35]. In vitro studies have found that MAPK pathway can be involved in the upregulation of calcitonin gene-related peptide (CGRP) expression in rat trigeminal ganglion (TG) organ culture [36], and the release of CGRP and other neuropeptides is closely related to meningeal vascular inflammation and migraine symptoms. In addition, the transcription of COX-2 ′s PTGS2 gene is associated with multiple intracellular signals that come together to activate mitogen-activated protein kinase (MAPK)

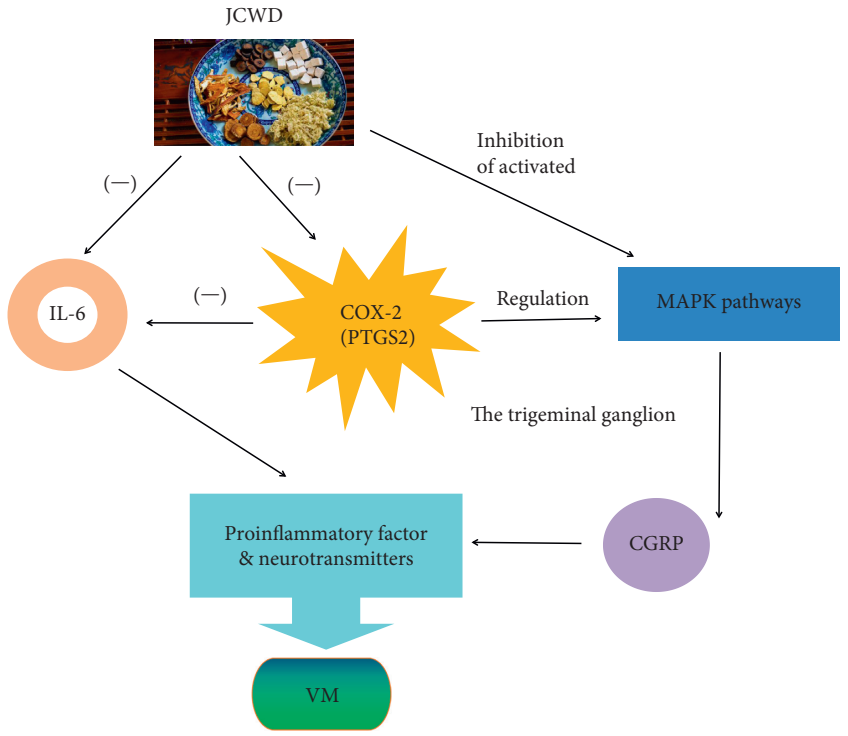

Figure 10: Possible mechanism of JCWD for VM.

[37]. Based on the above discussion, we speculate that the possible mechanism of JCWD in the treatment of VM is shown in Figure 10.

5. Conclusion

In this study, the active components of JCWD and the potential targets and key pathways acting on vestibular migraine were predicted by the method of network pharmacology, which once again confirmed the process of multicomponent, multitarget, and multipathway treatment of diseases with traditional Chinese medicine compound prescription. The active components such as quercetin, kaempferol, luteolin, wogonin, and tanshinone II as in Jiawei Chaiqin Wendan decoction may regulate the levels of inflammatory factors and neurotransmitters (such as CGRP) by acting on IL6, MAPK3, MAPK1, PTGS2, and other targets, thus playing a role in the treatment of vestibular migraine. Due to the limitations of the database and the software itself, the above results need to be further verified by experiments.

Data Availability

The datasets used and/or analyzed during the current study are available from the corresponding author on reasonable request.

Conflicts of Interest

The authors declare no conflicts of interest regarding the publication of this article.

Acknowledgments

This work was supported by Zhang Huailiang National Heritage Project of Famous Old Chinese Medicine Experts (National Traditional Chinese Medicine Education and Culture [2018]134) and Clinical study on the treatment of persistent postural perceptual dizziness by TCM Optimization Program (2018JDZX012).

References

[1] V. Li, H. McArdle, and S. A. Trip, "Vestibular migraine," *BMJ*, vol. 366, p. l4213, 2019.

[2] G. Ashish, A. M. Augustine, A. K. Tyagi, A. Lepcha, and A. Balraj, "Subjective visual vertical and horizontal in vestibular migraine," *The journal of international advanced otology*, vol. 13, no. 2, pp. 254–258, 2017.

[3] H. Neuhauser, M. Leopold, M. von Brevern, G. Arnold, and T. Lempert, "The interrelations of migraine, vertigo, and migrainous vertigo," *Neurology*, vol. 56, no. 4, pp. 436–441, 2001.

[4] M. Ashina, J. M. Hansen, T. P. Do, A. Melo-Carrillo, R. Burstein, and M. A. Moskowitz, "Migraine and the trigeminovascular system-40 years and counting," *The Lancet Neurology*, vol. 18, no. 8, pp. 795–804, 2019.

[5] Yu, Q. Wan, and W. Wang, "Expert consensus on diagnosis and treatment of vestibular migraine(2018)," *Chinese Journal of PainMedicine*, vol. 7, pp. 481–488, 2018.

[6] T.-C. Huang, S.-J. Wang, and A. Kheradmand, "Vestibular migraine: an update on current understanding and future directions," *Cephalalgia*, vol. 40, no. 1, pp. 107–121, 2020.

[7] M. Maldonado Fernández, G. J. Irving, L. Murdin, I. Kivekäs, and M. Strupp, "Pharmacological agents for the prevention of vestibular migraine," *Cochrane Database of Systematic Reviews*, vol. 6, Article ID CD010600, 2015.

[8] Wei and J. Q. Cai, "Comparison of the curative effect of TCM syndrome differentiation andconventional western medicine in the treatment of patients with vertigo," *Internal Medicine*, vol. 12, no. 5, pp. 677-678, 2017.

[9] Duan, F. F. Wang, and H. L. Zhang, "Chaiqin wendan decoction in the treatment of 31 cases of frequent tension-type headache," *Journal of Traditional Chinese Medicine Research*, vol. 30, no. 6, pp. 34–36, 2017.

[10] Huang, Y. H. Guo, and J. X. Zhao, "Diagnosis and treatment strategies and reflections on the prevention and treatment of Meniere's disease with traditional Chinese medicine," *China Journal of Traditional Chinese Medicine and Pharmacy*, vol. 33, no. 12, pp. 5490–5492, 2018.

[11] Yue, S. X. Qian, and T. Y. Yuan, "Clinical observation of Chaiqin Wendan Decoction combined with paroxetine in the treatment of chronic subjective dizziness," *China Journal of Traditional Chinese Medicine and Pharmacy*, vol. 37, no. 3, pp. 673–676, 2019.

[12] J. Ru, P. Li, J. Wang et al., "TCMSP: a database of systems pharmacology for drug discovery from herbal medicines," *Journal of Cheminformatics*, vol. 6, no. 1, 2014.

[13] Y.-Y. Lee, Y.-P. Yang, P.-I. Huang et al., "Exercise suppresses COX-2 pro-inflammatory pathway in vestibular migraine," *Brain Research Bulletin*, vol. 116, pp. 98–105, 2015.

[14] Wang and R. Ke, "The clinical and pharmacological research progress of Wendan Decoction and its modified formulas in the treatment of circulatory system diseases," *Journal of Liaoning University of Traditional Chinese Medicine*, vol. 23, no. 1, pp. 186–190, 2021.

[15] Lin, S. Zhong, and X. G. Cai, "Effects of Wendan Decoction on the expression of inflammatory mediators in rats with metabolic syndrome," *Journal of Guangzhou University of Traditional Chinese Medicine*, vol. 35, no. 4, pp. 664–668, 2018.

[16] Liu and Y. B. Sui, "Effects of Huanglian Wendan Decoction on insulin resistance and adipocytokines in rats with metabolic syndrome," *Journal of LiaoningUniversity of Traditional Chinese Medicine*, vol. 3, pp. 385–387, 2011.

[17] Yu, Q. Shu, Y. Bai et al., "Effects of Wendan Decoction on the immune and inflammatory cytokine expression of obesity with phlegm-dampness syndrome," *China Journal of Traditional Chinese Medicine and Pharmacy*, vol. 2, pp. 378–381, 2019.

[18] Dou, H. Y. Chen, and L. Liu, "Effects of huanglian wendan decoction on inflammatory response in rats with vascular dementia," *Chinese Traditional Patent Medicine*, vol. 7, pp. 1702–1705, 2019.

[19] Liu, Y. Y. Wei, and H. H. Xiong, "Effects of Wendan Decoctioncontaining serum on P38MAPK and PKC of primary astrocytes under glutamaeconditions," *Pharmacology and Clinics of Chinese Materia Medica*, vol. 31, no. 1, pp. 5–8, 2015.

[20] J. Lee and W. Park, "Anti-inflammatory effect of wogonin on RAW 264.7 mouse macrophages induced with polyinosinic-polycytidylic acid," *Molecules*, vol. 20, no. 4, pp. 6888–6900, 2015.

[21] T.-L. Si, Q. Liu, Y.-F. Ren et al., "Enhanced anti-inflammatory effects of DHA and quercetin in lipopolysaccharide-induced RAW264.7 macrophages by inhibiting NF-κB and MAPK activation," *Molecular Medicine Reports*, vol. 14, no. 1, pp. 499–508, 2016.

[22] Lei, A. Chen, and Y. Liu, "Research progress on the pharmacological effects of kaempferol," *Studies of Trace Elements and Health*, vol. 34, no. 2, pp. 61-62, 2017.

[23] Xu, J. Yang, and Q. Li, "Progress in the pharmacological research of luteolin and its glycosides in dense Mongolian flowers," *Chinese Wild Plant Resources*, vol. 38, no. 4, pp. 53–57, 2019.

[24] Chen, *The Effect of Wogonin on the MAPK/NF-κB Signaling Pathway in the Inflammatory Response of Spinal Dorsal Root Neurons Induced by Lipopolysaccharide*, Nanchang University, Nanchang, China, 2015.

[25] Pang, X. M. Qin, and G. H. Du, "Research progress on the pharmacological effects and mechanisms of Scutellaria baicalensis flavone based on the aging hypothesis," *Chinese Traditional and Herbal Drugs*, vol. 50, no. 13, pp. 3207–3216, 2019.

[26] S. Il Jang, H. Jin Kim, Y.-J. Kim, S.-I. Jeong, and Y.-O. You, "Tanshinone IIA inhibits LPS-induced NF-κB activation in RAW 264.7 cells: possible involvement of the NIK-IKK, ERK1/2, p38 and JNK pathways," *European Journal of Pharmacology*, vol. 542, no. 1–3, pp. 1–3, 2006.

[27] Zhang and W. C. Li, "Clinical study of gastrodin capsule combined with lomelizine in the treatment of angioneurotic migraine," *Drugs & Clinic*, vol. 34, no. 2, pp. 327–331, 2019.

[28] Yue, S. Li, and D. D. Wei, "The role of neuregulin/epidermal growth factor receptor pathway in a rat model of migraine," *Stroke and Nervous Diseases*, vol. 28, no. 2, pp. 187–191, 2019.

[29] Li, X. Y. Wang, N. Li, and H. Zhang, "Research status of mitogen-activated protein kinase (MAPK) and nuclear factor-κB (NF-κB) pathways in the pathogenesis of migraine," *The Chinese Journal of Clinical Pharmacology*, vol. 35, no. 10, pp. 1071–1074, 2019.

[30] Gao, Y. N. Meng, and L. K. Su, "Effect of flunarizine combined with tonganning capsule on patients with migraine and its effect on serum MMP-9, TNF-α and LPA," *Journal of Clinical and Experimental Medicine*, vol. 16, no. 4, pp. 379–382, 2017.

[31] E. Kaiser, P. Chiba, and K. Zaky, "Phospholipases in biology and medicine," *Clinical Biochemistry*, vol. 23, no. 5, pp. 349–370, 1990.

[32] B. Nuvoli and R. Galati, "Cyclooxygenase-2, epidermal growth factor receptor, and aromatase signaling in inflammation and mesothelioma," *Molecular Cancer Therapeutics*, vol. 12, no. 6, pp. 844–852, 2013.

[33] A. G. Turjanski, J. P. Vaqué, and J. S. Gutkind, "MAP kinases and the control of nuclear events," *Oncogene*, vol. 26, no. 22, pp. 3240–3253, 2007.

[34] S. Impey, K. Obrietan, and D. R. Storm, "Making new connections: role of ERK/MAP kinase signaling in neuronal plasticity," *Neuron*, vol. 23, no. 1, pp. 11–14, 1999.

[35] S. Kumar, J. Boehm, and J. C. Lee, "p38 MAP kinases: key signalling molecules as therapeutic targets for inflammatory diseases," *Nature Reviews Drug Discovery*, vol. 2, no. 9, pp. 717–726, 2003.

[36] L. Lei, X. Yuan, S. Wang et al., "Mitogen-activated protein kinase pathways are involved in the upregulation of calcitonin gene-related peptide of rat trigeminal ganglion after organ culture," *Journal of Molecular Neuroscience*, vol. 48, no. 1, pp. 53–65, 2012.

[37] Z.-Z. Lai, H.-L. Yang, S.-Y. Ha et al., "Cyclooxygenase-2 in endometriosis," *International Journal of Biological Sciences*, vol. 15, no. 13, pp. 2783–2797, 2019.

Hindawi
Evidence-Based Complementary and Alternative Medicine
Volume 2021, Article ID 6079305, 12 pages
https://doi.org/10.1155/2021/6079305

Research Article

Paeoniflorin Effect of Schwann Cell-Derived Exosomes Ameliorates Dorsal Root Ganglion Neurons Apoptosis through IRE1α Pathway

Yanbo Zhu,[1,2] **Shuo Han**,[1,2] **Xiao Li**,[1,2] **Yingying Gao**,[1,2] **Jiayue Zhu**,[1,2] **Xinwei Yang**,[1,2] **and Liping Xu**[1,2]

[1]*School of Traditional Chinese Medicine, Capital Medical University, Beijing, China*
[2]*Beijing Key Lab of TCM Collateral Disease Theory Research, Capital Medical University, Beijing, China*

Correspondence should be addressed to Liping Xu; xulp@ccmu.edu.cn

Received 30 June 2021; Accepted 20 August 2021; Published 27 September 2021

Academic Editor: Rajeev K Singla

Copyright © 2021 Yanbo Zhu et al. This is an open access article distributed under the Creative Commons Attribution License, which permits unrestricted use, distribution, and reproduction in any medium, provided the original work is properly cited.

Background. Diabetic peripheral neuropathy (DPN) is a common complication of diabetes but its pathogenesis is not fully clarified. Endoplasmic reticulum (ER) stress has been confirmed to be involved in the development of DPN. Dorsal root ganglion neuron (DRGn) is the target cell of DPN injure in the peripheral neurons system. Schwann cell (SCs)-derived exosomes (SC-EXOs) can carry IRE1α signal transduction factors in ER stress to DRGn. The aim of this study is to investigate the effect of SC-EXOs treated with paeoniflorin (PF) on DRGn stimulated by high glucose. *Methods*. SCs were divided into Control group (Control), 150 mM glucose group (HG), high osmotic pressure group (HOP), and low, middle, and high dose PF group (PF1, PF10, and PF100). Exosomes were obtained from SCs by ultracentrifugation and identified according to marker proteins, including CD63, Alix, Hsp70, and TSG101. ER stress initiating factor GRP78, the IRE1α pathway information transmission factor IRE1α, and the phosphorylation level of IRE1α were detected by Western blot, DRGn is divided into Control group (Control), 50 mM glucose group + Control exosomes group (HG + EXOs Control), 50 mM glucose group (HG), and 50 mM glucose group + administration exosomes group (HG + EXOs PF1, HG + EXOs PF10, and HG + EXOs PF100); ER morphology of primary DRGn was observed by using the transmission electron microscope, the level of DRGn apoptosis was analyzed by TUNEL, and the downstream proteins of ER stress including CHOP, XBP1S, JNK, and p-JNK in DRG and the expression of apoptosis-related proteins Bcl-2, Bax, Caspase-3, and Caspase-12 were measured by Western blot. *Results*. Compared with the exosomes in the HG group, the exosomes after the intervention of PF can significantly reduce the expression of GRP78, IRE1α, and the phosphorylation level of IRE1α ($P < 0.05$); compared with the DRGn in the HG group, the SC-EXOs treated with PF could regulate the expression of proteins downstream of IRE1α pathway in ER stress ($P < 0.05$ or $P < 0.01$), improve the morphological integrity of ER, and reduce apoptosis in DRGn ($P < 0.05$ or $P < 0.01$). *Conclusion*. PF regulates the information of ER stress carried by SC-EXOs and further affects downstream of IRE1α pathway in DRGn, thus reducing ER stress-induced apoptosis. PF can interfere with DPN through affecting information communication carried by EXOs between SCs and DRGn.

1. Introduction

Diabetic peripheral neuropathy (DPN) is one of the most common long-term complications of diabetes, with a prevalence of over 50%, and is characterized by sensory and motor neuron damage [1, 2]. The pathogenesis of DPN is complex, including microvascular ischemia, polyol pathway, oxidative stress, and endoplasmic reticulum stress (ER stress) [3]. Our previous studies have shown that apoptosis induced by ER stress is one of the important mechanisms of the pathogenesis of DPN [4–6]. Endoplasmic reticulum (ER) is an important organelle for protein synthesis, folding and modification, lipid synthesis, and calcium storage. ER stress is caused by the accumulation of unfolded or misfolded proteins, interruption of lipid synthesis, or depletion of calcium storage. High glucose stimulation can cause ER

stress in cells, and the cells respond to ER stress through unfolded protein response (UPR) to maintain ER homeostasis. UPR mainly contains PERK, ATF6, and IRE1α signal pathways [7]. IRE1α pathway is the most conservative branch of UPR in evolution, which can reduce the protein folding load and increase the ER proteins folding ability [8].

Dorsal root ganglion (DRG) is one kind of cell bodies, and the susceptibility of dorsal root ganglion neurons (DRGn) to high glucose concentration stress in vivo and in vitro is involved in the occurrence and development of diabetic neuropathy. At the same time, ER stress can also cause abnormal DRGn ion channel function, gene expression, transcription regulation, metabolism, and protein folding [9].

As a kind of lipid bilayer membrane vesicles involved in cell-to-cell communication, exosomes play a key role in intracellular communication [10]. Exosomes are wrapped in bilayer membranes to protect their genetic material. In this way, exosomes can be used as stable and effective carriers to carry specific goods such as proteins, lipids, and genetic materials, so they can be used as a promising tool to transport anti-infective goods to target tissues or organs [11]. Extracellular pathway is an effective way to regulate apoptosis, angiogenesis, and target cell inflammation [12]. The SC-EXOs can significantly promote axonal growth and regeneration both in vitro and in vivo [13, 14]. Axon regeneration is an important process for functional recovery after being stimulated by high glucose [15, 16]. Therefore, SC-EXOs may be used as carriers to participate in the regulation of DRGn axon regeneration and growth and promote the repair of peripheral nerves after injury [17]. The study showed that the secretion of exosomes would increase under ER stress, but in the IRE1α-deficient cells, the secretion of exosomes did not increase. This indicated that the IRE1α pathway was involved in the release of exosomes [18]. At the same time, with ER stress, the endoribonuclease activity activated by IRE1α will cleave XBP1 (X-box binding protein 1) mRNA which could play the role of transcription factor. The IRE1α-XBP1 pathway was involved in insulin resistance and dyslipidemia. It has been previously demonstrated that IRE1α was essential for the release of exosomes from palmitate-treated liver cells [19, 20]. However, the role of exosomes stimulated by IRE1a and the regulation of the IRE1a pathway are still unclear.

Paeoniflorin (PF) is a monoterpene glycoside isolated from Ranunculaceae plant *Paeonia lactiflora*, which acts as antioxidant and anti-inflammatory and performs vasodilatation and other biological activities [21]. PF can block the PERK pathway by inhibiting the expression of GRP78 and finally reduce ER stress [22]. At the same time, the anti-inflammatory effect of PF is achieved by inhibiting the phosphorylation level of IRE1α [23, 24]. Therefore, this article studies the effect of PF on SC-EXOs in IRE1α signaling pathway of DRGn.

2. Materials and Methods

2.1. Primary DRGn Extraction and SCs Culture. DRGn was prepared from SD neonatal rats regardless of gender (3–5 days old, Charles River Experimental Animal Technology Co., Ltd.). The DRG is taken from the intervertebral foramen of both vertebrae. The tail of the DRG is cut off, and its head is retained. The head is cut into pieces and incubated in 4 mL trypsin with 1% collagenase for 1-2 hours at 37°C. Dissociated cells were seeded in Petri dish coated with poly-L-lysine (PLL, Sigma-Aldrich), incubated for 7 days, and the medium is replaced every 2-3 days [25, 26].

SCs line was cultured in DMEM complete medium containing 10% fetal bovine serum (FBS) and 1% penicillin-streptomycin. The incubator was kept at 37°C and 5% CO_2. They were divided into Control group (25 mmol/L glucose DMEM + 10% FBS, Control), high glucose group (150 mmol/L glucose DMEM + 10% FBS, HG), high osmotic pressure group (25 mmol/L glucose DMEM + 44.4 mmol/L Mannitol + 10% FBS, HOP), PF low dose group (150 mmol/L glucose DMEM + 10%FBS + 1 μM PF, PF1), PF medium dose group (150 mmol/L glucose DMEM + 10%FBS+10 μM PF, PF10), and PF high dose group (150 mmol/L glucose DMEM + 10%FBS + 100 μM PF, PF100). After 24 hours of modeling, the supernatant was collected to extract exosomes.

2.2. Exosomes Extraction. SC-EXOs were extracted by ultracentrifugation from the culture supernatants. SC-EXOs were extracted by ultracentrifugation from the culture supernatants. The supernatants were collected and sequentially centrifuged firstly at 300 × g for 10 min, then the supernatants were collected and secondly at 2,000 × g for 20 min. Then again they were collected; next 30 min with 10,000 × g. The supernatant was transferred into the 8.9 mL centrifugal tube (Beckman, USA) to ultracentrifugation at 100,000 × g for 70 min twice at 4°C to get the exosomes. Our extraction method was the same as described in the previous study [27]. After sucking out all the supernatant, the precipitate was dissolved in 200 μL PBS and collected in 1.5 mL centrifuge tube for follow-up experiments.

2.3. Cell CCK8 Assay. 100 uL SCs suspension was inoculated in each well of 96-well plate, and Control group (25 mmol/L glucose DMEM + 10% FBS), HG group (150 mmol/L glucose DMEM + 10% FBS, HG), and HOP group (25 mmol/L glucose DMEM + 44.4 mmol/L Mannitol + 10% FBS) were set up. Six multiple holes were set in each group. After 24 hours, 10 μl CCK8 solution was added to each hole. The culture plate was incubated in the incubator for 3 hours. The absorbance value was measured by enzyme labeling instrument at 450 nm. Cytoactive rate*(%) = [(As − Ab)/(Ac − Ab)] × 100%, where As is HG or HOP group absorbance; Ac is Control group absorbance; and Ab is Blank hole absorbance.

2.4. Confocal Laser Microscopy. The primary DRGn was identified, and the SC-EXOs internalized by DRGn were observed with immunofluorescence.

DRGn identification: DRG was extracted and inoculated into cell climbing tablets and cultured for 7 days. DRGn was stained with NF-H polyclonal antibody (18934-1-AP,

Proteintech, NF200) for specific immunofluorescence staining, and the morphology of DRGn was observed by using laser confocal microscope.

DRGn internalized SC-EXOs: DRGn was stained by immunofluorescence with NF-H polyclonal. The exosomes were labeled with PKH26 (MINI26-1KT, Sigma) and co-cultured with DRGn for 24 hours. The situation of SC-EXOs internalized by DRGn was observed by immunofluorescence.

2.5. Transmission Electron Microscopy. The primary DRGn was inoculated on a six-well culture plate and cultured for 7 days. DRGn collected by centrifugation was fixed with glutaraldehyde for 2 hours, and the samples were rinsed 3 times with phosphate buffer. It is taken to Core Facility Center of Capital Medical University. The ER in DRGn was observed by using the HT7700 transmission electron microscope (Hitachi, Japan). The clear ER image was finally obtained by using the CCD camera and the microscope host.

2.6. Western Blot. The treated DRGn and SC-EXOs were collected. Cellular protein was extracted by RIPA lysis buffer. The equal proteins were separated on an SDS-PAGE, and then they are transferred to the PVDF membrane. The membrane was blocked with 5% nonfat dry milk for 1 hour. The PVDF membrane was incubated overnight at 4°C with primary antibodies, including Alix (1 : 2000, ab275377, Abcam), Hsp70 (1 : 2000, ab2787, Abcam), CD63 (1 : 2000, ab134045, Abcam), TSG101 (1 : 2000, ab125011, Abcam), GRP78 (1 : 2000, ab108613, Abcam), IRE1α (1 : 500, sc-390960, Santa cruz), p-IRE1α (1 : 2000, ab124945, Abcam), CHOP (1 : 500, sc-46661, Santa cruz), JNK (1 : 2000, ab208035, Abcam), p-JNK (1 : 2000, ab124956, Abcam), XBP1 (1 : 500, sc-8015, Santa cruz), Bcl-2 (1 : 2000, ab182858, Abcam), Bax (1 : 2000, ab32503, Abcam), Caspase-3 (1 : 2000, ab32351, Abcam), Caspase-12 (1 : 2000, ab62484, Abcam), and β-actin (1 : 2000, ab8226, Abcam). The membranes were incubated with the appropriate horseradish peroxidase-conjugated secondary antibodies. The specific bands were observed by using the hypersensitive ECL chemiluminescence kit (New Cell & Molecular Biotech Co., Ltd, P10200).

2.7. TUNEL Assay. DRGn was cultured in groups on the cell climbing slice; the cells were fixed by 4% paraformaldehyde, 0.1%TritonX-100 permeated through the membrane, dripped with TUNEL reaction solution (G1501-50T, Servicebio), and incubated at 37°C for 2 h. The nuclei were stained with DAPI and then sealed with antifluorescence quenchant. Under the 880 Airyscan laser confocal microscope (Zeiss, Germany), 8 visual fields were randomly selected in each group, the number of apoptotic cells and total cells were counted, and the percentage of apoptosis was calculated.

2.8. Statistical Analysis. The software used to process data includes GraphPad Prism8.0 and Image J. The results are shown as mean ± standard error of mean (SEM). Differences were analyzed by one-way ANOVA followed by Tukey's multiple comparisons test. Student's unpaired *t*-test was used to analyze data between 2 groups. $P < 0.05$ was considered statistically significant.

3. Result

3.1. The Cytoactivity of SCs Was Not Affected by High Osmotic Pressure. Compared with Control group, the cytoactivity in HG group was significantly decreased ($P < 0.01$), while the HOP group had no significant difference (Figure 1). This experiment confirmed that high osmotic pressure had no effect on cell cytoactivity. The changes in SCs and SC-EXOs were caused by high glucoses concentration, not osmotic pressure.

3.2. Identification of SC-EXOs Incubated in High Glucose. Figure 2 shows the results of Western blot. The exosomes specific proteins Alix, Hsp70, CD63, and TSG101 were detected. They were expressed in the exosomes of each group. The expression of the marker protein indicated the presence of exosomal components which proved that SCs can secrete exosomes, and using the ultracentrifugation to extract exosomes was reliable.

3.3. Identification of Primary DRGn and Internalization of SC-EXOs. Identification of primary DRGn: in order to verify whether the primary DRGn could be grown adherently after extracting the DRG by our method, we used the currently recognized DRGn specific antibody NF200 for identification. Cultured for 7 days, the immunofluorescence results showed that the adherent cells could appear green fluorescence, indicating that the adherent cells could bind to the specific antibody NF200, and the cells also showed the characteristics of DRGn: the whole cell was triangular and had slender axons (Figure 3(a)). This proved that our extraction method is correct, and the cell was primary DRGn.

The DRGn showed green fluorescence, and the nucleus showed blue fluorescence by using the laser confocal microscope. The exosomes showed red fluorescence. After merging, the red exosomes were located in the cytoplasm of green DRGn cells and distributed around the blue DRGn nucleus (Figure 3(b)). This proved that DRGn can internalize exosomes.

3.4. PF Regulated GRP78 and IRE1α in SC-EXOs Incubated in High Glucose. Compared with the Control group, the expression of GRP78 in the HG group increased ($P < 0.05$); compared with the HG group, the expression of the PF1 group decreased ($P < 0.05$; Figure 4(b)). Compared with the Control group, the expression of IRE1α and p-IRE1α in the HG group increased ($P < 0.01$); compared with the HG group, the PF10 group decreased ($P < 0.05$; Figures 4(c) and 4(d)). Thus, it could be seen that high glucose can lead to ER stress, PF can play a role in anti-ER stress, and exosomes participate in the information transmission of IRE1α pathway.

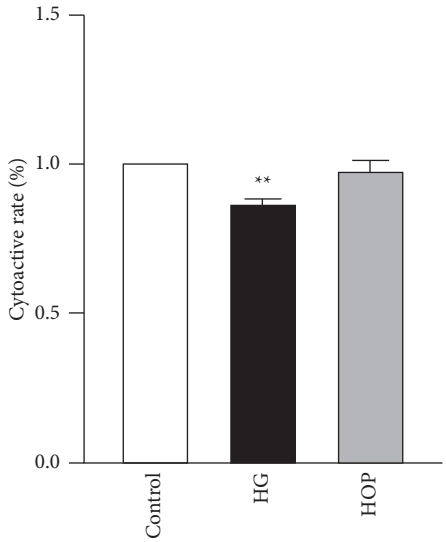

Figure 1: Determination of SCs high glucose and high osmotic pressure cell cytoactivity by CCK8 ** $P < 0.01$ vs. Control, $n = 6$ for each group.

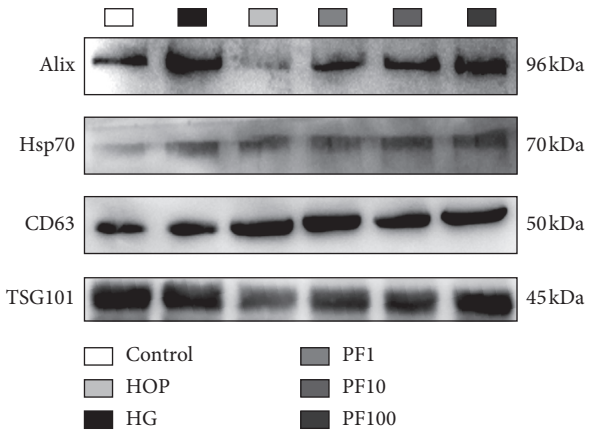

Figure 2: Exosomes marker protein of SC-EXOs. Western blot showed specific markers Alix, CD9, Hsp70, CD63, and TSG101 in exosomes.

3.5. Effect of PF Intervention of SC-EXOs on the Downstream Protein Expression of IRE1α Signal Pathway in DRGn. CHOP, XBP1s, C-Jun N-terminal kinase (JNK), and p-JNK are regarded as the downstream indexes of ER stress IRE1α pathway [28, 29]. We verify their expression by Western blot. Compared with the Control group, the expression of CHOP, JNK, and p-JNK increased, and the expression of XBP1s decreased in the HG group ($P < 0.05$ or $P < 0.01$). Compared with the HG group, the expression of CHOP, JNK, and p-JNK significantly decreased and the expression of XBP1s increased in the exosomes intervention group ($P < 0.05$ or $P < 0.01$; Figures 5(b)–5(e)). This proved that the exosomes after the intervention of PF can reduce the ER stress.

3.6. Effect of PF Intervention of SC-EXOs on the Morphological Integrity of ER in DRGn. We can see that the shape of ER in the Control group is uniform (Figure 6(a)). After 24 hours of 50 mM glucose intervention, the morphology of ER was partially enlarged, broken, and fragmented (Figure 6(c)). In the 50 mM glucose + EXOs PF group, the structure of ER tended to be intact (Figures 6(d) and 6(e)). This can explain that the PF interferes with SC-EXOs to maintain the intact morphology of ER. The morphology of ER in SC-EXOs PF100 and SC-EXOs Control group has improved but the effect was not obvious (Figures 6(b) and 6(e)).

3.7. PF Interfered with SC-EXOs to Reduce Apoptosis of DRGn

3.7.1. PF Interfered with SC-EXOs on Apoptosis of DRGn in High Glucose Concentration by TUNEL Kit. The TUNEL kit method is currently recognized as one of the methods to detect the level of apoptosis. Compared with the Control group, a large number of green fluorescence appeared in the HG group (Figure 7(a)), and the level of apoptosis increased in the HG group ($P < 0.01$; Figure 7(b)). Compared with the HG group, different doses of PF interfere with the SC-EXOs to reduce apoptosis of DRGn ($P < 0.01$; Figure 7(b)). Compared with the HG + EXOs PF1 group, the apoptosis rate of DRGn in the HG + EXOs PF10 group and HG + EXOs PF100 group was significantly decreased ($P < 0.01$). The intervention effect of PF with doses of 10 μM and 100 μM was the best.

3.7.2. PF Interfered with SC-EXOs on DRGn Apoptotic Protein in High Glucose Concentration. In addition to using the TUNEL kit to detect the degree of apoptosis in DRGn, we also verified the expression of anti-apoptotic protein Bcl-2 and pro-apoptotic protein Bax and Caspase family proteins Caspase-12 and Caspase-3 by Western blot. Compared with the Control group, the expression of Bax, Caspase-3, and Caspase-12 was significantly increased and the expression of Bcl-2 was decreased in the HG group ($P < 0.05$ or $P < 0.01$); compared with the HG group, the expression of Bax, Caspase-3, and Caspase-12 was significantly decreased and the expression of Bcl-2 was significantly increased in the HG + EXOs PF group ($P < 0.05$ or $P < 0.01$; Figures 8(b)–8(e)). Western blot showed that EXOs interfered with PF could inhibit the expression of apoptotic protein in DRGn, which was consistent with the results of the previous TUNEL kit. It was more confirmed that EXOs after the intervention of PF can reduce the apoptosis induced by high glucose.

4. Discussion

In diabetic peripheral neuropathy, the research group has found that exosomes could play the role of antioxidative stress through information communication and then improve DPN. There was a variety of pathogenesis of DPN. The studies have shown that exosomes can improve DPN by regulating the communication between SCs and DRGn. ER stress is one of the pathogenesis of DPN [30]. PF can improve the apoptosis of SCs in high glucose concentration by reducing ER stress and has the potential to interfere with DPN [6]. However, can PF interfere with DPN by improving the communication between SCs and DRGn? What is the

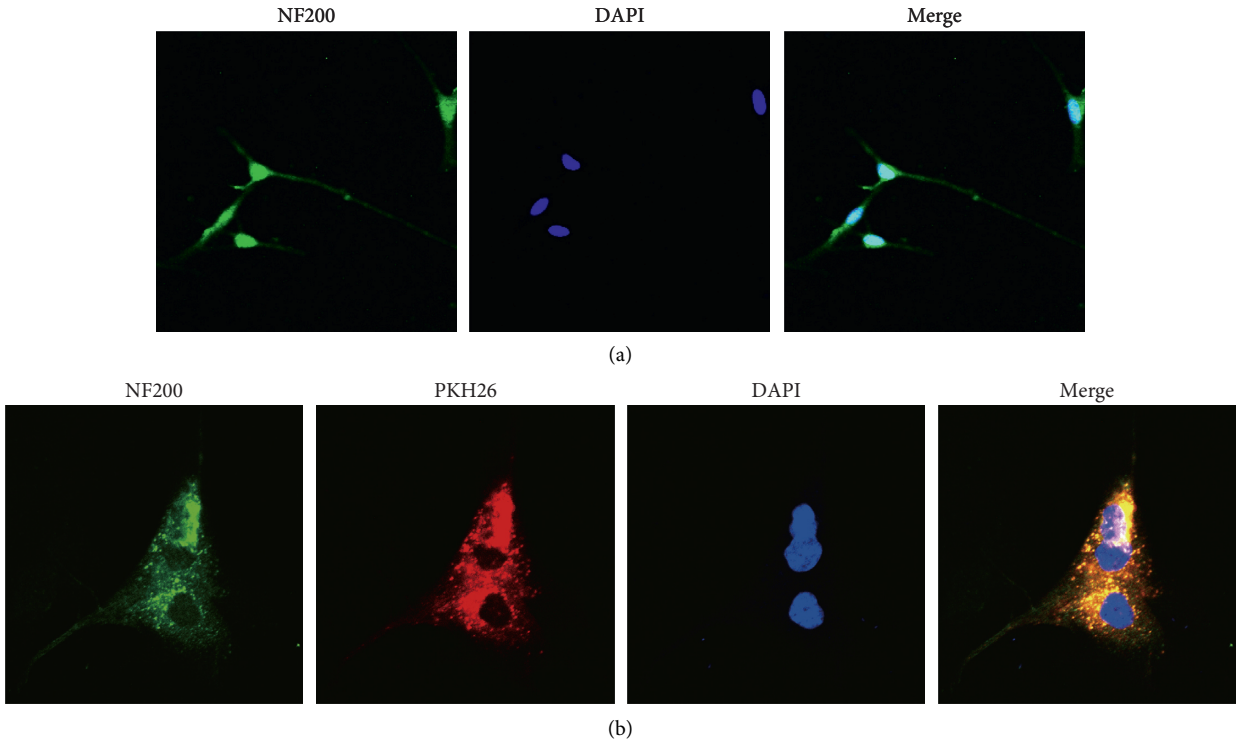

Figure 3: Identification of the DRGn and the internalization of SC-EXOs. (a) NF200 specific identification of DRGn (×200), scale bar, 100 μm. (b) DRGn internalized SC-EXOs (×400), scale bar, 50 μm.

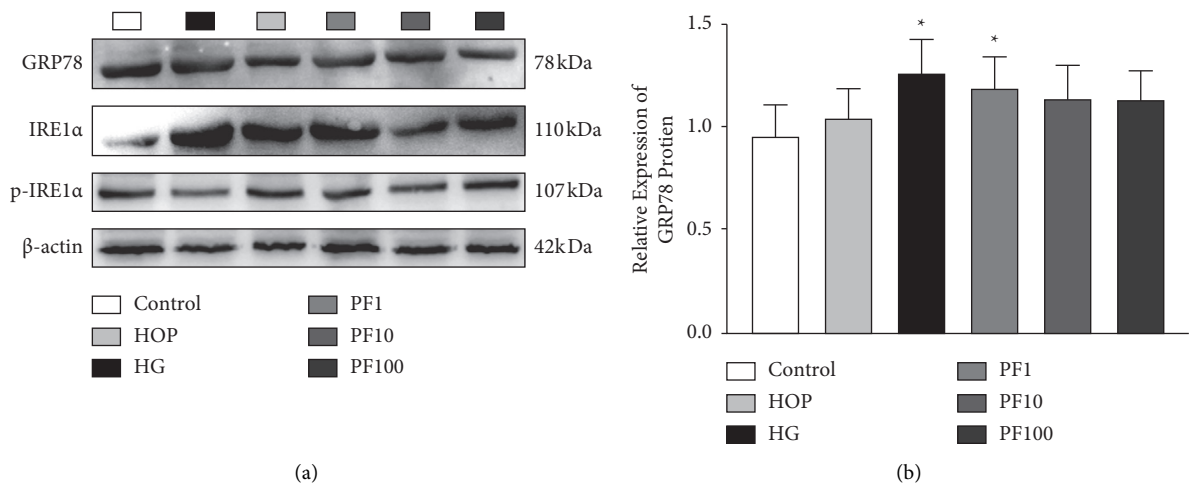

Figure 4: Continued.

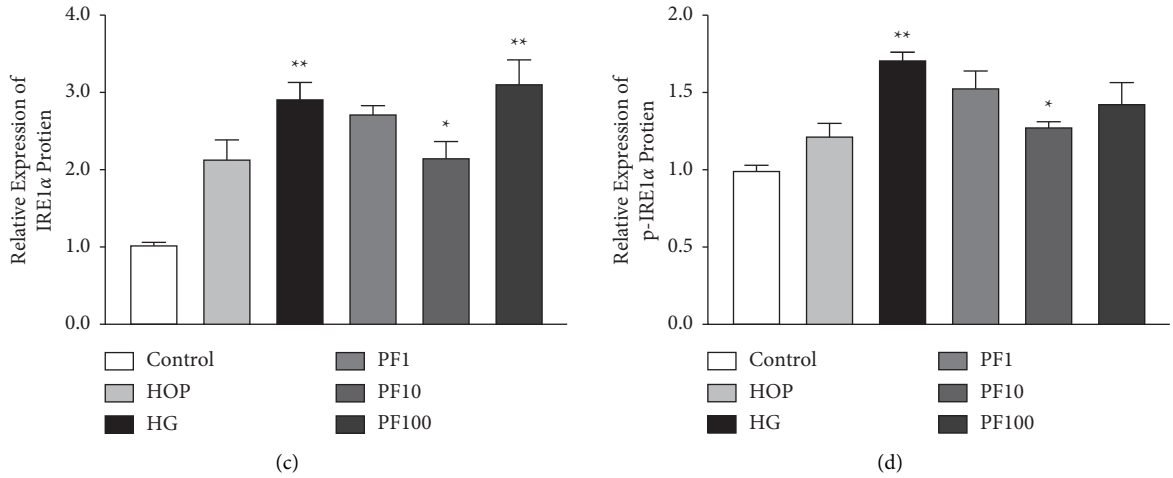

Figure 4: PF interfered with SC-EXOs carrying ER stress information. (a) The expression of ER stress initiating factors in exosomes. The protein expression level for (b) GRP78, (c) IRE1α, and (d) p-IRE1α was determined by Western blotting, $n = 4$ for each group. The results are expressed as the mean ± standard error.

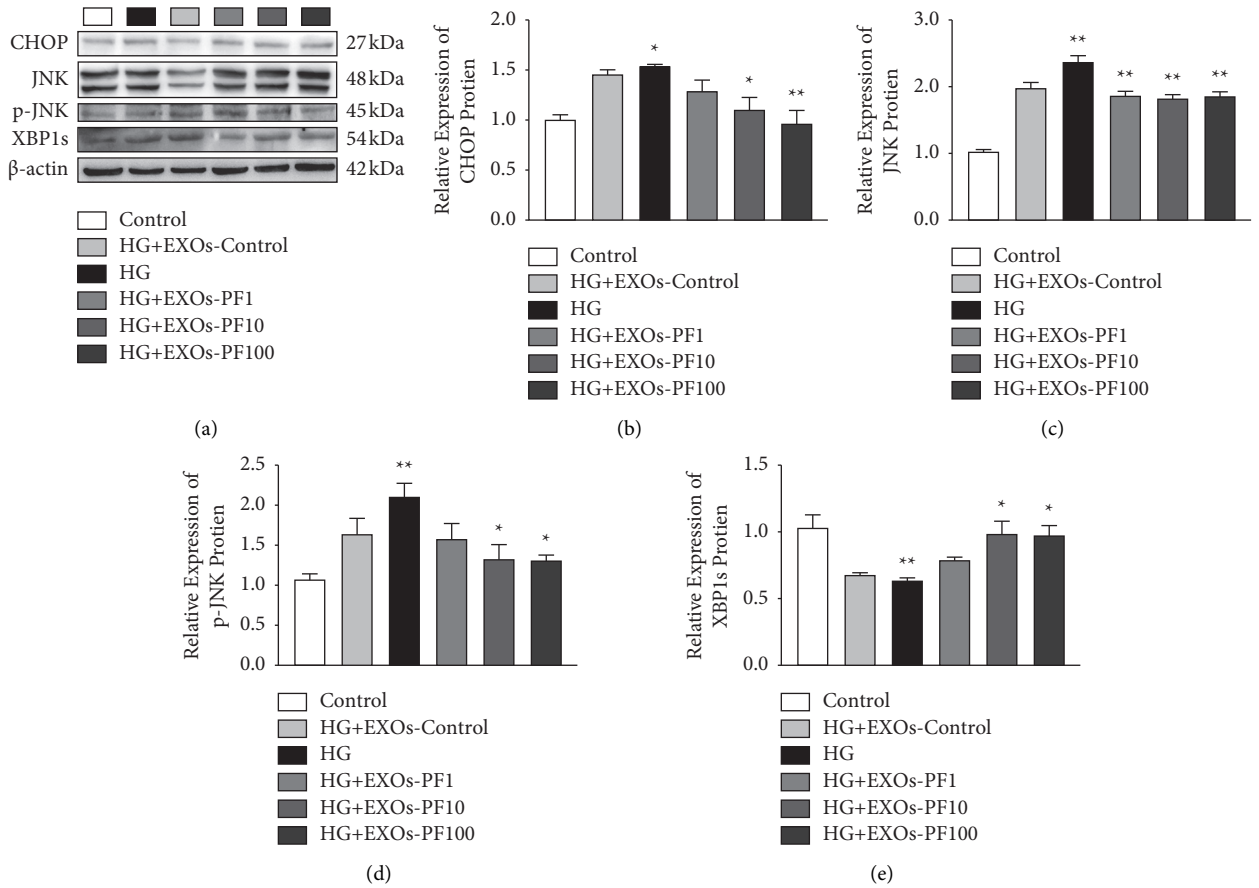

Figure 5: The effect of PF interfered with SC-EXOs on the downstream proteins of ER stress in DRGn. (a) The expression of ER stress downstream protein in DRGn. The expression level of (b) CHOP, (c) JNK, (d) p-JNK, and (e) XBP1s was determined by Western blotting, $n = 4$ for each group. The results are expressed as the mean ± standard error.

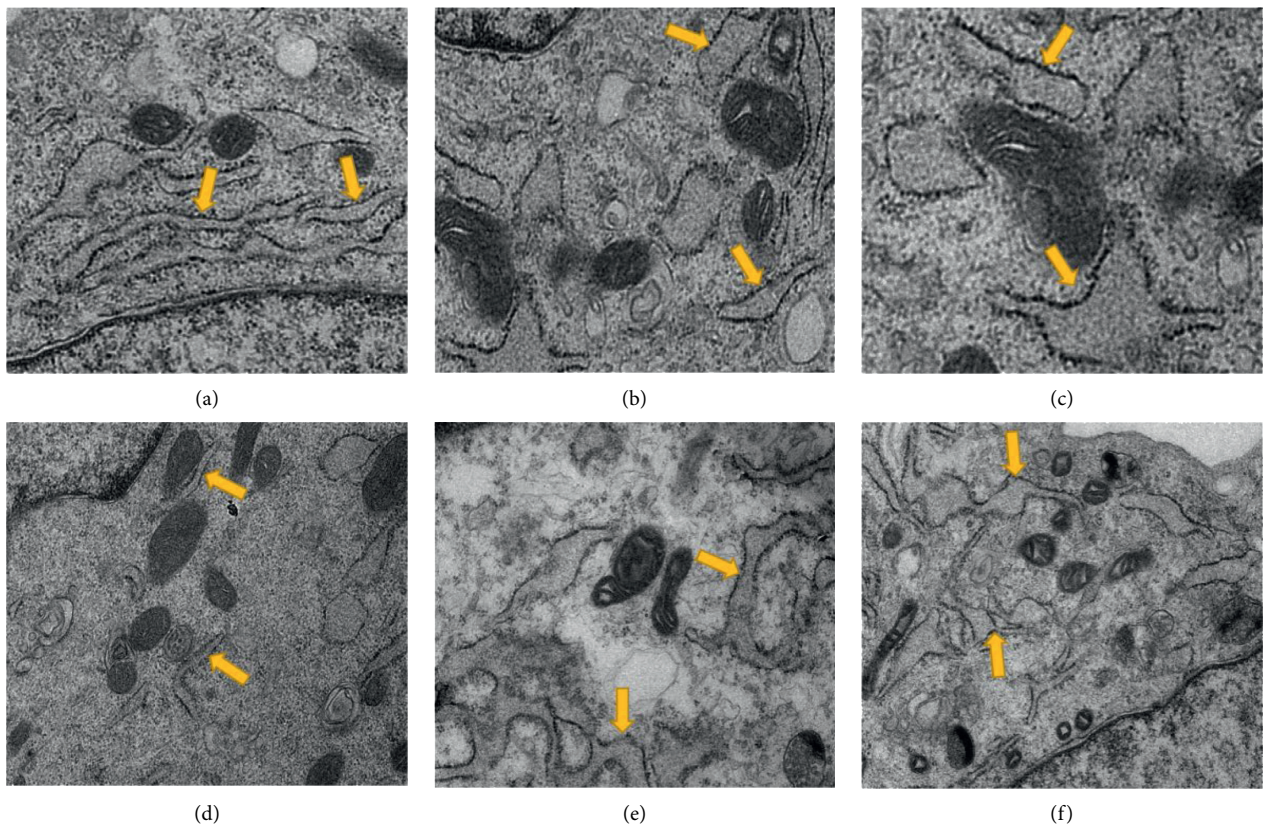

Figure 6: Ultrastructural observation of ER (7,000x). The yellow arrow refers to the ER. (a–f) The Control group, HG + EXOs Control group, HG group, HG + EXOs PF1 group, HG + EXOs PF10 group, and HG + EXOs PF100 group.

specific way of action? These have not been fully clarified at present. Our study confirmed that PF can reduce the apoptosis of DRGn by regulating the signal proteins related to ER stress in SC-EXOs.

In this study, ER stress was used as a breakthrough point to further explain the role of SC-EXOs. We used an in vitro model to verify this hypothesis. The results of this study are as follows: (1) SC-EXOs can carry ER stress initiating factor and IRE1α pathway initiating factor; (2) the hyperosmotic condition does not affect the activity of SCs and the SC-EXOs; (3) DRGn can internalize the SC-EXOs and use the exosomes communication mechanism to transmit information; (4) high glucose can aggravate the ER stress and change the morphology of ER in DRGn; and (5) SC-EXOs under the intervention of PF can reduce the apoptosis of DRGn in high concentration.

DPN as a disease of the peripheral nervous system, high glucose stimulation can cause damage to SCs and DRGn axons [31]. SC-EXOs can promote the activity of nerve cells [32]. At the same time, the SC-EXOs also can significantly promote axonal growth and axonal regeneration. Axon regeneration is an important process of functional recovery after peripheral nervous system injury [33]. Therefore, the SC-EXOs may be involved in the axonal regeneration and growth regulation of DRGn and promote the repair of peripheral nerve injury. Then, the molecular mechanism of SC-EXOs is explained to promote DRGn axonal growth, and thus ER stress is inhibited to reduce cell apoptosis; this is the core problem solved in this study.

We previously found that hyperglycemia can cause axonal damage in DRGn and trigger DPN. The degeneration of distal sensory axons in DRGn is the main cause of DPN [34, 35]. SCs can interact with the axons of DRGn, and SCs in the normal concentration can secrete exosomes to promote the proliferation of injured DRGn [36]. SC-EXOs were internalized by DRGn axons, and miR-27a in exosomes promoted neurite growth of diabetic DRGn [30]. Our results showed that DRGn could internalize SC-EXOs, and exosomes were involved in the recovery of damaged DRGn. However, our results showed that the exosomes under the intervention of PF significantly alleviated the ER stress and apoptosis of DRGn. SC-EXOs under normal conditions can have a therapeutic effect on DRGn stimulated by high glucose, but the results are not significantly different. Therefore, it can be shown that PF intervention can help exosomes carry IRE1α pathway information to inhibit apoptosis.

It has been proved that the condition of high glucose concentration can increase the number of exosomes and interfere with the biological activity of exosomes [37]. SCs with axonal damage can also release a large number of exosomes [38]. Therefore, it is proved that high glucose concentration can affect the exosomes, and we have previously proved that high glucose concentration can increase

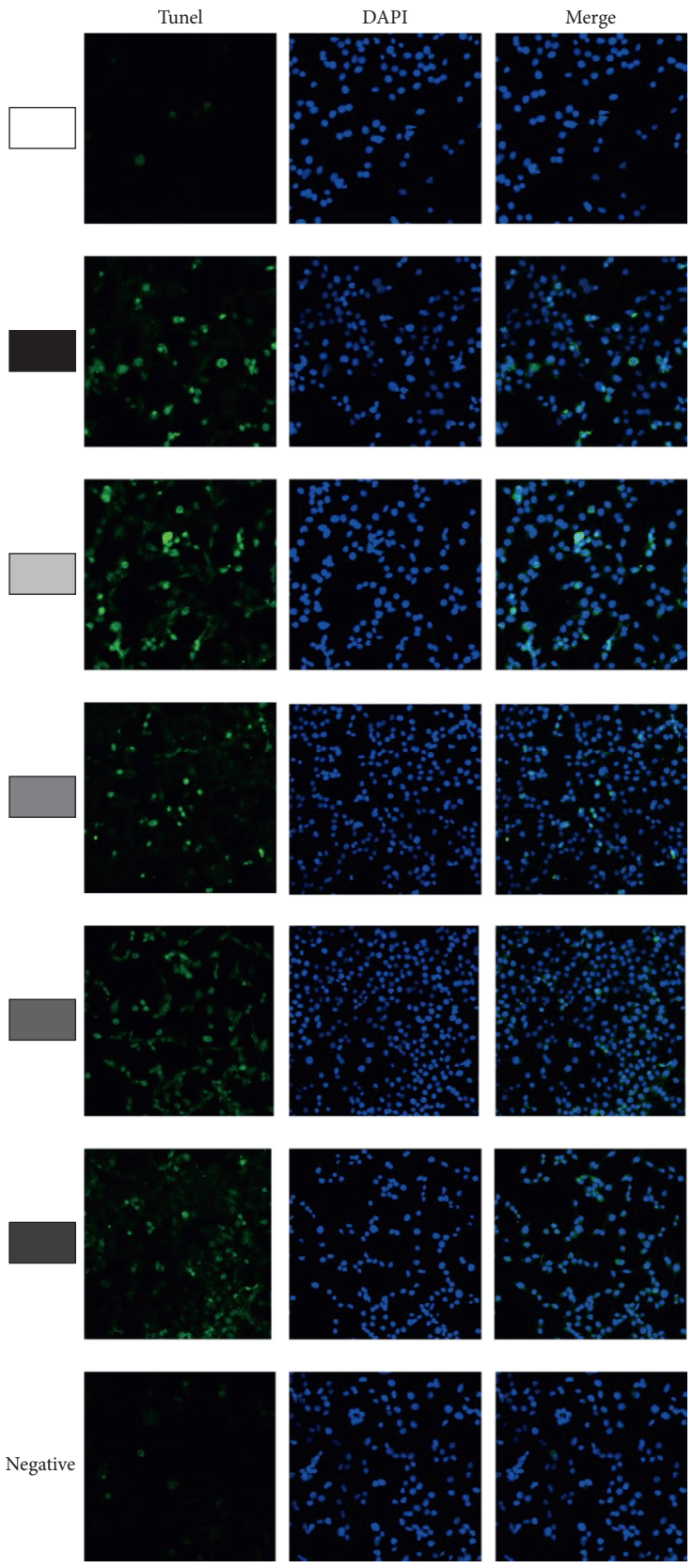

(a)

Figure 7: Continued.

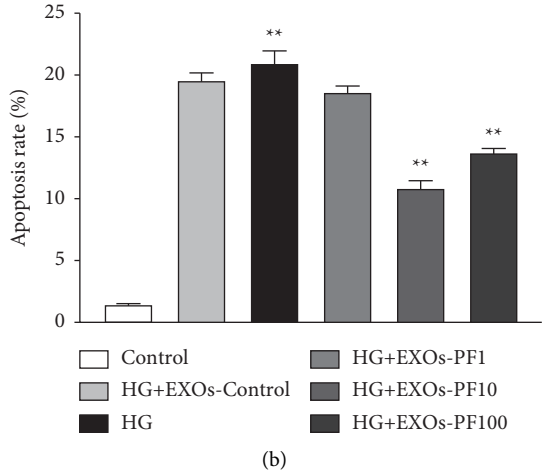

Figure 7: The apoptosis level of DRGn was detected by immunofluorescence (×200) dcale bar, 100 μm. The green fluorescence was the apoptotic cells stained by TUNEL kit, and the blue fluorescence was the nucleus. Blue-green overlap was the apoptotic cells. $n = 6$ for each group.

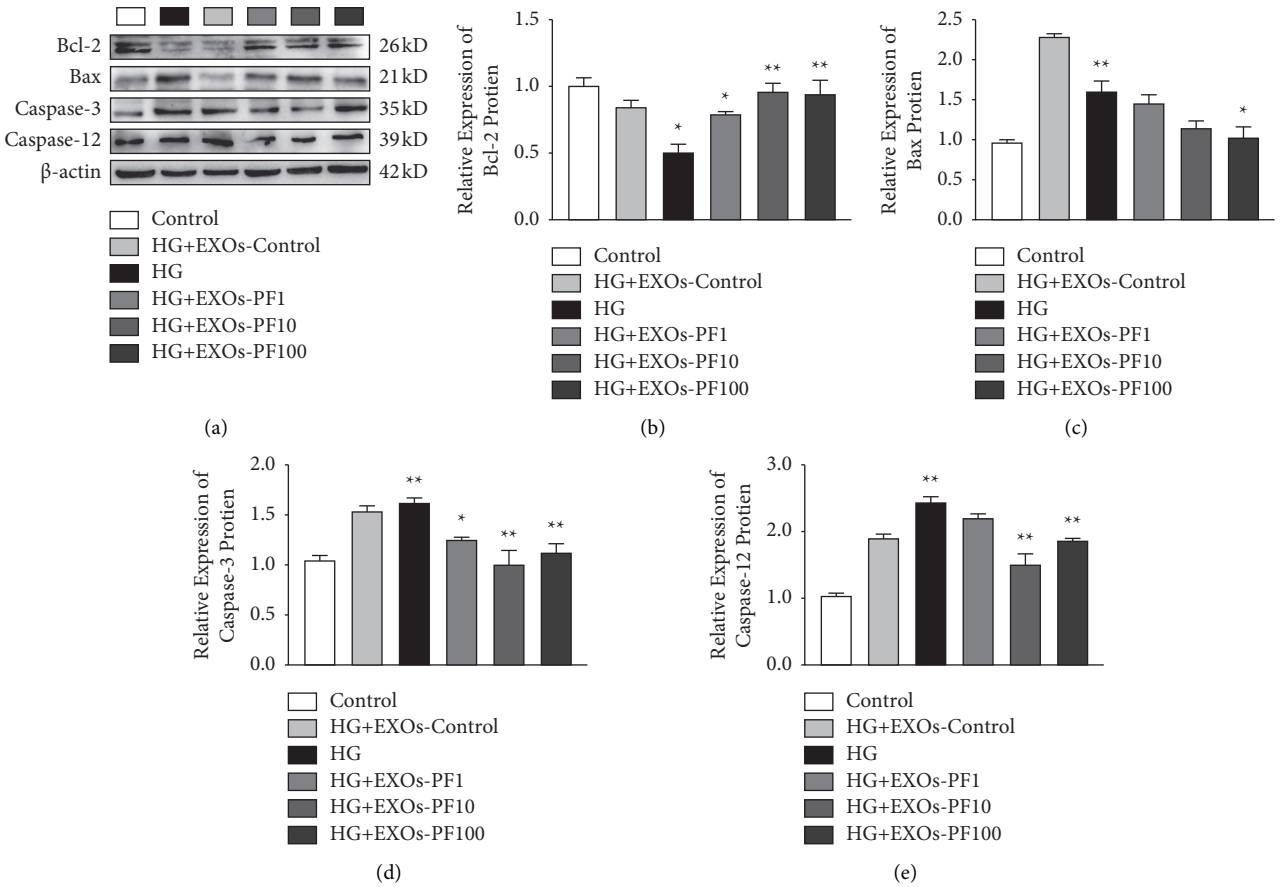

Figure 8: The effect of PF interfered with SC-EXOs on the apoptotic proteins in DRGn. (a) The expression of apoptotic protein in DRGn. DRGn apoptosis protein expression for (b) Bax, (c) Bcl-2, (d) Caspase-3, and (e) Caspase-12 was determined by the western blot. The results were expressed as the mean ± standard error, $n = 4$ for each group.

the expression of exosomal marker protein CD63 compared with the Control group [39], which is consistent with our experimental results. In order to eliminate the effect of other conditions on the exosomes derived from SCs, we also treated SCs with high osmotic pressure. At the same time, we tested the SCs and SC-EXOs after intervention and found

that high osmotic pressure did not affect the activity of SCs and the information transmission between exosomes and DRGn.

The research group previously proved that DPN was characterized by demyelination caused by SCs apoptosis induced by ER stress. The pathogenesis of DPN is complicated, but ER stress is closely related to apoptosis. In the process of UPR, IRE1α dissociates with GRP78 and then undergoes autophosphorylation to activate downstream reactions [40]. The results showed that both IRE1α and GRP78 were expressed in exosomes, and their expression increased significantly in high glucose concentration, indicating that exosomes can carry information transmission factor and activate IRE1α signal pathway. At the same time, the expression of both exosomes decreased after the intervention of PF. C/EBP homologous protein (CHOP), as a downstream protein of ER stress, is upregulated in SCs of the diabetic nephropathy rat model. Under ER stress, activated IRE1α can no longer regulate the expression of transcription factors CHOP and Caspase-12 and further activate the expression of Caspase-3, aggravating apoptosis-mediated DPN damage. All these are consistent with our experimental results. CHOP played a key role in cell apoptosis induced by ER stress. It was considered to play a central role in cell apoptosis induced by ER stress. It is strongly induced by IRE1α signal. Inhibiting the expression of IRE1α can inhibit the expression of CHOP [41]. At the same time, in the diabetic model, the expression level of XBP1s in hippocampus decreased significantly, suggesting that the decrease in XBP-1s expression is closely related to the damage of the peripheral nervous system caused by diabetes [42]. Excessive or persistent ER stress can also activate the phosphokinase activity of IRE1α. Activated ASK1 induces and increases the expression of JNK by increasing the transcription of JNK. It has been found that the expression of JNK is significantly decreased after the application of IRE1α phosphokinase inhibitor [43]. Our results of Western blot also show that PF interferes with SC-EXOs to affect the expression of ER stress downstream factors in DRGn, inhibits the expression of apoptotic factors Caspase-12 and Caspase-3, reduce apoptosis, and alleviates ER stress by exosomes.

In summary, our study shows that SCs can release exosomes, and the method of extracting exosomes by ultracentrifugation is feasible. Exosomes can carry ER stress initiating factor and IRE1α signaling pathway information transmission factor for cell-to-cell information exchange. High glucose concentration will affect SCs secretion of exosomes, while high osmotic pressure will not affect SCs activity and exosomes secretion. PF can improve the ER stress of DRGn and affect the expression of downstream proteins such as JNK and CHOP; improve the morphology in ER of DRGn damaged by high glucose; and increase the expression of anti-apoptotic protein Bcl-2, decrease the expression of pro-apoptotic protein Bax, inhibit the expression of Caspase family Caspase-12 and Caspase-3, and ultimately improve DPN. As a carrier of cellular communication, exosomes provide new ideas for the treatment of DPN, diabetes, and its complications.

5. Conclusion

This study proved that SCs can secrete exosomes. PF can affect the expression of IRE1α and GRP78 which were the key proteins of IRE1α signal pathway in exosomal ER stress. DRGn can absorb SC-EXOs. PF carries ER stress information by exosomes, which plays the role of anti-ER stress and reduces DRGn apoptosis, thus ameliorating DPN. Our research provided a new method for the treatment of DPN from the molecular mechanism level.

Data Availability

The data used to support the results of this study are included in the article.

Conflicts of Interest

The authors declare that they have no conflicts of interest.

Acknowledgments

This work was supported by the National Natural Science Fund Projects (Nos. 81873125 and 81473642) and the National Natural Science Fund for Youths (No. 81704014).

References

[1] P. Yan, Y. Xu, Z. Zhang et al., "Decreased plasma neuregulin 4 levels are associated with peripheral neuropathy in Chinese patients with newly diagnosed type 2 diabetes: a cross-sectional study," *Cytokine*, vol. 113, pp. 356–364, 2019.

[2] E. S. Kim, S. W. Lee, E. Y. Mo, S. D. Moon, and J. H. Han, "Inverse association between serum total bilirubin levels and diabetic peripheral neuropathy in patients with type 2 diabetes," *Endocrine*, vol. 50, no. 2, pp. 405–412, 2015.

[3] M. Kobayashi and D. W. Zochodne, "Diabetic neuropathy and the sensory neuron: new aspects of pathogenesis and their treatment implications," *Journal of Diabetes Investigation*, vol. 9, no. 6, pp. 1239–1254, 2018.

[4] Y. P. Liu, S. J. Shao, and H. D. Guo, "Schwann cells apoptosis is induced by high glucose in diabetic peripheral neuropathy," *Life Sciences*, vol. 248, Article ID 117459, 2020.

[5] H. Pan, H. Huang, L. Zhang, S. Ma, H. Yang, and H. Wang, "Adjusting internal organs and dredging channel" electroacupuncture treatment prevents the development of diabetic peripheral neuropathy by downregulating glucose-related protein 78 (GRP78) and caspase-12 in streptozotocin-diabetic rats," *Journal of Diabetes*, vol. 11, no. 12, pp. 928–937, 2019.

[6] W. Yao, X. Yang, J. Zhu, B. Gao, R. Liu, and L. Xu, "Tang-Luo-Ning, a traditional Chinese medicine, inhibits endoplasmic reticulum stress-induced apoptosis of schwann cells under high glucose environment," *Evidence Based Complementary and Alternative Medicine*, vol. 2017, Article ID 5193548, 9 pages, 2017.

[7] B. L. L. Clayton and B. Popko, "Endoplasmic reticulum stress and the unfolded protein response in disorders of myelinating glia," *Brain Research*, vol. 1648, pp. 594–602, 2016.

[8] S. S. Cao and R. J. Kaufman, "Unfolded protein response," *Current Biology*, vol. 22, no. 16, pp. R622–R626, 2012.

[9] D. Sharma, J. N. Singh, and S. S. Sharma, "Effects of 4-phenyl butyric acid on high glucose-induced alterations in dorsal root

ganglion neurons," *Neuroscience Letters*, vol. 635, pp. 83–89, 2016.

[10] S. K. Fineberg, K. S. Kosik, and B. L. Davidson, "MicroRNAs potentiate neural development," *Neuron*, vol. 64, no. 3, pp. 303–309, 2009.

[11] S. Mathivanan, C. J. Fahner, G. E. Reid, and R. J. Simpson, "ExoCarta 2012: database of exosomal proteins, RNA and lipids," *Nucleic Acids Research*, vol. 40, pp. D1241–D1244, 2012.

[12] D. G. Phinney, M. Di Giuseppe, J. Njah et al., "Mesenchymal stem cells use extracellular vesicles to outsource mitophagy and shuttle microRNAs," *Nature Communications*, vol. 6, no. 1, p. 8472, 2015.

[13] N. P. Gonçalves, Y. Yan, M. Ulrichsen et al., "Modulation of small RNA signatures in schwann-cell-derived extracellular vesicles by the p75 neurotrophin receptor and sortilin," *Biomedicines*, vol. 8, no. 11, p. 450, 2020.

[14] R. López-Leal, F. Díaz-Viraqué, R. J. Catalán et al., "Schwann cell reprogramming into repair cells increases miRNA-21 expression in exosomes promoting axonal growth," *Journal of Cell Science*, vol. 133, no. 12, Article ID jcs239004, 2020.

[15] K. Elmasry, R. Mohamed, I. Sharma et al., "Epigenetic modifications in hyperhomocysteinemia: potential role in diabetic retinopathy and age-related macular degeneration," *Oncotarget*, vol. 9, no. 16, pp. 12562–12590, 2018.

[16] V. La Marca and A. Fierabracci, "Insights into the diagnostic potential of extracellular vesicles and their miRNA signature from liquid biopsy as early biomarkers of diabetic micro/macrovascular complications," *International Journal of Molecular Sciences*, vol. 18, no. 9, p. 1974, 2017.

[17] X. J. Ning, X. H. Lu, J. C. Luo et al., "Molecular mechanism of microRNA-21 promoting schwann cell proliferation and axon regeneration during injured nerve repair," *RNA Biology*, vol. 17, no. 10, pp. 1508–1519, 2020.

[18] S. Kanemoto, R. Nitani, T. Murakami et al., "Multivesicular body formation enhancement and exosome release during endoplasmic reticulum stress," *Biochemical and Biophysical Research Communications*, vol. 480, no. 2, pp. 166–172, 2016.

[19] E. Kakazu, A. S. Mauer, M. Yin, and H. Malhi, "Hepatocytes release ceramide-enriched pro-inflammatory extracellular vesicles in an IRE1α-dependent manner," *Journal of Lipid Research*, vol. 57, no. 2, pp. 233–245, 2016.

[20] D. Dasgupta, Y. Nakao, A. S. Mauer et al., "IRE1A stimulates hepatocyte-derived extracellular vesicles that promote inflammation in mice with steatohepatitis," *Gastroenterology*, vol. 159, no. 4, pp. 1487–1503, 2020.

[21] J. S. Wang, Y. Huang, S. Zhang et al., "A protective role of paeoniflorin in fluctuant hyperglycemia-induced vascular endothelial injuries through antioxidative and anti-inflammatory effects and reduction of PKCβ1," *Oxidative Medicine and Cellular Longevity*, vol. 2019, Article ID 5647219, 11 pages, 2019.

[22] X. Zhu, K. Wang, F. Zhou, and L. Zhu, "Paeoniflorin attenuates atRAL-induced oxidative stress, mitochondrial dysfunction and endoplasmic reticulum stress in retinal pigment epithelial cells via triggering Ca2+/CaMKII-dependent activation of AMPK," *Archives Pharmacal Reserach*, vol. 41, no. 10, pp. 1009–1018, 2018.

[23] J. Chen, M. Zhang, M. Zhu et al., "Paeoniflorin prevents endoplasmic reticulum stress-associated inflammation in lipopolysaccharide-stimulated human umbilical vein endothelial cells via the IRE1α/NF-κB signaling pathway," *Food & Function*, vol. 9, no. 4, pp. 2386–2397, 2018.

[24] J. Chen, X. F. Hou, G. Wang et al., "Terpene glycoside component from moutan cortex ameliorates diabetic nephropathy by regulating endoplasmic reticulum stress-related inflammatory responses," *Journal of Ethnopharmacology*, vol. 193, pp. 433–444, 2016.

[25] X. L. Wang, L. W. Cui, Z. Liu et al., "Effects of TRPA1 activation and inhibition on TRPA1 and CGRP expression in dorsal root ganglion neurons," *Neural Regeneration Research*, vol. 14, no. 1, pp. 140–148, 2019.

[26] X. B. Wang, W. Ma, T. Luo et al., "A novel primary culture method for high-purity satellite glial cells derived from rat dorsal root ganglion," *Neural Regeneration Research*, vol. 14, no. 2, pp. 339–345, 2019.

[27] Z. Wu, P. Pu, Z. Su, X. Zhang, L. Nie, and Y. Chang, "Schwann cell-derived exosomes promote bone regeneration and repair by enhancing the biological activity of porous Ti6Al4V scaffolds," *Biochemical and Biophysical Research Communications*, vol. 531, no. 4, pp. 559–565, 2020.

[28] R. Iurlaro and C. Muñoz-Pinedo, "Cell death induced by endoplasmic reticulum stress," *The FEBS Journal*, vol. 283, no. 14, pp. 2640–2652, 2016.

[29] H. Dong, N. M. Adams, Y. Xu et al., "The IRE1 endoplasmic reticulum stress sensor activates natural killer cell immunity in part by regulating c-Myc," *Nature Immunology*, vol. 20, no. 7, pp. 865–878, 2019.

[30] L. Wang, M. Chopp, A. Szalad et al., "Exosomes derived from schwann cells ameliorate peripheral neuropathy in type 2 diabetic mice," *Diabetes*, vol. 69, no. 4, pp. 749–759, 2020.

[31] M. Zhang, Inam-U-Llah, X. Shi et al., "Taurine promotes neuritic growth of dorsal root ganglion cells exposed to high glucose in vitro," *Advances in Experimental Medicine and Biology*, vol. 1155, pp. 923–934, 2019.

[32] M. Hu, L. Hong, C. Liu et al., "Electrical stimulation enhances neuronal cell activity mediated by Schwann cell derived exosomes," *Scientific Reports*, vol. 9, no. 1, p. 4206, 2019.

[33] I. Allodi, E. Udina, and X. Navarro, "Specificity of peripheral nerve regeneration: interactions at the axon level," *Progress in Neurobiology*, vol. 98, no. 1, pp. 16–37, 2012.

[34] L. Jia, M. Chopp, L. Wang et al., "MiR-34a regulates axonal growth of dorsal root ganglia neurons by targeting FOXP2 and VAT1 in postnatal and adult mouse," *Molecular Neurobiology*, vol. 55, no. 12, pp. 9089–9099, 2018.

[35] E. L. Feldman, K. A. Nave, T. S. Jensen, and D. L. H. Bennett, "New horizons in diabetic neuropathy: mechanisms, bioenergetics, and pain," *Neuron*, vol. 93, no. 6, pp. 1296–1313, 2017.

[36] M. Zhou, M. Hu, S. He et al., "Effects of RSC96 schwann cell-derived exosomes on proliferation, senescence, and apoptosis of dorsal root ganglion cells in vitro," *Medical Science Monitor: International Medical Journal of Experimental and Clinical Research*, vol. 24, pp. 7841–7849, 2018.

[37] A. da Silva Novaes, F. T. Borges, E. Maquigussa, V. A. Varela, M. V. S. Dias, and M. A. Boim, "Influence of high glucose on mesangial cell-derived exosome composition, secretion and cell communication," *Scientific Reports*, vol. 9, no. 1, p. 6270, 2019.

[38] R. Lopez-Leal and F. A. Court, "Schwann cell exosomes mediate neuron-glia communication and enhance axonal regeneration," *Cellular and Molecular Neurobiology*, vol. 36, no. 3, pp. 429–436, 2016.

[39] S. Han, X. Li, X. Yang, J. Zhu, Y. Zhu, and L. Xu, "Effect of paeoniflorin on apoptosis of dorsal root neurons induced by schwann cell exosomes," *Journal of Medical Research*, vol. 49, no. 11, pp. 49–53, 2020.

[40] M. C. Kopp, P. R. Nowak, N. Larburu, C. J. Adams, and M. M. Ali, "In vitro FRET analysis of IRE1 and BiP association and dissociation upon endoplasmic reticulum stress," *Elife*, vol. 7, Article ID e30257, 2018.

[41] W. Yao, X. Yang, J. Zhu, B. Gao, H. Shi, and L. Xu, "IRE1α siRNA relieves endoplasmic reticulum stress-induced apoptosis and alleviates diabetic peripheral neuropathy in vivo and in vitro," *Scientific Reports*, vol. 8, no. 1, p. 2579, 2018.

[42] J. Yang, X. Wu, X. Wu et al., "The multiple roles of XBP1 in regulation of glucose and lipid metabolism," *Current Protein & Peptide Science*, vol. 18, no. 6, pp. 630–635, 2017.

[43] S. Yi, K. Chen, L. Zhang et al., "Endoplasmic reticulum stress is involved in stress-induced hypothalamic neuronal injury in rats via the PERK-ATF4-CHOP and IRE1-ASK1-JNK pathways," *Frontiers in Cellular Neuroscience*, vol. 13, p. 190, 2019.

Hindawi
Evidence-Based Complementary and Alternative Medicine
Volume 2021, Article ID 6773260, 9 pages
https://doi.org/10.1155/2021/6773260

Research Article

A Novel Supplement Attenuates Oxidative Stress-Induced TDP-43-Related Pathogenesis in TDP-43-Expressed Cells

Eun Jin Yang

KM Medicine Science Research Division, Korea Institute of Oriental Medicine, 1672 Yuseong-Daero, Yuseong-Gu, Daejeon 305811, Republic of Korea

Correspondence should be addressed to Eun Jin Yang; yej4823@gmail.com

Received 9 July 2021; Accepted 9 September 2021; Published 27 September 2021

Academic Editor: Rajeev K Singla

Copyright © 2021 Eun Jin Yang. This is an open access article distributed under the Creative Commons Attribution License, which permits unrestricted use, distribution, and reproduction in any medium, provided the original work is properly cited.

Amyotrophic lateral sclerosis (ALS) is caused by selective the loss of spinal motor neurons by multifactorial pathological mechanisms and results in muscle atrophy. Incidence rates of ALS are increasing over time, but there are no effective treatments at present due to limitations on approved therapies (riluzole and edaravone). Therefore, this study investigated whether combined treatment with Bojungikgi-tang and riluzole could act synergistically in transactive response DNA-binding protein 43 (TDP-43) stress granule cells. To examine the effect of combined treatment on oxidative stress-induced cell death, the CCK8 assay was performed for the detection of cell viability. The expression of oxidative stress-induced proteins was determined by Western blot. Quantification of sodium arsenite-induced reactive oxygen species (ROS) was measured in TDP-43 stress granular cells using 2,7-diacetyl dichlorofluorescein diacetate. To investigate the effect of combined treatment on TDP-43 aggregation, immunofluorescence and immunoblotting were performed in TDP-43 stress granular cells. This combined treatment alleviated oxidative stress-induced cell death by increasing the expression levels of antioxidation proteins, such as heme oxygenase-1 and B cell lymphoma-2-associated X protein. Furthermore, it reduced oxidative stress-induced TDP-43 aggregates and lowered the levels of autophagy-related proteins, including p62, light chain 3b, and ATG8, in TDP-43-expressing cells. Our results suggest that this combined treatment could be helpful for autophagy regulation in other neurodegenerative diseases.

1. Introduction

Amyotrophic lateral sclerosis (ALS) is caused by selective loss of spinal motor neurons by multifactorial pathological mechanisms and results in muscle atrophy [1]. ALS-related genes include mutations in superoxide dismutase 1, fused in sarcoma (FUS), transactive response DNA-binding protein 43 (TDP-43), C9orf72, optineurin, sequestosome 1, ubiquilin 2, dynactin, MATR3, and valosin-containing protein (VCP) [2]. The pathological mechanisms of ALS include excitotoxicity, apoptosis, inflammation, and oxidative stress at the cellular level [2]. TDP-43 is involved in frontotemporal lobar degeneration (FTLD), and ALS and its pathological mechanisms include oxidative stress [3], neuroinflammation [4], and mitochondrial dysfunction [5]. In particular, oxidative stress activates pathological pathways leading to neuronal degeneration and motor neuron death [6]. Furthermore, TDP-43 has been associated with the RNA-related metabolism, stress granule formation, the ubiquitin-proteasome system (UPS), autophagy, and mitochondrial dysfunction [7]. The TDP-43 protein is a significant component of the characteristic ubiquitinated neuronal inclusions [8, 9]. Abnormal TDP-43 is displaced from the nucleus to the cytoplasm and forms aggregates due to defects in the machinery regulating protein homeostasis, such as the autophagy-lysosome pathway and UPS [10]. The research is inconsistent as to whether the aggregation of TDP-43 protein is beneficial or induces neurotoxicity. Xu et al. and Wegorzewska et al. have shown that mutant TDP-43 protein is toxic to neurons in several TDP-43 animal models [11, 12]. However, Vander Broeck et al. suggested that the loss of TDP-43 induces TDP-43-related proteinopathies rather than toxic effects by aggregates [13]. Significant research has focused on finding a drug to prevent or

alleviate TDP-43-related disease conditions. The multiple complex pathomechanisms have complicated finding an effective drug for ALS. Although riluzole has been used to treat patients with ALS, it does not appear to extend patients' survival. Furthermore, riluzole does not improve neuropathology in TDP-43 expressed animal models [14, 15].

Herbal medicines, such as the Huolingshengji formula and Jiawei Sijunzi, have been shown to improve neurological and muscle function in patients with ALS [16, 17]. In patients with ALS, herbal medicines, such as the Huolingshengji formula and Jiawei Sijunzi, have been shown to improve neurological and muscle functions [16, 17]. Chang et al. showed that berberine could be a potential therapy as an activator of mTOR-autophagy signals TDP-43-related neuropathology [18]. Bojungikgi-tang (BJIGT) is a traditional herbal medicine in traditional Chinese medicine (TCM), is known as Bu Zhong Yi Qi Tang (BZYQT) in Chinese and Hochuekkito in Japanese, and comprises eight herbs. Several studies have demonstrated the effects on tumor suppression [19], chronic fatigue syndrome [20], and immune function [21]. Furthermore, we have shown that BJIGT treatment improved motor activity with anti-inflammatory and antioxidative effects in the spinal cord and gastrocnemius muscle of the hSOD1^{G93A} animal model [22]. We have investigated the effects of combined treatment with BJIGT and riluzole in TDP-43 stress granular cells to examine the synergistic effect of combined treatment. The combined treatment reduced oxidative stress-induced cell death and regulated autophagy dysfunction compared with sodium arsenite (SA) only-treated TDP-43 cells. From those findings, we suggest that combined treatment could be helpful for aggregate clearance in other neurodegenerative diseases.

2. Methods

2.1. Cell Subculture and Drug Preparation. TDP-43 stress granules cells were purchased from Innovative Technologies in Biological Systems (Innoprot, Spain). The TDP-43 stress granules cells were maintained in Dulbecco's MEM/Nut MIX F-12 medium (Sigma Aldrich, USA) supplemented with 10% fetal bovine serum (Thermo Fischer Scientific, CA, USA) and 5 μg/mL puromycin (Thermo Fischer Scientific, CA, USA) and 80 μg/mL hygromycin (Thermo Fischer Scientific, CA, USA). Cells were grown at 37°C and 5% CO_2 incubator and subcultured every 3 days. For the induction of fluorescent TDP-43 expression, 50% confluence cells were added 5 mM isopropyl β-d-1-thiogalactopyranoside (IPTG) in a complete medium. For the study, BJIGT and riluzole were purchased from Hankookshinyak (Chungnam, Korea) and Millipore (Billerica, MA, USA). BJIGT was dissolved with distilled PBS (dPBS) and filtered with 0.45 μm syringe filter. Riluzole was dissolved in dimethyl sulfoxide (Sigma Aldrich, USA).

2.2. Cell Viability (CCK-8 Assay). Cell viability was observed using the Cell Counting Kit-8 (CCK-8) (Sigma Aldrich, USA). TDP-43 stress granules cells were subcultured in a 96-well plate, pretreated with 100 μg/mL BJIGT or 50 μM riluzole or combined BJIGT (100 μg/mL) and riluzole (50 μM), and then exposed to 150 μM sodium arsenite (SA) for 18 h or sterilized water as a solvent control. Treated cells were added 10 μL of CCK-8 solution. The assay was repeated three times. The optical density value was measured at absorbance 450 nm by a microplate reader (SpectraMAX 340, molecular devices, USA) for cell viability.

2.3. Western Blot. After incubation with 150 μM SA for 18 h, the cells were rinsed twice with PBS. We used radioimmunoprecipitation assay (RIPA) buffer (50 mM Tris-HCl, pH 8.0, 150 mM NaCl, 1% NP-40, 0.5% sodium deoxycholate, and 0.1% sodium dodecyl sulfate (SDS)), which included phosphatase and protease inhibitors (GenDEPOT, Barker, TX, USA), to lyse the cells; this sample was called "RIPA-soluble." The lysed cells were centrifuged at 4°C at 12,000 rpm for 20 min. We evaluated the supernatants with the bicinchoninic acid (BCA) protein assay (Thermo Fischer Scientific, CA, USA) to determine the protein concentration of the lysates. The RIPA-insoluble pellets were lysed with 10% SDS buffer, sonicated, and supplemented with SDS-polyacrylamide gel electrophoresis (PAGE). The soluble and insoluble proteins were separated on 4–12% SD-PAGE gels and transferred to PVDF membranes. PVDF blocked with 5% skim milk for elimination of nonspecific binding and then incubated with the following primary antibodies: heme oxygenase (HO) 1, ATG7, and tubulin (Abcam, Cambridge, MA, USA); B cell lymphoma-2-associated X protein (Bax) and green fluorescent protein (GFP) (Santa Cruz Biotechnology, Santa Cruz, CA, USA); microtubule-associated protein 1A/1B light chain (LC) 3b and P62 (Cell Signaling Technology, Danvers, MA, USA); and ubiquitin (Vector Laboratories, Burlingame, CA, USA) at 4°C overnight. After rinsing with 0.1% Tween in Tris-buffered saline, the PVDF was incubated with anti-rabbit of anti-mouse IgG antibodies (Santa Cruz Biotechnology). For chemiluminescent detection, the membrane was incubated with SuperSignal West Femto Substrate Maximum Sensitivity Substrate (Thermo Fisher Scientific, CA, USA). Immunoblots were detected using a ChemiDoc Imaging System (BioRad), and quantification was performed using ImageJ software (National Institutes of Health, Bethesda, MD, USA).

2.4. Determination of Reactive Oxygen Species Generation. Quantification of SA-induced reactive oxygen species (ROS) was measured in TDP-43 stress granular cells using 2,7-diacetyl dichlorofluorescein diacetate (DCFH-DA). DCFH-DA penetrates the intracellular matrix of cells and oxidizes DCFH-DA, depending on ROS, and then forms fluorescent DCF. TDP-43 stress granular cells (4×10^3/mL) were treated with DCFH-DA (5 μM) and incubated at 37°C for 10 min. Stained cells were rinsed with dPBS and added trypsin to remove excess DCFH-DA. Fluorescent intensity was performed with excitation, and emission filters were set at 490 nm and 535 nm, respectively, using SpectraMax i3 (Molecular devices, San Jose, USA).

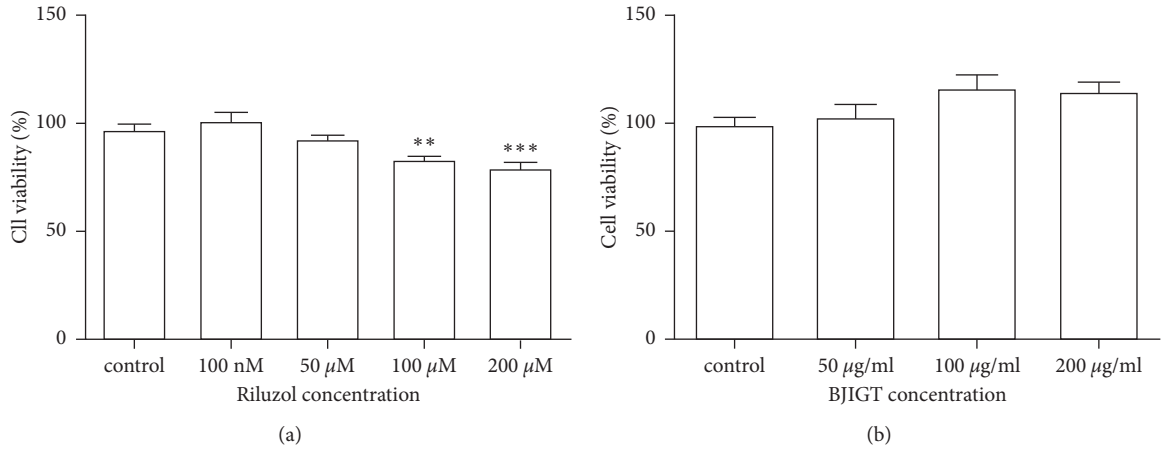

Figure 1: Cell viability under differing BJIGT and riluzole concentrations. TDP-43 stress granular cells incubated with riluzole (a) and BJIGT (b) at indicated concentrations for 24 h. Barplots are represented as a percentage of the control value. BJIGT, Bojungikgi-tang.

2.5. Immunofluorescence and Aggregation Analysis. TDP-43 stress granular cells were treated with 70% ice-cold ethanol on ice for fixation. Permeabilized cells with PBST (PBS, 0.5% Triton X-100) were blocked with 5% bovine serum albumin. After blocking, TDP-43 stress granular cells were incubated with anti-GFP, at 4°C overnight. TDP-43 stress granular cells were treated with Alexa Fluor 488-conjugated goat anti-mouse immunoglobulin G secondary antibody (1 : 500; Invitrogen). The cell images were observed on an Eclipse Ti-U (Nikon, Tokyo, Japan) fluorescence microscope. For quantification of aggregates in cells, three representative microscopy fields per sample were analyzed. The aggregated cells by SA treatment were calculated by the number of GFP-positive aggregated cells/total number of cells.

2.6. Statistical Analyses. Statistical analysis was analyzed using GraphPad Prism 9.0 (GraphPad Software, San Diego, CA, USA), and barplot presented with the mean ± standard error of the mean (SEM) were indicated. Statistical significance of Western blotting, CCK8 assay, and ROS assay were analyzed using one-way analysis of variance followed by the Newman–Keuls test.

3. Results

3.1. Combined Herbal Medicine and a Drug Prevented SA-Induced Cell Death of TDP-43 Stress Granular Cells. We examined cell viability as a function of the concentration of riluzole and BJIGT in TDP-43 stress granular cells to determine cell toxicity. We observed a 14% reduction of cell viability with 100 μM riluzole comparing with the control group ($p < 0.01$ and $p < 0.001$, Figures 1(a) and 1(b)). BJIGT did not reduce cell viability for doses up to 200 μg/mL for 24 h in TDP-43 stress granular cells (Figures 1(a) and 1(b)). To investigate the combined treatment effect on SA-induced cell death, we preincubated cells with BJIGT (100 μg/mL), riluzole (50 μM), and combined BJIGT (100 μg/mL) and riluzole (50 μM) for 6 h before treatment with SA (150 μM) over 18 h. BJIGT and riluzole treatment increased cell viability by 1.7- and 1.8-fold, respectively, compared with SA-treated TDP-43 stress granular cells. The combined treatment inhibited SA-induced cell death by 2.1-fold compared with the SA-treated group ($p < 0.05$ and $p < 0.01$, Figure 2). Our results suggest that combined treatment could have synergistic effects in the regulation of ALS pathology.

3.2. Combined Treatment Regulates Oxidative Stress-Induced Mechanism in TDP-43 Stress Granular Cells. To find the molecular mechanism of the combined treatment, we investigated the effects of oxidative stress-related proteins in SA-treated TDP-43 stress granular cells. As shown in Figures 3(a) and 3(b), we observed the reduction in HO1 and Bax protein levels by 2- and 3.2-folds, respectively, in BJIGT pretreatment in SA-treated TDP-43 expressing cells ($p < 0.05$). In addition, riluzole pretreatment reduced the expression of HO1 and Bax proteins by 3.1- and 8.7-folds, respectively, compared with SA-treated TDP-43 stress granular cells. Furthermore, the combined treatment significantly decreased the levels of HO1 and Bax proteins by 6- and 10.9-folds, respectively, compared with SA-treated cells ($p < 0.05$). To confirm the antioxidation effect of the combined treatment, we performed a DCFDA assay in SA-treated TDP-43 cells in the presence or absence of BJIGT and riluzole. The level of ROS generation using DCF fluorescence intensity increased by 1.2-fold in SA-treated cells compared with the generation in control ($p < 0.05$ and $p < 0.01$, Figures 3(c) and 3(d)). Interestingly, BJIGT and riluzole treatment reduced ROS production by 1.2- and 1.1-folds, respectively, compared with the SA-treated group. The combined treatment reduced 1.3-fold fluorescence intensity induced by SA treatment in TDP-43 stress granular cells ($p < 0.01$, Figures 3(c) and 3(d)).

3.3. Combined Treatment Regulated SA-Induced Autophagy Dysfunction in TDP-43 Stress Granular Cells. Ubiquitinated or hyperphosphorylated TDP-43 is detected in the nucleus due to oxidative stress or inflammation. It interacts with autophagy and UPS-related ubiquitin [9, 23].

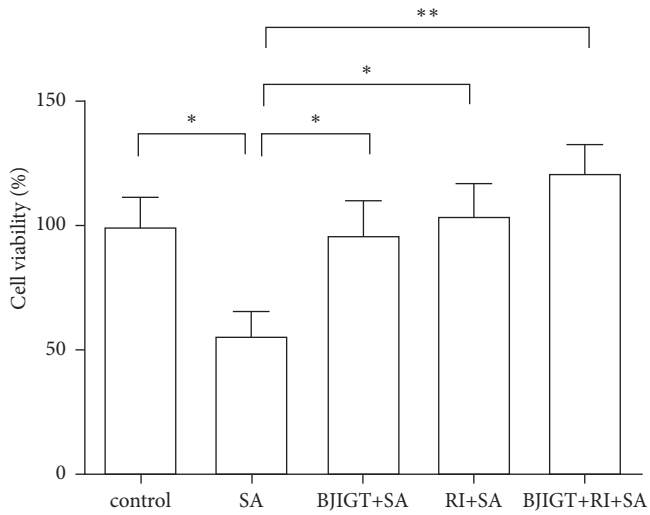

Figure 2: SA-induced cell death from BJIGT combined with riluzole in TDP-43-expressed stress granular cells. TDP-43 stress granular cells were pretreated with BJIGT (100 μg/mL), riluzole (50 μM), and combined BJIGT (100 μg/mL)/riluzole (50 μM) for 6 h before treatment of SA (150 μM) for 18 h. Combined treatment prevented SA-induced cell death in TDP-43 stress granular cells. SA, sodium arsenite; BJIGT, Bojungikgi-tang; RI, riluzole.

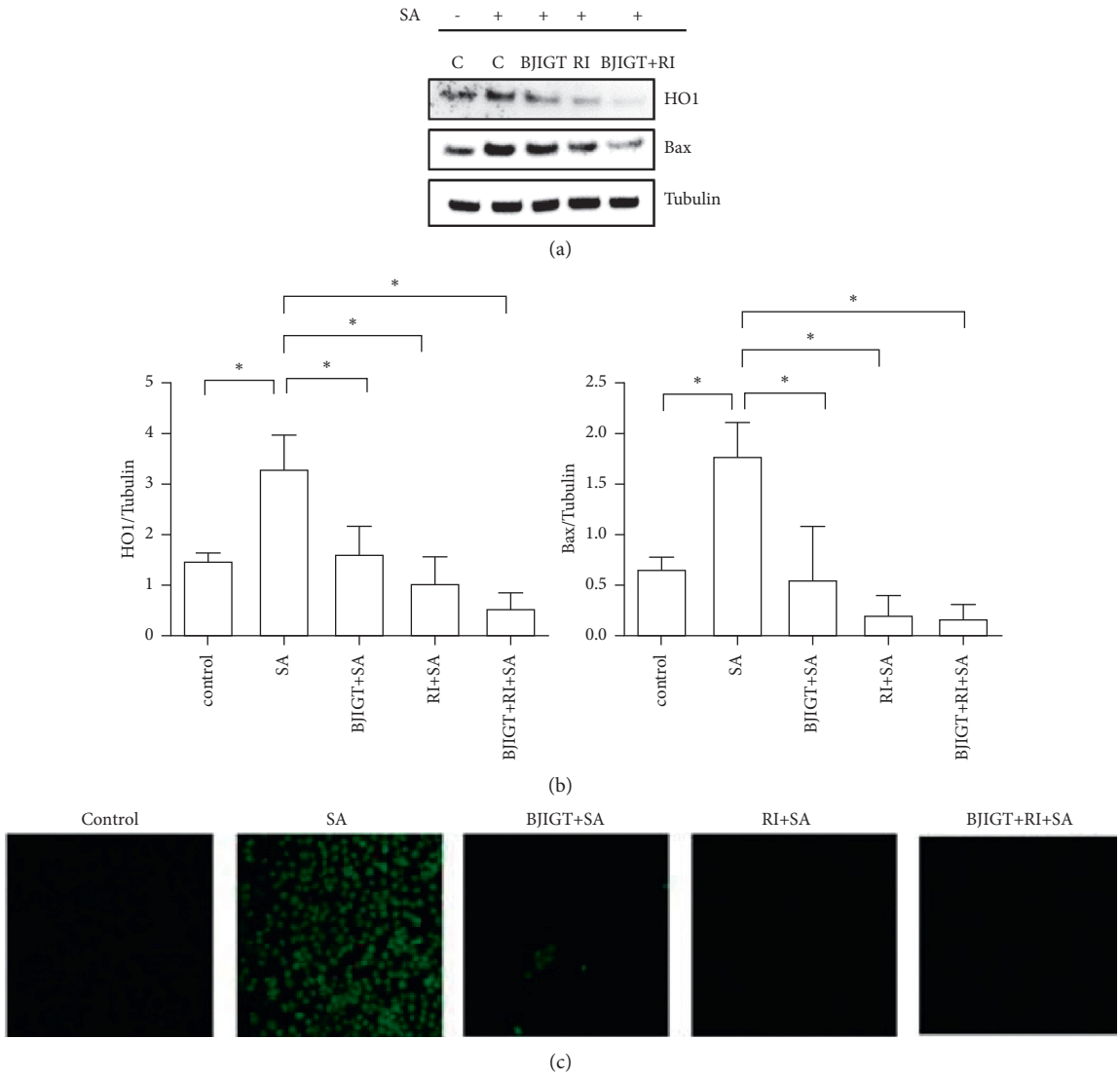

Figure 3: Continued.

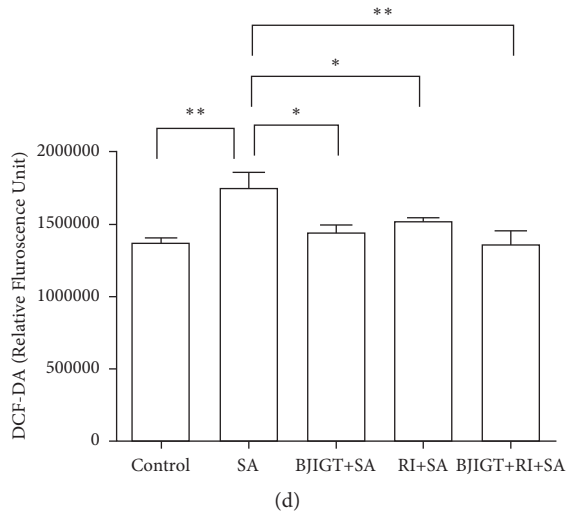

Figure 3: Oxidative stress effects of BJIGT combined with riluzole in TDP-43-expressed stress granular cells. TDP-43 stress granular cells were pretreated with BJIGT (100 μg/mL), riluzole (50 μM), and combined BJIGT (100 μg/mL)/riluzole (50 μM) for 6 h before treatment of SA (150 μM) for 18 h. (a) Representative data of HO1 and Bax expression in TDP-43 stress granular cells. SA-induced oxidative stress-related proteins (HO1 and Bax) were reduced by BJIGT/riluzole in TDP-43-expressed stress granular cells. Tubulin was used as loading control. (b) Quantification of immunoblots. Bars represent the means ± SEMs of more than three independent experiments. $^{*}P < 0.05$ vs. the SA-treated control group. (c) TDP-43 stress granular cells were treated with SA (150 μM) for 18 h in the absence or presence of BJIGT (100 μg/mL), riluzole (50 μM), and combined BJIGT (100 μg/mL)/riluzole (50 μM), and then incubated with 5 μM DCFH-DA. Cells were captured with a fluorescent microscope (40× magnification). (d) Relative fluorescence was quantified with a microplate reader. Bars represent the means ± SEMs of more than three independent experiments. $^{*}P < 0.05$ and $^{**}p < 0.01$ vs. the SA-treated group. C, control; SA, sodium arsenite; BJIGT, Bojungikgi-tang; RI, riluzole.

To investigate the effect of combined treatment on TDP-43 aggregation, we performed immunofluorescence and immunoblotting in TDP-43 stress granular cells. As shown in Figure 4, we found TDP-43 aggregates in SA-treated TDP-43-expressed cells. The combined treatment significantly reduced the aggregates by 2.9-fold in SA-treated TDP-43 expressed cells ($p < 0.001$, Figures 4(a) and 4(b)). Furthermore, we found that combined treatment reduced ubiquitinated high molecular proteins in SA-treated TDP-43 expressing cells compared with SA-treated TDP-43 expressing cells ($p < 0.001$, Figure 4(c)). These findings suggest that combined treatment can regulate SA-induced autophagy dysfunction in TDP-43-expressed cells.

To demonstrate the combined treatment effect on autophagy function, we investigated the levels of autophagy-related proteins, including P62, LC3b, and ATG7, in TDP-43-expressing cells. SA treatment significantly increased the expression levels of P62, LC3b, and ATG7 by 2.2-, 2.7-, and 2.3-folds, respectively, compared with the control in TDP-43 stress granular cells ($p < 0.05$, Figures 5(a) and 5(b)). However, combined treatment reduced P62, LC3b, and ATG7 protein levels by 2.8-, 3.4-, and 2.4-folds, respectively, compared with SA-treated TDP-43 stress granular cells ($p < 0.05$, Figures 5(a) and 5(b)).

4. Discussion

TDP-43 is important for regulating RNA biogenesis, such as splicing, translation, and stability [7]. However, TDP-43 overexpression and displacement to the cytoplasm are related to neurodegeneration, including motor nerve degeneration, as observed in ALS. Furthermore, TDP-43 proteinopathy induces neurodegenerative pathomechanisms, such as autophagy dysfunction [10], neuroinflammation [4], and mitochondrial dysfunction [5]. Several researchers have tried unsuccessfully to find an effective treatment or therapy for TDP-43-induced ALS. Although riluzole has been treated for patients with ALS, it is limited by improving survival for only 2-3 months [24], an unclear mechanism of action and adverse effects, such as nausea, asthenia, and gastrointestinal problems [25].

TCM has been used for disease treatment for centuries in China, Japan, and South Korea. BJIGT is a traditional herbal formula of TCM that has been known as BZYQT in Chinese and Hochuekkito in Japanese and comprises eight herbs. Several studies have demonstrated the effects on tumors [19], chronic fatigue syndrome [20], and immune function [21]. In our previous study, we demonstrated the anti-inflammatory and antioxidative effects of BJIGT in the muscle of the spinal cord of $hSOD1^{G93A}$ mice [22]. In addition, Yu et al. showed that cotreatment with BZYQT and cisplatin enhanced apoptosis and autophagy, leading to increased intracellular ROS levels in human lung carcinoma A549/DDP cells (cisplatin-resistant cells) [26]. They suggested that BZYQT could be a potential chemotherapy sensitizer to reverse cisplatin resistance.

Oxidative stress is induced by excessive production of ROS by disruption of the antioxidant systems, leading to protein misfolding and causing inflammation and mitochondrial dysfunction [8]. In ALS, oxidative stress is a

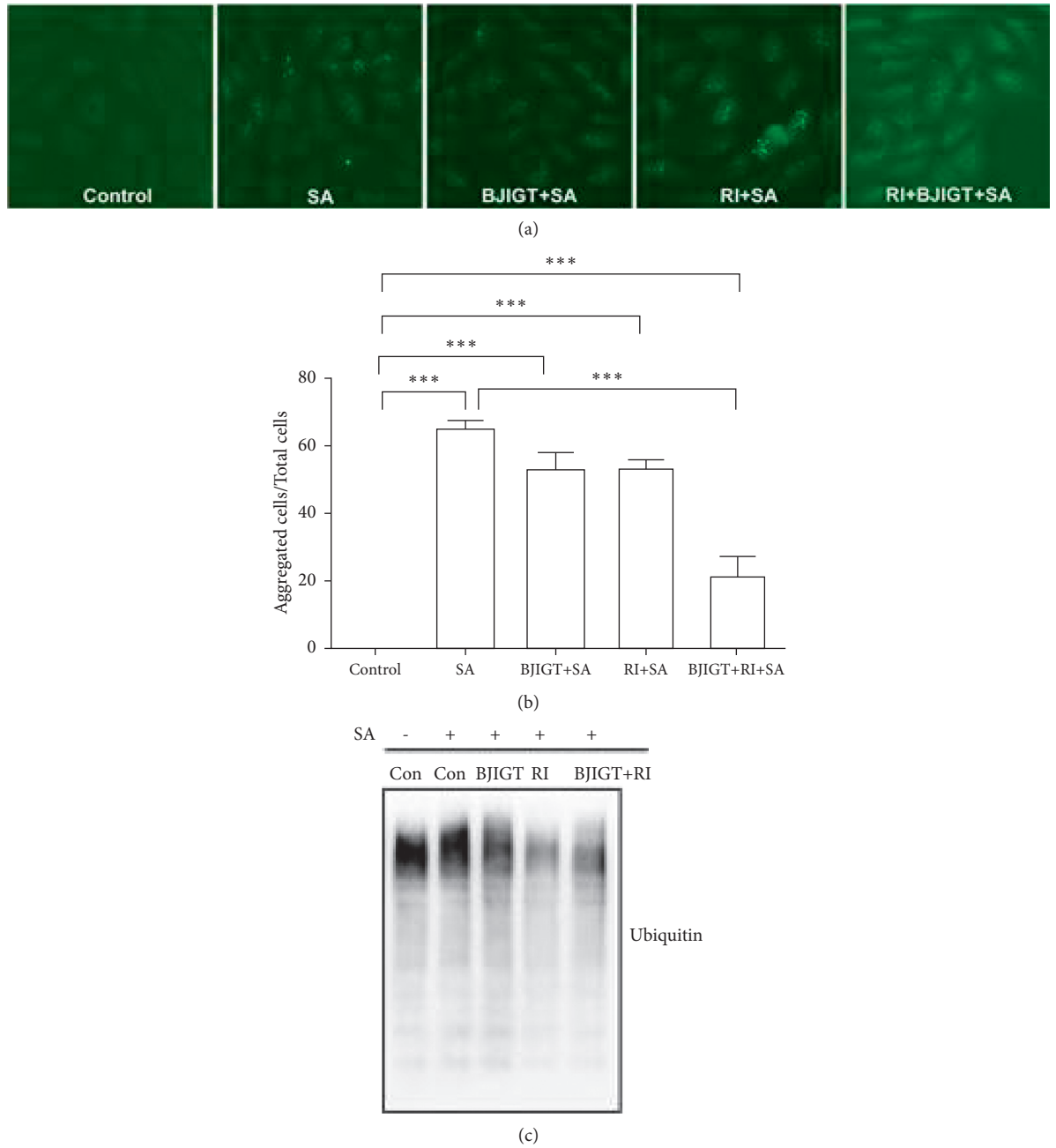

Figure 4: Aggregation effects of BJIGT combined with riluzole in TDP-43-expressed stress granular cells. TDP-43 stress granular cells were pretreated with BJIGT (100 μg/mL), riluzole (50 μM), and combined BJIGT (100 μg/mL) and riluzole (50 μM) for 6 h before treatment with SA (150 μM) for 18 h. (a) The cells treated with anti-GFP immunofluorescence, the primary antibody, and captured with a fluorescent microscope (200× magnification). (b) Quantification of inclusions. Three representative microscopy fields per sample were analyzed. The aggregated cells by SA treatment were calculated by the number of GFP-positive aggregated cells/total number of cells. (c) Cell lysates identified with immunoblots using antiubiquitin. Con, control; SA, sodium arsenite; BJIGT, Bojungikgi-tang; RI, riluzole.

critical factor driving disease progression and disease pathogenesis [27]. TDP-43 is expressed as stress granules under cellular oxidative stress [28]. Liu et al. demonstrated that antioxidant oxidation resistance 1 extended survival and disease progression in an SOD1-mediated ALS animal model [29]. Edaravone was shown to remove lipid peroxide and hydroxyl radicals for neuronal protection and nitrosative stress in ALS [30]. However, acetylcysteine and creatine, as antioxidants, did not affect ALS symptom recovery [31]. This finding implies that oxidative stress is related to other pathological mechanisms, such as mitochondrial dysfunction, protein aggregation, and cytoskeletal dysfunction in ALS. Therefore, multiple target treatments are needed to improve complex diseases, such as ALS.

In this study, we investigated the effects of combined treatment with BJIGT and riluzole on SA-induced oxidative stress in TDP-43 stress granular cells. We found that combined treatment significantly reduced the

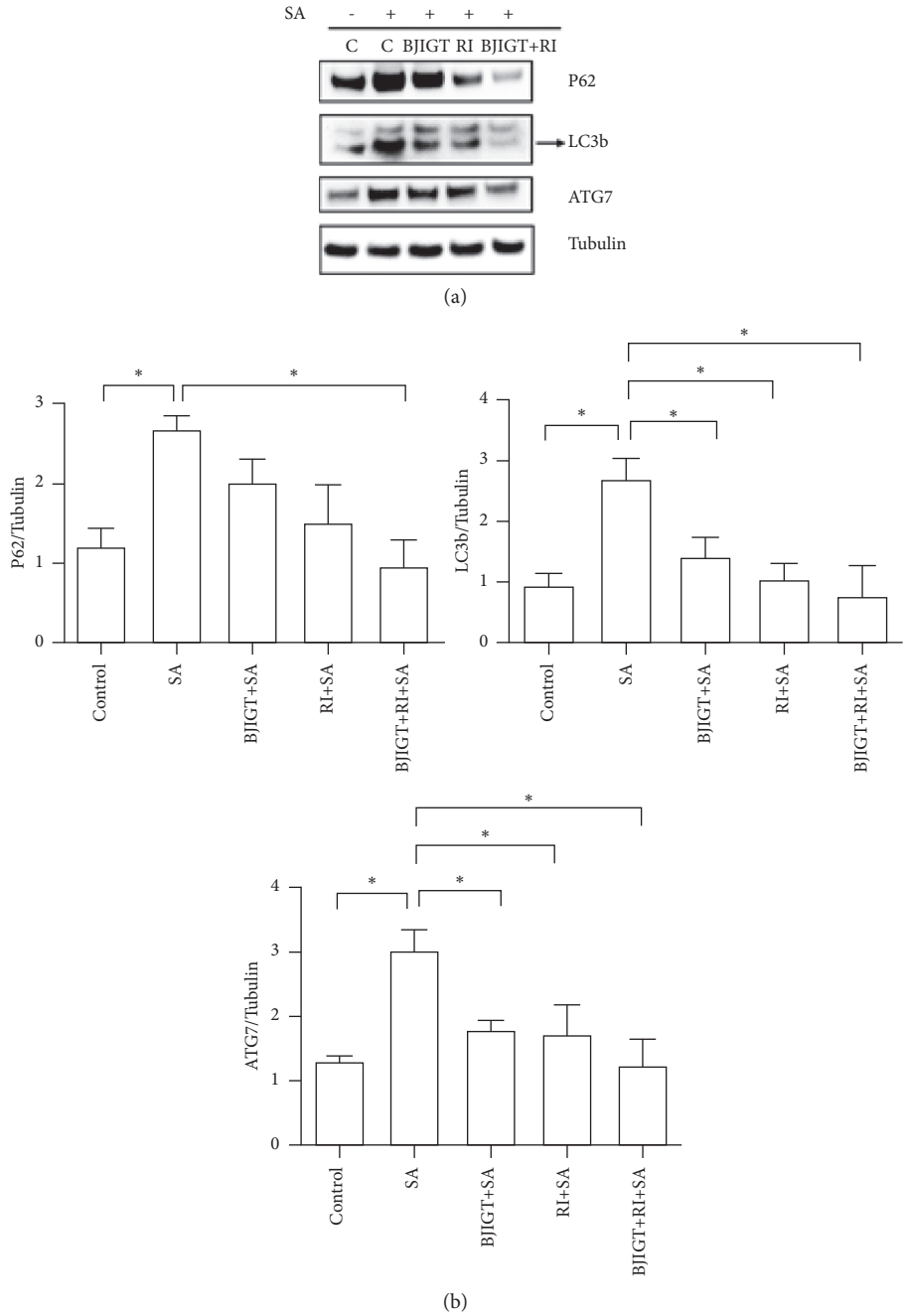

Figure 5: Autophagy function effects of BJIGT combined with riluzole in TDP-43-expressed stress granular cells. Cell lysates were used to detect P62, LC3b, and ATG7 expression by Western blots. Combined treatment reduced SA-induced autophagy dysfunction in TDP-43 stress granular cells. (a) Representative data of autophagy-related protein expressions (P62, LC3b, and ATG7) in TDP-43 stress granular cells. Tubulin was used as loading control. (b) Quantification of immunoblots. Bars show the means ± SEMs of more than three independent experiments. $^{*}P < 0.05$ vs. the SA-treated control group.

expression levels of oxidative stress-induced HO1 and Bax proteins, as well as ROS generation. These findings suggest that cotreatment with BJIGT and riluzole could help the regulation of mitochondrial dysfunction in ALS. Zuo et al. demonstrated that TDP-43 aggregation induced by oxidative stress leads to mitochondrial imbalance [32]. SOD1-, TDP-43-, FUS-, and C9orf72-associated ALS causes toxicity by ubiquitin inclusions and is a common pathological feature of familial ALS or sporadic ALS [33, 34].

TDP-43 is expressed in the nucleus but represents cytosolic mislocalisation in a ubiquitinated or hyperphosphorylated form by oxidative stress or inflammation and interacts with autophagy and UPS-related ubiquitin [9, 23, 35]. Usually, autophagy and the UPS are important cellular mechanisms to clear protein aggregation. However,

these functions are disrupted by oxidative stress in AD, PD, and ALS [36]. ALS genes are related to autophagic systems, such as p62, optineurin, VCP, ubiquilin 2, and TANK-binding kinase 1 (TBK1) [37]. Tanji et al. demonstrated that the interaction between TDP-43 and p62 was disrupted in the cerebral cortex of patients with FTLD-TDP [38].

As autophagy dysfunction is a critical pathological feature in ALS, AD, PD, and HD, Cipolat Mis et al. have investigated autophagy-regulating molecules in ALS models [39]. The autophagy inducer rapamycin is mTOR-dependently reduced protein aggregation, although it is only effective at the early stage of $SOD1^{G93A}$ mice [40]. However, mTOR inhibition by rapamycin worsens the disease, although phosphatidic acid (an mTOR agonist) improved movement and developmental viability in a TDP-43-depleted *Drosophila* model [41]. Trehalose reduced SOD1 aggregation to prevent neuronal loss in $SOD1^{G93A}$ mice [42] and induced TDP-43 clearance by autophagic activation in TDP-43 expressing SH-SY5Y cells [43]. These autophagic inductors, including rapamycin and trehalose, showed positive or negative effects in a non-clinical ALS model. Thus, further studies are needed in various experimental models before clinical translation. Our study found that combined treatment reduced insoluble ubiquitinated proteins, and TDP-43 aggregates via modulation of autophagy dysfunction under oxidative stress. These findings suggest that combined treatment could induce TDP-43 clearance via the autophagic degradation pathway. However, it is necessary to investigate autophagy regulation by combined treatment in other ALS-related animal models, such as $hSOD1^{G93A}$ and FUS. Further studies will be performed to determine whether combined treatment activates mTOR-dependent or independent pathways in TDP-43-expressing cells. Furthermore, the interaction between BJIGT and riluzole should be investigated for translation into clinical studies.

5. Conclusion

In conclusion, this is the first study demonstrating that pretreatment with BJIGT and riluzole alleviates SA-induced oxidative stress and regulates autophagy in TDP-43 stress granule cells.

Data Availability

The datasets that support the findings of this study are included within this article.

Conflicts of Interest

The author declares that there are no conflicts of interest.

Authors' Contributions

E. J. Y. conceptualized the study, performed formal analysis, investigated the study, prepared the original draft, and reviewed and edited the article. The author read and confirmed to the published version of the manuscript.

Acknowledgments

This work was supported by the Basic Science Research Program through the National Research Foundation of Korea funded by the Ministry of Science, ICT and Future Planning, South Korea, under grant NRF-2020R1A2C2006703.

References

[1] P. Pasinelli and R. H. Brown, "Molecular biology of amyotrophic lateral sclerosis: insights from genetics," *Nature Reviews Neuroscience*, vol. 7, no. 9, pp. 710–723, 2003.

[2] M. Cassato, *The Cause of Amyotrophic Lateral Sclerosis*, Taylor & Francis, New York, NY, USA, 2009.

[3] W. A. Pedersen, W. Fu, and J. N. Keller, "Protein modification by the lipid peroxidation product 4-hydroxynonenal in the spinal cords of amyotrophic lateral sclerosis patients," *Annals of Neurology*, vol. 44, no. 5, pp. 819–824, 2003.

[4] J. S. Henkel, D. R. Beers, L. Siklos, and S. H. Appel, "The chemokine MCP-1 and the dendritic and myeloid cells it attracts are increased in the mSOD1 mouse model of ALS," *Molecular and Cellular Neuroscience*, vol. 31, no. 3, pp. 427–437, 2003.

[5] M. F. Beal, R. J. Ferrante, S. E. Browne, R. T. Matthews, N. W. Kowall, and R. H. Brown Jr., "Increased 3-nitrotyrosine in both sporadic and familial amyotrophic lateral sclerosis," *Annals of Neurology*, vol. 42, no. 4, pp. 644–654, 2004.

[6] S. C. Barber and P. J. Shaw, "Oxidative stress in ALS: key role in motor neuron injury and therapeutic target," *Free Radical Biology and Medicine*, vol. 48, no. 5, pp. 629–641, 2005.

[7] E. L. Scotter, H. J. Chen, and C. E. Shaw, "TDP-43 proteinopathy and ALS: insights into disease mechanisms and therapeutic targets," *Neurotherapeutics*, vol. 12, no. 2, pp. 352–363, 2007.

[8] P. M. Abdul-Muneer, N. Chandra, and J. Haorah, "Interactions of oxidative stress and neurovascular inflammation in the pathogenesis of traumatic brain injury," *Molecular Neurobiology*, vol. 51, no. 3, pp. 966–979, 2009.

[9] F. Geser, M. Martinez-Lage, L. K. Kwong, V. M. Lee, and J. Q. Trojanowski, "Amyotrophic lateral sclerosis, frontotemporal dementia and beyond: the TDP-43 diseases," *Journal of Neurology*, vol. 256, no. 8, pp. 1205–1214, 2010.

[10] J. K. Bose, C. C. Huang, and C. K. Shen, "Regulation of autophagy by neuropathological protein TDP-43," *Journal of Biological Chemistry*, vol. 286, no. 52, pp. 44441–44448, 2003.

[11] Y. F. Xu, T. F. Gendron, and Y. J. Zhang, "Wild-type human TDP-43 expression causes TDP-43 phosphorylation, mitochondrial aggregation, motor deficits, and early mortality in transgenic mice," *Journal of Neuroscience*, vol. 30, no. 32, pp. 10851–10859, 2003.

[12] I. Wegorzewska, S. Bell, N. J. Cairns, T. M. Miller, and R. H. Baloh, "TDP-43 mutant transgenic mice develop features of ALS and frontotemporal lobar degeneration," *Proceedings of the National Academy of Sciences of the United States of America*, vol. 106, no. 44, pp. 18809–18814, 2003.

[13] L. Vanden Broeck, P. Callaerts, and B. Dermaut, "TDP-43-mediated neurodegeneration: towards a loss-of-function hypothesis?" *Trends in Molecular Medicine*, vol. 20, no. 2, pp. 66–71, 2020.

[14] M. C. Hogg, L. Halang, I. Woods, K. S. Coughlan, and J. H. M. Prehn, "Riluzole does not improve lifespan or motor function in three ALS mouse models," *Amyotroph Lateral Scler Frontotemporal Degener*, vol. 19, no. 5-6, pp. 438–445, 2003.

[15] Y. Chen, H. Wang, Z. Ying, and Q. Gao, "Ibudilast enhances the clearance of SOD1 and TDP-43 aggregates through TFEB-mediated autophagy and lysosomal biogenesis: the new molecular mechanism of ibudilast and its implication for neuroprotective therapy," *Biochemical and Biophysical Research Communications*, vol. 526, no. 1, pp. 231–238, 2011.

[16] H. Qiu, J. H. Li, S. B. Yin, J. Q. Ke, C. L. Qiu, and G. Q. Zheng, "Dihuang yinzi, a classical Chinese herbal prescription, for amyotrophic lateral sclerosis: a 12-year follow-up case report," *Medicine (Baltimore)*, vol. 95, no. 14, Article ID e3324, 2018.

[17] W. Pan, X. Su, J. Bao, and J. Wang, "Open randomized clinical trial on JWSJZ decoction for the treatment of ALS patients," *Evidence-based Complementary and Alternative Medicine*, vol. 2013, Article ID 347525, 3 pages, 2013.

[18] C. F. Chang, Y. C. Lee, K. H. Lee, C. H. Lin, C. L. Chen, and C. C. Huang, "Therapeutic effect of berberine on TDP-43-related pathogenesis in FTLD and ALS," *Journal of Biomedical Science*, vol. 23, no. 1, p. 72, 2013.

[19] M. Utsuyama, H. Seidlar, M. Kitagawa, and K. Hirokawa, "Immunological restoration and anti-tumor effect by Japanese herbal medicine in aged mice," *Mechanism of Ageing and Development*, vol. 122, no. 3, pp. 341–352, 2013.

[20] M. Ouyang, Y. Liu, and W. Tan, "Bu-zhong-yi-qi pill alleviate the chemotherapy-related fatigue in 4 T1 murine breast cancer model," *BMC Complementary and Alternative Medicine*, vol. 14, p. 497, 2019.

[21] Y. Yamaoka, T. Kawakita, and K. Nomoto, "Protective effect of a traditional Japanese medicine, Bu-zhong-yi-qi-tang (Japanese name: hochu-ekki-to), on the restraint stress-induced susceptibility against Listeria monocytogenes," *Immunopharmacology*, vol. 48, no. 1, pp. 35–42, 2012.

[22] M. Cai, S. H. Lee, and E. J. Yang, "Bojungikgi-tang improves muscle and spinal cord function in an amyotrophic lateral sclerosis model," *Molecular Neurobiology*, vol. 56, no. 4, pp. 2394–2407, 2013.

[23] S. H. Kim, Y. Shi, and K. A. Hanson, "Potentiation of amyotrophic lateral sclerosis (ALS)-associated TDP-43 aggregation by the proteasome-targeting factor, ubiquilin 1," *Journal of Biological Chemistry*, vol. 284, no. 12, pp. 8083–8092, 2013.

[24] V. Kumar, A. Islam, M. I. Hassan, and F. Ahmad, "Therapeutic progress in amyotrophic lateral sclerosis-beginning to learning," *European Journal of Medicinal Chemistry*, vol. 121, pp. 903–917, 2012.

[25] M. K. Jaiswal, "Riluzole and edaravone: a tale of two amyotrophic lateral sclerosis drugs," *Medicinal Research Reviews*, vol. 39, no. 2, pp. 733–748, 2011.

[26] N. Yu, Y. Xiong, and C. Wang, "Bu-Zhong-Yi-Qi decoction, the water extract of Chinese traditional herbal medicine, enhances cisplatin cytotoxicity in A549/DDP cells through induction of apoptosis and autophagy," *BioMed Research International*, vol. 2017, Article ID 3692797, 9 pages, 2017.

[27] E. D'Amico, P. Factor-Litvak, R. M. Santella, and H. Mitsumoto, "Clinical perspective on oxidative stress in sporadic amyotrophic lateral sclerosis," *Free Radical Biology and Medicine*, vol. 65, pp. 509–527, 2011.

[28] C. Colombrita, E. Zennaro, and C. Fallini, "TDP-43 is recruited to stress granules in conditions of oxidative insult," *Journal of Neurochemistry*, vol. 111, no. 4, pp. 1051–1061, 2012.

[29] K. X. Liu, B. Edwards, and S. Lee, "Neuron-specific antioxidant OXR1 extends survival of a mouse model of amyotrophic lateral sclerosis," *Brain*, vol. 138, no. 5, pp. 1167–1181, 2011.

[30] H. Yoshino and A. Kimura, "Investigation of the therapeutic effects of edaravone, a free radical scavenger, on amyotrophic lateral sclerosis (Phase II study)," *Amyotroph Lateral Scler*, vol. 7, no. 4, pp. 241–245, 2011.

[31] E. S. Louwerse, G. J. Weverling, P. M. Bossuyt, F. E. Meyjes, and J. M. de Jong, "Randomized, double-blind, controlled trial of acetylcysteine in amyotrophic lateral sclerosis," *Archives of Neurology*, vol. 52, no. 6, pp. 559–564, 2009.

[32] X. Zuo, J. Zhou, and Y. Li, "TDP-43 aggregation induced by oxidative stress causes global mitochondrial imbalance in ALS," *Nature Structural & Molecular Biology*, vol. 28, no. 2, pp. 132–142, 2009.

[33] M. Neumann, D. M. Sampathu, and L. K. Kwong, "Ubiquitinated TDP-43 in frontotemporal lobar degeneration and amyotrophic lateral sclerosis," *Science*, vol. 314, no. 5796, pp. 130–133, 2008.

[34] D. A. Bosco, G. Morfini, and N. M. Karabacak, "Wild-type and mutant SOD1 share an aberrant conformation and a common pathogenic pathway in ALS," *Nature Neuroscience*, vol. 13, no. 11, pp. 1396–1403, 2007.

[35] C. Rothenberg, D. Srinivasan, and L. Mah, "Ubiquilin functions in autophagy and is degraded by chaperone-mediated autophagy," *Human Molecular Genetics*, vol. 19, no. 16, pp. 3219–3232, 2011.

[36] A. Singh, R. Kukreti, L. Saso, and S. Kukreti, "Oxidative stress: a key modulator in neurodegenerative diseases," *Molecules*, vol. 24, no. 8, 2015.

[37] D. K. H. Nguyen, R. Thombre, and J. Wang, "Autophagy as a common pathway in amyotrophic lateral sclerosis," *Neuroscience Letters*, vol. 697, pp. 34–48, 2014.

[38] K. Tanji, H. X. Zhang, F. Mori, A. Kakita, H. Takahashi, and K. Wakabayashi, "p62/sequestosome 1 binds to TDP-43 in brains with frontotemporal lobar degeneration with TDP-43 inclusions," *Journal of Neuroscience Research*, vol. 90, no. 10, pp. 2034–2042, 2013.

[39] M. S. Cipolat Mis, S. Brajkovic, E. Frattini, A. Di Fonzo, and S. Corti, "Autophagy in motor neuron disease: key pathogenetic mechanisms and therapeutic targets," *Molecular and Cellular Neuroscience*, vol. 72, pp. 84–90, 2011.

[40] X. Zhang, L. Li, and S. Chen, "Rapamycin treatment augments motor neuron degeneration in SOD1(G93A) mouse model of amyotrophic lateral sclerosis," *Autophagy*, vol. 7, no. 4, pp. 412–425, 2013.

[41] Q. Xia, H. Wang, and Z. Hao, "TDP-43 loss of function increases TFEB activity and blocks autophagosome-lysosome fusion," *The EMBO Journal*, vol. 35, no. 2, pp. 121–142, 2008.

[42] X. Zhang, S. Chen, and L. Song, "MTOR-independent, autophagic enhancer trehalose prolongs motor neuron survival and ameliorates the autophagic flux defect in a mouse model of amyotrophic lateral sclerosis," *Autophagy*, vol. 10, no. 4, pp. 588–602, 2010.

[43] Y. Wang, F. T. Liu, and Y. X. Wang, "Autophagic modulation by trehalose reduces accumulation of TDP-43 in a cell model of amyotrophic lateral sclerosis via TFEB activation," *Neurotoxicity Research*, vol. 34, no. 1, pp. 109–120, 2013.

Hindawi
Evidence-Based Complementary and Alternative Medicine
Volume 2021, Article ID 6789835, 21 pages
https://doi.org/10.1155/2021/6789835

Research Article

Mechanism of *Radix Rhei Et Rhizome* Intervention in Cerebral Infarction: A Research Based on Chemoinformatics and Systematic Pharmacology

Wang Xiang,[1] Zhiyong Long,[2] Jinsong Zeng,[3,4] Xiaofei Zhu,[4] Mengxia Yuan,[2] Jiamin Wu,[5] Yonghe Wu,[4] and Liang Liu[4]

[1]*The Affiliated Hospital of Guilin Medical University, Guilin, Guangxi Province, China*
[2]*Shantou University Medical College, Shantou University, Shantou, Guangdong, China*
[3]*The First Affiliated Hospital of Hunan University of Chinese Medicine, Changsha, Hunan Province, China*
[4]*Hunan University of Chinese Medicine, Changsha, Hunan Province, China*
[5]*Shanghai University of Traditional Chinese Medicine, Shanghai, China*

Correspondence should be addressed to Jinsong Zeng; zengjingsong321@outlook.com

Received 31 May 2021; Accepted 13 August 2021; Published 7 September 2021

Academic Editor: Rajeev K Singla

Copyright © 2021 Wang Xiang et al. This is an open access article distributed under the Creative Commons Attribution License, which permits unrestricted use, distribution, and reproduction in any medium, provided the original work is properly cited.

Objective. To explore the therapeutic targets, network modules, and coexpressed genes of *Radix Rhei Et Rhizome* intervention in cerebral infarction (CI), and to predict significant biological processes and pathways through network pharmacology. To explore the differential proteins of *Radix Rhei Et Rhizome* intervention in CI, conduct bioinformatics verification, and initially explain the possible therapeutic mechanism of *Radix Rhei Et Rhizome* intervention in CI through proteomics. *Methods*. The TCM database was used to predict the potential compounds of Radix Rhei Et Rhizome, and the PharmMapper was used to predict its potential targets. GeneCards and OMIM were used to search for CI-related genes. Cytoscape was used to construct a protein-protein interaction (PPI) network and to screen out core genes and detection network modules. Then, DAVID and Metascape were used for enrichment analysis. After that, in-depth analysis of the proteomics data was carried out to further explore the mechanism of *Radix Rhei Et Rhizome* intervention in CI. *Results*. (1) A total of 14 *Radix Rhei Et Rhizome* potential components and 425 potential targets were obtained. The core components include sennoside A, palmidin A, emodin, toralactone, and so on. The potential targets were combined with 297 CI genes to construct a PPI network. The targets shared by *Radix Rhei Et Rhizome* and CI include ALB, AKT1, MMP9, IGF1, CASP3, etc. The biological processes that *Radix Rhei Et Rhizome* may treat CI include platelet degranulation, cell migration, fibrinolysis, platelet activation, hypoxia, angiogenesis, endothelial cell apoptosis, coagulation, and neuronal apoptosis. The signaling pathways include Ras, PI3K-Akt, TNF, FoxO, HIF-1, and Rap1 signaling pathways. (2) Proteomics shows that the top 20 proteins in the differential protein PPI network were Syp, Syn1, Mbp, Gap43, Aif1, Camk2a, Syt1, Calm1, Calb1, Nsf, Nefl, Hspa5, Nefh, Ncam1, Dcx, Unc13a, Mapk1, Syt2, Dnm1, and Cltc. Differential protein enrichment results show that these proteins may be related to synaptic vesicle cycle, vesicle-mediated transport in synapse, presynaptic endocytosis, synaptic vesicle endocytosis, axon guidance, calcium signaling pathway, and so on. *Conclusion*. This study combined network pharmacology and proteomics to explore the main material basis of *Radix Rhei Et Rhizome* for the treatment of CI such as sennoside A, palmidin A, emodin, and toralactone. The mechanism may be related to the regulation of biological processes (such as synaptic vesicle cycle, vesicle-mediated transport in synapse, presynaptic endocytosis, and synaptic vesicle endocytosis) and signaling pathways (such as Ras, PI3K-Akt, TNF, FoxO, HIF-1, Rap1, and axon guidance).

1. Introduction

Cerebral infarction (CI) or ischemic stroke (IS) mainly results from blood supply disturbances in local brain tissue areas, leading to necrosis of ischemic hypoxic lesions in the brain tissue, which results in the manifestation of corresponding neurological deficits [1]. Epidemiological studies have shown that stroke has become the disease with the highest mortality rate in China [2, 3]. CI is divided into cerebral thrombosis, cerebral embolism, and lacunar infarction according to the different pathogenesis. Among them, cerebral thrombosis is the most common type of CI, accounting for about 60% [4]. Timely thrombolysis to restore blood supply after infarction is the most important measure to save the ischemic area. Although reperfusion after ischemia can restore its function, ischemia-reperfusion injury makes the irreversible damage to the brain tissue after the blood flow restored [5–7]. Cerebral ischemia-reperfusion injury (CIR) is mainly related to the formation of free radicals (oxygen and lipid free radicals), oxidative stress, energy metabolism disorders, apoptosis, excitatory amino acid toxicity, calcium overload, inflammation, and so on [6–9]. Currently, the preventive and therapeutic drugs for CIR include excitatory amino acid-regulating drugs, neurotrophic growth factors, free radical scavengers, nitric oxide synthase inhibitors, intracellular calcium overload inhibitors, and natural plant active compounds (flavonoids, saponins, polysaccharides) [8, 10–13]. Of particular importance is that natural plant active compounds are becoming potential CIR drugs.

Radix Rhei Et Rhizome is an important part of the traditional Chinese medicine (TCM) formulas for the treatment of CI in the acute phase, which has a long history of medicinal use [14–18]. Modern medical research proves that rhubarb aglycones have significant protective effects on ischemic brain tissue: it can maintain the integrity of the blood-brain barrier, reduce inflammation, inhibit apoptosis, and protect nerves [15–19]. However, its specific mechanism is still unclear. Therefore, this research hopes to propose a new method to analyze the regulatory mechanism of *Radix Rhei Et Rhizome* on CI biological networks. The development of high-throughput omics and chemoinformatics has given the opportunity to analyze the mechanisms of natural plant components for disease treatment [20–24]. Therefore, based on previous research, this study will integrate proteomics and chemoinformatics strategies to further explore the molecular mechanism of *Radix Rhei Et Rhizome*'s intervention in CI and provide reference information for new drug development and its clinical application. The idea and process of this research are shown in Figure 1.

2. Material and Methods

2.1. Construction of Pharmacodynamic Molecular Database and Radix Rhei Et Rhizome's Compounds Prediction. All compounds of *Radix Rhei Et Rhizome* were obtained from the traditional Chinese medicine database and analysis platforms TCMSP database (http://lsp.nwu.edu.cn/) [25] and TCM@Taiwan (http://tcm.cmu.edu.tw/zh-tw/) [26]. In order to obtain potential active compounds from these compounds, this study used drug-likeness (DL), Caco-2 permeability, and oral bioavailability (OB) indicators [20–24, 27–30] and combined literature [31] to predict potential pharmacological compounds in *Radix Rhei Et Rhizome*. The standard was OB ≥ 30%, DL ≥ 0.18, and Caco-2 permeability > −0.4. After the potential compound prediction, a total of 9 *Radix Rhei Et Rhizome*'s potential compounds were obtained: (-)-catechin, aloe-emodin, beta-sitosterol, daucosterol, eupatin, mutatochrome, palmidin A, rhein, and toralactone. Meanwhile, due to the limitation of the pharmacokinetic parameter model, in order to avoid the omission of potential compounds, a large number of studies related to *Radix Rhei Et Rhizome* were searched to supplement its active compounds. Finally, according to references [32, 33], a total of 5 oral absorbable compounds with bioactivity were supplemented: chrysophanol, danthron, emodin, sennoside A, and physcion. The 3D structure of all screened compounds was saved in mol2 format.

2.2. Potential Targets Prediction and CI Gene Collection. In addition to screening the active components of *Radix Rhei Et Rhizome*, determining the targets of the active ingredients is also an important step to clarify the biological basis of TCM. The PharmMapper server platform (http://lilab-ecust.cn/pharmmapper/) was used to predict potential targets. After importing the "mol2" format file, the number of returned targets was set to 300, and the pharmacophore model was selected as the setting condition [34]. The PDB ID of the protein target was imported into UniProt KB (https://www.uniprot.org/uniprot/), with the species restricted to "Homo sapiens" (for potential targets) (Table S1) or "*Rattus norvegicus*" (for proteomics data) (Table S2), to obtain the official symbol of *Radix Rhei Et Rhizome* potential target.

The keyword "cerebral infarction" was entered into the GeneCards database (http://www.genecards.org/) [35] and the OMIM database (http://www.ncbi.nlm.nih.gov/omim) [36] to search for reported CI-related genes. The genes in the GeneCards database with relevance score >1 were selected. After removing duplicate genes and false positive genes, the CI gene set was obtained (Table S3).

2.3. Network Construction and Analysis Methods. In system pharmacology, the construction and analysis of biological network diagrams are very important for TCM pharmacological analysis. The network formed by nodes and edges (connections between nodes) is a mathematical-based and quantifiable mapping of various regulatory relationships under complex biological systems. String 11.0 (https://string-db.org/) was used to query protein-protein interaction (PPI) relationships [37]. The results were saved in TSV format, and the node1, node2, and Combinedscore information in the file was retained and imported into Cytoscape 3.7.1 software to draw the relevant network [38]. The "NetworkAnalyzer" plugin that comes with Cytoscape software was used to analyze the degree and betweenness of the network. These two parameters are often used to illustrate the importance of nodes, that is, the higher the degree and betweenness, the more important the

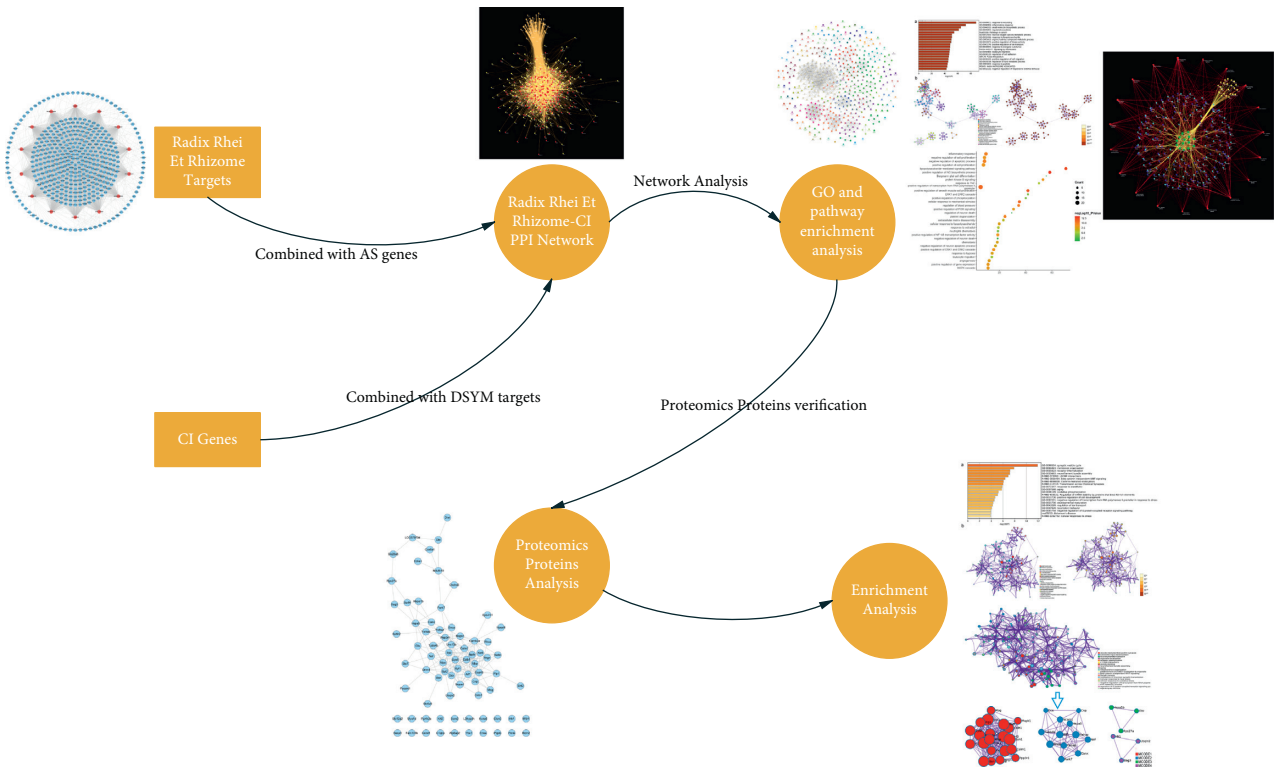

Figure 1: The idea and process of this research.

node in the network. The clusters of networks were detected by MCODE (Cytoscape's plugin). The MCODE algorithm was originally a clustering algorithm designed to detect protein complexes in PPI networks, which can detect tightly connected regions (i.e., molecular complexes) in large-scale protein interaction networks [38]. This method can now also be used to detect clusters in other types of networks.

2.4. Gene Ontology (GO) Enrichment, Pathway Enrichment, and Reactome Enrichment Analysis. DAVID ver. 6.8 (https://david-d.ncifcrf.gov) was used for the GO enrichment analysis of targets and genes in clusters and for the pathway enrichment analysis of targets and genes in PPI networks [39]. The Reactome Pathway Database (https://reactome.org/) was used for reactome pathway enrichment [40].

3. Results and Discussion

3.1. Potential Compound-Potential Target Network of Radix Rhei Et Rhizome. A total of 14 components and 425 targets were used to construct the potential compound-potential target network of *Radix Rhei Et Rhizome*. In this network, nodes near the center have a greater degree than nodes near the periphery (Figure 2).

3.2. Radix Rhei Et Rhizome-CI PPI Network Analysis

3.2.1. Radix Rhei Et Rhizome-CI PPI Network Construction. The *Radix Rhei Et Rhizome*-CI PPI network is composed of 645 nodes (371 potential target nodes, 231 CI gene nodes, and 43 *Radix Rhei Et Rhizome*-CI target nodes) and 14,119 edges. The following are the top 20 nodes in the network: (1) *Radix Rhei Et Rhizome* targets: EGFR (203 edges), SRC (201 edges), MAPK1 (193 edges), and MAPK8 (167 edges). (2) CI genes: INS (292 edges), IL6 (273 edges), VEGFA (244 edges), TNF (241 edges), TP53 (235 edges), EGF (210 edges), CXCL8 (178 edges), IL10 (163 edges), IL1B (160 edges), CCL2 (159 edges), and APP (157 edges). (3) *Radix Rhei Et Rhizome*-CI targets: ALB (302 edges), AKT1 (266 edges), MMP9 (191 edges), IGF1 (182 edges), and CASP3 (170 edges) (Figure 3). The preliminary enrichment results of biological processes and signaling pathways are shown in Figures 4 and 5.

In this study, a total of 14 *Radix Rhei Et Rhizome* compounds and 425 potential targets were predicted for analysis using the network pharmacological method. Although the number of predicted targets for each potential compound is different, the overlap of the target set of some compounds is large. In other words, Radix Rhei Et Rhizome's compounds have common targets probably because these compounds come from the same structural parent. For example, rhein, aloe-emodin, chrysophanol, physcion, and emodin are known as rhubarb aglycones.

In terms of the blood-brain barrier, studies have shown that emodin can maintain the integrity of the blood-brain barrier, reduce inflammation, and inhibit apoptosis [41–45]. In another study, emodin reduced blood-brain barrier permeability and reduced infarct size by inhibiting the expression of connexin 43 (Cx43) and aquaporin 4 (AQP4) in cerebral ischemia/reperfusion model rats [46]. In terms of inhibiting inflammation,

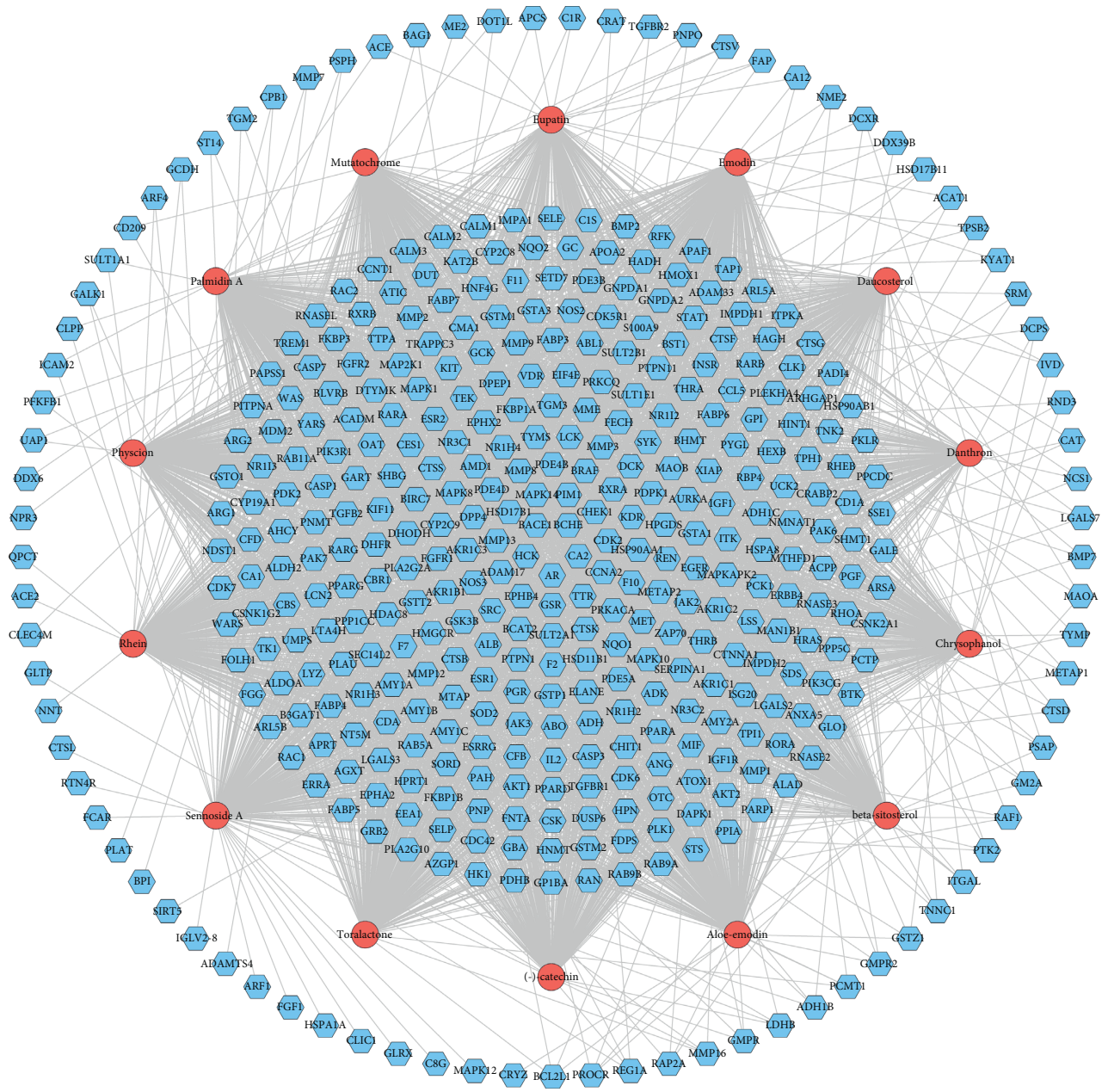

Figure 2: Potential Compound-Potential Target Network of *Radix Rhei Et Rhizome* (Blue hexagons stand for potential targets. Red circles stand for potential compounds.).

emodin can inhibit transforming growth factor (TGF)-β, tumor necrosis factor (TNF)-α, interleukin (IL)-1β, and intercellular adhesion molecule 1 (ICAM-1), so as to protect the brain [42]. Chrysophanol inhibits the inflammatory response by reducing the expression of IL-1β, caspase-1, and NALP3, thereby improving neurological deficits, infarct volume, cerebral edema, and blood-brain barrier permeability in mice with ischemia-reperfusion injury. Chrysophanol can also improve the survival rate, nervous system score, and motor function of mice with middle cerebral artery occlusion by reducing the expression of TNF-α, IL-1β, and NF-κB p65 [47]. In terms of inhibiting apoptosis, emodin can inhibit neuronal apoptosis [43, 44, 48]. Its specific mechanism may be that emodin can increase Bcl-2 and inhibit caspase-3 and Bax expression to reduce glutamate-induced HT22 cell apoptosis [43]. Rhein increases the expression of mature brain-derived neurotrophic factor (BDNF) and phosphorylation of Akt and cAMP response element binding protein (CREB), which improves the behavior and function of CI mice [49]. Rhein also reduced the expression of BAX, caspase-9, caspase-3, and cleaved caspase-3 and increased the expression of Bcl-2, thereby reducing the infarcted area of cerebral ischemia-reperfusion injury mice [50]. In addition, chrysophanol can inhibit NO-related neuronal cell death by attenuating nitrite and nitrate (NOx-) and 3-nitrotyrosine (3-NT) levels and reducing lysed caspase-3 protein expression [51].

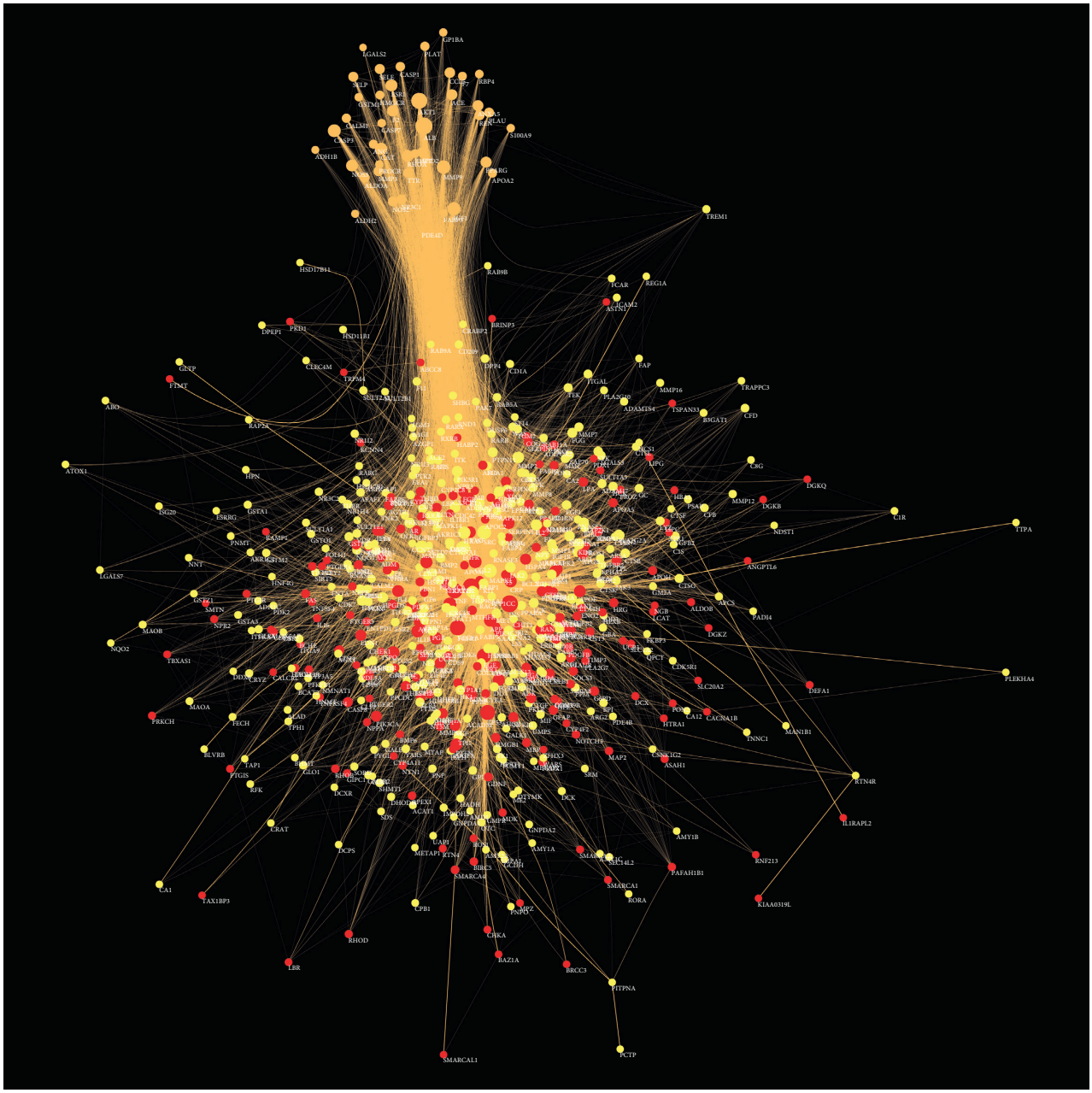

Figure 3: *Radix Rhei Et Rhizome*-CI PPI network (Red, yellow, and orange circles stand for CI genes, *Radix Rhei Et Rhizome* targets, and *Radix Rhei Et Rhizome*-CI targets, respectively. The larger the node size, the higher the degree of the node. The thicker the line, the greater the edge betweenness of the node.).

In terms of oxidative stress, emodin inhibits the apoptosis of primary rat cortical neurons induced by hydrogen peroxide (H_2O_2) [44]. It was also found that emodin can inhibit the apoptosis of neurons after oxyglucose deprivation and reduce the damage of PC12 nerve cells by increasing the expression of activin A [45]. Chrysophanol also increases total superoxide dismutase (SOD) and manganese-dependent SOD (MnSOD) activities in cerebral ischemia-reperfusion injury models and inhibits the production of reactive oxygen species (ROS) [51]. In addition, rhein can reduce malondialdehyde (MDA) and increase the activities of SOD, catalase (CAT), and glutathione peroxidase (GSH-Px) and improve neurological function scores [50]. Chrysophanol can improve endoplasmic reticulum (ER) stress by reducing ER stress-related factors (such as glucose-regulated protein 78 (GRP78), phosphorylated eukaryotic initiation factor 2α (p-eIF2α), CCAAT-enhancer-binding protein homologous protein (CHOP), caspase-12, and NF-κB/κB-α) [52].

In terms of various compound combinations and synergies, rhubarb aglycones (aloe-emodin, rhein, emodin, chrysophanol, and physcion) can improve disorders of amino acid, energy, and lipid metabolism caused by cerebral ischemia-reperfusion injury [15]. Further research shows that rhubarb aglycones can reduce IgG content and increase type IV collagen (CoLIV) and laminin (LN) levels, thereby

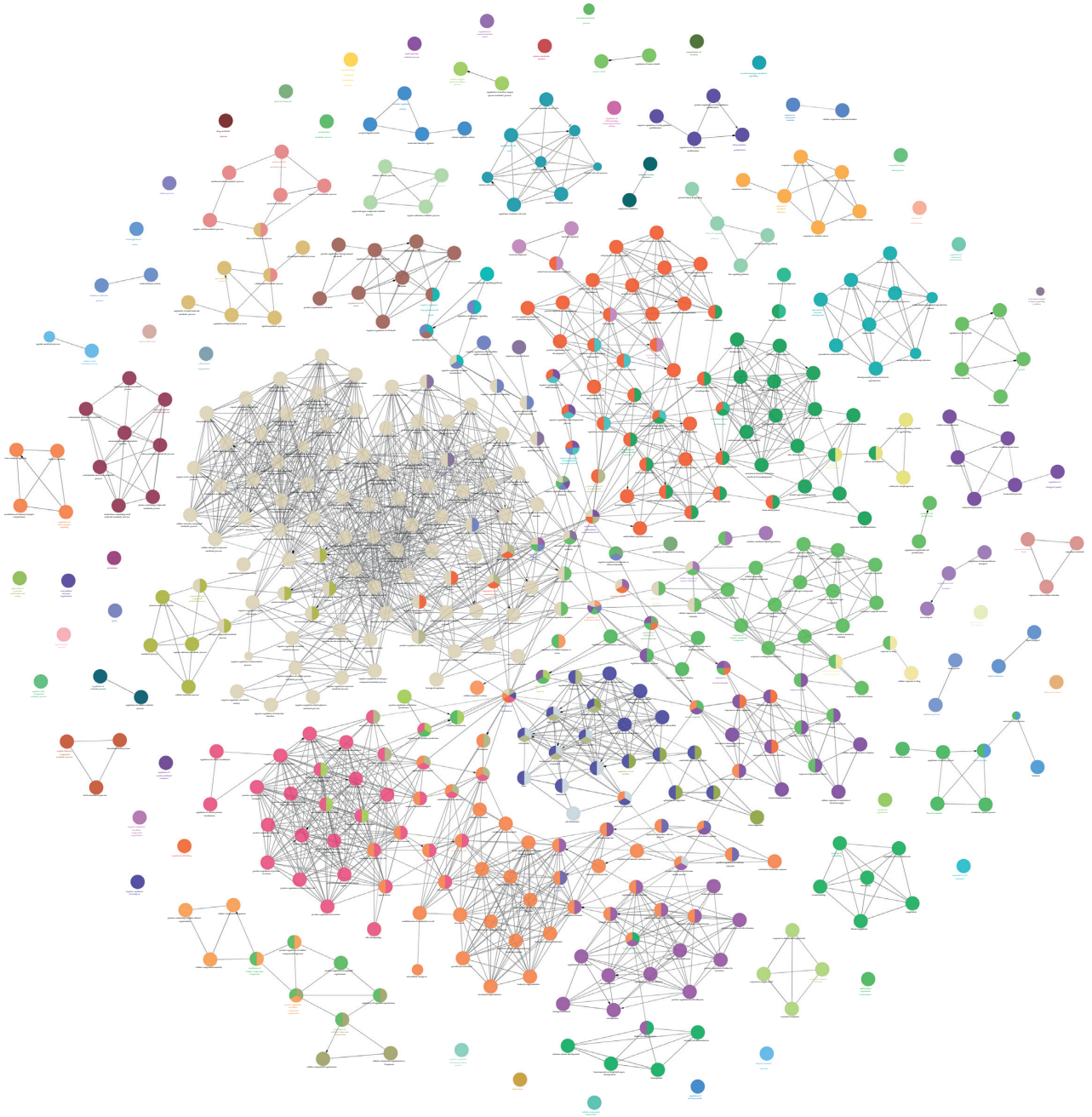

Figure 4: The preliminary enrichment results by ClueGO.

reducing cerebral microvascular basement membrane damage caused by thrombolysis [53]. Pharmacokinetic studies have shown that in CI model rats, the maximum plasma concentration (C max), half-life (t 1/2), and area under the curve (AUC 0-t) increased significantly, but the overall clearance (CL) value decreased significantly, indicating that rhubarb anthraquinones are more easily absorbed after coadministration [54].

3.2.2. Biological Processes of Radix Rhei Et Rhizome-CI PPI Network. Eighteen (18) clusters returned after analyzed by MCODE (Table 1 and Figure 6). The cluster score (complex score) is defined as the product of the complex subgraph, $C = (V, E)$, density, and the number of vertices in the complex subgraph ($DC \times |V|$). The higher the score, the denser the cluster.

The potential targets and CI genes in the cluster were introduced into DAVID for GO enrichment analysis. The biological process of the top 10 clusters is taken as an example (Table S4). For example, cluster 1 is related to GO: 0045429, GO:0031663, GO:0048661, GO:0071260, GO: 0045944, GO:0008217, GO:0006954, GO:0043066, GO: 0002576, GO:0070374, and GO:0051092; cluster 2 is associated with GO:0002576, GO:0070374, GO:0043066, GO: 0030335, GO:0001934, GO:0010628, GO:0042730, GO:

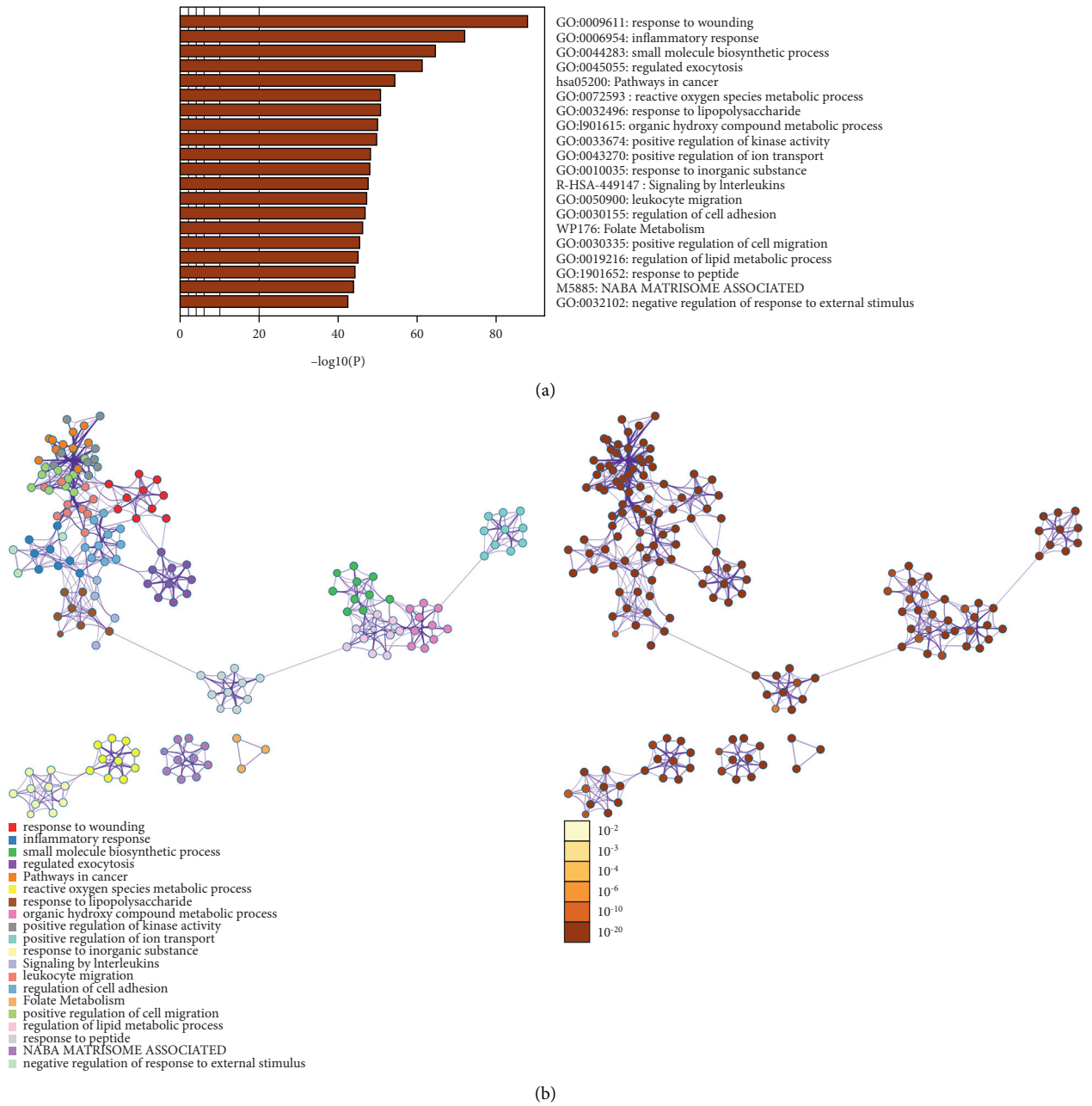

Figure 5: The Metascape results: (a) top biological processes, signaling pathways, and reactome pathways and (b) PPI network colored by enrichment results or *P*-values.

0030168, GO:0007165, GO:0043406, and GO:0043065; and cluster 3 is involved in GO:0042632, GO:0019433, GO:0042157, GO:0017187, GO:0007584, GO:0034375, GO:0043691, GO:0019915, GO:0006465, and GO:0070328. The details of clusters and biological processes are shown in Table S4. Since the biological processes in cluster 1 are representative, the main biological processes of cluster 1 are shown as an example (Figure 7).

3.2.3. Signaling Pathways of Radix Rhei Et Rhizome-CI PPI Network. Nineteen (19) CI-related signal pathways were returned. The relationship among signaling pathways, targets, and components is shown in Figure 8. The details of signaling pathways are shown in Figure 9 and Table S5. The number of targets regulated by the components of *Radix Rhei Et Rhizome* is shown in Table 2.

3.2.4. Reactome Pathways of Radix Rhei Et Rhizome-CI PPI Network. Ninety-three (93) CI-related signal pathways were returned. The relationship among reactome pathways, targets, and components is shown in Figure 10. The details of reactome pathways are shown in Figure 11 (Table S6). The number of targets regulated by the components of *Radix Rhei Et Rhizome* is shown in Table 3.

Table 1: Clusters of *Radix Rhei Et Rhizome*-CI PPI network.

Cluster	Score	Nodes	Edges	Targets and genes
1	44	67	1452	IGF1, NOS3, SERPINE1, MMP2, CRP, CCL5, VWF, PTEN, CASP8, MYD88, CD40, TLR4, MMP1, PLG, NGF, CTGF, HRAS, HSPA4, HIF1A, MMP9, RHOA, ANXA5, CREB1, SOD2, REN, CYCS, GRB2, MAPK1, MMP3, BCL2L1, IL2, TGFB1, ADIPOQ, AGT, FGF2, SELE, CD40LG, PTGS2, ALB, IL10, IL1B, HGF, MAP2K1, CCL2, IL4, ACE, CAT, THBS1, CXCL8, PPARG, AR, JAK2, ESR1, HMOX1, MMP7, CSF3, EDN1, BDNF, EGFR, SELP, MAPK14, CDC42, ICAM1, MMP13, STAT1, APOE, APP
2	25.821	79	1007	AKT1, XIAP, PIK3CA, SRC, F13A1, ALDOA, F3, NFKB1, AKT2, PTPN11, FGA, FGG, AGTR1, NR3C1, AIF1, PPBP, HSP90AA1, SERPINF2, NQO1, NOS2, ABL1, FGB, SOCS3, CD34, MIF, BMP2, PDGFRB, PDGFB, MET, HMGB1, IL6, KIT, PGF, MDM2, HPGDS, TEK, MBP, LGALS3, ENG, SOD1, MAPK8, TNF, PLAU, GFAP, PTK2, INS, RAF1, IL1A, GSK3B, TP53, CASP3, FAS, PTPN1, PROS1, TGFB2, VEGFA, HRG, ELANE, IGFBP3, TLR3, MAPK10, PGR, NCF1, CCNA2, CASP1, FGF1, IGF1R, F8, PLAUR, RETN, ADAM17, LDLR, KDR, CFD, MMP14, F5, PARP1, S100B, EGF
3	6.846	27	89	PAH, LPL, ARSA, RNASE2, APCS, CTSK, IMPDH1, CTSL, PON1, FABP4, RBP4, LPA, BPI, CST3, PROZ, RNASE3, SCARB1, F7, LIPG, FABP5, GM2A, PROC, HMGCR, GC, HABP2, HEXB, APOA1
4	5.706	35	97	F11, SERPINC1, HP, APOM, AKR1B1, HK1, HSP90AB1, SERPINA1, APOB, ENO2, ABCA1, OLR1, ATIC, PIK3CG, PLA2G7, CDK6, F10, ANG, SERPIND1, ZAP70, RHEB, LCAT, BACE1, HCK, MMP12, BTK, TTR, COG2, LIPC, ITGAL, AURKA, SYK, BRAF, APOC2, F12
5	4.783	24	55	PNP, BHMT, HADH, NR1I3, NT5M, SHMT1, YARS, TPI1, RAN, STS, UCK2, UCP3, ACADM, TYMS, RXRA, AHCY, LDHB, IVD, CYP1A1, PDE3B, PSPH, ADK, SULT1A1, AKR1C3
6	4	21	40	G6PD, MAP2, RAC2, GLRX, PTGER3, GSTP1, RHOB, RHOD, ASAH1, DCX, PSAP, CHIT1, CALM1, CRYZ, CTSS, CDA, PRDX1, HTR1A, LTA4H, QPCT, NPY
7	4	8	14	GLO1, GMPR, APRT, APEX1, IMPDH2, UMPS, DTYMK, TK1
8	4	4	6	RXRB, THRB, RARG, RARB
9	4	5	8	GALE, GNPDA2, UAP1, GALK1, GNPDA1
10	3.818	34	63	APOH, FBN1, TIMP3, THBD, HSPA8, EPHA2, INSR, PF4, ADAM10, PLAT, F2, RAC1, APAF1, PIK3R1, ERBB4, GSR, CASP7, CDK2, CHEK1, NOS1, EIF4E, HSPA1A, ESR2, CCL11, CYBA, FGFR2, ARG1, JAK3, APOA2, CSK, LCK, TGFBR1, MMP8, LCN2
11	3.75	17	30	GSTO1, CYP2C8, AGXT, GSTA1, FCAR, PCK1, BST1, ADH1C, P2RY12, ITK, ITGB2, CYP3A5, ADH1B, PYGL, NR1H4, HLA-DRB1, CYP2C9
12	3.571	15	25	SLC9A1, FABP1, KAT2B, SAA1, APOA5, TBXA2R, PPARA, ACTA2, TGFBR2, PRKACA, CPB2, RARA, EDNRA, COL3A1, NR1H3
13	3.333	4	5	GSTM2, SOD3, GSTA3, GSTM1
14	3	3	3	GPI, PKLR, ALDOB
15	3	3	3	SMARCA1, DOT1L, HDAC8
16	3	3	3	MAOA, PNMT, MAOB
17	3	3	3	AMY1A, AMY1B, AMY1C
18	2.889	10	13	GART, DCK, HFE, FECH, DHFR, PDE4B, ALAD, CLPP, PDE4D, DHODH

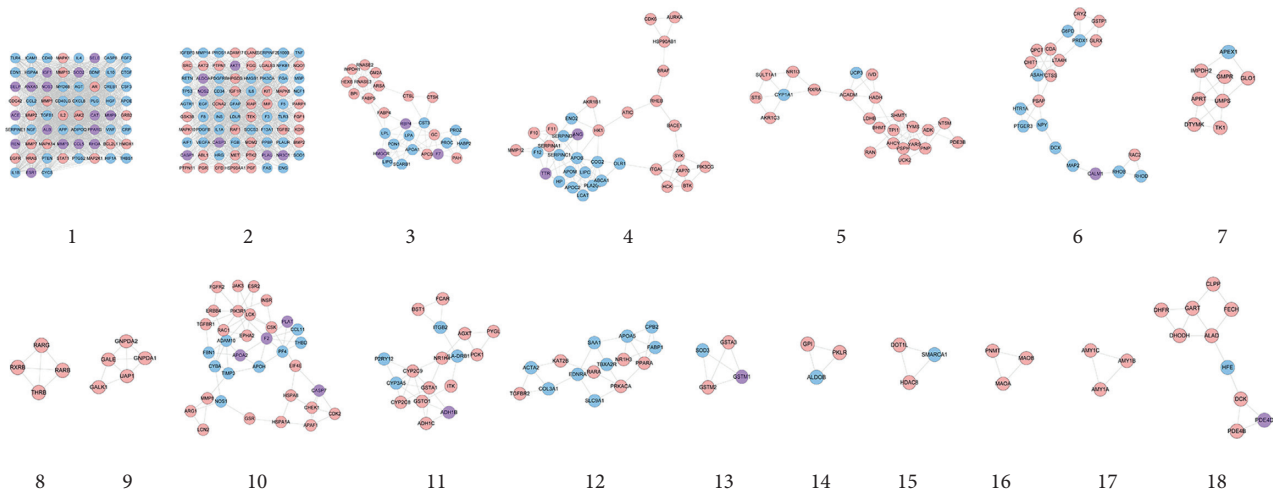

Figure 6: Clusters of *Radix Rhei Et Rhizome*-CI PPI network (Blue, pink, and purple circles stand for CI genes, *Radix Rhei Et Rhizome* targets, and *Radix Rhei Et Rhizome*-CI targets, respectively.).

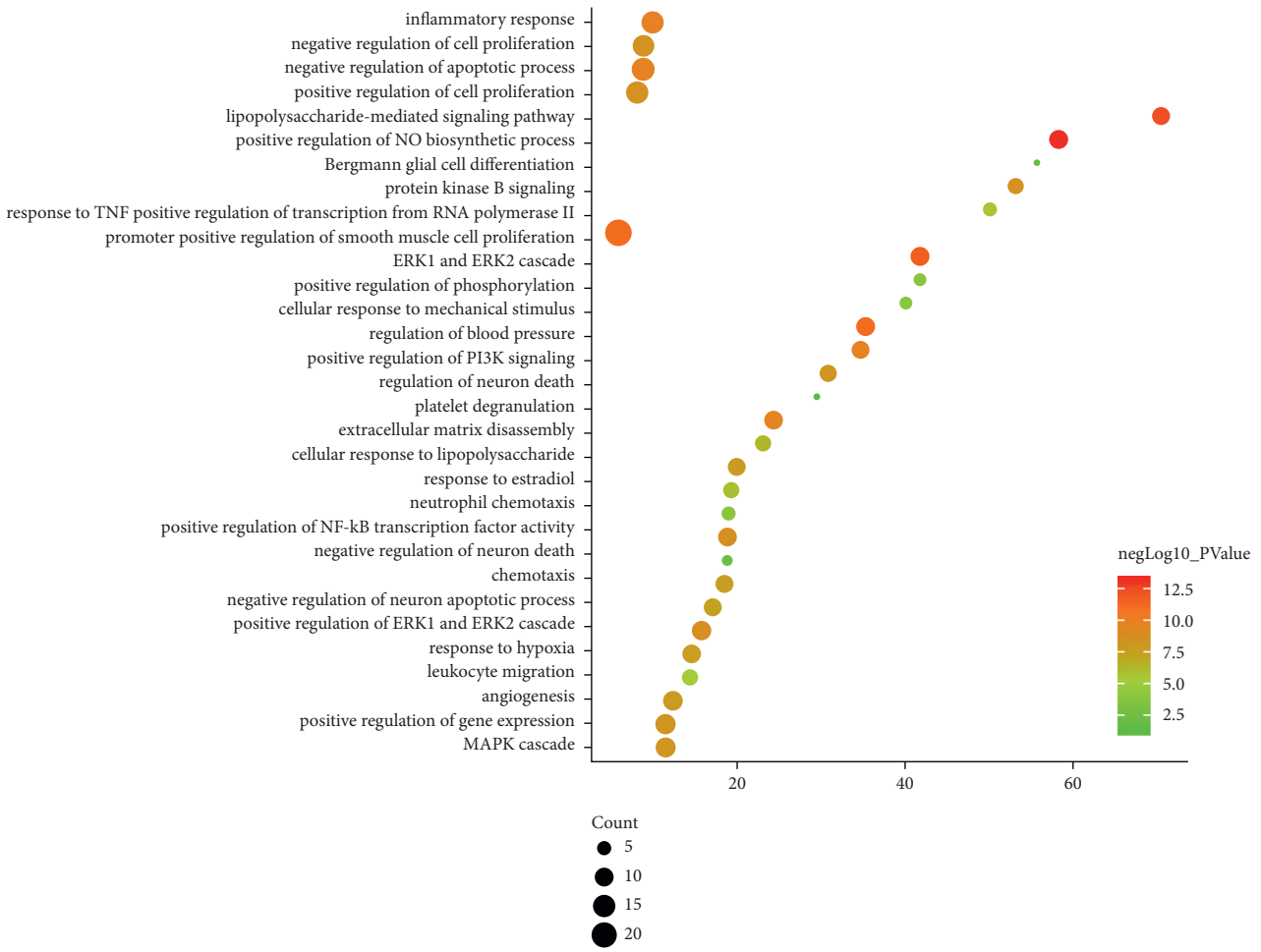

Figure 7: Bubble chart of biological processes (The *X*-axis is fold enrichment.).

The main biological processes, signaling pathways, and reactome pathways are shown in Figures 7, 9, and 10, respectively. Current studies have found that the occurrence and development of CI have slowed blood flow and vascular sclerosis in the cerebral vessels [55]. Astrocytes, endothelial cells, and pericytes constitute the neurovascular units required for neuronal metabolism [56, 57]. When CI occurs, the neurovascular unit is abnormal: hypoxia results in the dysfunction of the endothelial cell barrier of the blood-brain barrier, leading to a decrease in intracellular cAMP levels and an increase in vascular permeability [58, 59]. Ischemia and reperfusion cause various cells in the neurovascular unit to initiate cell death programs, including apoptosis, autophagy-related cell death, iron death, cell scoring, and necrosis [60, 61]. During CI, these cells contribute to postischemic inflammation at multiple stages of the ischemic cascade [62]. In the inflammatory response, microglia and astrocytes and infiltrating immune cells release a variety of inflammatory factors, including cytokines, chemokines, enzymes, and free radicals, which not only cause brain damage but also affect brain tissue repair [63, 64]. Recent studies have also shown that anti-inflammatory is an important treatment strategy for CI [65]. After thrombolysis, oxidative stress becomes the central link in cerebral ischemia-reperfusion. During reperfusion, oxygen is replenished, which is essential for maintaining the viability of neurons [66]. However, prooxidase and mitochondria also use oxygen as a substrate, and a large amount of oxygen free radicals (oxidants) are generated during reperfusion. Endogenous antioxidant enzymes, including SOD, can clear oxidants and reduce oxidant-induced brain damage [67, 68].

The network pharmacology strategy was used above to predict the mechanism of *Radix Rhei Et Rhizome* intervention in CI. In order to further explore it, the previous proteomics data were analyzed in depth. The proteomics data come from reference [69].

3.3. Bioinformatics Analysis of Proteomics Proteins

3.3.1. Proteomics Proteins' PPI Network. The proteomics proteins of reference [69] are shown in Table S2. A total of 76 proteins were input into String for PPI data. The proteomics proteins' PPI data were composed of 76 proteomics protein nodes and 182 edges (Figure 12).

3.3.2. Enrichment Analysis Results. DAVID and Metascape (http://metascape.org/gp/index.html#/main/step1) were utilized to analyze the proteins in the proteomics proteins'

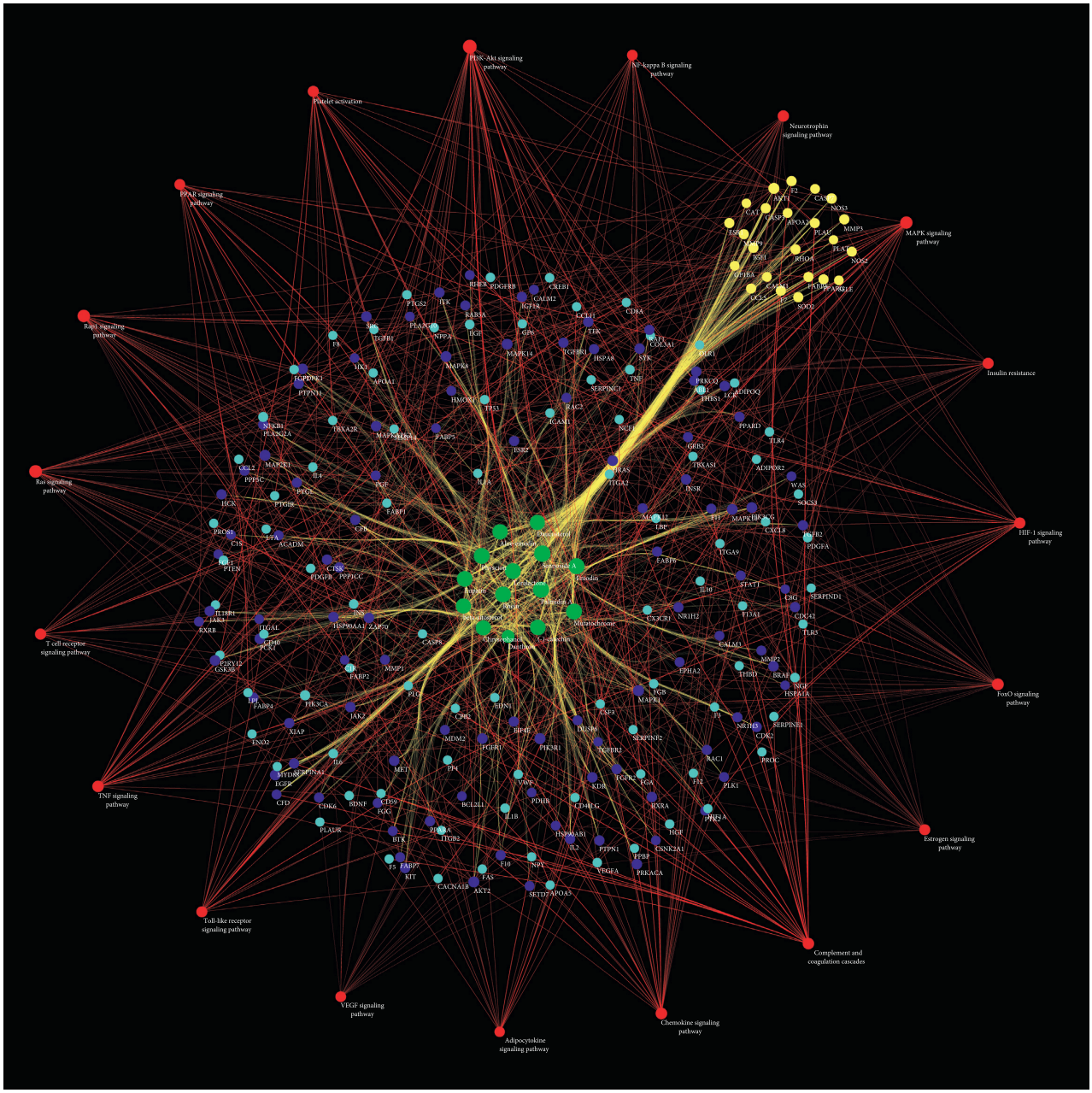

FIGURE 8: Signaling pathways of *Radix Rhei Et Rhizome*-CI PPI network (Red circles stand for signaling pathways. Dark blue circles stand for *Radix Rhei Et Rhizome* targets. Light blue circles stand for CI genes. Yellow circles stand for *Radix Rhei Et Rhizome*-CI targets. Green circles stand for *Radix Rhei Et Rhizome* compounds. The larger the node size, the higher the degree of the node. The thicker the line, the greater the edge betweenness of the node.).

PPI network (Figure 13). The details of biological processes, signaling pathways, and reactome pathways are shown in Table S7. The clusters are shown in Figure 14.

The top 20 proteins in Figure 12 were Syp, Syn1, Mbp, Gap43, Aif1, Camk2a, Syt1, Calm1, Calb1, Nsf, Nefl, Hspa5, Nefh, Ncam1, Dcx, Unc13a, Mapk1, Syt2, Dnm1, and Cltc. These proteins may be the key targets of *Radix Rhei Et Rhizome* in the treatment of CI. As a specific marker protein of synaptic vesicles, synaptophysin (SYP) is a sign of synapse occurrence. Its density and distribution can indirectly reflect the number and distribution of synapses in the body [70, 71]. Studies have found that after CI in rats, the synaptophysin immune response was significantly enhanced compared with the sham operation group, and the expression reached a peak at 2 weeks after cerebral ischemia, and it significantly decreased at 3 weeks [72]. This experimental study found that after Radix Rhei Et Rhizome treatment, its expression was significantly increased compared with the model group, indicating that Radix Rhei Et Rhizome may resist synapse damage or promote synaptic regeneration after cerebral ischemia. Synapse protein I gene (SYN1) mainly mediates the delivery of synaptic vesicles and circulation [73] and plays an important role in neurodegenerative diseases [74], such as Alzheimer's disease, Parkinson's disease, and

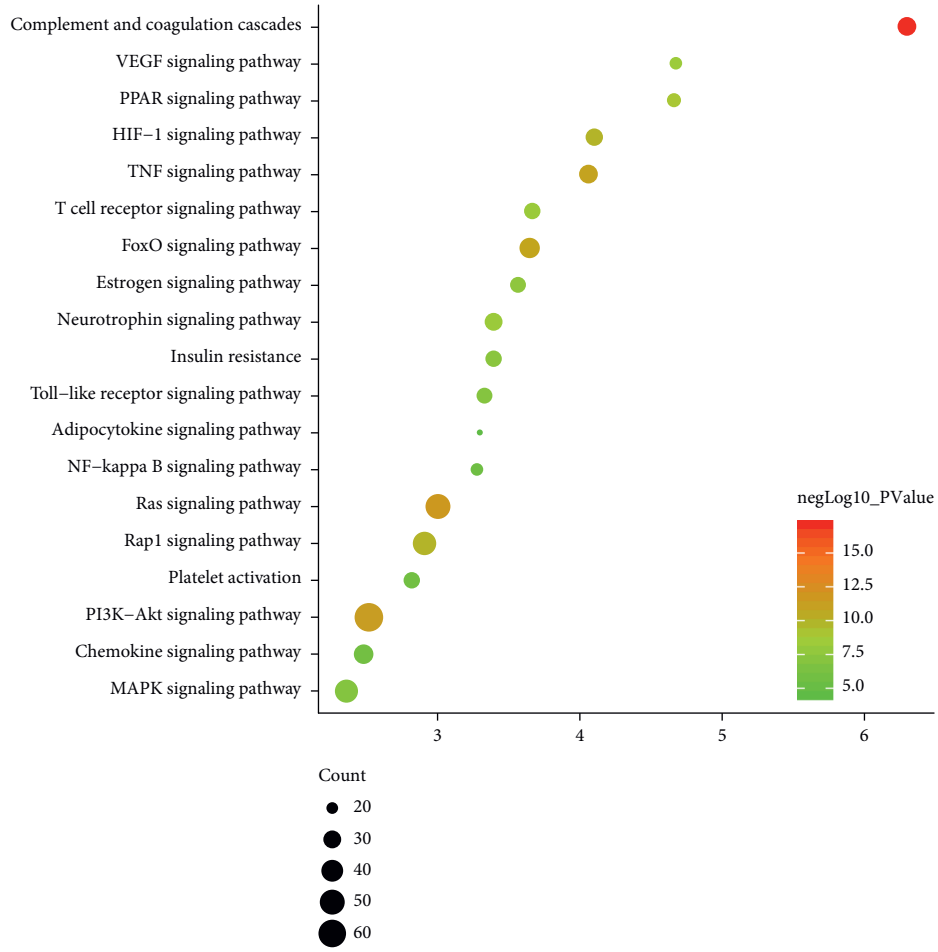

Figure 9: Signaling pathways of biological processes (The *X*-axis is fold enrichment.).

Table 2: The number of targets regulated by the components of *Radix Rhei Et Rhizome*.

Components	Number of targets
Sennoside A	103
Palmidin A	99
Emodin	98
Toralactone	96
Mutatochrome	96
Rhein	95
Physcion	95
Eupatin	93
(-)-Catechin	91
Aloe-emodin	88
Chrysophanol	86
Beta-sitosterol	85
Daucosterol	85
Danthron	53

amyotrophic lateral sclerosis. This study suggests that SYN1 may be a potential drug target for neurodegenerative diseases caused by CI, among which *Radix Rhei Et Rhizome* can reduce CI by interfering with SYN1.

GAP-43 is a calmodulin-binding phosphoprotein that has been isolated and identified in recent years [75]. In the process of neuron development and regeneration, GAP-43 is synthesized in large quantities along with the growth of axons and is a marker of axon growth. The expression product is mainly located on the plasma membrane surface of the axon growth cone [76]. Studies have shown that the increase in GAP-43 content in the penumbra of the ischemic penumbra of one middle cerebral artery 3 to 14 days after the embolization of the middle cerebral artery is synchronized with the recovery of the function of the affected limb [77]. Another study found that the expression of GAP-43 in the brain increased significantly after cerebral infarction, peaked at 1 week after ischemia-reperfusion, and began to decrease after 2 weeks [78, 79]. This experiment found that *Radix Rhei Et Rhizome* can significantly enhance the expression of GAP-43 in the cortical ischemic penumbra, suggesting that *Radix Rhei Et Rhizome* can effectively promote the regeneration of axons in CI model rats and induce the recovery of nerve function.

MBP is mainly located on the serosal surface of the myelin sheath and is the main protein of the myelin sheath of the central nervous system. Its main function is to maintain the integrity and functional stability of the myelin sheath of the central nervous system, and its neural tissue specificity is high [80]. When acute cerebral infarction (ACI) occurs, when the human central nervous system is damaged, the blood-brain barrier function is unbalanced, which increases

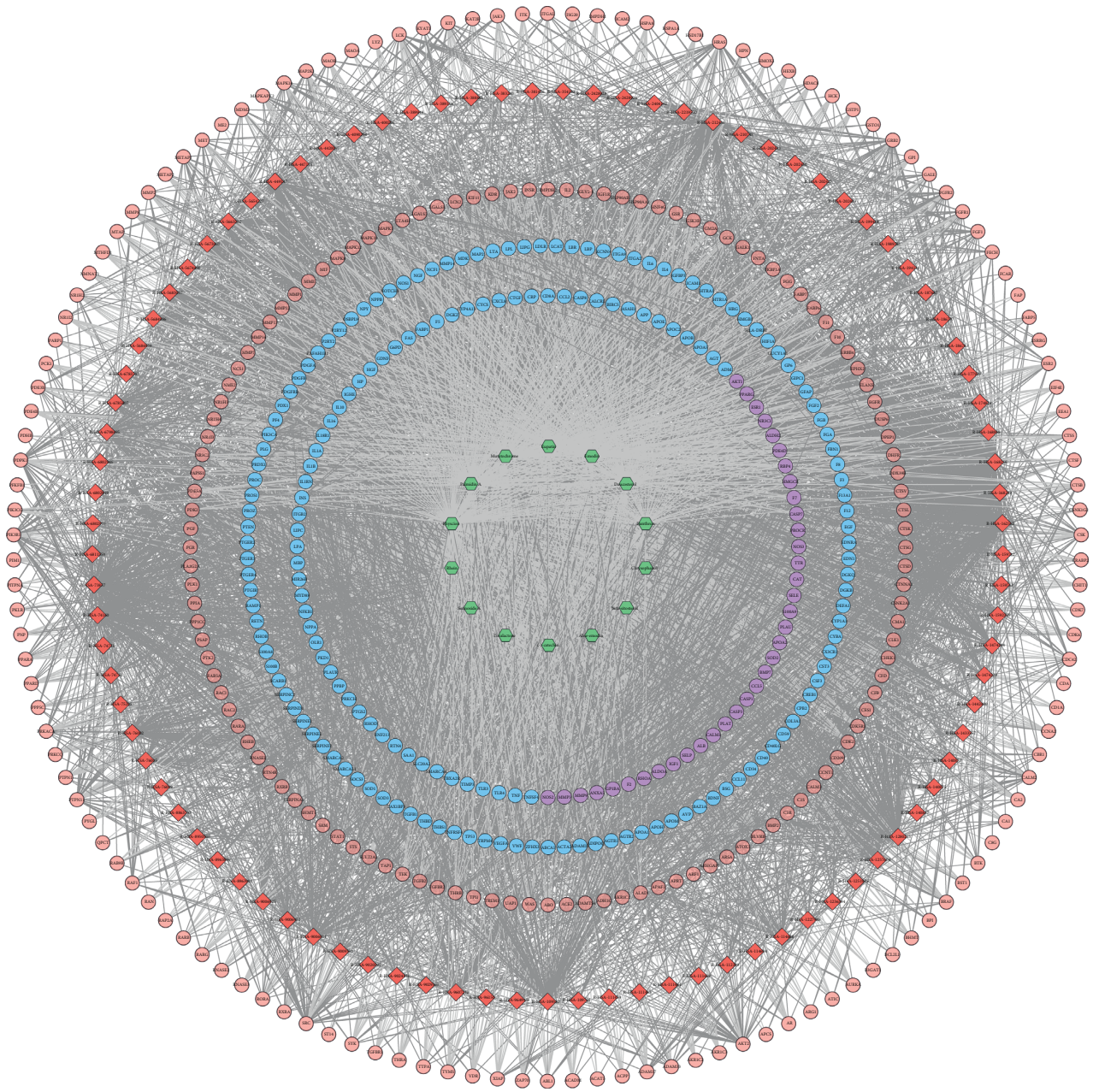

Figure 10: Reactome pathways of *Radix Rhei Et Rhizome*-CI PPI Network (Green hexagons stand for potential compounds. Blue, pink, and purple circles stand for CI genes, *Radix Rhei Et Rhizome* targets, and *Radix Rhei Et Rhizome*-CI targets, respectively. Red diamonds stand for reactome pathways. Dark lines stand for relationships among reactome pathways and targets. Light lines stand for relationships among herbs and targets.).

its permeability, and MBP can easily pass through the blood-brain barrier and be released into the blood. At present, the detection of serum NSE and MBP expression levels is of great value in assessing the prognosis of ACI disease [81]. The results of this study showed that the MBP level of the CI group increased rapidly and the MBP level decreased after Radix Rhei Et Rhizome treatment, suggesting that Radix Rhei Et Rhizome treatment of the ACI rat model can promote the disease outcome and reduce the MBP level.

Allogeneic inflammatory factor-1 (AIF-1) is a 17 kDa cytoplasmic calcium-binding inflammatory response scaffold protein, which is mainly expressed in immune cells [82]. AIF-1 affects the immune system at several key points, thereby regulating inflammatory diseases [83]. AIF-1 promotes the expression of inflammatory mediators such as cytokines, chemokines, and inducible nitric oxide synthase (iNOS) and promotes the proliferation and migration of inflammatory cells. Current research shows that it regulates central nervous system (CNS) damage [82, 83]. The results of this study showed that the level of cerebral infarction (AIF-1) increased rapidly, and the level of AIF-1 decreased after *Radix Rhei Et Rhizome* treatment. It is suggested that *Radix Rhei Et Rhizome* can promote the outcome of CI and reduce the level of inflammation.

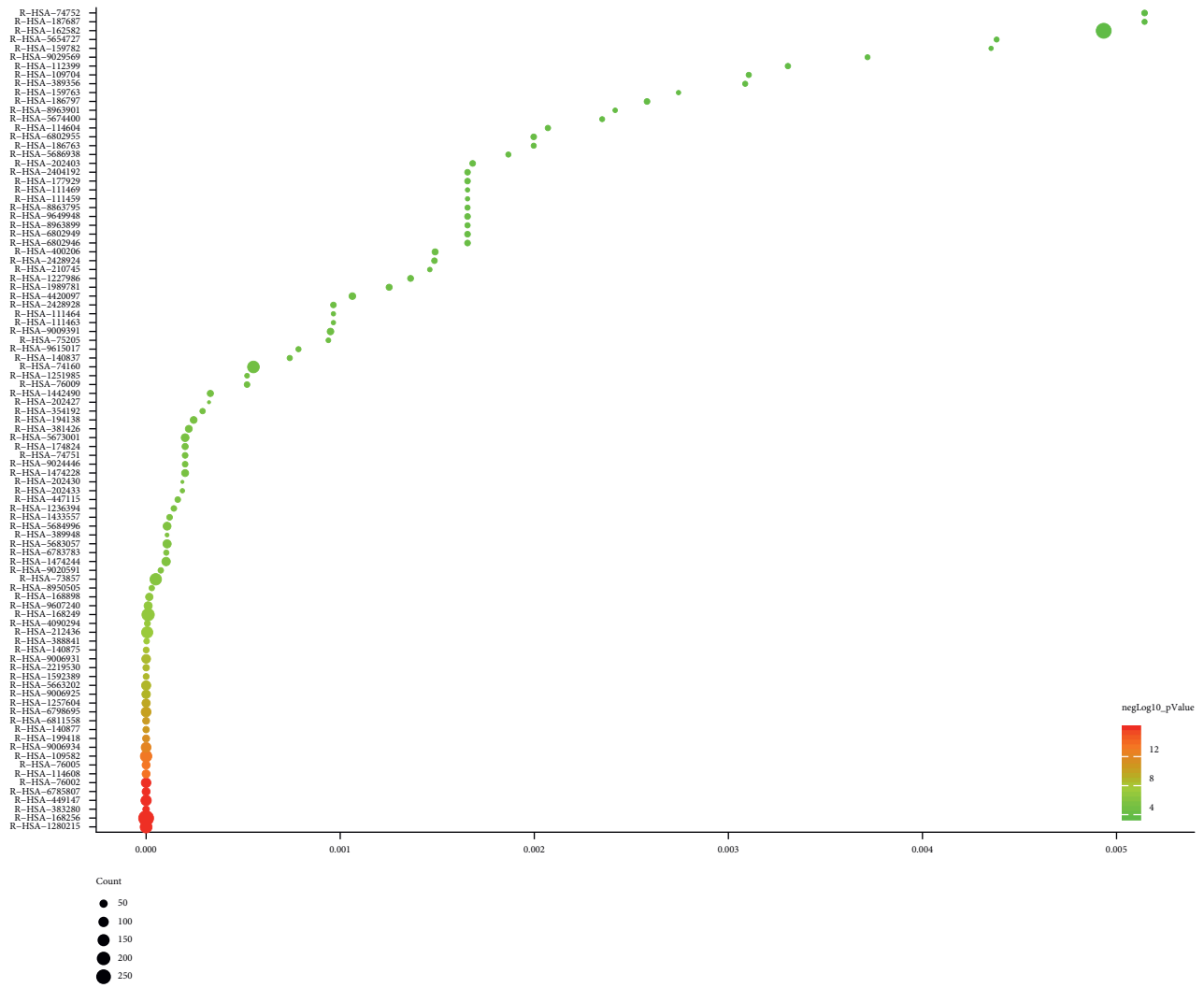

Figure 11: Reactome pathways of biological processes (The *X*-axis is FDR.).

Table 3: The number of targets regulated by the components of *Radix Rhei Et Rhizome*.

Components	Number of targets
Palmidin A	222
Sennoside A	213
Toralactone	212
Emodin	209
Rhein	209
Eupatin	207
(-)-Catechin	205
Aloe-emodin	202
Physcion	202
Mutatochrome	193
Chrysophanol	178
Beta-sitosterol	171
Daucosterol	168
Danthron	116

The alpha (CAMK2A) of calcium/calmodulin-dependent protein kinase II (CaMKII) plays a key role in neuronal plasticity and brain learning and memory [84, 85]. After *Radix Rhei Et Rhizome* intervention, the expression of CAMK2A was upregulated. The main biological function of Syt1 is to trigger vesicle fusion [86], which is related to the molecular mechanism of neuronal endocytosis and exocytosis coupling [87]. This study found that Syt1 was upregulated after *Radix Rhei Et Rhizome* intervention. Calmodulin 1 (CALM1) is highly expressed in the human brain tissue, and its biological function is mainly related to axon transmission [88]. In addition, the Calm1 signaling pathway is crucial for the migration of precerebellar neurons in mice [89]. Calm1-L plays a functional role in the central and peripheral nervous system [90]. This study found that Calm1 was upregulated after *Radix Rhei Et Rhizome* intervention. A recent study also showed that CALM1 rs3179089 gene polymorphism is associated with CI in Chinese Han population [91].

Calbindin 1 (Calb1) acts as a buffer, sensor, and transporter of intracellular Ca^{2+}. Different types of hippocampal neurons have different Calb1 concentrations. Since Calb1 can inhibit the increase of free Ca^{2+}, it accelerates the collapse of the Ca^{2+} gradient after the influx of Ca^{2+} stops [92, 93]. Current research shows that it plays a role in neurotransmitter and hormone release, neuron differentiation, brain wiring, and neuron development [94, 95]. The

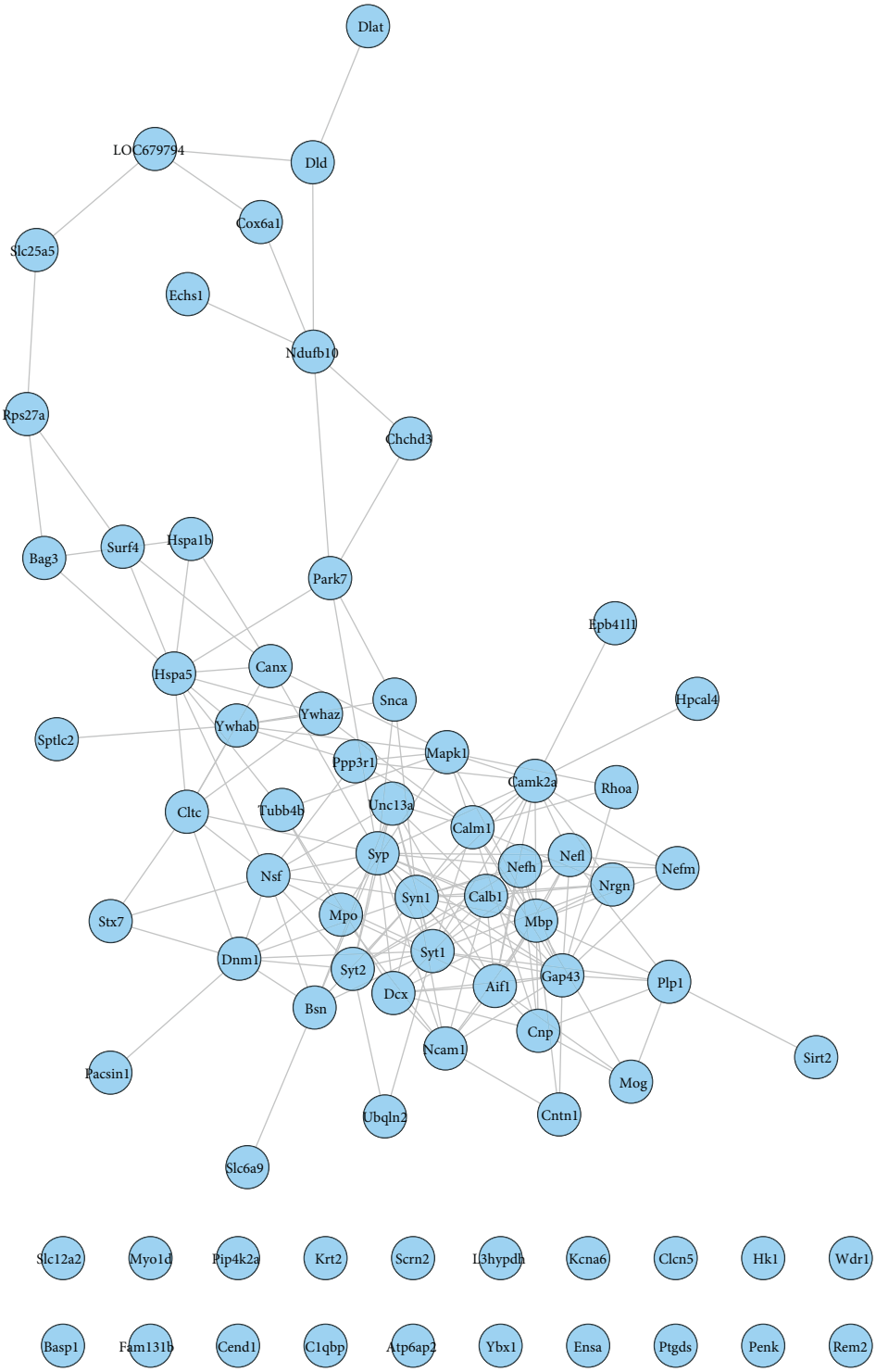

Figure 12: Proteomics proteins' PPI network.

results of this study showed that the level of Calb1 was downregulated in the CI group, and the level of Calb1 was upregulated after Radix Rhei Et Rhizome treatment. It is suggested that *Radix Rhei Et Rhizome* may promote disease outcome through neurotransmitter and other methods.

N-ethylmaleimide-sensitive fusion protein (NSF) is an ATPase that plays an important role in intracellular membrane vesicle transport [96]. It is highly conservative in evolution and participates in the secretion process of different species and different cell types [96, 97]. Current research shows that it plays an important role in the process of neurotransmitter release by synaptic vesicle exocytosis at presynaptic nerve terminals [97, 98]. The results of this study showed that the level of NSF in the cerebral infarction group was downregulated and the level of NSF was upregulated after treatment.

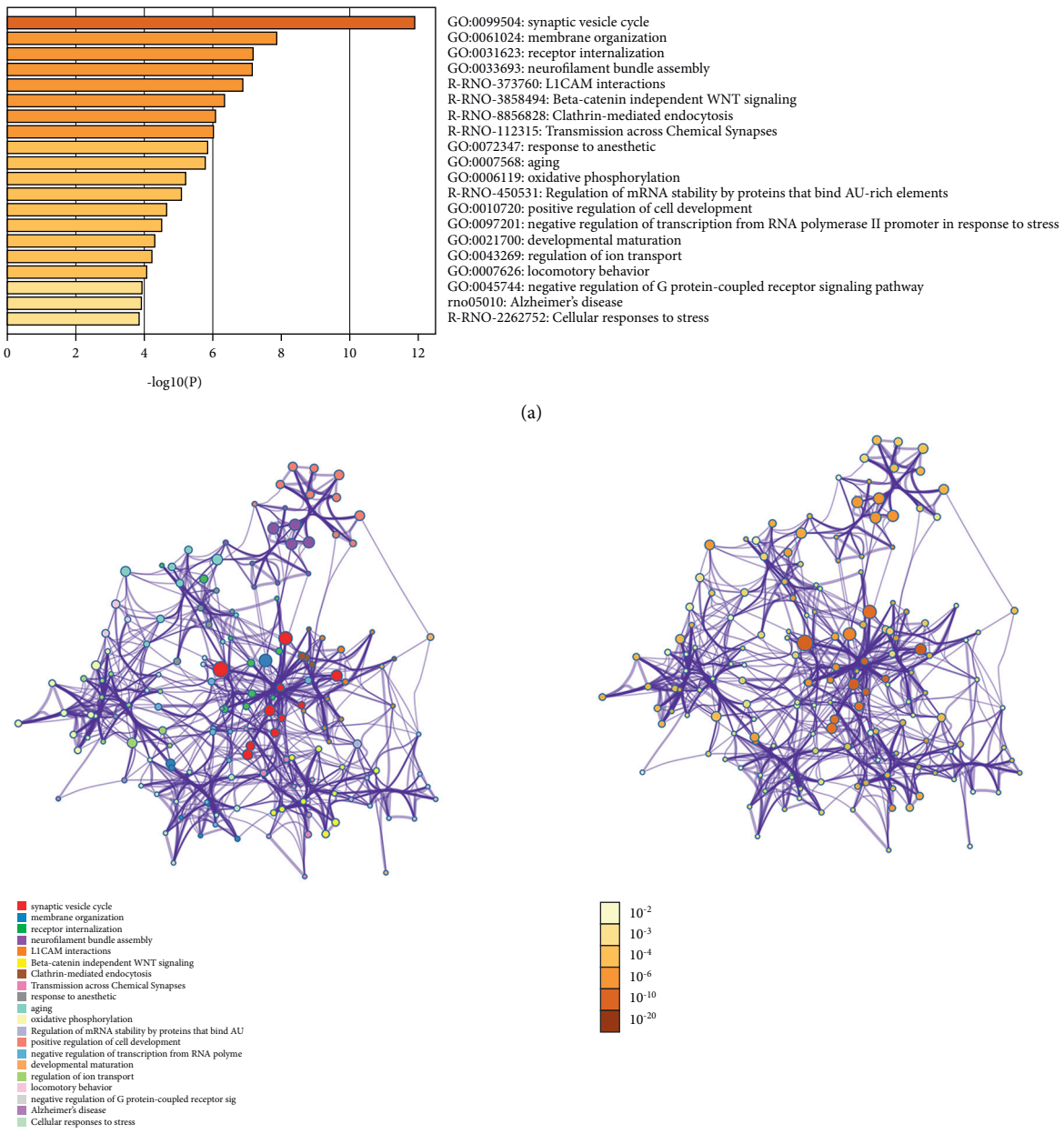

Figure 13: The Metascape results: (a) top biological processes, signaling pathways, and reactome pathways of the proteomics proteins' PPI network and (b): PPI networks colored by enrichment results or *P*-values.

Neurofilament light chain (Nefl) belongs to one of the main subtypes of neurofilament protein. It is the main cytoskeleton structural protein of neurons, which is distributed in axons [99, 100]. Nefl is also an important indicator for judging acute axonal injury [99]. In clinical studies of relapsing multiple sclerosis, Nefl is used as an effective evaluation index for drug anti-inflammatory therapy [101]. Recent studies have shown that emodin activates mTOR and Notch pathways in hypoxic PC12 cells by inhibiting Nefl [102]. In this study, the expression level of Nefl in CI model rats was higher but decreased after intervention, indicating that there is acute axon damage in acute stroke and *Radix Rhei Et Rhizome* may be able to protect axons.

The endoplasmic reticulum stress chaperone protein HSPA5 is mainly related to endoplasmic reticulum stress. Current studies have shown that endoplasmic reticulum stress can induce autophagy activation [103]. Previous studies have confirmed that in the mouse brain I/R model, the expression of HSPA5 protein is increased, and it has a neuroprotective effect [104]. At present, by injecting HSPA5 siRNA into the anterior ventricle of CI mice, the expression of LC3-1/LC3-I is significantly reduced, and it will also lead to the loss of nerve cells in the cerebral ischemic cortex of mice and aggravation of neurobehavioral damage. This is similar to the effect of the autophagy inhibitor 3-MA, indicating that HSPA5-mediated autophagy may play a

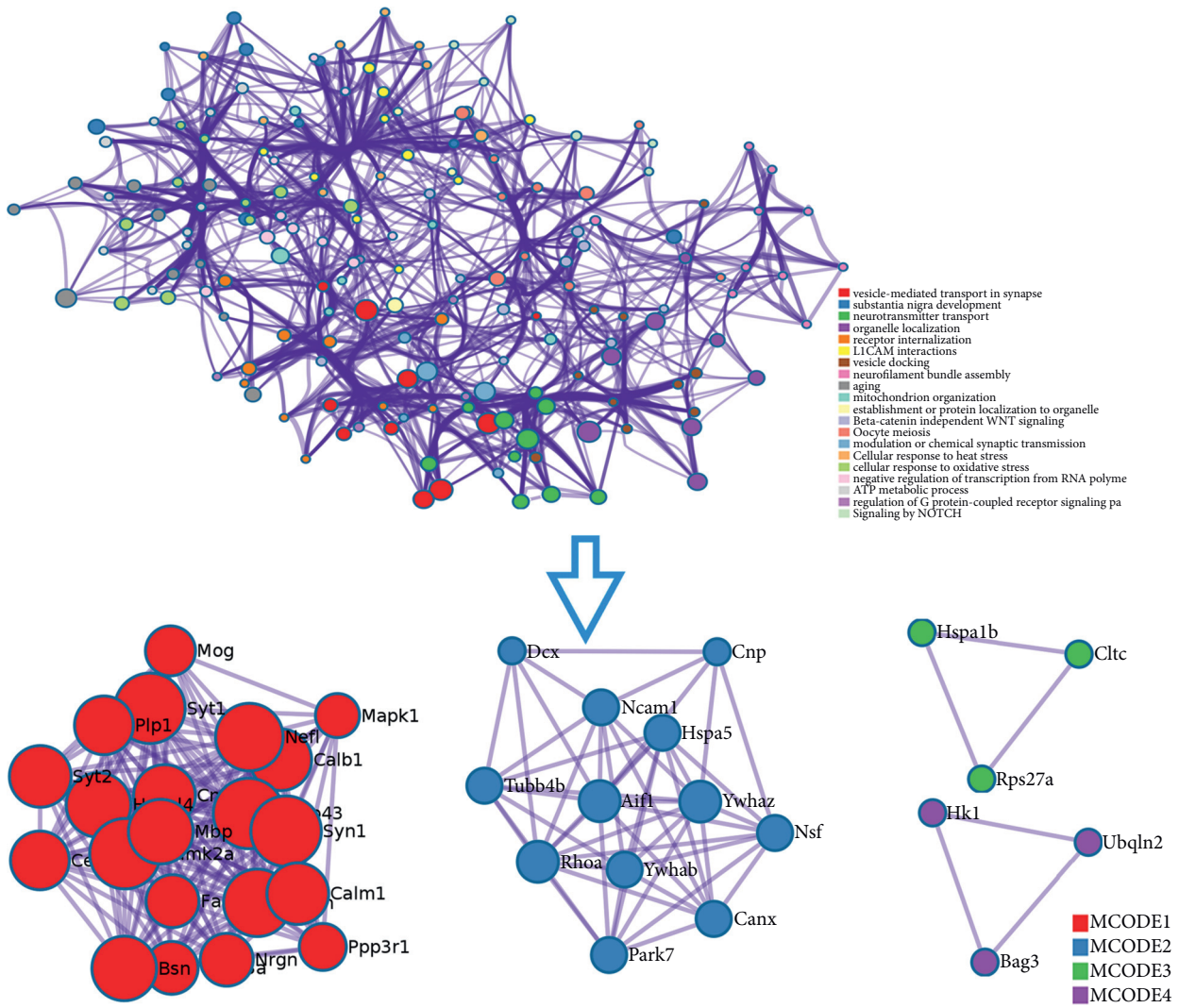

Figure 14: Clusters of proteomics proteins' PPI network.

neuroprotective effect in mouse I/R [105, 106]. The results of this study showed that the level of HSPA5 in the CI group was downregulated, but after treatment, the level of HSPA5 was upregulated.

NCAM1 is a member of the cell adhesion molecule family and is a molecular cleavage of the immunoglobulin superfamily. NCAM1 is a membrane protein that includes three subtypes: NCAM-120, NCAM-140, and NCAM-180. It is mainly expressed in the nervous system and is involved in regulating the function of nerve cells and neuron migration [107]. NCAM1 is expressed in neural stem cells. In addition, astrocytes also express many adhesion molecules, such as VCAM1, NCAM1, and ICAM1, which represent many potential drug targets for inflammatory diseases of the central nervous system [108–110]. This study showed that the level of NCAM1 in the CI group was downregulated. After *Radix Rhei Et Rhizome* treatment, the level of NCAM1 was upregulated, suggesting that *Radix Rhei Et Rhizome* may inhibit adhesion molecules and is related to inflammatory factors.

Dcx is a microtubule-associated phosphoprotein, which is specifically expressed in newborn neuroblasts and immature neurons in DG [111, 112]. Therefore, Dcx has been widely used to label the cell bodies, processes, and growth cones of newborn neurons. Studies have reported that after CI, Dcx strengthens the differentiation of nerve cells in the DG area of the hippocampus and promotes the rehabilitation of nerve function [113]. This study showed that the level of Dcx in the CI group was downregulated, and after treatment, the level of Dcx was upregulated, suggesting that *Radix Rhei Et Rhizome* may regulate the generation of new neurons and promote the outcome of CI.

The limitation of this study is that although the pharmacokinetic parameters are used to predict the composition of *Radix Rhei Et Rhizome* and the composition was supplemented as much as possible by searching the literature, due to the limitations of the current detection technology, there are still active ingredients that may not be included. Since the intestinal flora may metabolize and secondary modify the active components of *Radix Rhei Et Rhizome*, these components may be traced in the blood. In the future, better technology is needed to detect these components. In

addition, although this study analyzed the main active components of *Radix Rhei Et Rhizome* in the treatment of CI through chemoinformatics and explored its possible synergistic effects, there is still a lack of in vivo and in vitro experiments related to their intervention in CI. In the future, we will explore the synergistic compatibility of these components in the CI in vitro model and the CI in vivo model and look forward to further development of new drugs for the treatment of CI, laying the foundation for its clinical application.

Our previous research evaluated the therapeutic effect of *Radix Rhei Et Rhizome* on cerebral hemorrhage [114], while this study explored the mechanism of Radix Rhei Et Rhizome in the treatment of CI, and this study found that Radix Rhei Et Rhizome may regulate the synaptic remodeling and the regeneration of nerve cell axons after cerebral ischemia. Compared with previous research [114], this study explored the mechanism of *Radix Rhei Et Rhizome* intervention in CI. This study found that *Radix Rhei Et Rhizome* may treat CI through biological process (such as platelet degranulation, cell migration, fibrinolysis, platelet activation, hypoxia, angiogenesis, endothelial cell apoptosis, coagulation, and neuronal apoptosis), signaling pathways (such as Ras, PI3K-Akt, TNF, FoxO, HIF-1, and Rap1), and reactome pathways (such as inflammatory cytokines, platelet activation, response to elevated platelet cytoplasmic Ca^{2+}, and hemostasis).

4. Conclusion

Radix Rhei Et Rhizome may play the therapeutic role for CI through regulating biological modules such as synaptic vesicles and neurotransmitter secretion and transport, energy metabolism, neuronal programmed death (apoptotic autophagy) module, calcium ion regulation of exocytosis and cytoplasmic calcium ion release, endoplasmic reticulum oxidative stress, and neuroplasticity (neuron and synaptic plasticity).

Data Availability

The data used to support the findings of this study are included within the article and the supplementary information files.

Conflicts of Interest

The authors declare no competing interests.

Authors' Contributions

Jinsong Zeng, Xiaofei Zhu, and Liang Liu are responsible for the study concept and design. Jinsong Zeng, Xiaofei Zhu, Mengxia Yuan, Jiamin Wu, Wang Xiang, Yonghe Wu, Zhiyong Long, and Liang Liu are responsible for data analysis and interpretation. Jinsong Zeng and Xiaofei Zhu drafted the paper. Liang Liu supervised the study. All the authors participated in the analysis and interpretation of data and approved the final paper. Wang Xiang and Zhiyong Long should be considered joint first authors.

Acknowledgments

This research was supported by the Natural Science Foundation of Hunan Province (2020JJ5442) and Open Fund for First-class Discipline of Integrated Traditional Chinese and Western Medicine of the Hunan University of Chinese Medicine (2020ZXYJH09).

Supplementary Materials

Table S1: potential targets for potential compounds; Table S2: proteomics data; Table S3: CI gene; Table S4: enrichment analysis of clusters based on gene ontology (GO) annotation of *Radix Rhei Et Rhizome*-CI PPI network; Table S5: pathway enrichment analysis of *Radix Rhei Et Rhizome*-CI PPI network; Table S6: reactome pathways of *Radix Rhei Et Rhizome*-CI PPI network; and Table S7: the biological processes, signaling pathways, and reactome of proteomics proteins' PPI network. (*Supplementary Materials*)

References

[1] H. Slyter, "Guidelines for the management of patients with acute ischemic stroke," *Stroke*, vol. 26, no. 1, pp. 137-138, 1995.

[2] Z. Wang, S. Hu, S. Sang, L. Luo, and C. Yu, "Age-period-cohort analysis of stroke mortality in China," *Stroke*, vol. 48, no. 2, pp. 271–275, 2017.

[3] J. Cao, E. S. Eshak, K. Liu, K. Gero, Z. Liu, and C. Yu, "Age-period-cohort analysis of stroke mortality attributable to high sodium intake in China and Japan," *Stroke*, vol. 50, no. 7, pp. 1648–1654, 2019.

[4] R. A. Radu, E. O. Terecoasă, O. A. Băjenaru, and C. Tiu, "Etiologic classification of ischemic stroke: where do we stand?" *Clinical Neurology and Neurosurgery*, vol. 159, pp. 93–106, 2017.

[5] H. K. Eltzschig and T. Eckle, "Ischemia and reperfusion-from mechanism to translation," *Nature Medicine*, vol. 17, no. 11, pp. 1391–1401, 2011.

[6] T. Kalogeris, C. P. Baines, M. Krenz, and R. J. Korthuis, "Cell biology of ischemia/reperfusion injury," *International Review of Cell and Molecular Biology*, vol. 198, pp. 229–317, 2012.

[7] W. Cai, H. Liu, J. Zhao et al., "Pericytes in brain injury and repair after ischemic stroke," *Translational Stroke Research*, vol. 8, no. 2, pp. 107–121, 2017.

[8] J. H. Choi and J. Pile-Spellman, "Reperfusion changes after stroke and practical approaches for neuroprotection," *Neuroimaging Clinics of North America*, vol. 28, no. 4, pp. 663–682, 2018.

[9] J. Yang, M. Chen, R. Y. Cao, Q. Li, and F. Zhu, "The role of circular RNAs in cerebral ischemic diseases: ischemic stroke and cerebral ischemia/reperfusion injury," *Advances in Experimental Medicine and Biology*, vol. 1087, no. 2, pp. 309–325, 2018.

[10] C. Hentia, A. Rizzato, E. Camporesi et al., "An overview of protective strategies against ischemia/reperfusion injury: the role of hyperbaric oxygen preconditioning," *Brain and Behavior*, vol. 8, no. 5, Article ID e00959, 2018.

[11] B. P. Gaire, "Herbal medicine in ischemic stroke: challenges and prospective," *Chinese Journal of Integrative Medicine*, vol. 24, no. 4, pp. 243–246, 2018.

[12] P.-f. Wu, Z. Zhang, F. Wang, and J.-g. Chen, "Natural compounds from traditional medicinal herbs in the treatment of cerebral ischemia/reperfusion injury," *Acta Pharmacologica Sinica*, vol. 31, no. 12, pp. 1523–1531, 2010.

[13] N. Ghosh, R. Ghosh, Z. A. Bhat et al., "Advances in herbal medicine for treatment of ischemic brain injury," *Natural product communications*, vol. 9, no. 7, pp. 1045–1055, 2014.

[14] A.-j. Liu, L. Song, Y. Li et al., "Active compounds of rhubarb root and Rhizome in animal model experiments of focal cerebral ischemia," *Evidence-Based Complementary and Alternative Medicine*, vol. 2015, Article ID 210546, 13 pages, 2015.

[15] Q. Guan, S. Liang, Z. Wang, Y. Yang, and S. Wang, "1H NMR-based metabonomic analysis of the effect of optimized rhubarb aglycone on the plasma and urine metabolic fingerprints of focal cerebral ischemia-reperfusion rats," *Journal of Ethnopharmacology*, vol. 154, no. 1, pp. 65–75, 2014.

[16] R.-R. Li, X.-F. Liu, S.-X. Feng et al., "Pharmacodynamics of five anthraquinones (aloe-emodin, emodin, rhein, chysophanol, and physcion) and reciprocal pharmacokinetic interaction in rats with cerebral ischemia," *Molecules*, vol. 24, no. 10, p. 1898, 2019.

[17] N. Zhang, X. Zhang, X. Liu et al., "Chrysophanol inhibits NALP3 inflammasome activation and ameliorates cerebral ischemia/reperfusion in mice," *Mediators of Inflammation*, vol. 2014, Article ID 370530, 12 pages, 2014.

[18] W.-T. Yang, Y. Wang, Y.-H. Shi et al., "Herbal compatibility of ginseng and rhubarb exerts synergistic neuroprotection in cerebral ischemia/reperfusion injury of rats," *Frontiers in Physiology*, vol. 10, p. 1174, 2019.

[19] X. Li, S. Chu, Y. Liu, and N. Chen, "Neuroprotective effects of anthraquinones from rhubarb in central nervous system diseases," *Evidence-Based Complementary and Alternative Medicine*, vol. 2019, Article ID 3790728, 12 pages, 2019.

[20] T. Bao, K. Yang, Z. Long, L. Zeng, and Y. Li, "Systematic pharmacological methodology to explore the pharmacological mechanism of siwu decoction for osteoporosis," *Medical Science Monitor*, vol. 25, pp. 8152–8171, 2019.

[21] K. Yang, L. Zeng, T. Bao, Z. Long, and B. Jin, "Exploring the pharmacological mechanism of quercetin-resveratrol combination for polycystic ovary syndrome: a systematic pharmacological strategy-based research," *Scientific Reports*, vol. 9, no. 1, p. 18420, 2019.

[22] L. Zeng, K. Yang, and J. Ge, "Uncovering the pharmacological mechanism of Astragalus salvia compound on pregnancy-induced hypertension syndrome by a network pharmacology approach," *Scientific Reports*, vol. 7, no. 1, p. 16849, 2017.

[23] L. Zeng and K. Yang, "Exploring the pharmacological mechanism of Yanghe decoction on HER2-positive breast cancer by a network pharmacology approach," *Journal of Ethnopharmacology*, vol. 199, pp. 68–85, 2017.

[24] K. Yang, L. Zeng, A. Ge et al., "Investigating the regulation mechanism of baicalin on triple negative breast cancer's biological network by a systematic biological strategy," *Biomedicine & Pharmacotherapy*, vol. 118, p. 109253, 2019.

[25] J. Ru, P. Li, J. Wang et al., "TCMSP: a database of systems pharmacology for drug discovery from herbal medicines," *Journal of Cheminformatics*, vol. 6, no. 1, p. 13, 2014.

[26] F.-P. Chen, C.-M. Chang, S.-J. Hwang, Y.-C. Chen, and F.-J. Chen, "Chinese herbal prescriptions for osteoarthritis in Taiwan: analysis of national health insurance dataset," *BMC Complementary and Alternative Medicine*, vol. 14, no. 1, p. 91, 2014.

[27] X. Xu, W. Zhang, C. Huang et al., "A novel chemometric method for the prediction of human oral bioavailability," *International Journal of Molecular Sciences*, vol. 13, no. 6, pp. 6964–6982, 2012.

[28] R. Ano, Y. Kimura, M. Shima, R. Matsuno, T. Ueno, and M. Akamatsu, "Relationships between structure and high-throughput screening permeability of peptide derivatives and related compounds with artificial membranes: application to prediction of Caco-2 cell permeability," *Bioorganic & Medicinal Chemistry*, vol. 12, no. 1, pp. 257–264, 2004.

[29] G. X. Hu, C. H. Zhang, W. N. Zhao, and Q. S. Yu, "QSPR study on the permeability of drugs across Caco-2 monolayer," *Journal of Zhejiang University*, vol. 3, pp. 304–308, 2009.

[30] W. P. Walters and M. A. Murcko, "Prediction of "drug-likeness"" *Advanced Drug Delivery Reviews*, vol. 54, no. 3, pp. 255–271, 2002.

[31] D. Metodiewa, A. Kochman, and S. Karolczak, "Evidence for antiradical and antioxidant properties of four biologically active N,N-diethylaminoethyl ethers of flavaone oximes: a comparison with natural polyphenolic flavonoid rutin action," *IUBMB Life*, vol. 41, no. 5, pp. 1067–1075, 1997.

[32] T. Pang, Z. Xie, Y. Chen, Y. H. Li, and M. R. Wen, "Simultaneous determination of 7 anthraquinone compounds in rhubarb compatible drugs by HPLC," *Chinese Journal of New Drugs*, vol. 26, no. 9, pp. 1079–1088, 2017, in Chinese.

[33] X. Y. Gao and J. Q. Lu, "Simultaneous determination of seven anthraquinones in rhubarb by HPLC-DAD," *Journal of Pharmaceutical Analysis*, vol. 30, no. 4, pp. 1636–1641, 2010, in Chinese.

[34] X. Wang, Y. Shen, S. Wang et al., "PharmMapper 2017 update: a web server for potential drug target identification with a comprehensive target pharmacophore database," *Nucleic Acids Research*, vol. 45, no. W1, pp. W356–W360, 2017.

[35] G. Stelzer, R. Rosen, I. Plaschkes et al., "The GeneCards suite: from gene data mining to disease genome sequence analysis," *Current Protocols in Bioinformatics*, vol. 54, pp. 1.30.1–1.30.33, 2016.

[36] A. Hamosh, A. F. Scott, J. S. Amberger, C. A. Bocchini, and V. A. McKusick, "Online Mendelian Inheritance in Man (OMIM), a knowledge base of human genes and genetic disorders," *Nucleic Acids Research*, vol. 33, no. Database issue, pp. D514–D517, 2004.

[37] D. Szklarczyk, A. Franceschini, S. Wyder et al., "STRING v10: protein-protein interaction networks, integrated over the tree of life," *Nucleic Acids Research*, vol. 43, no. D1, pp. D447–D452, 2015.

[38] G. D. Bader and C. W. Hogue, "An automated method for finding molecular complexes in large protein interaction networks," *BMC Bioinformatics*, vol. 4, no. 1, pp. 2–57, 2003.

[39] D. W. Huang, B. T. Sherman, and R. A. Lempicki, "Systematic and integrative analysis of large gene lists using DAVID bioinformatics resources," *Nature Protocols*, vol. 4, no. 1, pp. 44–57, 2009.

[40] A. Fabregat, S. Jupe, L. Matthews et al., "The reactome pathway knowledgebase," *Nucleic Acids Research*, vol. 46, no. D1, pp. D649–D655, 2018.

[41] Y. Li, Q.-Q. Xu, C.-S. Shan, Y.-H. Shi, Y. Wang, and G.-Q. Zheng, "Combined use of emodin and ginsenoside Rb1 exerts synergistic neuroprotection in cerebral ischemia/

reperfusion rats," *Frontiers in Pharmacology*, vol. 9, p. 943, 2018.

[42] J.-S. Lu, J.-X. Liu, W.-Y. Zhang, S.-W. Liang, D. Wang, and J. Fang, "Preventive effects of Emodin on cerebral ischemia injury and expression of the inflammatory factors in rats with cerebral ischemia," *China Journal of Chinese Materia Medica*, vol. 30, no. 24, pp. 1939–1943, 2005.

[43] S. M. Ahn, H. N. Kim, Y. R. Kim et al., "Emodin from Polygonum multiflorum ameliorates oxidative toxicity in HT22 cells and deficits in photothrombotic ischemia," *Journal of Ethnopharmacology*, vol. 188, pp. 13–20, 2016.

[44] T. Liu, H.-T. Hu, and Q.-R. Sun, "Neuroprotective effects of emodin on primary rat cortical neurons apoptosis induced by hydrogen peroxide," *Zhong Yao Cai*, vol. 33, no. 7, pp. 1116–1119, 2010.

[45] H. Guo, X. Shen, Y. Xu, J. Yuan, D. Zhao, and W. Hu, "Emodin prevents hypoxic-ischemic neuronal injury: involvement of the activin a pathway," *Neural Regeneration Research*, vol. 8, no. 15, pp. 1360–1367, 2013.

[46] A. B. Belousov, J. D. Fontes, M. Freitas-Andrade, and C. C. Naus, "Gap junctions and hemichannels: communicating cell death in neurodevelopment and disease," *BMC Cell Biology*, vol. 18, no. S1, p. 1, 2017.

[47] Y. Zhao, Y. Fang, J. Li et al., "Neuroprotective effects of chrysophanol against inflammation in middle cerebral artery occlusion mice," *Neuroscience Letters*, vol. 630, pp. 16–22, 2016.

[48] H. Ageta, A. Murayama, R. Migishima et al., "Activin in the brain modulates anxiety-related behavior and adult neurogenesis," *PLoS One*, vol. 3, no. 4, p. e1869, 2008.

[49] S. W. Leung, J. H. Lai, J. C.-C. Wu et al., "Neuroprotective effects of emodin against ischemia/reperfusion injury through activating ERK-1/2 signaling pathway," *International Journal of Molecular Sciences*, vol. 21, no. 8, pp. 2899–2020, 2020.

[50] Q. Zhao, X. Wang, A. Chen et al., "Rhein protects against cerebral ischemic/reperfusion induced oxidative stress and apoptosis in rats," *International Journal of Molecular Medicine*, vol. 41, no. 5, pp. 2802–2812, 2018.

[51] Y. Zhao, Y. Huang, Y. Fang et al., "Chrysophanol attenuates nitrosative/oxidative stress injury in a mouse model of focal cerebral ischemia/reperfusion," *Journal of Pharmacological Sciences*, vol. 138, no. 1, pp. 16–22, 2018.

[52] Y. Zhao, Y. Fang, H. Zhao et al., "Chrysophanol inhibits endoplasmic reticulum stress in cerebral ischemia and reperfusion mice," *European Journal of Pharmacology*, vol. 818, no. 5, pp. 1–9, 2018.

[53] J. Li, J. Liu, D. Wang et al., "Effects of rhubarb aglycone combined with thrombolysis on brain microvascular basement membrane impairment in rats with thrombus-occluded cerebral ischemia," *Zhongguo Zhongyao Zazhi*, vol. 35, no. 21, pp. 2908–2911, 2010.

[54] S.-X. Feng, J.-S. Li, L.-B. Qu, Y.-M. Shi, and D. Zhao, "Comparative pharmacokinetics of five rhubarb anthraquinones in normal and thrombotic focal cerebral ischemia-induced rats," *Phytotherapy Research*, vol. 27, no. 10, 2012.

[55] J. S. Kim and L. R. Caplan, "Clinical stroke syndromes," *Frontiers of Neurology and Neuroscience*, vol. 40, pp. 72–92, 2016.

[56] C. Iadecola, "The neurovascular unit coming of age: a journey through neurovascular coupling in health and disease," *Neuron*, vol. 96, no. 1, pp. 17–42, 2017.

[57] J. H. Zhang, J. Badaut, J. Tang, A. Obenaus, R. Hartman, and W. J. Pearce, "The vascular neural network-a new paradigm in stroke pathophysiology," *Nature Reviews Neurology*, vol. 8, no. 12, pp. 711–716, 2012.

[58] L. Zan, X. Zhang, Y. Xi et al., "SRC regulates angiogenic factors and vascular permeability after focal cerebral ischemia-reperfusion," *Neuroscience*, vol. 262, pp. 118–128, 2014.

[59] T. Hansen, A. Moss, and N. Brindle, "Vascular endothelial growth factor and angiopoietins in neurovascular regeneration and protection following stroke," *Current Neurovascular Research*, vol. 5, no. 4, pp. 236–245, 2008.

[60] B. R. Stockwell, J. P. Friedmann Angeli, H. Bayir et al., "Ferroptosis: a regulated cell death nexus linking metabolism, redox biology, and disease," *Cell*, vol. 171, no. 2, pp. 273–285, 2017.

[61] E. Sekerdag, I. Solaroglu, and Y. Gursoy-Ozdemir, "Cell death mechanisms in stroke and novel molecular and cellular treatment options," *Current Neuropharmacology*, vol. 16, no. 9, pp. 1396–1415, 2018.

[62] J. Anrather and C. Iadecola, "Inflammation and stroke: an overview," *Neurotherapeutics*, vol. 13, no. 4, pp. 661–670, 2016.

[63] R. Jin, L. Liu, S. Zhang, A. Nanda, and G. Li, "Role of inflammation and its mediators in acute ischemic stroke," *Journal of Cardiovascular Translational Research*, vol. 6, no. 5, pp. 834–851, 2013.

[64] K. J. Becker, "Inflammation and the silent sequelae of stroke," *Neurotherapeutics*, vol. 13, no. 4, pp. 801–810, 2016.

[65] Y. Gu, J. Chen, and J. Shen, "Herbal medicines for ischemic stroke: combating inflammation as therapeutic targets," *Journal of Neuroimmune Pharmacology*, vol. 9, no. 3, pp. 313–339, 2014.

[66] A. Janyou, P. Wicha, J. Jittiwat, A. Suksamrarn, C. Tocharus, and J. Tocharus, "Dihydrocapsaicin attenuates blood brain barrier and cerebral damage in focal cerebral ischemia/reperfusion via oxidative stress and inflammatory," *Scientific Reports*, vol. 7, no. 1, p. 10556, 2017.

[67] A. Neves Carvalho, O. Firuzi, M. Joao Gama, J. van Horssen, and L. Saso, "Oxidative stress and antioxidants in neurological diseases: is there still hope?" *Current Drug Targets*, vol. 18, no. 6, pp. 705–718, 2017.

[68] H. E. de Vries, M. Witte, D. Hondius et al., "Nrf2-induced antioxidant protection: a promising target to counteract ROS-mediated damage in neurodegenerative disease?" *Free Radical Biology and Medicine*, vol. 45, no. 10, pp. 1375–1383, 2008.

[69] X. Lin, T. Liu, P. Li et al., "iTRAQ-based proteomics analysis reveals the effect of rhubarb in rats with ischemic stroke," *BioMed Research International*, vol. 2018, Article ID 6920213, 13 pages, 2018.

[70] C. N. Egbujo, D. Sinclair, and C.-G. Hahn, "Dysregulations of synaptic vesicle trafficking in schizophrenia," *Current Psychiatry Reports*, vol. 18, no. 8, p. 77, 2016.

[71] F. Valtorta, M. Pennuto, D. Bonanomi, and F. Benfenati, "Synaptophysin: leading actor or walk-on role in synaptic vesicle exocytosis?" *BioEssays*, vol. 26, no. 4, pp. 445–453, 2004.

[72] X. K. Zhao, N. Xiao, J. B. Zhou et al., "Effects of ephedrine on the recovery of motor function in cerebral ischemic rats and the molecular mechanism," *Chinese Journal of Rehabilitation Medicine*, vol. 20, no. 3, pp. 172–175, 2005.

[73] A. John, E. Ng-Cordell, N. Hanna, D. Brkic, and K. Baker, "The neurodevelopmental spectrum of synaptic vesicle cycling disorders," *Journal of Neurochemistry*, vol. 157, no. 2, pp. 208–228, 2021.

[74] A. Margiotta, "Role of SNAREs in neurodegenerative diseases," *Cells*, vol. 10, no. 5, pp. 991–2021, 2021.

[75] L. I. Benowitz and A. Routtenberg, "GAP-43: an intrinsic determinant of neuronal development and plasticity," *Trends in Neurosciences*, vol. 20, no. 2, pp. 84–91, 1997.

[76] S. M. Strittmatter, T. Vartanian, and M. C. Fishman, "GAP-43 as a plasticity protein in neuronal form and repair," *Journal of Neurobiology*, vol. 23, no. 5, pp. 507–520, 1992.

[77] R. P. Stroemer, T. A. Kent, and C. E. Hulsebosch, "Enhanced neocortical neural sprouting, synaptogenesis, and behavioral recovery with d -amphetamine therapy after neocortical infarction in rats," *Stroke*, vol. 29, no. 11, pp. 2381–2395, 1998.

[78] K. Miyake, W. Yamamoto, M. Tadokoro et al., "Alterations in hippocampal GAP-43, BDNF, and L1 following sustained cerebral ischemia," *Brain Research*, vol. 935, no. 1-2, pp. 24–31, 2002.

[79] Y. Li, N. Jiang, C. Powers, and M. Chopp, "Neuronal damage and plasticity identified by microtubule-associated protein 2, growth-associated protein 43, and cyclin D1 immunoreactivity after focal cerebral ischemia in rats," *Stroke*, vol. 29, no. 9, pp. 1972–1981, 1998.

[80] W. Hua, H. Wu, M. Zhou et al., "Protective effects of recombinant human erythropoietin on oligodendrocyte after cerebral infarction," *Zhonghua Bing Li Xue Za Zhi*, vol. 44, no. 5, pp. 323–328, 2015, in Chinese.

[81] M. Zuo, H. Guo, T. Wan et al., "Wallerian degeneration in experimental focal cortical ischemia," *Brain Research Bulletin*, vol. 149, pp. 194–202, 2019.

[82] Y.-Y. Zhao, D.-J. Yan, and Z.-W. Chen, "Role of AIF-1 in the regulation of inflammatory activation and diverse disease processes," *Cellular Immunology*, vol. 284, no. 1-2, pp. 75–83, 2013.

[83] R. von Bernhardi, F. Heredia, N. Salgado, and P. Muñoz, "Microglia function in the normal brain," *Advances in Experimental Medicine and Biology*, vol. 949, pp. 67–92, 2016.

[84] N. Gupta, S. Jadhav, K.-L. Tan, G. Saw, K. B. Mallilankaraman, and S. T. Dheen, "miR-142-3p regulates BDNF expression in activated rodent microglia through its target CAMK2A," *Frontiers in Cellular Neuroscience*, vol. 14, pp. 132–2020, 2020.

[85] T. Akita, K. Aoto, M. Kato et al., "De novo variants in CAMK2A and CAMK2B cause neurodevelopmental disorders," *Annals of Clinical and Translational Neurology*, vol. 5, no. 3, pp. 280–296, 2018.

[86] Y. Park and J.-K. Ryu, "Models of synaptotagmin-1 to trigger Ca^{2+}-dependent vesicle fusion," *FEBS Letters*, vol. 592, no. 21, pp. 3480–3492, 2018.

[87] Z. Xie, J. Long, J. Liu, Z. Chai, X. Kang, and C. Wang, "Molecular mechanisms for the coupling of endocytosis to exocytosis in neurons," *Frontiers in Molecular Neuroscience*, vol. 10, p. 47, 2017.

[88] B. Wang, L. Pan, M. Wei et al., "FMRP-mediated axonal delivery of miR-181d regulates axon elongation by locally targeting Map1b and Calm1," *Cell Reports*, vol. 13, no. 12, pp. 2794–2807, 2015.

[89] H. Kobayashi, S. Saragai, A. Naito, K. Ichio, D. Kawauchi, and F. Murakami, "Calm1 signaling pathway is essential for the migration of mouse precerebellar neurons," *Development*, vol. 142, no. 2, pp. 375–384, 2015.

[90] B. Bae, H. N. Gruner, M. Lynch et al., "Elimination of Calm1 long 3′-UTR mRNA isoform by CRISPR-Cas9 gene editing impairs dorsal root ganglion development and hippocampal neuron activation in mice," *RNA*, vol. 26, no. 10, pp. 1414–1430, 2020.

[91] L. Gu, J. Huang, J. Li et al., "Association of CALM1 rs3179089 polymorphism with ischemic stroke in Chinese Han population," *NeuroMolecular Medicine*, vol. 20, no. 2, pp. 271–279, 2018.

[92] A. Muller, "Endogenous Ca^{2+} buffer concentration and Ca^{2+} microdomains in hippocampal neurons," *Journal of Neuroscience*, vol. 25, no. 3, pp. 558–565, 2005.

[93] Q. Guo, S. Christakos, N. Robinson, and M. P. Mattson, "Calbindin D28k blocks the proapoptotic actions of mutant presenilin 1: reduced oxidative stress and preserved mitochondrial function," *Proceedings of the National Academy of Sciences*, vol. 95, no. 6, pp. 3227–3232, 1998.

[94] B. Schwaller, "Cytosolic Ca^{2+} buffers," *Cold Spring Harbor Perspectives in Biology*, vol. 2, no. 11, Article ID a004051, 2010.

[95] B. Schwaller, "The use of transgenic mouse models to reveal the functions of Ca^{2+} buffer proteins in excitable cells," *Biochimica et Biophysica Acta (BBA)-General Subjects*, vol. 1820, no. 8, pp. 1294–1303, 2012.

[96] M. Zhao and A. T. Brunger, "Recent advances in deciphering the structure and molecular mechanism of the AAA+ ATPase N-Ethylmaleimide-Sensitive factor (NSF)," *Journal of Molecular Biology*, vol. 428, no. 9, pp. 1912–1926, 2016.

[97] T. C. Südhof and J. Rizo, "Synaptic vesicle exocytosis," *Cold Spring Harbor Perspectives in Biology*, vol. 3, no. 12, Article ID a005637, 2011.

[98] X. Lou, "Sensing exocytosis and triggering endocytosis at synapses: synaptic vesicle exocytosis-endocytosis coupling," *Frontiers in Cellular Neuroscience*, vol. 12, p. 66, 2018.

[99] T. Ziemssen, K. Akgün, and W. Brück, "Molecular biomarkers in multiple sclerosis," *Journal of Neuroinflammation*, vol. 16, no. 1, p. 272, 2019.

[100] T. M. Evans, H. V. Remmen, A. Purkar et al., "Microwave and magnetic (M2) proteomics of a mouse model of mild traumatic brain injury," *Translational Proteomics*, vol. 3, pp. 10–21, 2014.

[101] M. Gunnarsson, C. Malmeström, M. Axelsson et al., "Axonal damage in relapsing multiple sclerosis is markedly reduced by natalizumab," *Annals of Neurology*, vol. 69, no. 1, pp. 83–89, 2011.

[102] M. Cao, Y. Fang, W. Jia, Y. Wang, J. Sun, and D. Tao, "Emodin relieves hypoxia-triggered injury via elevation of microRNA-25 in PC-12 cells," *Artificial Cells, Nanomedicine, and Biotechnology*, vol. 47, no. 1, pp. 2678–2687, 2019.

[103] J. Liu, F. Kuang, G. Kroemer, D. J. Klionsky, R. Kang, and D. Tang, "Autophagy-dependent ferroptosis: machinery and regulation," *Cell Chemical Biology*, vol. 27, no. 4, pp. 420–435, 2020.

[104] Z. Peng, J. Li, Y. Li et al., "Downregulation of miR-181b in mouse brain following ischemic stroke induces neuroprotection against ischemic injury through targeting heat shock protein A5 and ubiquitin carboxyl-terminal hydrolase isozyme L1," *Journal of Neuroscience Research*, vol. 91, no. 10, pp. 1349–1362, 2013.

[105] Z. F. Peng, J. Meng, and J. H. Zhang, "The role of heat shock protein A5-mediated autophagy in cerebral ischemia/reperfusion injury in mice," *Chinese Journal of Applied Physiology*, vol. 33, no. 3, pp. 234–238, 2017.

[106] C. F. Peng, "Role of microRNA-181b in ischemic stroke mice through regulation of heat shock protein A5," *Journal of Anatomy*, vol. 48, no. 1, pp. 25–29, 2017.

[107] S. Liddelow and D. Hoyer, "Astrocytes: adhesion molecules and immunomodulation," *Current Drug Targets*, vol. 17, no. 16, pp. 1871–1881, 2016.

[108] M. Winther, V. Berezin, and P. S. Walmod, "NCAM2/OCAM/RNCAM: cell adhesion molecule with a role in neuronal compartmentalization," *The International Journal of Biochemistry & Cell Biology*, vol. 44, no. 3, pp. 441–446, 2012.

[109] M. Mehrabian, H. Hildebrandt, and G. Schmitt-Ulms, "NCAM1 polysialylation," *ASN Neuro*, vol. 8, no. 6, 2016.

[110] V. Berezin, P. S. Walmod, M. Filippov, and A. Dityatev, "Targeting of ECM molecules and their metabolizing enzymes and receptors for the treatment of CNS diseases," *Progress in Brain Research*, vol. 214, pp. 353–388, 2014.

[111] O. Reiner, "LIS1 and DCX: implications for brain development and human disease in relation to microtubules," *Scientific*, vol. 2013, Article ID 393975, 17 pages, 2013.

[112] O. Reiner, A. Gdalyahu, I. Ghosh et al., "DCX's phosphorylation by not just another kinase (JNK)," *Cell Cycle (Georgetown, Tex.)*, vol. 3, no. 6, pp. 747–751, 2004.

[113] F. Wang, *Neural Differentiation of Hippocampal Dentate Gyrus after Ischemic Stroke in Youth and the Role and Mechanism of Paclitaxel Intervention in Ischemic Stroke*, Yangzhou University, Yangzhou, China, 2021.

[114] X. Zhu, Z. Long, T. Bao, L. Liu, and K. Yang, "Exploring the mechanism of radix rhei et rhizome intervention in intracerebral hemorrhage based on systematic pharmacology and proteomics strategy," *Bioscience Reports*, vol. 41, no. 3, Article ID BSR20201910, 2021.

Hindawi
Evidence-Based Complementary and Alternative Medicine
Volume 2021, Article ID 6854860, 12 pages
https://doi.org/10.1155/2021/6854860

Research Article

Poria cocos Regulates Cell Migration and Actin Filament Aggregation in B35 and C6 Cells by Modulating the RhoA, CDC42, and Rho Signaling Pathways

Chia-Yu Lee,[1] Chang-Ti Lee,[1] I-Shiang Tzeng,[2] Chan-Yen Kuo,[2] Fu-Ming Tsai,[2] and Mao-Liang Chen[2]

[1]*Department of Chinese Medicine, Taipei Tzu Chi Hospital, Buddhist Tzu Chi Medical Foundation, New Taipei 231, Taiwan*
[2]*Department of Research, Taipei Tzu Chi Hospital, Buddhist Tzu Chi Medical Foundation, New Taipei 231, Taiwan*

Correspondence should be addressed to Mao-Liang Chen; cater0656@hotmail.com

Received 16 June 2021; Revised 13 August 2021; Accepted 26 August 2021; Published 1 September 2021

Academic Editor: Ghulam Ashraf

Copyright © 2021 Chia-Yu Lee et al. This is an open access article distributed under the Creative Commons Attribution License, which permits unrestricted use, distribution, and reproduction in any medium, provided the original work is properly cited.

Poria is used as a traditional Chinese herbal medicine with anti-inflammatory, anticancer, and mood-stabilizing properties. Poria contains triterpenoids and polysaccharides, which are reported to regulate the cytoplasmic free calcium associated with the *N*-methyl-D-aspartate receptor and affect the cell function of neonatal rat nerve cells and hippocampal neurons. Although the modulatory effects of Poria on neuronal function have been widely reported, the molecular mechanism of these effects is unclear. Cell migration ability and the reorganization of actin filaments are important biological functions during neuronal development, and they can be regulated mainly by the Rho signaling pathway. We found that the cell migration ability and actin condensation in B35 cells enhanced by *P. cocos* (a water solution of *P. cocos* cum Radix Pini (PRP) or White Poria (WP)) might be caused by increased RhoA and CDC42 activity and increased expression of downstream ROCK1, p-MLC2, N-WASP, and ARP2/3 in B35 cells. Similar modulations of cell migration ability, actin condensation, and Rho signaling pathway were also observed in the C6 glial cell line, except for the PRP-induced regulation of RhoA and CDC42 activities. Ketamine-induced inhibition of cell migration and actin condensation can be restored by *P. cocos*. In addition, we observed that the increased expression of RhoA and ROCK1 or the decreased expression of CDC42 and N-WASP caused by ketamine in B35 cells could also be restored by *P. cocos*. The results of this study suggest that the regulatory effects of *P. cocos* on cell migration and actin filament aggregation are closely related to the regulation of RhoA, CDC42, and Rho signaling pathways in both B35 and C6 cells. PRP and WP have the potential to restore neuronal cell Rho signaling abnormalities involved in some mental diseases.

1. Introduction

Poria cocos (Schw.) is a parasitic fungus that exists in various species of *Pinus*. *P. cocos* cum Radix Pini (PRP; Sclerotium Pararadicis, also known as *Fu Shen* in traditional Chinese herbal medicine), and White Poria (WP; also known as *Bai Fu Ling* in traditional Chinese herbal medicine) are medicinal herbs from the dry sclerotium of Polyporaceae fungi that have diuretic, sedative, and tonic effects [1]. They both contain two major types of chemical substances, namely, triterpenoids and polysaccharides. Their other minor ingredients include histidine, amino acids, choline, steroids, and potassium salts [2, 3]. *P. cocos* mediates its pharmacological anti-inflammatory properties via two triterpenoids, namely, pachymic acid and dehydrotumulosic acid [4]. *P. cocos* also has immunomodulatory properties that can alter immune function through dynamically regulated cytokine expression [5, 6]. It has also been reported to possess anticancer properties [2, 7–9]. Moreover, *P. cocos* has been found to regulate the concentration of free calcium in the cytoplasm of brain neurons in neonatal rats [10]. Water extracts of *P. cocos* have been demonstrated to dose-dependently increase cytosolic free calcium [2] and inhibit glutamate-induced cytosolic free calcium [10] in cells.

Similar results have been observed in the primary culture of hippocampal neurons from neonatal rats. Thus, *P. cocos* water extracts can regulate cytoplasmic free calcium in brain nerve cells by affecting a variety of glutamate receptors, such as *N*-methyl-D-aspartate receptor (NMDAR) [10].

The integration of the hippocampus and posterior splenic cortex into a high-level cognitive circuit supports learning and memory in the form of relationships (space, context, and situation) [11]. Impairments in hippocampal neurons might cause abnormal cognitive function in animals [12]. Reduced hippocampal neuronal activities, caused by a reduction in hippocampal neurogenesis or an abnormality of the hippocampal neuronal structure, are always accompanied by cognitive impairments in NMDAR antagonist-treated rats [13, 14]. Schubert et al. [15] reported that active Ras homolog family member A (RhoA) interacts with NMDAR, α-amino-3-hydroxy-5-methyl-4-isoxazolepropionic acid receptor, and metabotropic glutamate receptor 1 at the excitatory postsynapsis to maintain NMDAR stabilization and modulate spine actin remodeling [15]. They also mentioned that the activation of RhoA can induce dendritic spine morphology regulation in cultured hippocampal neurons [15]. Cell division cycle 42 (CDC42) levels and dendritic spine density have also been observed to decrease in patients with schizophrenia. A recent report revealed that ketamine can reduce the expression levels of RhoA and Rho-associated coiled-coil containing protein kinase 1 (ROCK1) while simultaneously reducing the proportion of mushroom spines and increasing the proportion of stubby spines in rat hippocampal neurons, which could be involved in the cognitive impairments of schizophrenia [16].

The formation of actin filaments in neuronal cells can induce cytoskeletal rearrangement, which can lead to changes in cell shape and cell function [17]. Cytoskeletal rearrangement also induces synaptic spine elongation, cell migration [18–20], and neuronal plasticity [21, 22], which are important for neuron development and have the same molecular mechanism, namely, the Rho signaling pathway. Furthermore, various studies have mentioned that the calcium concentration in cells plays important roles in regulating Rho signaling regulation and further directional movement, mesodermal sheet migration, cytoskeletal reorganization, and cancer metastasis [18, 23–25]. Our previous study found that APDs might differentially regulate Rho protein expression and activation to further modulate cytoskeletal rearrangement by altering the expression of proteins that are involved in the Rho signaling pathway in B35 and C6 cells and APD-treated rat cortex [26]. We also found that APDs could reverse MK801-induced Rho protein regulation, migration, and actin filament (F-actin) condensation in B35 and C6 cells. In this study, we proposed that *P. cocos* might also provide potential regulatory and modulatory effects on neuronal cell activities by affecting the NMDAR-mediated calcium-related Rho signaling pathway. We aimed to determine whether PRP and WP can regulate the expression and activity of Rho family proteins in B35 and C6 cells. We also examined the effects of PRP and WP on proteins related to Rho signaling. We further investigated whether PRP and WP could enhance the migration ability and F-actin condensation of B35 and C6 cells. Additionally, ketamine-induced B35 cell migration inhibition, which was used to mimic the damaging effect on neuronal cells, was restored by PRP and WP. Ketamine-induced RhoA, CDC42, N-WASP, and ROCK1 expression regulation was also recovered by PRP and WP. We concluded that PRP and WP can modulate the Rho signaling pathway by regulating the expression level and activity of RhoA and CDC42 but not Rac1, thereby increasing cell migration and the F-actin concentration.

2. Materials and Methods

2.1. Preparation of PRP and WP. Herbal powder extracts of PRP and WP were obtained from Sun Ten Pharmaceutical Company (New Taipei City, Taiwan). To prepare the PRP and WP solutions, herbal powder extracts of PRP and WP were added to sterilized double-distilled H_2O and left at room temperature for 6 h at a final concentration of 10 mg/ml. The PRP and WP solutions were then centrifuged, and the corresponding supernatants were collected and stored at −20°C until use.

2.2. Cell Culture and PRP/WP Treatment. B35 and C6 cells were obtained from the Bioresource Collection and Research Center of the Food Industry Research and Development Institute (Hsinchu City, Taiwan). B35 cells are a rat neuroblastoma cell line used to observe drug effects on neuronal cells. Glial cells can provide nutritional and physiological support, such as neurotransmitter reuptake and recycling to neuronal cells. C6 cells are a glioblastoma cell line used for observing drug effects on glial cells. C6 cells were also used to compare the drug effects between B35 and C6 cells. B35 cells were cultured in modified Eagle's medium (Invitrogen Life Technologies) with fetal bovine serum (10%) (Invitrogen Life Technologies). PRP or WP was added once a day to a final concentration of 10 μg/ml for seven days. To examine the effects of PRP or WP on ketamine-treated B35 cells, B35 cells were treated with ketamine (100 μg/ml) daily for seven days followed by the addition of ketamine (100 μg/ml) and ketamine in combination with PRP (10 μg/ml) or WP (10 μg/ml) daily for another seven days. C6 cells were cultured in high-glucose Dulbecco's modified Eagle's medium (Invitrogen Life Technologies, Carlsbad, CA, USA) containing L-glutamine (2 mm), fetal bovine serum (2%) (Invitrogen Life Technologies), and heat-inactivated horse serum (10%) (Invitrogen Life Technologies). The C6 cells were subcultured when the cell density reached 70% confluence to prevent abnormal S100 protein production. Both cell lines were cultured in a CO_2 incubator with 5% CO_2 at 37°C. The cells were harvested for examination after they had been treated with PRP or WP for seven days.

2.3. Total Protein Extraction and Western Blot Analysis. B35 and C6 cells were lysed in mammalian protein extraction buffer (GE Healthcare Bio-Sciences, Uppsala, Sweden) to extract total proteins according to the manufacturer's procedures. Protease inhibitor mix (GE

Healthcare Bio-Sciences) and phosphatase inhibitors (2 mm NaF and 1 mm Na_3VO_4) were added to the lysis buffer to prevent protein degradation. In total, 10–50 μg of the total protein extracts was analyzed using 8%, 10%, or 12.5% sodium dodecyl sulfate-polyacrylamide gel electrophoresis according to the molecular weight of the target proteins. The separated proteins were then transferred from the gels to polyvinylidene difluoride membranes and blocked with membrane blocking solution (Life Technology, Frederick, MD, USA). β-Actin was used as an internal calibration control for all of the target proteins. Specific primary antibodies and horseradish peroxidase-conjugated goat anti-mouse or anti-rabbit antibodies (cat. nos. 401215 and 401315; Calbiochem, Darmstadt, Germany) were used to detect the target protein bands. An Amersham ECL kit (Amersham, Bucks, UK) was then used to reveal the protein bands.

2.4. RhoA/Rac1/Cdc42 Activity Assay. Rho protein activity was analyzed using the RhoA/Rac1/Cdc42 activity assay kit (Cell Biolab, San Diego, CA, USA). In brief, cells cultured in a 10 cm dish were washed with PBS and lysed in 0.5 mL of lysis buffer containing protease inhibitor mix (GE Healthcare Bio-Sciences) and phosphatase inhibitors (2 mm NaF and 1 mm Na_3VO_4). After centrifugation at $14{,}000 \times g$ for 5 min, 300 μg of protein from each cellular lysate was adjusted to a total volume of 1 ml with 1 × assay lysis buffer. Then, each sample received 40 μl of resuspended Rhotekin RBD or PAK PBD agarose beads, and all assay mixtures were incubated for one hour at 4°C with gentle shaking. The beads were then collected by centrifugation at $14{,}000 \times g$ for 10 s followed by removing the supernatants and washing the bead pellets three times with 0.5 ml of 1 × assay lysis buffer. The beads were resuspended in 40 μl of 2 × SDS-PAGE sample buffer and boiled for 5 min. The samples were then analyzed by western blot and detected with anti-RhoA, anti-CDC42, or anti-Rac1 antibodies.

2.5. Cell Migration Assay. To examine the migration ability of B35 and C6 cells, they were treated with PRP or WP for seven days followed by seeding 10^4 PRP- or WP-treated B35 cells and 5×10^3 PRP- or WP-treated C6 cells into a Transwell insert (pore size, 8 μm) (Costar; Corning Incorporation, Kennebunk, ME, USA) set in a 24-well tissue culture plate. The cells were cultured for another 24 h with PRP or WP for continuous stimulation. To examine the effects of PRP or WP on the migration ability of ketamine-treated B35 cells, B35 cells were treated with ketamine for seven days, followed by treatment with ketamine, ketamine with PRP, or ketamine with WP for another seven days. A total of 10^4 drug-treated B35 cells were seeded into Transwell inserts and cultured for another 24 h with ketamine, PRP, or WP for continuous stimulation. The migrated B35 and C6 cells were washed with 1 × phosphate-buffered saline (PBS) and fixed with methanol and stained with 50 μg/ml propidium iodide solution (Sigma, Saint Louis, MO, USA) for 30 min. The number of cells on the membrane was then counted under a microscope at 40 × magnification. The experiments were performed in triplicate for statistical analysis.

2.6. Phalloidin Staining of B35 and C6 Cell F-Actin. Fluorescently labeled phalloidin can stably and specifically bind to F-actin filaments in cells. To observe the F-actin condensation induced by PRP and WP, B35 and C6 cells (5×10^3) treated with PRP or WP for seven days were seeded into a 6-well plate with poly-L-lysine-coated coverslips and then cultured with PRP or WP for another two days accordingly. After the two-day incubation, the coverslips were collected and washed with 1 × PBS. Cells on the coverslips were then fixed in methanol. Subsequently, the cells were washed with 1 × PBS and stained with 1 × phalloidin solution (CytoPainter Phalloidin-iFluor 488 Reagent, ab176753; Abcam, Waltham, MA, USA) at room temperature for 90 min. Residual phalloidin was washed off two to three times with 1 × PBS. The coverslips were mounted and sealed on glass slides and then viewed under a fluorescence microscope.

2.7. Statistical Analysis. Student's *t*-tests were performed to analyze differences in the cell migration ability and normalized expression levels of the examined target proteins between the control cells and PRP- or WP-treated B35 and C6 cells. SPSS 20.0 was used for statistical analysis. p values of <0.05 (*) and <0.01 (**) were defined as statistically significant.

3. Results

3.1. PRP and WP Induced Regulation of the Rho Family Proteins. RhoA, CDC42, and Rac1 are major Rho family proteins that can be regulated by RhoGDP-dissociation inhibitor 1 (RhoGDI1) and affect the modulation of Rho signaling. We found that PRP and WP increased the expression of RhoGDI1 ($p < 0.05$ for PRP and $p < 0.01$ for WP) in B35 cells (Figures 1(a) and 1(b)). Moreover, PRP and WP increased the expression of RhoA ($p < 0.05$ for PRP and $p < 0.01$ for WP) and CDC42 ($p < 0.05$ for PRP and $p < 0.01$ for WP) in B35 cells (Figures 1(a) and 1(b)). Downregulation of RhoGDI1 ($p < 0.05$) was observed in C6 cells treated with PRP (Figures 1(c) and 1(d)). PRP also reduced the expression of RhoA ($p < 0.01$) and CDC42 ($p < 0.01$) in C6 cells (Figures 1(c) and 1(d)). In contrast, WP increased the expression of RhoGDI1 ($p < 0.05$), RhoA ($p < 0.01$), and CDC42 ($p < 0.01$) in C6 cells (Figures 1(c) and 1(d)). Furthermore, neither PRP nor WP affected Rac1 expression in B35 and C6 cells (Figure 1). A pulldown assay was also performed to examine the activation of the Rho family proteins by measuring the expression of GTP form Rho family proteins. We observed that the GTP forms of RhoA (activated RhoA; RhoA-GTP) and CDC42 (activated CDC42; CDC42-GTP) were increased by either PRP ($p < 0.01$) or WP ($p < 0.05$) in B35 cells (Figures 2(a) and 2(b)). In C6 cells, PRP increased RhoA-GTP ($p < 0.05$) and decreased CDC42-GTP ($p < 0.05$) levels, while WP decreased RhoA-GTP ($p < 0.05$) and CDC42-GTP ($p < 0.05$) levels (Figures 2(c) and 2(d)). No GTP form of Rac1

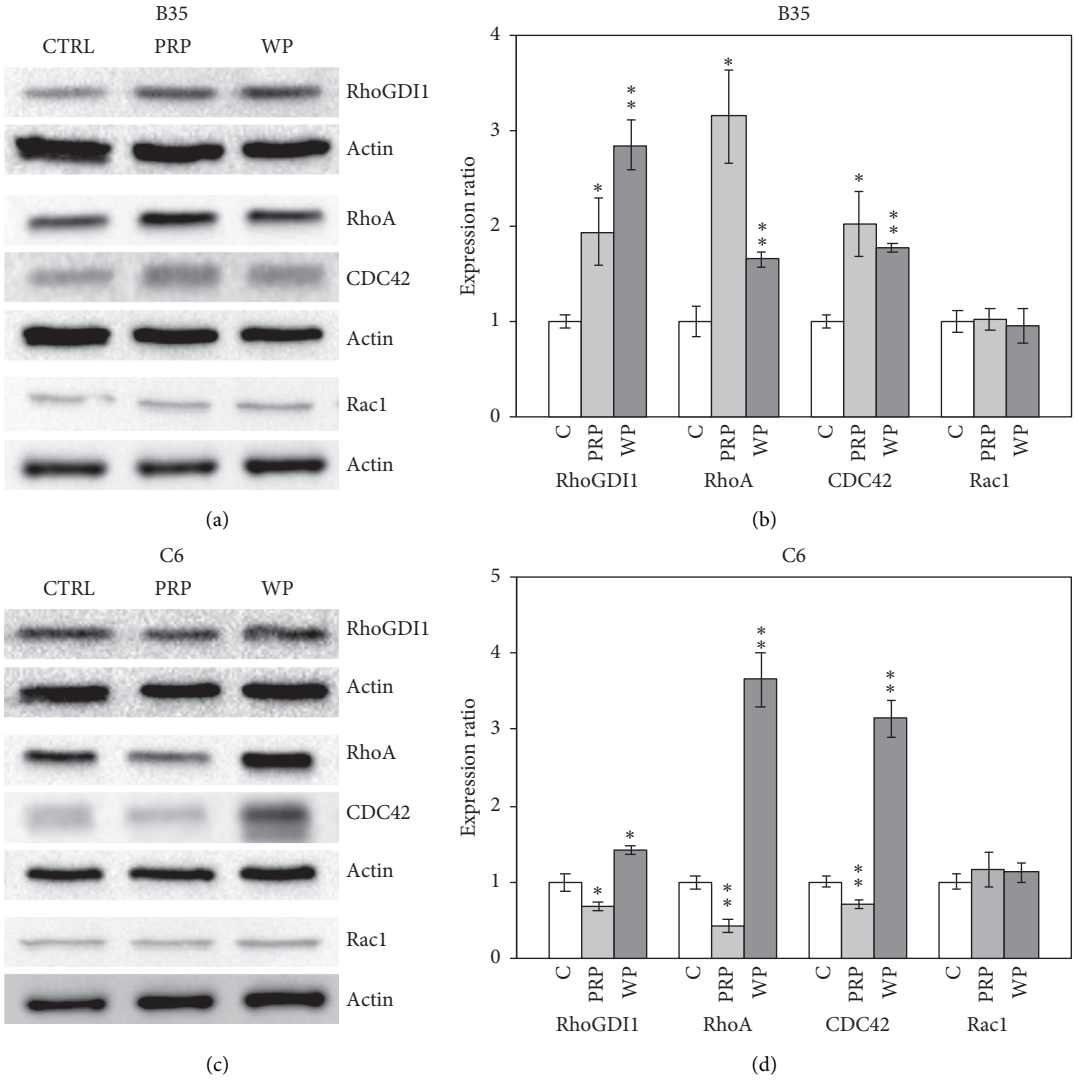

Figure 1: *Poria cocos* regulated RhoGDI1, RhoA, and CDC42 expression in B35 and C6 cells. The expression levels of RhoGDI1, RhoA, CDC42, and Rac1 were examined using western blotting in this experiment. B35 (a, b) and C6 (c, d) cells were treated with PRP (10 μg/ml) or WP (10 μg/ml). The bar charts were calculated based on triplicate western blot data from three batches of PRP- or WP-treated cells using Student's *t*-test ($^{*}p < 0.05$; $^{**}p < 0.01$). C/CTRL: control; PRP: *Poria cocos* cum Radix Pini; WP: White Poria.

(activated Rac1; Rac1-GTP) was detected in either the B35 or C6 cells in this study.

3.2. PRP and WP Modulated F-Actin Condensation and RhoA-Related Rho Signaling. Rho proteins, including ROCK1, phosphorylated myosin light chain 2 (p-MLC2), and profilin 1 (PFN1), have been proposed to be able to regulate RhoA-related signaling to further modulate F-actin assembly and condensation. Usually, F-actin is evenly distributed in cells (indicated with a blue arrow in Figure 3) and will be condensed (indicated with a red arrow in Figure 3) when regulated. In this study, F-actin condensation in B35 cells was induced by PRP and WP (Figure 3). In addition, PRP and WP also induced F-actin condensation in C6 cells (Figure 3). The expression of ROCK1 was increased by PRP ($p < 0.01$) and WP ($p < 0.01$) in B35 cells (Figures 4(a) and 4(b)). PFN1 expression was reduced by PRP ($p < 0.05$), but not by WP in B35 cells (Figures 4(a) and 4(b)). An increase in the expression of p-MLC2 induced by PRP ($p < 0.01$) and WP ($p < 0.05$) was also observed in B35 cells (Figures 4(a) and 4(b)). Moreover, PRP-induced increased expression of ROCK1 ($p < 0.05$), PFN1 ($p < 0.05$), and p-MLC2 ($p < 0.01$) in C6 cells (Figures 4(c) and 4(d)), whereas WP induced the expression of ROCK1 ($p < 0.05$), PFN1 ($p < 0.05$), and p-MLC2 ($p < 0.05$) in C6 cells (Figures 4(c) and 4(d)).

3.3. PRP and WP Modulated CDC42 Migration-Related Rho Signaling. CDC42 signaling can modulate filopodia and the migration of cells by regulating CDC42 and CDC42 signaling-related proteins, including neuronal Wiskott–Aldrich syndrome protein (N-WASP), p21 (RAC1)-activated kinase 1 (PAK1), and RhoA protein–modulated actin-related protein 2/3 (ARP2/3). Activated CDC42 can modulate cell migration by regulating N-WASP or PAK1.

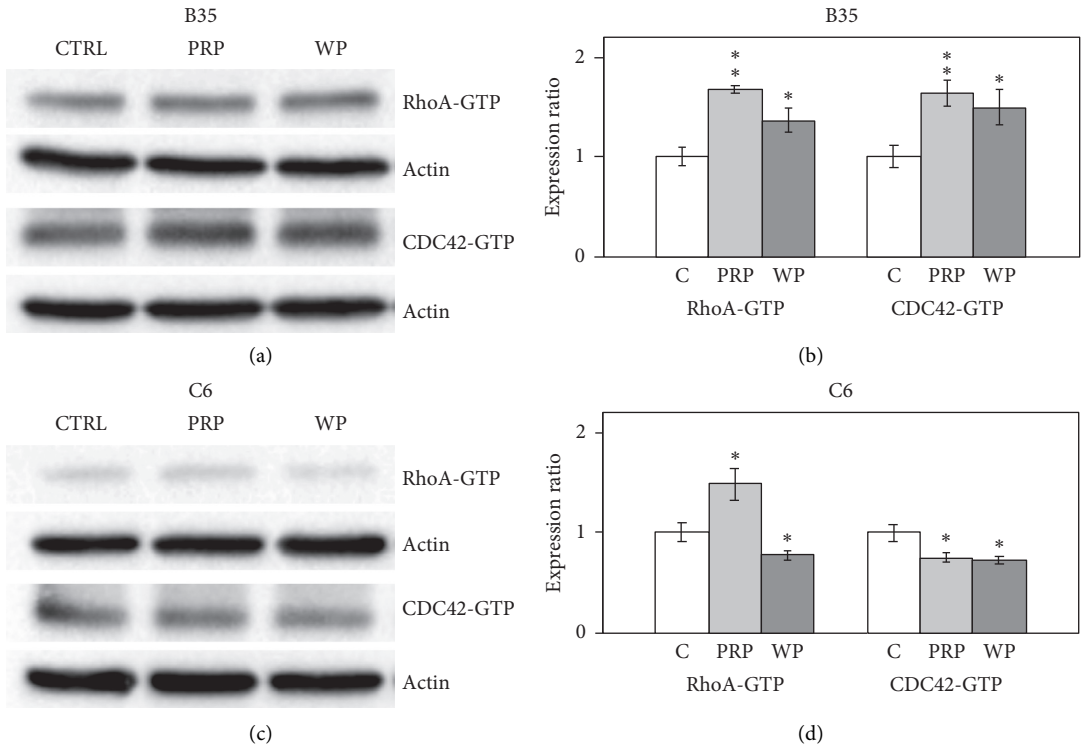

Figure 2: *Poria cocos* induced activation of RhoA and CDC42 in B35 and C6 cells. The expression levels of activated RhoA, CDC42, and Rac1 were examined using western blotting in this experiment. B35 (a, b) and C6 (c, d) cells were treated with PRP (10 μg/ml) or WP (10 μg/ml). The GTP form of Rho protein was pulled down and analyzed. The bar charts were calculated based on triplicate western blot data from three batches of PRP- or WP-treated cells using Student's *t*-test ($^{*}p < 0.05$; $^{**}p < 0.01$). C/CTRL: control; PRP: *Poria cocos* cum Radix Pini; WP: White Poria.

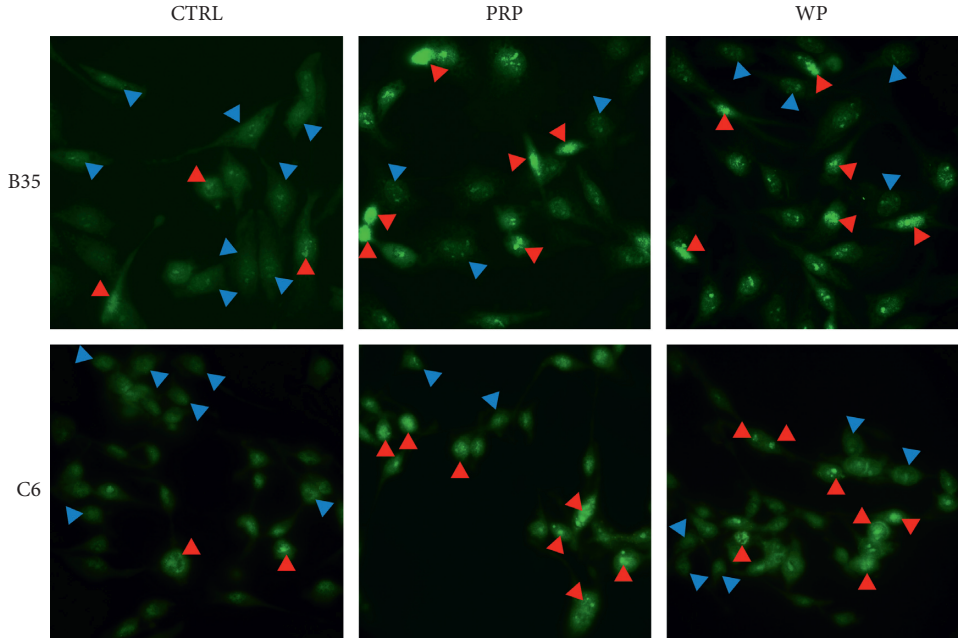

Figure 3: *Poria cocos* induced actin filament condensation in B35 and C6 cells. B35 and C6 cells were treated with PRP (10 μg/ml) or WP (10 μg/ml) for seven days and then stained with CytoPainter Phalloidin-iFluor 488 Reagent. The blue arrows indicate uniformly distributed F-actin, and the red arrows indicate condensed F-actin. C/CTRL: control; PRP: *Poria cocos* cum Radix Pini; WP: White Poria.

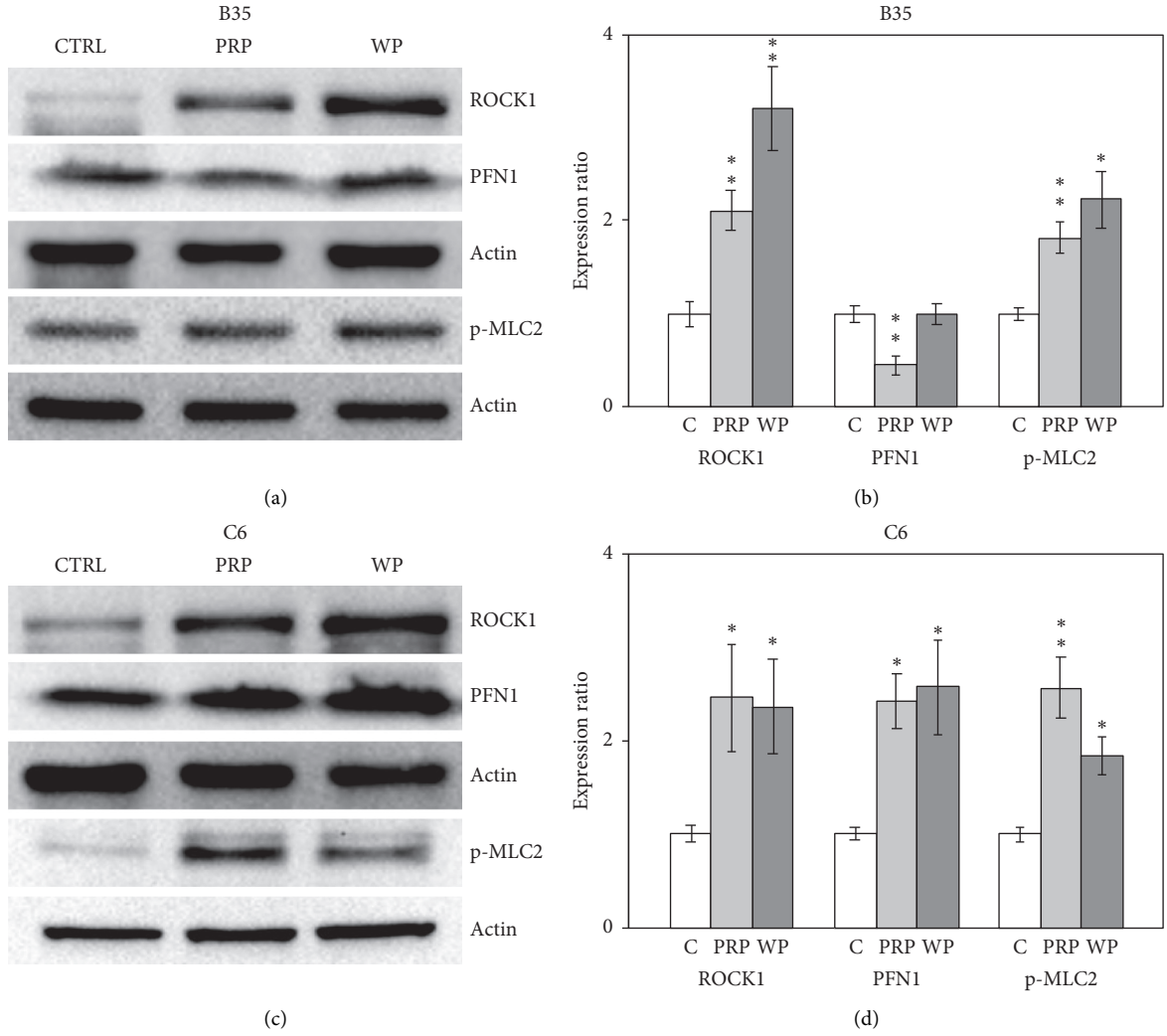

Figure 4: *Poria cocos* induced RhoA-related Rho signaling regulation. The expression levels of ROCK1, N-PFN1, and p-MLC2 were examined using western blotting in this experiment. B35 (a, b) and C6 (c, d) cells were treated with PRP (10 μg/ml) or WP (10 μg/ml). The bar charts were calculated based on triplicate western blot data from three batches of PRP- or WP-treated cells using Student's *t*-test ($^{*}p < 0.05$; $^{**}p < 0.01$). C/CTRL: control; PRP: *Poria cocos* cum Radix Pini; WP: White Poria.

N-WASP can modulate ARP2/3 to further manage actin polymerization and subsequent cell migration. PAK1 can regulate cofilin function to control actin polymerization and cell migration. PRP- or WP-treated B35 and C6 cells were seeded into a Transwell insert, incubated with PRP or WP for another 24 h, and then analyzed to confirm PRP- or WP-induced cell migration. As shown in Figure 5, PRP and WP increased the migration ability of B35 ($p < 0.01$ for both PRP and WP) and C6 ($p < 0.01$ for both PRP and WP) cells.

CDC42 signaling-related proteins were also analyzed with western blotting. N-WASP expression in B35 cells was enhanced by PRP ($p < 0.05$) and WP ($p < 0.01$) (Figures 6(a) and 6(b)). Interestingly, PRP and WP reduced N-WASP expression in C6 cells ($p < 0.01$ for PRP and $p < 0.05$ for WP) (Figures 6(c) and 6(d)). The expression of PAK1 was induced by PRP and WP in B35 ($p < 0.01$ for PRP and $p < 0.05$ for WP) (Figures 6(a) and 6(b)) and C6 ($p < 0.05$ for PRP and $p < 0.01$ for WP) cells (Figures 6(c) and 6(d)). ARP2/3 expression was induced by PRP but inhibited by WP in B35 cells. Both PRP ($p < 0.01$) and WP ($p < 0.01$) increased the expression of ARP2/3 in C6 cells (Figures 6(c) and 6(d)).

3.4. PRP and WP Modulated c-jun Expression in B35 and C6 Cells. Rho proteins have been reported to regulate c-jun expression and subsequently regulate apoptotic gene expression. As shown in Figures 6(a) and 6(b), increased expression of c-jun was induced by PRP ($p < 0.05$) and WP ($p < 0.05$) in B35 cells. c-jun expression in C6 cells was also increased by PRP ($p < 0.05$) and WP ($p < 0.01$) (Figures 6(c) and 6(d)).

3.5. PRP and WP Restored Cell Migration Inhibition and Rho Signaling Regulation in Ketamine-Treated B35 Cells. Ketamine has been reported to induce Rho family protein regulation *in vitro* and *in vivo*. We treated B35 cells with

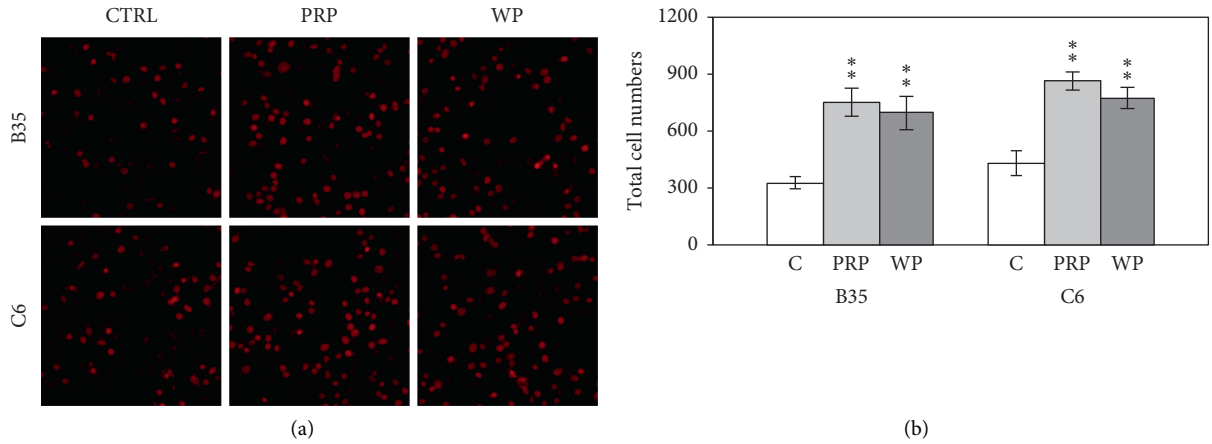

Figure 5: Cell migration regulation induced by PRP and WP in B35 and C6 cells. (a) Propidium iodide staining revealed increased migration of B35 and C6 cells treated with PRP or WP. (b) The bar chart was calculated from three cell migration assays of PRP- or WP-treated cells and analyzed using Student's *t*-test ($^{*}p < 0.05$; $^{**}p < 0.01$). C/CTRL: control; PRP: *Poria cocos* cum Radix Pini; WP: White Poria.

ketamine followed by PRP or WP treatment to further clarify the roles of PRP or WP in Rho signaling-related cytoskeletal regulation in neuronal cells. As Figure 7 shows, B35 cell migration was inhibited by ketamine and was restored by either PRP or WP treatment. We also examined the expression level of some of the Rho signaling proteins in B35 cells treated with ketamine or in combination with PRP/WP. We found that ketamine increased RhoA ($p < 0.01$) and decreased CDC42 ($p < 0.05$) expression in B35 cells, while both PRP and WP reversed ketamine-induced RhoA and CDC42 regulation (Figures 8(a) and 8(b)). Ketamine enhanced Rock1 expression, while PRP ($p < 0.01$)/WP ($p < 0.01$) reversed ketamine-induced ROCK1 induction in B35 cells (Figures 8(c) and 8(d)). We also found that ketamine could induce a reduction in N-WASP expression, which could be restored by PRP or WP treatment (both $p < 0.01$) in B35 cells (Figures 8(c) and 8(d)). Ketamine-reduced PAK1 expression ($p < 0.05$) was further reduced by PRP ($p < 0.01$) but not WP in B35 cells (Figures 8(e) and 8(f)).

Postsynaptic density protein 95 (PSD-95) is a scaffold protein that can promote excitatory synapse maturation of neurons. The expression and accumulation of PSD-95 in postsynaptic dendrites is closely related to Rho protein-dependent cell cytoskeleton regulation [15, 27]. We observed that ketamine decreased PSD-95 expression, which was recovered by WP treatment in B35 cells (Figures 8(e) and 8(f)).

4. Discussion

P. cocos (Schw.) is a saprophytic fungus that parasitizes various species of *Pinus*, such as *Pinus densiflora* and *Pinus massoniana* [28]. Recent pharmacological research has revealed that *P. cocos* polysaccharides have antinephritic, immunomodulatory, anti-inflammatory, antioxidant, and antitumor effects [29–31]. *P. cocos* has been proposed to treat insomnia through the neurotransmitter γ-aminobutyric acid or by stimulating the γ-aminobutyric acid AA receptor [32]. *P. cocos* water extracts have also been suggested as herbal medicines for treating depression [33]. A recent study reported that *P. cocos* polysaccharides exhibited neuroprotective effects by regulating various cell functions in an Alzheimer's disease rat model [34]. *P. cocos* has also been found to exhibit antioxidant ability against oxidative stress and to prevent PC12 β-amyloid-induced cell death [35].

Rho protein signaling could modulate cell apoptotic gene expression, migration, morphological modulation, and cytoskeletal reorganization by regulating ROCK1 function and downstream MLC2 phosphorylation [16]. The phosphorylation of MLC2 will then induce myosin activation and stress fiber contraction in cells [36, 37]. In addition, the RhoA protein can regulate the expression of ARP2/3 to control cell filopodia and migration [38, 39]. CDC42-induced PAK1/N-WASP activation can also regulate ARP2/3-mediated cytoskeletal remodeling [40]. Recent studies also reported that, in addition to RAC1, PAK1 can be regulated by CDC42 signaling to affect cell migration [41–43]. These findings indicate that neuronal dysfunction caused by abnormal Rho protein expression/activation and downstream Rho protein-mediated pathway signaling may be corrected by reconstructing Rho protein signaling.

In this study, we found that PRP and WP could enhance RhoA, RhoA-GTP, ROCK1, and p-MLC2 expression in B35 neuronal cells. We also observed that PRP and WP could induce CDC42, CDC42-GTP, and N-WASP expression in B35 cells. In addition, PRP and WP enhanced the migration ability and induced F-actin condensation in B35 cells. These results indicate that PRP and WP can regulate cell migration and F-actin aggregation by regulating the Rho signaling pathway, especially by affecting RhoA and CDC42 instead of Rac1.

We also investigated whether ketamine inhibits the migration ability of B35 cells and modulates RhoA, CDC42, ROCK1, and N-WASP expression levels. Ketamine-induced Rho signaling regulation has been linked to various mental disorders. Our results show that PRP and WP can restore ketamine-induced cell migration inhibition and can reverse

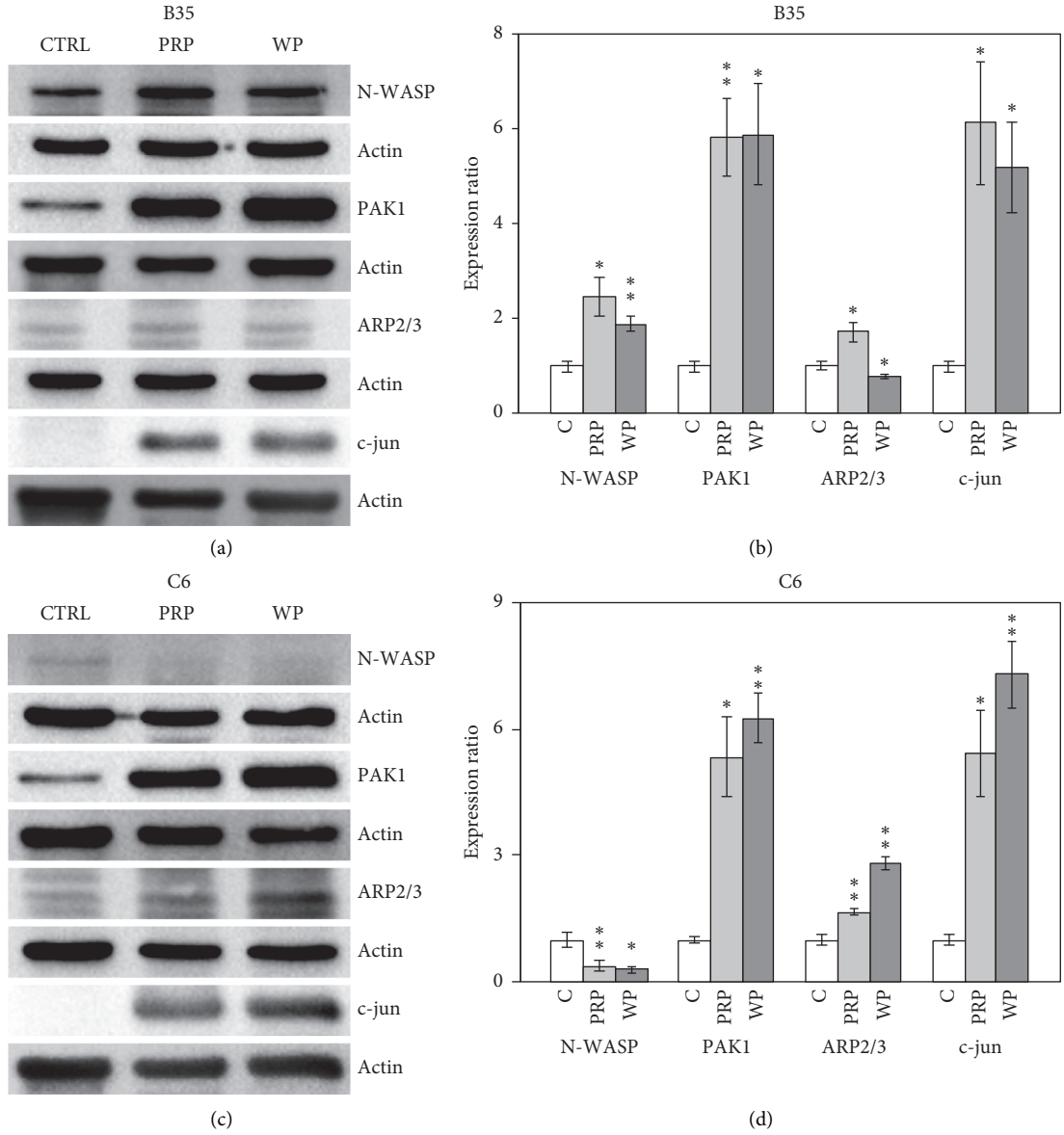

Figure 6: *Poria cocos* induced CDC42/cell migration-related Rho signaling regulation and c-jun expression. The expression levels of N-WASP, PAK1, ARP2/3, and c-jun were examined using western blotting in this experiment. B35 (a, b) and C6 (c, d) cells were treated with PRP (10 μg/ml) or WP (10 μg/ml). The bar charts were calculated based on triplicate western blot data from three batches of PRP- or WP-treated cells using Student's *t*-test ($^{*}p < 0.05$; $^{**}p < 0.01$). C/CTRL: control; PRP: *Poria cocos* cum Radix Pini; WP: White Poria.

the ketamine-induced expression regulation of RhoA, CDC42, ROCK1, and N-WASP. These findings suggest that PRP and WP have the potential to correct dysfunction in impaired neurons by regulating abnormal Rho protein signaling.

ROCK1 and PAK1 act as regulators of cofilin activity by modulating LIM kinase activity. High expression levels of ROCK1 and PAK1 can inhibit cofilin activity, leading to further actin polymerization and F-actin stabilization [44, 45]. Our results showed that the expression of ROCK1 and N-WASP induced by PRP/WP enhanced the expression of p-MLC2 and ARP2/3, together with the expression of ROCK1 and PAK1 induced by PRP/WP, leading to cell migration, actin polymerization, and F-actin stabilization. In addition, we found unstable PAK1 expression levels among different control B35 samples and drug-treated B35 cells. We propose that the expression levels of PAK1 might be dynamically controlled by some unrevealed factors. Further studies should be performed to come to a reasonable conclusion about the unstable PAK1 expression.

We also found that WP exhibited effects on Rho protein signaling regulation in C6 cells similar to those observed in B35 cells. WP also induced ROCK1, PAK1, N-WASP, and p-MLC2 expression. These findings suggest that WP could enhance migration and F-actin aggregation in C6 cells by controlling Rho protein expression. Interestingly, the downregulation of RhoA and CDC42 expression induced by PRP could still increase the expression of ROCK1, PAK1,

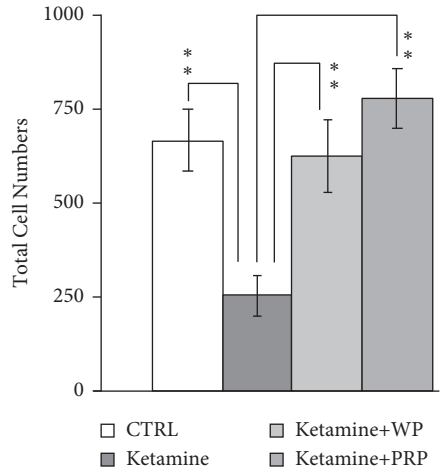

Figure 7: *Poria cocos* reversed ketamine-induced cell migration inhibition in B35 cells. The bar chart was calculated from three batches of cell migration assays. Data were calculated and analyzed by using Student's *t*-test ($^{*}p < 0.05$; $^{**}p < 0.01$). C/CTRL: control; PRP: *Poria cocos* cum Radix Pini; WP: White Poria.

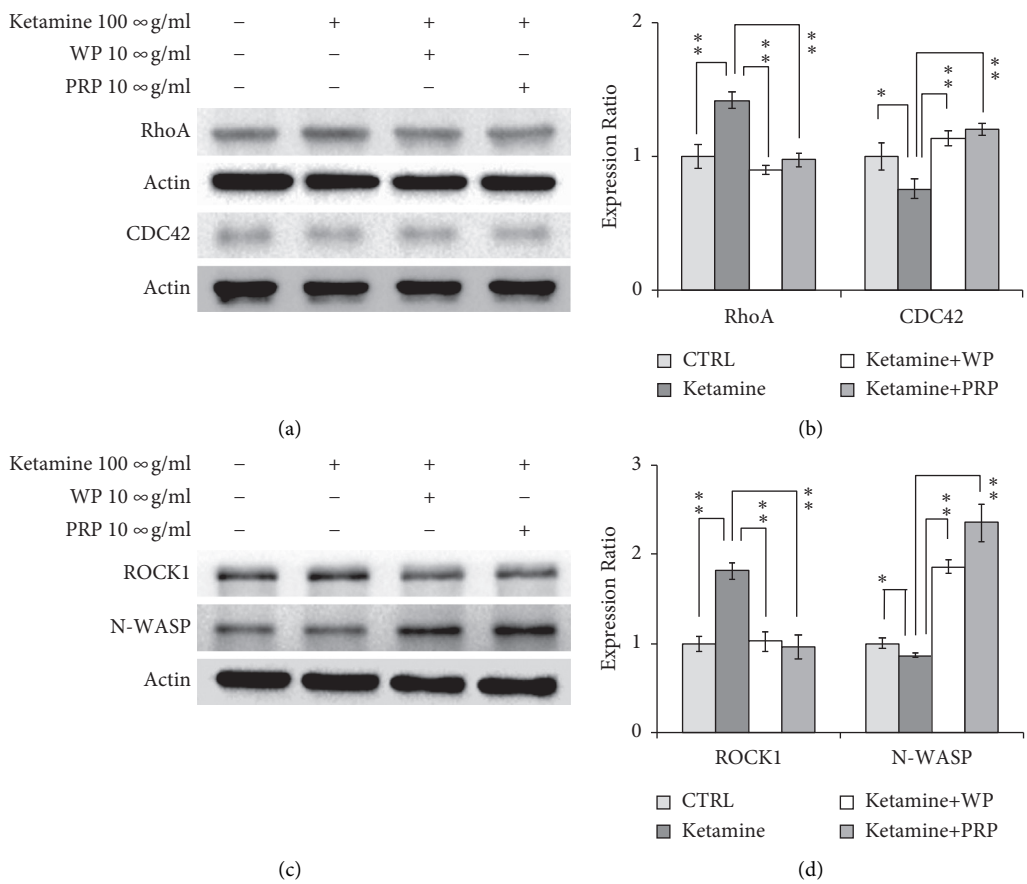

Figure 8: Continued.

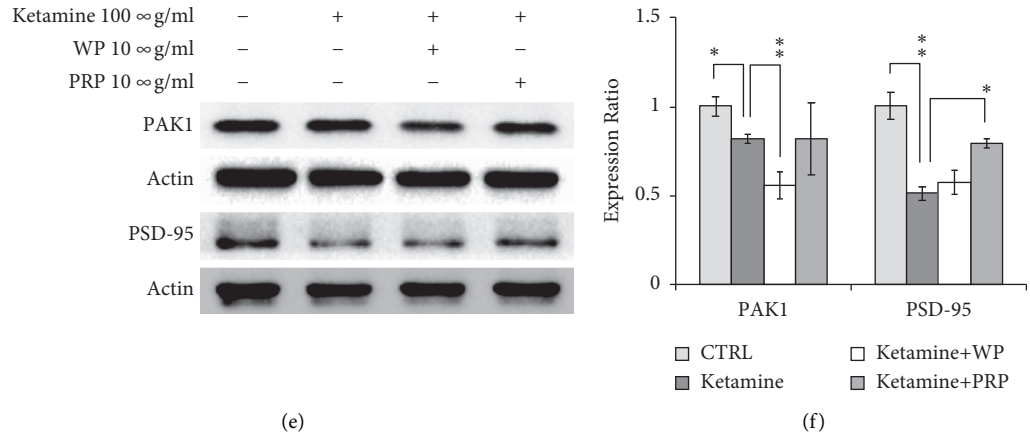

Figure 8: *Poria cocos* reversed ketamine-induced Rho signaling regulation in B35 cells. B35 cells treated with ketamine for seven days were then treated with ketamine or ketamine in combination with PRP or WP for another seven days. The expression levels of RhoA, CDC42, ROCK1, N-WASP, and PAK1 were examined using western blotting in this experiment. The bar charts were calculated based on triplicate western blot data from three batches of drug-treated cells using Student's *t*-test ($^{*}p < 0.05$; $^{**}p < 0.01$). C/CTRL: control; PRP: *Poria cocos* cum Radix Pini; WP: White Poria.

N-WASP, and p-MLC2 in C6 cells and induce cell migration and F-actin concentration.

There may be two reasons for these observations. First, the feedback inhibition of RhoGDI1, RhoA, and CDC42, as well as cross-talk between Rho protein signaling in C6 cells, may be the possible regulatory mechanisms by which cells maintain the signal balance between Rho proteins and related cell functions. Second, the lower expression levels of RhoA and CDC42 in C6 cells may be because there are components in PRP that are different from WP that can specifically reduce the expression levels of RhoA and CDC42 in C6 cells.

5. Conclusions

In summary, we found that PRP and WP could enhance migration and F-actin condensation in B35 and C6 cells. We also observed that PRP and WP regulated Rho protein signaling. Ketamine-induced cell migration inhibition and some Rho signaling regulation can be reversed by PRP and WP treatment. These findings suggest that PRP and WP regulate cell migration and F-actin condensation by differentially modulating Rho protein signaling in B35 and C6 cells. These results also show that PRP and WP can regulate Rho protein signaling in neurons and glial cells and, therefore, have the potential to further regulate abnormal cell functions related to mental disorders.

Abbreviations

APD: Antipsychotic drug
ARP2/3: Actin-related protein 2/3
CDC42: Cell division cycle 42
F-actin: Actin filament
NMDAR: N-Methyl-D-aspartate receptor
N-WASP: Neuronal Wiskott–Aldrich Syndrome protein
p-MLC2: Phosphorylated myosin light chain 2
PAK1: p21 (RAC1) activated kinase 1
PFN1: Profilin 1
PRP: *Poria cocos* cum Radix Pini
PSD-95: Postsynaptic density protein 95
RhoA: Ras homolog family member A
RhoGDI1: Rho GDP dissociation inhibitor 1
ROCK1: Rho-associated coiled-coil containing protein kinase 1
WP: White Poria.

Data Availability

The datasets used or analyzed in the current study are available from the corresponding author on reasonable request.

Conflicts of Interest

The authors declare that they have no conflicts of interest.

Authors' Contributions

CY Lee and CY Kuo designed and conducted the experiments. CT Lee and FM Tsai designed the experiments and analyzed the data. IS Tzeng performed statistical analysis. ML Chen conceived the study, designed, and conducted the experiments, analyzed the data, and drafted the manuscript. All authors have read and agreed to the published version of the manuscript.

Acknowledgments

This study was supported by a grant (TCRD–TPE–108–13) from the Taipei Tzu Chi Hospital through the Buddhist Tzu Chi Medical Foundation, Taipei, Taiwan.

References

[1] M. J. Cuella, R. M. Giner, M. C. Recio, M. J. Just, S. Manez, and J. L. Rios, "Two fungal lanostane derivatives as phospholipase

A2 inhibitors," *Journal of Natural Products*, vol. 59, no. 10, pp. 977–979, 1996.

[2] J. L. Rios, "Chemical constituents and pharmacological properties of Poria cocos," *Planta Medica*, vol. 77, no. 7, pp. 681–691, 2013.

[3] Y. L. Feng, Y. Y. Zhao, F. Ding et al., "Chemical constituents of surface layer of Poria cocos and their pharmacological properties (I)," *Zhongguo Zhongyao Zazhi*, vol. 38, no. 7, pp. 1098–1102, 2013.

[4] M. J. Cuellar, R. M. Giner, M. C. Recio, M. J. Just, S. Manez, and J. L. Rios, "Effect of the basidiomycete Poria cocos on experimental dermatitis and other inflammatory conditions," *Chemical & Pharmaceutical Bulletin*, vol. 45, no. 3, pp. 492–494, 1997.

[5] K. Spelman, J. Burns, D. Nichols, N. Winters, S. Ottersberg, and M. Tenborg, "Modulation of cytokine expression by traditional medicines: a review of herbal immunomodulators," *Alternative Medicine Review*, vol. 11, no. 2, pp. 128–150, 2010.

[6] S. J. Yu and J. Tseng, "Fu-Ling, a Chinese herbal drug, modulates cytokine secretion by human peripheral blood monocytes," *International Journal of Immunopharmacology*, vol. 18, no. 1, pp. 37–44, 1996.

[7] T. Kaminaga, K. Yasukawa, H. Kanno, T. Tai, Y. Nunoura, and M. Takido, "Inhibitory effects of lanostane-type triterpene acids, the components of Poria cocos, on tumor promotion by 12-O-tetradecanoylphorbol-13-acetate in two-stage carcinogenesis in mouse skin," *Oncology*, vol. 53, no. 5, pp. 382–385, 1996.

[8] H. M. Kang, S. K. Lee, D. S. Shin et al., "Dehydrotrametenolic acid selectively inhibits the growth of H-ras transformed rat2 cells and induces apoptosis through caspase-3 pathway," *Life Sciences*, vol. 78, no. 6, pp. 607–613, 2006.

[9] M. Ukiya, T. Akihisa, H. Tokuda et al., "Inhibition of tumor-promoting effects by poricoic acids G and H and other lanostane-type triterpenes and cytotoxic activity of poricoic acids A and G from Poria cocos," *Journal of Natural Products*, vol. 65, no. 4, pp. 462–465, 2002.

[10] W. Chen, W. An, and J. Chu, "Effect of water extract of Poria on cytosolic free calcium concentration in brain nerve cells of neonatal rats," *Zhongguo Zhong Xi Yi Jie He Za Zhi*, vol. 18, no. 5, pp. 293–295, 1956.

[11] H. Buchtova, I. Fajnerova, A. Stuchlik, and S. Kubik, "Acute systemic MK-801 induced functional uncoupling between hippocampal areas CA3 and CA1 with distant effect in the retrosplenial cortex," *Hippocampus*, vol. 27, no. 2, pp. 134–144, 2017.

[12] A. S. Ivy, C. S. Rex, Y. Chen et al., "Hippocampal dysfunction and cognitive impairments provoked by chronic early-life stress involve excessive activation of CRH receptors," *Journal of Neuroscience*, vol. 30, no. 39, pp. 13005–13015, 2010.

[13] D. Han, L. Xu, H. Xiao, G. C. Prado Schmidt, and S. Shi, "Dizocilpine reduces head diameter of dendritic spines in the hippocampus of adolescent rats," *Psychiatry Research*, vol. 210, no. 1, pp. 351–356, 2013.

[14] B. Juliandi, K. Tanemura, K. Igarashi et al., "Reduced adult hippocampal neurogenesis and cognitive impairments following prenatal treatment of the antiepileptic drug valproic acid," *Stem Cell Reports*, vol. 5, no. 6, pp. 996–1009, 2015.

[15] V. Schubert, J. S. Da Silva, and C. G. Dotti, "Localized recruitment and activation of RhoA underlies dendritic spine morphology in a glutamate receptor-dependent manner," *The Journal of Cell Biology*, vol. 172, no. 3, pp. 453–467, 2006.

[16] S. Jiang, Z. Hao, X. Li et al., "Ketamine destabilizes growth of dendritic spines in developing hippocampal neurons in vitro via a Rhodependent mechanism," *Molecular Medicine Reports*, vol. 18, no. 6, pp. 5037–5043, 2018.

[17] D. A. Fletcher and R. D. Mullins, "Cell mechanics and the cytoskeleton," *Nature*, vol. 463, no. 7280, pp. 485–492, 2010.

[18] F. C. Tsai, G. H. Kuo, S. W. Chang, and P. J. Tsai, "Ca2+ signaling in cytoskeletal reorganization, cell migration, and cancer metastasis," *BioMed Research International*, vol. 2015, Article ID 409245, 13 pages, 2015.

[19] D. D. Tang and B. D. Gerlach, "The roles and regulation of the actin cytoskeleton, intermediate filaments and microtubules in smooth muscle cell migration," *Respiratory Research*, vol. 18, no. 1, p. 54, 2017.

[20] D. Yamazaki, S. Kurisu, and T. Takenawa, "Regulation of cancer cell motility through actin reorganization," *Cancer Science*, vol. 96, no. 7, pp. 379–386, 2005.

[21] Y. Nakahata and R. Yasuda, "Plasticity of spine structure: local signaling, translation and cytoskeletal reorganization," *Frontiers in Synaptic Neuroscience*, vol. 10, p. 29, 2018.

[22] T. Kuriu, A. Inoue, H. Bito, K. Sobue, and S. Okabe, "Differential control of postsynaptic density scaffolds via actin-dependent and -independent mechanisms," *Journal of Neuroscience*, vol. 26, no. 29, pp. 7693–7706, 2006.

[23] K. Hayashi, T. S. Yamamoto, and N. Ueno, "Intracellular calcium signal at the leading edge regulates mesodermal sheet migration during Xenopus gastrulation," *Scientific Reports*, vol. 8, no. 1, p. 2433, 2018.

[24] C. Wei, X. Wang, M. Zheng, and H. Cheng, "Calcium gradients underlying cell migration," *Current Opinion in Cell Biology*, vol. 24, no. 2, pp. 254–261, 2012.

[25] S. Sakurada, N. Takuwa, N. Sugimoto et al., "Ca2+-dependent activation of Rho and Rho kinase in membrane depolarization-induced and receptor stimulation-induced vascular smooth muscle contraction," *Circulation Research*, vol. 93, no. 6, pp. 548–556, 2003.

[26] M. L. Chen, F. M. Tsai, M. C. Lee, and Y. Y. Lin, "Antipsychotic drugs induce cell cytoskeleton reorganization in glial and neuronal cells via Rho/Cdc42 signal pathway," *Progress In Neuro-Psychopharmacology & Biological Psychiatry*, vol. 71, pp. 14–26, 2016.

[27] M. J. Kim, K. Futai, J. Jo, Y. Hayashi, K. Cho, and M. Sheng, "Synaptic accumulation of PSD-95 and synaptic function regulated by phosphorylation of serine-295 of PSD-95," *Neuron*, vol. 56, no. 3, pp. 488–502, 2008.

[28] C. I. Esteban, "[Medicinal interest of Poria cocos (= Wolfiporia extensa)]," *Revista Iberoamericana De Micologia*, vol. 26, no. 2, pp. 103–107, 2009.

[29] T. Hattori, K. Hayashi, T. Nagao, K. Furuta, M. Ito, and Y. Suzuki, "Studies on antinephritic effects of plant components (3): effect of pachyman, a main component of Poria cocos Wolf on original-type anti-GBM nephritis in rats and its mechanisms," *The Japanese Journal of Pharmacology*, vol. 59, no. 1, pp. 89–96, 1992.

[30] H. Tian, Z. Liu, Y. Pu, and Y. Bao, "Immunomodulatory effects exerted by Poria Cocos polysaccharides via TLR4/TRAF6/NF-kappaB signaling in vitro and in vivo," *Biomedicine & Pharmacotherapy*, vol. 112, Article ID 108709, 2019.

[31] X. Li, Y. He, P. Zeng et al., "Molecular basis for Poria cocos mushroom polysaccharide used as an antitumour drug in China," *Journal of Cellular and Molecular Medicine*, vol. 23, no. 1, pp. 4–20, 2019.

[32] A. Singh and K. Zhao, "Treatment of insomnia with traditional Chinese herbal medicine," *International Review of Neurobiology*, vol. 135, pp. 97–115, 2017.

[33] Y. J. Huang, N. Y. Hsu, K. H. Lu et al., "Poria cocos water extract ameliorates the behavioral deficits induced by unpredictable chronic mild stress in rats by down-regulating inflammation," *Journal of Ethnopharmacology*, vol. 258, Article ID 112566, 2020.

[34] X. Zhou, Y. Zhang, Y. Jiang, C. Zhou, and Y. Ling, "Poria cocos polysaccharide attenuates damage of nervus in Alzheimer's disease rat model induced by D-galactose and aluminum trichloride," *NeuroReport*, vol. 32, no. 8, pp. 727–737, 2021.

[35] Y. H. Park, I. H. Son, B. Kim, Y. S. Lyu, H. I. Moon, and H. W. Kang, "Poria cocos water extract (PCW) protects PC12 neuronal cells from beta-amyloid-induced cell death through antioxidant and antiapoptotic functions," *Die Pharmazie*, vol. 64, no. 11, pp. 760–764, 2018.

[36] J. Shi, X. Wu, M. Surma et al., "Distinct roles for ROCK1 and ROCK2 in the regulation of cell detachment," *Cell Death & Disease*, vol. 4, p. e483, 2013.

[37] J. S. Da Silva, M. Medina, C. Zuliani, A. Di Nardo, W. Witke, and C. G. Dotti, "RhoA/ROCK regulation of neuritogenesis via profilin IIa-mediated control of actin stability," *The Journal of Cell Biology*, vol. 162, no. 7, pp. 1267–1279, 2003.

[38] M. C. Bischoff, S. Lieb, R. Renkawitz-Pohl, and S. Bogdan, "Filopodia-based contact stimulation of cell migration drives tissue morphogenesis," *Nature Communications*, vol. 12, no. 1, p. 791, 2021.

[39] Y. Huang, X. Yi, C. Kang, and C. Wu, "Arp2/3-Branched actin maintains an active pool of GTP-RhoA and controls RhoA abundance," *Cells*, vol. 810 pages, 2019.

[40] M. Parsons, J. Monypenny, S. M. Ameer-Beg et al., "Spatially distinct binding of Cdc42 to PAK1 and N-WASP in breast carcinoma cells," *Molecular and Cellular Biology*, vol. 25, no. 5, pp. 1680–1695, 2005.

[41] H. Imamura, K. Takaishi, K. Nakano et al., "Rho and Rab small G proteins coordinately reorganize stress fibers and focal adhesions in MDCK cells," *Molecular Biology of the Cell*, vol. 9, no. 9, pp. 2561–2575, 1998.

[42] M. A. Sells, J. T. Boyd, and J. Chernoff, "p21-activated kinase 1 (Pak1) regulates cell motility in mammalian fibroblasts," *The Journal of Cell Biology*, vol. 145, no. 4, pp. 837–849, 1999.

[43] M. A. Del Pozo, W. B. Kiosses, N. B. Alderson, N. Meller, K. M. Hahn, and M. A. Schwartz, "Integrins regulate GTP-Rac localized effector interactions through dissociation of Rho-GDI," *Nature Cell Biology*, vol. 4, no. 3, pp. 232–239, 2002.

[44] M. Cook, B. J. Bolkan, and D. Kretzschmar, "Increased actin polymerization and stabilization interferes with neuronal function and survival in the AMPKgamma mutant Loechrig," *PloS One*, vol. 9, no. 2, Article ID e89847, 2014.

[45] O. Geneste, J. W. Copeland, and R. Treisman, "LIM kinase and Diaphanous cooperate to regulate serum response factor and actin dynamics," *The Journal of Cell Biology*, vol. 157, no. 5, pp. 831–838, 2002.

Hindawi
Evidence-Based Complementary and Alternative Medicine
Volume 2021, Article ID 2126967, 14 pages
https://doi.org/10.1155/2021/2126967

Research Article

Exploring the Mechanism of Action of Herbal Medicine (*Gan-Mai-Da-Zao* Decoction) for Poststroke Depression Based on Network Pharmacology and Molecular Docking

Zhicong Ding,[1] **Fangfang Xu**,[1] **Qidi Sun**,[2] **Bin Li**,[1] **Nengxing Liang**,[1] **Junwei Chen**,[1] **and Shangzhen Yu**[1,3]

[1]*Jinan University, Guangzhou 510632, China*
[2]*Yangzhou University, Yangzhou 225009, China*
[3]*Wuyi Hospital of Traditional Chinese Medicine, Jiangmen 529000, China*

Correspondence should be addressed to Shangzhen Yu; ysz6521@163.com

Received 19 May 2021; Accepted 14 August 2021; Published 23 August 2021

Academic Editor: Ghulam Ashraf

Copyright © 2021 Zhicong Ding et al. This is an open access article distributed under the Creative Commons Attribution License, which permits unrestricted use, distribution, and reproduction in any medium, provided the original work is properly cited.

Background. Poststroke depression (PSD) is the most common and serious neuropsychiatric complication occurring after cerebrovascular accidents, seriously endangering human health while also imposing a heavy burden on society. Nevertheless, it is difficult to control disease progression. *Gan-Mai-Da-Zao* Decoction (GMDZD) is effective for PSD, but its mechanism of action in PSD is unknown. In this study, we explored the mechanism of action of GMDZD in PSD treatment using network pharmacology and molecular docking. *Material and methods*. We obtained the active components of all drugs and their targets from the public database TCMSP and published articles. Then, we collected PSD-related targets from the GeneCards and OMIM databases. Cytoscape 3.8.2 was applied to construct PPI and composite target disease networks. In parallel, the DAVID database was used to perform GO and KEGG enrichment analyses to determine the biological processes enriched in the treatment-related drugs in vivo. Finally, molecular docking was used to verify the association between the main active ingredients and their targets. *Results*. The network pharmacological analysis of GMDZD in PSD revealed 107 active ingredients with important biological effects, including quercetin, luteolin, kaempferol, naringenin, and isorhamnetin. In total, 203 potential targets for the treatment of this disease were screened, including STAT3, JUN, TNF, TPT53, AKT1, and EGFR. These drugs are widely enriched in a series of signaling pathways, such as TNF, HIF-1, and toll-like receptor. Moreover, molecular docking analysis showed that the core active components were tightly bound to their core targets, further confirming their anti-PSD effects. *Conclusion*. This prospective study was based on the integrated analysis of large data using network pharmacology technology to explore the feasibility of GMDZD for PSD treatment that was successfully validated by molecular docking. It reflects the multicomponent and multitarget characteristics of Chinese medicine and, more importantly, brings hope for the clinical treatment of PSD.

1. Introduction

Poststroke depression (PSD) is one of the most common and severe neuropsychiatric complications after stroke [1, 2]; it often starts insidiously, with mild symptoms of malaise and drowsiness in the early stages. Moreover, if patients with PSD are unable to express their feelings clearly due to language or cognitive impairment, the diagnosis is often compromised, and treatment is delayed [3]. This not only poses a great challenge to clinical work but also adds a heavy burden to the society and economy. A recent statistical study showed that approximately 795,000 people suffer from stroke each year in the United States. In detail, approximately 610,000 people experience stroke for the first time, and approximately 185,000 people experience recurrent stroke; more than 100,000 of these people die from stroke [4]. A meta-analysis of longitudinal studies showed that the prevalence of depression was 29% (95% CI 25–32) and remained stable up to 10 years after stroke, with a cumulative incidence of 39–52% within 5 years of stroke [5]. Studies

have reported that the cross-sectional prevalence of PSD is 18% and 33% [5–8]. To date, tricyclic antidepressants (TCAs) and selective serotonin reuptake inhibitors (SSRIs) have been used to treat PSD. However, the lack of a timely diagnosis, the adverse effects of these drugs on cardiovascular function, and an increased risk of bleeding lead to unsatisfactory treatment for patients with PSD [9, 10].

Traditional Chinese medicine (TCM) for PSD is characterized by few side effects and individualized treatment [11]. Therefore, the search for an herbal medicine for the treatment of PSD has become a hot topic in contemporary pharmacological research. *Gan-Mai-Da-Zao* Decoction (GMDZD) is derived from *Jingui Yaolue* and is composed of three Chinese herbal medicines: *Glycyrrhiza uralensis* Fisch. (gancao in Chinese), *Triticum aestivum* L. (xiaomai in Chinese), and *Ziziphus jujuba* Mill. (dazao in Chinese); it is mainly used for sleep disorders and depression-related psychiatric disorders [12]. A randomized controlled study showed that GMDZD intervention for 2 and 4 weeks could significantly improve the Hamilton Depression Rating Scale (HAM-D) score in postpartum women in depressive states [13]. Modern pharmacological studies have also confirmed that GMDZD could increase central excitability, sedation and hypnotism, antidepressant activity, and other pharmacological activities [14–16]. However, the mechanism by which the active ingredients in GMDZD alleviate depressive symptoms is unclear.

TCM with multiple components, multiple targets, and multiple pathways can bring very many new possibilities for clinical treatment. Network pharmacology is the result of the integration of multidisciplinary basic theories, such as those from biology, computer science, multidirectional pharmacology, molecular pharmacology, and medicine, and research tools that can systematically and comprehensively reflect the intervention mechanisms of drugs through disease networks. This has strong convergence with the principle of the overall dynamics of TCM treatment for diseases and the characteristics of multicomponent, multitarget, and multipathway interactions. Therefore, network pharmacology can provide new and powerful technical support for studying the mechanism of action of TCM compounding, which can help to reveal the scientific connotation of TCM compounding, discover drug targets, and develop TCM theories [17]. This study aimed to investigate the mechanism of action of GMDZD in the treatment of PSD through network pharmacology and molecular docking technology (Figure 1).

2. Materials and Methods

2.1. Screening Active Compounds and Predicting Putative Targets. Through the Traditional Chinese Medicine Systems Pharmacology Database and Analysis Platform (TCMSP, https://tcmspw.com/tcmsp.php), an authoritative public database that contains a large number of active ingredients, their related targets, and pharmacokinetic information [18], we searched for the active ingredients of three Chinese medicines and supplemented them with the published literature [19, 20]. Oral bioavailability (OB) is an important indicator used to evaluate the rate and extent of drug absorption into the human circulation, and drug-likeness (DL) is an indicator used to evaluate the similarity of a compound to a known drug [21, 22]. Based on these two absorption, distribution, metabolism, and excretion (ADME) mode values, we performed a preliminary screen of active ingredients to obtain the active compounds and their protein targets, where OB ≥ 30% and DL ≥ 0.18% were set as the criteria [23]. After screening, to standardize protein target information, the UniProt database (The Universal Protein Resource, https://www.uniprot.org/) was utilized to standardize the protein targets on which compounds act, resulting in more comprehensive target information such as gene IDs and gene symbols.

2.2. Identifying Disease-Related Targets and Filtering Intersecting Targets. Using "poststroke depression" as the keyword, we mined the GeneCards database (https://www.genecards.org/) and the OMIM database (https://omim.org/) for gene targets related to PSD [24]. The targets associated with PSD were obtained by merging the targets of the two databases and removing duplicates. The common targets were then screened by using Venny 2.1 (http://bioinformatics.psb.ugent.be/webtools/Venn/), and the common targets were defined as the potential targets of GMDZD in PSD.

2.3. Protein-Protein Interaction (PPI) Network Construction. A PPI network was constructed by submitting common disease-drug targets to the Search Tool for the Retrieval of Interacting Genes database (STRING, https://string-db.org/) [25]. The organism species was set as "*Homo sapiens*," and the confidence score with a correlation degree was set as ≥0.950; meanwhile, disconnected nodes were hidden. Then, the interaction information was further visually analysed by Cytoscape 3.8.2. The CytoNCA plug-in was used to analyse the topological attributes of the data submitted to Cytoscape [26, 27]. In this plug-in, betweenness centrality (BC), closeness centrality (CC), and degree centrality (DC) are used to estimate the importance of nodes in the network. The higher the quantitative value of these three numerical values, the more important the node in the network. In the PPI network, BC, CC, and DC are used as variables to screen out the core targets and build a network relationship diagram of the core targets based on the screening results.

2.4. Gene Ontology (GO) and Kyoto Encyclopedia of Genes and Genomes (KEGG) Pathway Enrichment Analyses. The previously obtained GMDZD targets for the treatment of PSD were imported into the DAVID database (https://david.ncifcrf.gov/summary.jsp), a repository with comprehensive annotation capability that is updated monthly with gene annotation data to analyse the biological processes and metabolic pathways in which they are enriched. We chose "*Homo sapiens*" for the species, and terms with a p value <0.05 were considered significant. The results were saved and visualized using Bioinformatics (http://www.bioinformatics.com.cn/) to obtain a bubble map of the results of the GO and KEGG enrichment analyses. GO

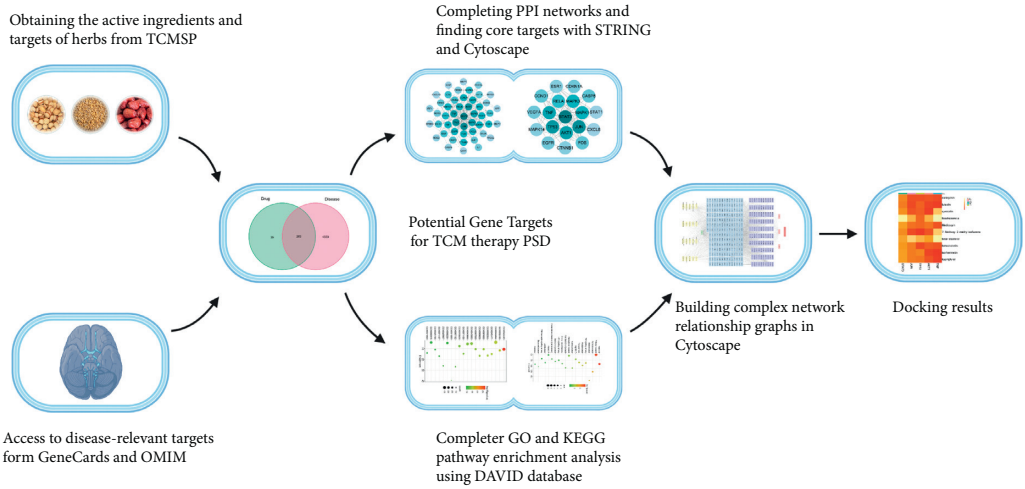

Figure 1: Detailed process of research design.

enrichment analysis covers three aspects of biology: cellular component, molecular function, and biological process. KEGG enrichment analysis can also suggest the biological mechanisms of action of drugs in the human body and the pathways involved in their regulation.

2.5. Network Construction. (1) Cytoscape 3.8.2 was implemented to draw the disease-herb-component-target (D-H-C-T) network to visualize the relationship between GMDZD and PSD. The different colours and shapes in the diagram represent the disease, drug, component, and target, and the "edges" represent the correlation between these parameters. (2) To more visually reflect the relationships of the target genes and the enriched pathways, a more complex but more intuitive network was constructed by combining the previous network, which includes more comprehensive information on the drugs and their active ingredients, targets, and pathways.

2.6. Molecular Docking Prediction

2.6.1. Preparation of Small-Molecule Ligands. To better evaluate the reliability of the network predictions, the core active ingredients were then molecularly docked to the core gene targets. First, small-molecule ligands were prepared by obtaining the 2D structures of their active ingredients in the *sdf* format through the PubChem database (https://pubchem.ncbi.nlm.nih.gov/) and then converting the 2D structures into 3D structures in the *mol2* format through ChemOffice software. Finally, the results were imported into AutoDockTools to convert to files into the *pdbqt* format [28].

2.6.2. Preparation of Protein Receptors. First, the core gene targets were entered into the UniProt database to obtain their UniProt IDs, and the 3D structures of the core gene targets were retrieved and downloaded from the Protein Data Bank database (PDB,http://www.rcsb.org/) in the *pdb* format. PyMOL 2.3.4 software was used to dewater and deligand the proteins, the core gene targets were hydrogenated and charge calculated using AutoDockTools [29], and the results were saved in the *pdbqt* format. Upon completion, ligand-receptor molecular docking was performed using AutoDockVina. Among the existing drugs that have been used to treat PSD, SSRIs have shown high efficacy and few side effects, with sertraline and escitalopram being the representative drugs [9, 10]. Notably, to make the conclusions more objective, we molecularly docked existing drugs already used for the treatment of PSD with the potential core gene targets we screened.

3. Results

3.1. Active Compounds and Targets of Gancao, Xiaomai, and Dazao. We found a total of 442 drug-related components from the TCMSP database as well as the available literature. Then, screening was performed according to the criteria DL ≥ 0.18 and OB ≥ 30%, and the gene targets associated with each active ingredient were obtained. Finally, duplicate targets were removed after comparison and correction by the UniProt database. A total of 109 active ingredients and 239 gene targets were obtained, among which some were derived from multiple drugs, reflecting the multicomponent and multitarget characteristics of TCM. Details on the active ingredients are shown in Supplementary Materials Table S1.

3.2. Gene Targets in PSD. In this study, 4733 PSD-related gene targets were obtained from the GeneCards database, and another 37 gene targets were obtained from the OMIM database, in which there were 8 identical targets. After removing duplicates, the total number of PSD-related gene targets was 4762. Next, 203 interacting gene targets were obtained by taking the intersection of the disease-related gene targets and the drug-related gene targets (Figure 2(a)). These targets were identified as the potential targets of GMDZD against PSD (Table 1).

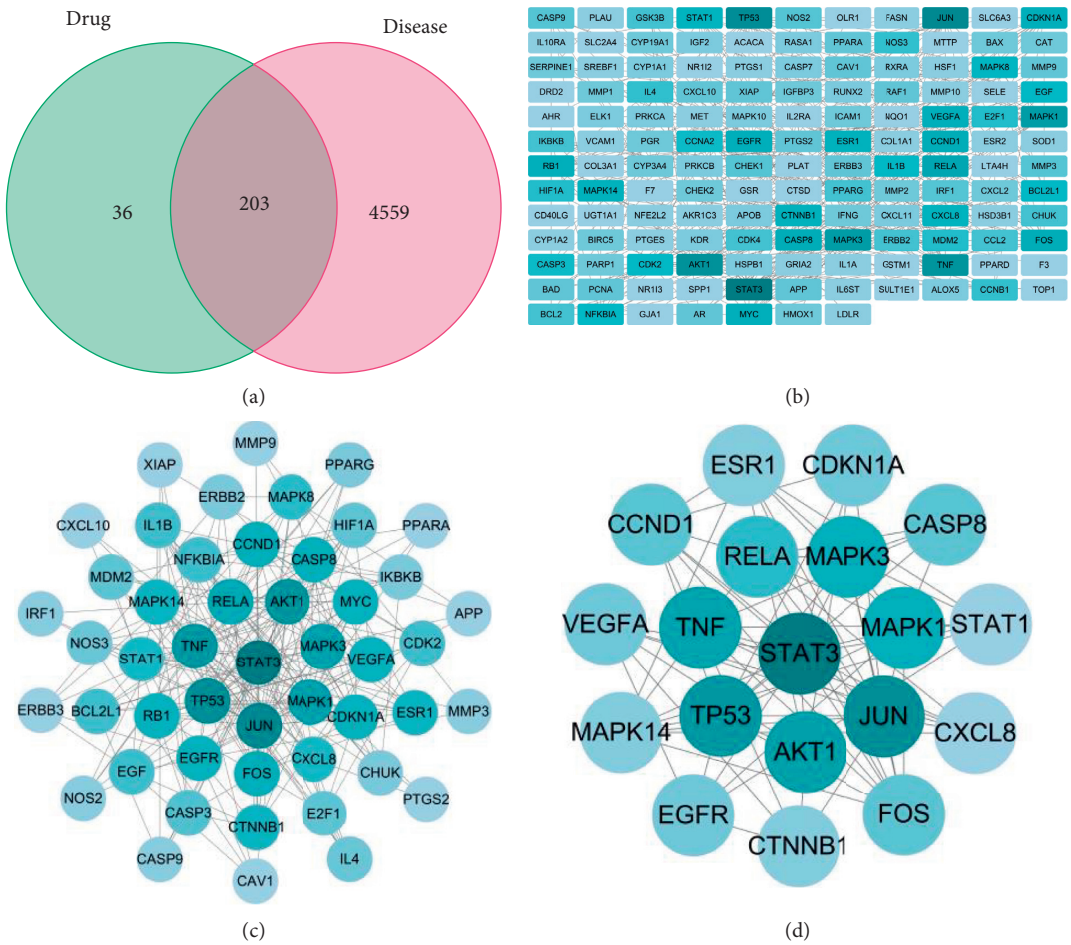

Figure 2: Drug-disease targets intersection Venn diagram and protein-protein interaction network. The darker the color means the larger the degree value, the more important it is in this network. (a) 203 intersection gene targets; (b) a protein-protein network from STRING; (c) one protein-protein cluster with 49 nodes and 230 edges; and (d) one protein-protein cluster with 19 nodes and 76 edges.

3.3. PPI Network Analysis. The 203 intersecting gene targets were submitted to the STRING database, and then, the data obtained from this platform were imported into Cytoscape 3.8.2 for visualization and topological analysis (Figure 2(b)). The PPI network consisted of 139 nodes and 426 edges. The topological properties of the intersecting gene targets were analysed using the CytoNCA plug-in, whose median BC, CC, and DC values were 22, 0.046184739, and 4, respectively. The values of 49 gene targets were above the median, and these genes were considered important for the treatment of PSD with GMDZD (Figure 2(c)). Among these genes, the values of AKT1, STAT3, TP53, CTNNB1, CDKN1A, ESR1, VEGFA, MAPK1, MAPK3, CASP8, CCND1, MAPK14, RELA, TNF, EGFR, FOS, JUN, CXCL8, and STAT1 were greater than the twofold median values of BC, CC, and DC (286.3560165, 0.046954747, and 11), indicating that these 19 genes are the core targets in the PPI network (Figure 2(d)), where STAT3 has the highest degree value, suggesting that it may be most relevant to this research. Details from the STRING analysis are shown in Supplementary Materials Table S2.

3.4. GO and KEGG Pathway Enrichment Analyses. The top 20 terms and pathways retrieved from the DAVID database were ranked according to their p value, and the data were then transformed into a bubble chart for display. The more the genes that are enriched, the larger the bubble, the deeper the colour, and the smaller the p value.

The main biological process terms were as follows: response to drug (GO: 0042493), response to lipopolysaccharide (GO: 0032496), positive regulation of transcription from RNA polymerase II promoter (GO: 0045944), response to ethanol (GO: 0045471), and response to estradiol (GO: 0032355) (Figure 3(a)). The main cellular component terms were as follows: extracellular space (GO: 0005615), cytosol (GO: 0005829), membrane raft (GO: 0045121), plasma membrane (GO: 0005886), and integral component of plasma membrane (GO: 0005887) (Figure 3(b)). The main molecular function terms were as follows: enzyme binding (GO: 0019899), identical protein binding (GO: 0042802), protein heterodimerization activity (GO: 0046982), drug binding (GO: 0008144), and protein binding (GO: 0005515) (Figure 3(c)). All of the abovementioned data suggest that GMDZD may treat PSD by modulating multiple GO functions.

Table 1: Potential targets of *Gan-Mai-Da-Zao* decoction against poststroke depression (PSD).

No.	Gene	No.	Gene	No.	Gene	No.	Gene	No.	Gene
1	PTGS1	42	PLAU	83	CDKN1A	124	THBD	165	CCNA2
2	DRD1	43	LTA4H	84	MMP9	125	SERPINE1	166	ESR2
3	CHRM1	44	MAOA	85	MAPK1	126	COL1A1	167	CDK2
4	DRD5	45	ADRB1	86	IL10RA	127	IFNG	168	MAPK10
5	SCN5A	46	BCL2	87	EGF	128	ALOX5	169	PYGM
6	CHRM5	47	BAX	88	RB1	129	IL1A	170	GRIA2
7	PTGS2	48	CASP9	89	TNF	130	MPO	171	OLR1
8	HTR3A	49	JUN	90	IL6ST	131	NCF1	172	IL4
9	RXRA	50	CASP3	91	AHSA1	132	ABCG2	173	HSD3B1
10	OPRD1	51	CASP8	92	TP53	133	GSTP1	174	IKBKB
11	SLC6A2	52	PRKCA	93	ELK1	134	NFE2L2	175	MAPK8
12	ADRA1A	53	PON1	94	NFKBIA	135	NQO1	176	PPP3CA
13	CHRM2	54	MAP2	95	POR	136	PARP1	177	AKR1C3
14	ADRA2B	55	CAT	96	ODC1	137	AHR	178	SLPI
15	ADRA1B	56	HAS2	97	TOP1	138	SLC2A4	179	MAPK3
16	SLC6A3	57	DRD4	98	RAF1	139	COL3A1	180	LDLR
17	ADRB2	58	ACHE	99	SOD1	140	CXCL11	181	BAD
18	CHRNA2	59	F7	100	HIF1A	141	CXCL2	182	MTTP
19	SLC6A4	60	CACNA1S	101	STAT1	142	NR1I3	183	APOB
20	DRD2	61	KDR	102	RUNX1T1	143	CHEK2	184	PLB1
21	OPRM1	62	AKT1	103	HSPA5	144	CLDN4	185	HMGCR
22	GABRA1	63	VEGFA	104	ERBB2	145	PPARA	186	CYP19A1
23	NR3C2	64	MMP2	105	ACACA	146	PPARD	187	UGT1A1
24	PPARG	65	MMP1	106	CYP1A1	147	HSF1	188	SREBF1
25	CYP3A4	66	HMOX1	107	ICAM1	148	CXCL10	189	GSR
26	NR1I2	67	CYP1A2	108	IL1B	149	CHUK	190	ABCC1
27	CYP2B6	68	CAV1	109	CCL2	150	SPP1	191	ADIPOR1
28	NOS2	69	CTNNB1	110	SELE	151	RUNX2	192	ABAT
29	KCNH2	70	MYC	111	VCAM1	152	E2F1	193	SOAT1
30	ESR1	71	CASP7	112	PTGER3	153	CTSD	194	BACE2
31	AR	72	F3	113	CXCL8	154	IGFBP3	195	STAT3
32	PRSS1	73	GJA1	114	PRKCB	155	IGF2	196	CDK4
33	PDE10A	74	MMP10	115	BIRC5	156	CD40LG	197	MDM2
34	MAOB	75	FASN	116	DUOX2	157	IRF1	198	APP
35	ADRA2A	76	DPP4	117	NOS3	158	ERBB3	199	PCNA
36	CA2	77	MMP3	118	HSPB1	159	HK2	200	TYR
37	ADRA2C	78	RELA	119	SULT1E1	160	RASA1	201	XIAP
38	ADRA1D	79	EGFR	120	IL2RA	161	GSTM1	202	PTGES
39	PGR	80	CCND1	121	CYP1B1	162	MAPK14	203	MET
40	ADH1C	81	BCL2L1	122	CCNB1	163	GSK3B		
41	AKR1B1	82	FOS	123	PLAT	164	CHEK1		

KEGG pathway enrichment analysis yielded a total of 122 pathways, and the same criteria used for GO enrichment analysis were used to obtain the top 20 pathways for graphic visualization. The main pathways of the relevant targets in PSD were as follows: hepatitis B (hsa05161), pathways in cancer (hsa05200), pancreatic cancer (hsa05212), bladder cancer (hsa05219), and the TNF signaling pathway (hsa04668). Among these pathways, "pathways in cancer" had the highest degree of target enrichment and were, thus, identified as an important critical pathway; similarly, "hepatitis B" had the lowest p value and was also identified as an important pathway (Figure 3(d)). Details on the GO and KEGG enrichment analyses from the DAVID database are shown in Supplementary Materials Table S3. Supplementary Materials Table S4 shows the specific information on the targets in the top 20 pathways.

3.5. Network Construction. There were 314 nodes and 1825 edges in the D-H-C-T network, among which the potential active ingredients icos-5-enoic acid (MOL004985) and gadelaidic acid (MOL004996) were hidden because the corresponding gene targets did not overlap with the disease targets (Figure 4). Details are shown in Supplementary Materials Table S5. The pathway information was imported into Cytoscape 3.8.2 and combined with the previous graph to obtain a new network with 335 nodes and 2300 edges (Figure 5).

3.6. Docking Results. The nodes with high degree values in the PPI network were considered core gene targets, and the five core gene targets with the highest degree values in the PPI network, namely, STAT3 (PDB ID: 6NJS), JUN (PDB ID: 5T01), TP53 (PDB ID: 6WQX), AKT1 (PDB ID: 5WBL),

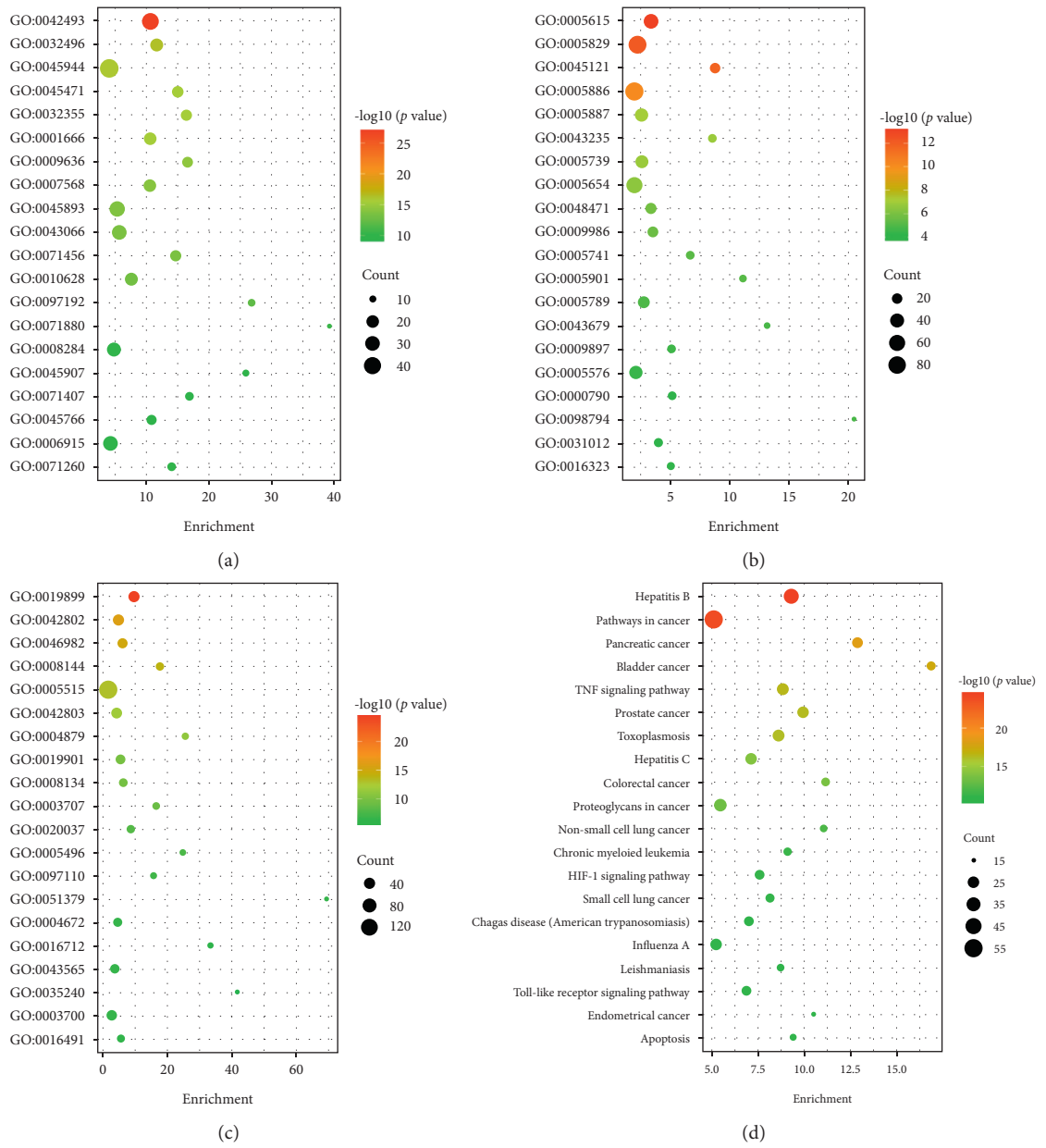

Figure 3: Bubble maps of GO and KEGG pathway enrichment analysis of *Gan-Mai-Da-Zao* decoction for PSD. (a) GO: biological process; (b) GO: cellular components; (c) GO: molecular functions; and (d) KEGG pathway enrichment analysis.

and TNF (PDB ID: 2E7A), were correlated with the 10 active ingredients with the highest degree in the "D-H-C-T" network (quercetin (MOL000098), luteolin (MOL000006), kaempferol (MOL000422), 7-methoxy-2-methyl isoflavone (MOL003896), naringenin (MOL004328), isorhamnetin (MOL000354), formononetin (MOL000392), licochalcone a (MOL000497), beta-sitosterol (MOL000358), and medicarpin (MOL002565)). These compounds were molecularly docked, and their binding energies were calculated. On this basis, we molecularly docked sertraline and escitalopram to the core genes to refine the comparative analysis (Table 2, Figure 6). Moreover, we graphically examined the specific docking details of the top core genes (STAT3 and JUN) with the top core components (quercetin, luteolin, kaempferol, and 7-methoxy-2-methyl isoflavone) (Figure 7). The lower the binding energy of both the ligand and receptor, the more stable the binding [30]. In general, a docking fraction value of less than $-4.25\ \text{kcal·mol}^{-1}$ indicates some binding activity, a value less than $-5.0\ \text{kcal·mol}^{-1}$ indicates good binding activity, and a value less than $-7.0\ \text{kcal·mol}^{-1}$ indicates strong binding activity [31]. A total of 60 groups of core components were determined to have good binding activity with the target proteins. The comparative analysis clearly showed that sertraline and escitalopram also showed good binding activity, but some of the active ingredients screened in this study showed higher binding activity with the core gene target to some extent, which also provides direction for the development of new drugs and subsequent research.

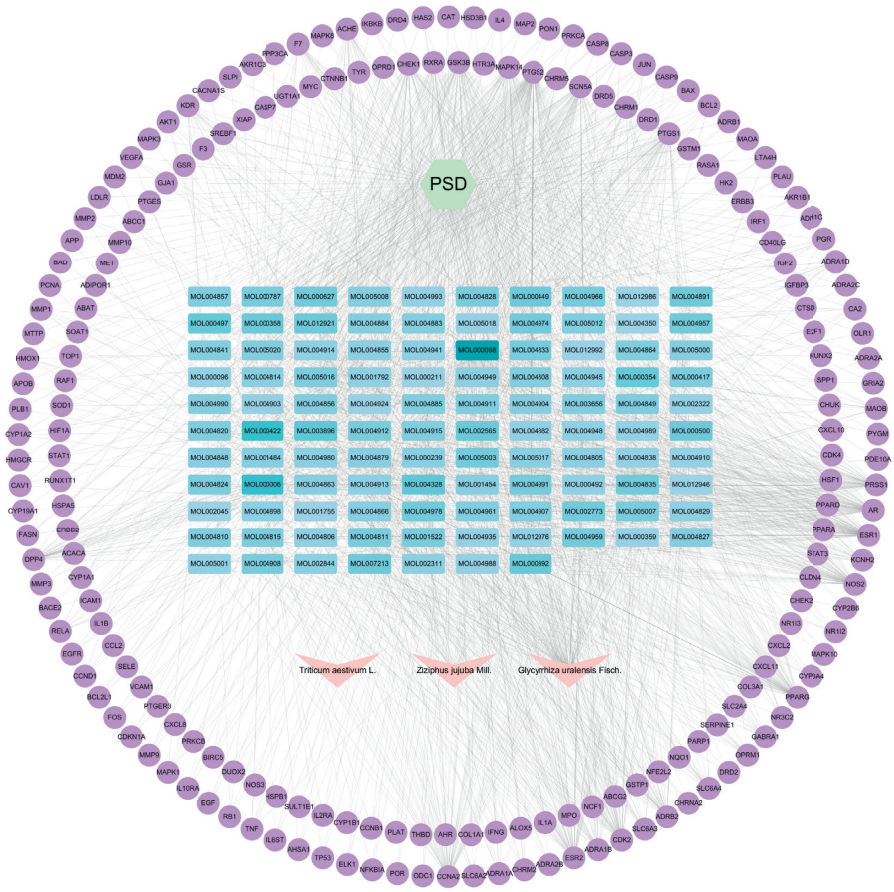

Figure 4: Disease-herb-compound-target (D-H-C-T) network of *Gan-Mai-Da-Zao* decoction against PSD. The purple circles represent genes, the green hexagons represent diseases, the pink V-shapes represent drugs, and finally, shades of blue rectangles represent active ingredients, and the darker the color, the greater the degree value in the network, indicating greater importance.

4. Discussion

Network pharmacology is a method used to predict the ability of a drug to treat a certain disease by searching for shared genes and identifying enriched pathways, which are then confirmed through available experimental evidence. Molecular docking can be used to predict the binding activity of active ingredients to their target proteins, which further confirms the therapeutic effect of the drugs. The use of these techniques has largely solved the great challenges posed to research due to the multicomponent and multitarget nature of TCM. Therefore, we used network pharmacology and molecular docking to reveal the possible mechanism of action of GMDZD in PSD.

In our study, the core active ingredients in the "D-H-C-T" network were identified as quercetin, luteolin, kaempferol, naringenin, and isorhamnetin. In recent years, flavonoids have been found to have significant effects on the central nervous system, with neuroprotective, antidepressant, and anxiolytic effects [32]. In our study, quercetin was derived from *Glycyrrhiza uralensis* Fisch. and *Ziziphus jujuba* Mill. A relevant animal study confirmed that quercetin could reverse stress-induced depression and anxiety in mice [33]. In addition, quercetin exerts antidepressant effects by exerting antioxidant and anti-inflammatory activities, decreasing cytotoxicity, and increasing 5-hydroxytryptamine levels [34]. Luteolin is derived from *Triticum aestivum* L. It has been reported that luteolin exerts an antidepressant effect by suppressing the endoplasmic reticulum [35] and inhibiting and downregulating plasma membrane monoamine transporters (PMAT, Slc29a4) [36]. It has also been found that luteolin may improve cognitive performance by inhibiting microglial activation and neuroinflammation in older mice [37]. Kaempferol, naringenin, and isorhamnetin are all derived from *Glycyrrhiza uralensis* Fisch. Kaempferol promotes the protein expression of brain-derived neurotrophic factor (BDNF) and nerve growth factor (NGF) in hippocampal tissue from aged rats with chronic stress/depression, and these changes resulted in neuroprotection and improved depression-like behaviour [38]. Naringenin is a flavonoid compound with strong antioxidant and anti-inflammatory effects. The literature has shown that naringin may produce functional behavioural effects by enhancing cholinergic transmission and antioxidant defence systems and inhibiting lipid peroxidation and nitrosative processes [39]. The application of isorhamnetin potentiates nerve growth factor- (NGF-) induced neurite outgrowth. In parallel, the expression of neurofilaments is

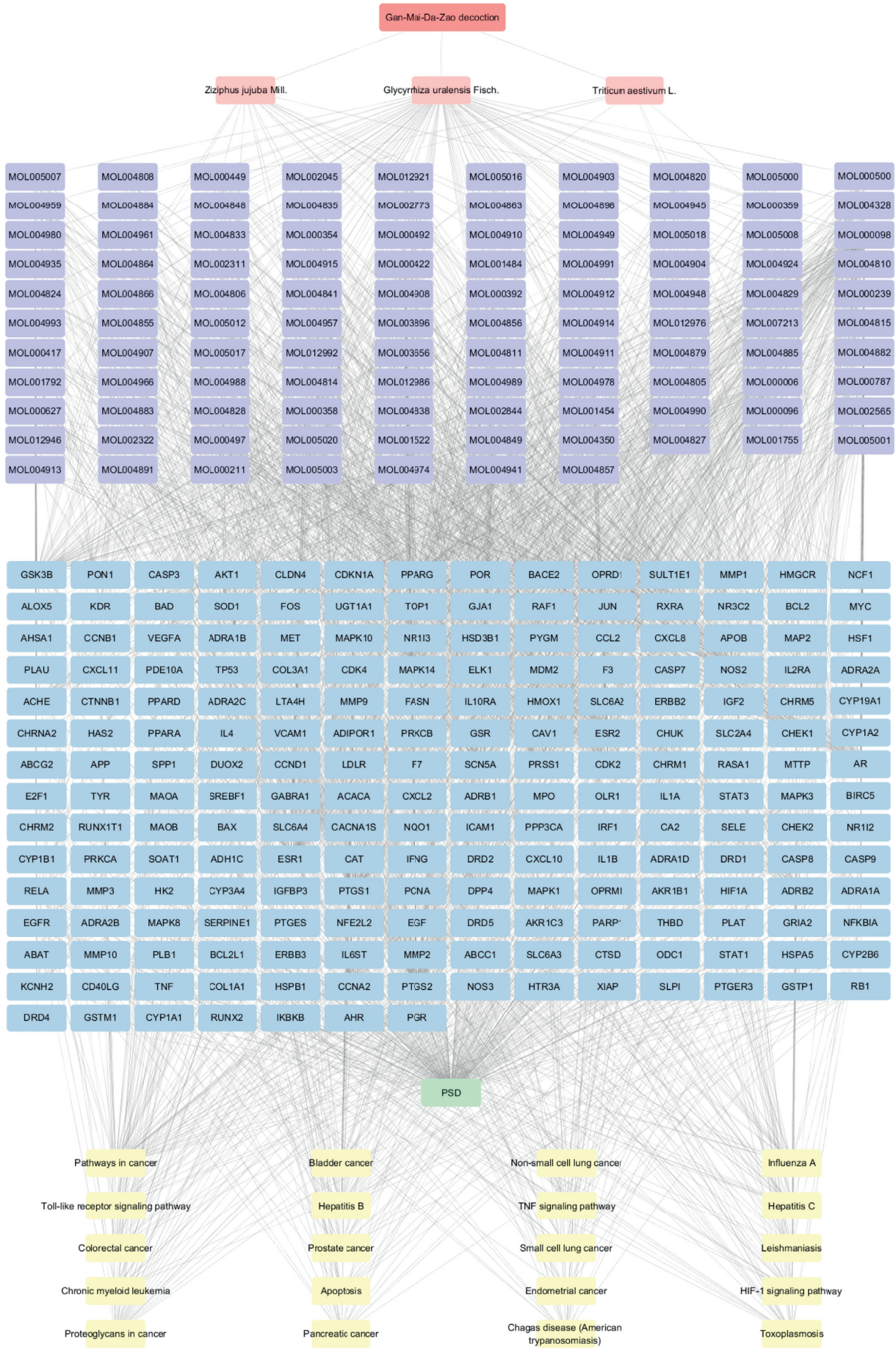

FIGURE 5: Network diagram containing pathway enrichment analysis. The different colored rectangles from top to bottom represent herbal medicine, herbs, active ingredients, targets, disease, and pathways.

Table 2: Binding energies of 10 main compounds and 2 drugs that have been used to treat PSD to 5 potential targets.

No.	Compound	Binding energy/kcal·mol^{-1}				
		STAT3	JUN	TP53	AKT1	TNF
1	Quercetin	−7.5	−8.4	−8.3	−8.9	−6.8
2	Luteolin	−7.8	−8.6	−8.2	−8.7	−8.9
3	Kaempferol	−7.3	−7.8	−7.9	−8.4	−8.9
4	7-Methoxy-2-methyl isoflavone	−7.6	−8.6	−9.0	−8.4	−6.7
5	Naringenin	−7.7	−8.5	−8.5	−8.4	−8.6
6	Isorhamnetin	−7.3	−7.8	−7.7	−8.7	−9.0
7	Formononetin	−7.4	−7.8	−8.6	−8.3	−8.4
8	Licochalcone a	−6.3	−7.0	−8.1	−7.0	−6.0
9	beta-Sitosterol	−7.2	−6.6	−7.0	−7.3	−6.2
10	Medicarpin	−7.3	−8.0	−8.1	−7.9	−8.4
11	Sertraline	−6.1	−5.9	−6.6	−7.3	−5.6
12	Escitalopram	−5.3	−6.4	−6.7	−7.1	−5.6

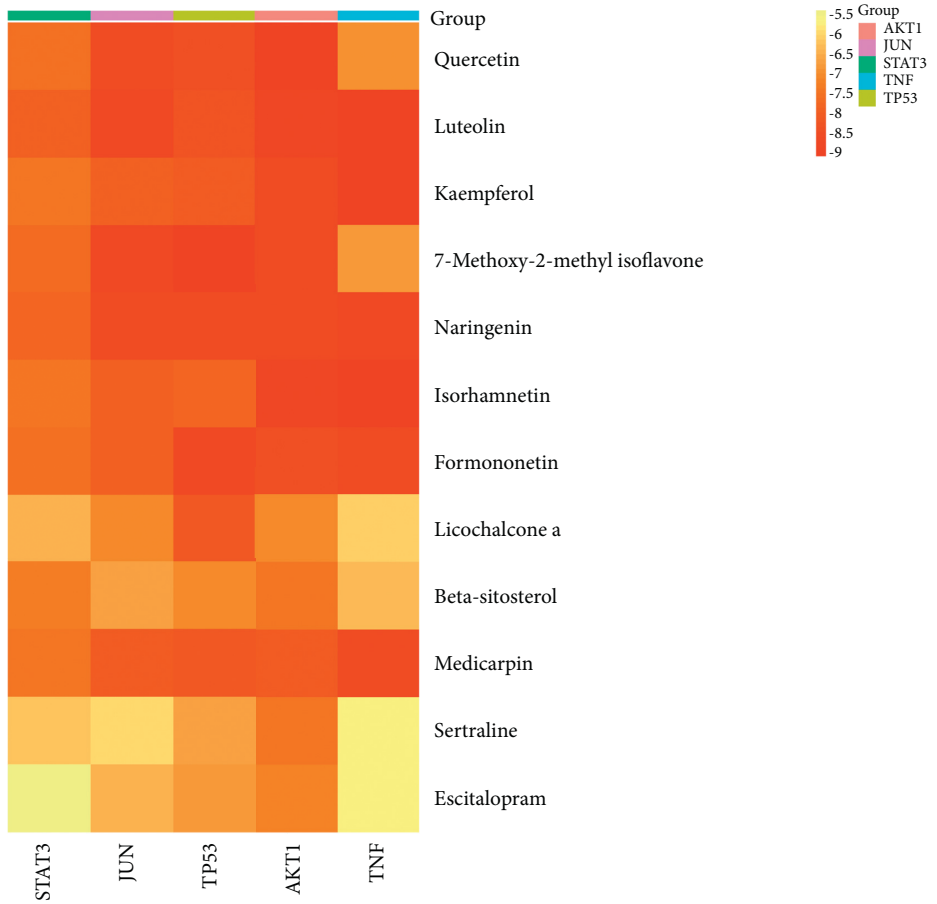

Figure 6: The heat map of the docking score.

markedly increased in the cultures cotreated with NGF and isorhamnetin. This suggests that isorhamnetin might be used to some extent to treat neurodegenerative diseases, including Alzheimer's disease and depression [40]. These important active ingredients are all sourced from GMDZD, and multiple active ingredients work together to exert their effects in the treatment of PSD.

In addition, a total of 19 core targets of GMDZD in PSD were screened in the PPI network: AKT1, STAT3, TP53, CTNNB1, CDKN1A, ESR1, VEGFA, MAPK1, MAPK3, CASP8, CCND1, MAPK14, RELA, TNF, EGFR, FOS, JUN, CXCL8, and STAT1. Among them, EGFR is highly expressed in a variety of malignancies, and depression is common in oncology patients (four times more prevalent than in the general population) [41, 42]. Moreover, EGFR-mutant non-small-cell lung cancer can lead to depression by mediating inflammatory factors [43]. Depressive-like behaviour can be induced by forced swimming, and MAPK1 overexpression in the hippocampus can exert antidepressant effects [44]. It has been reported that estrogen regulates neurotransmitter

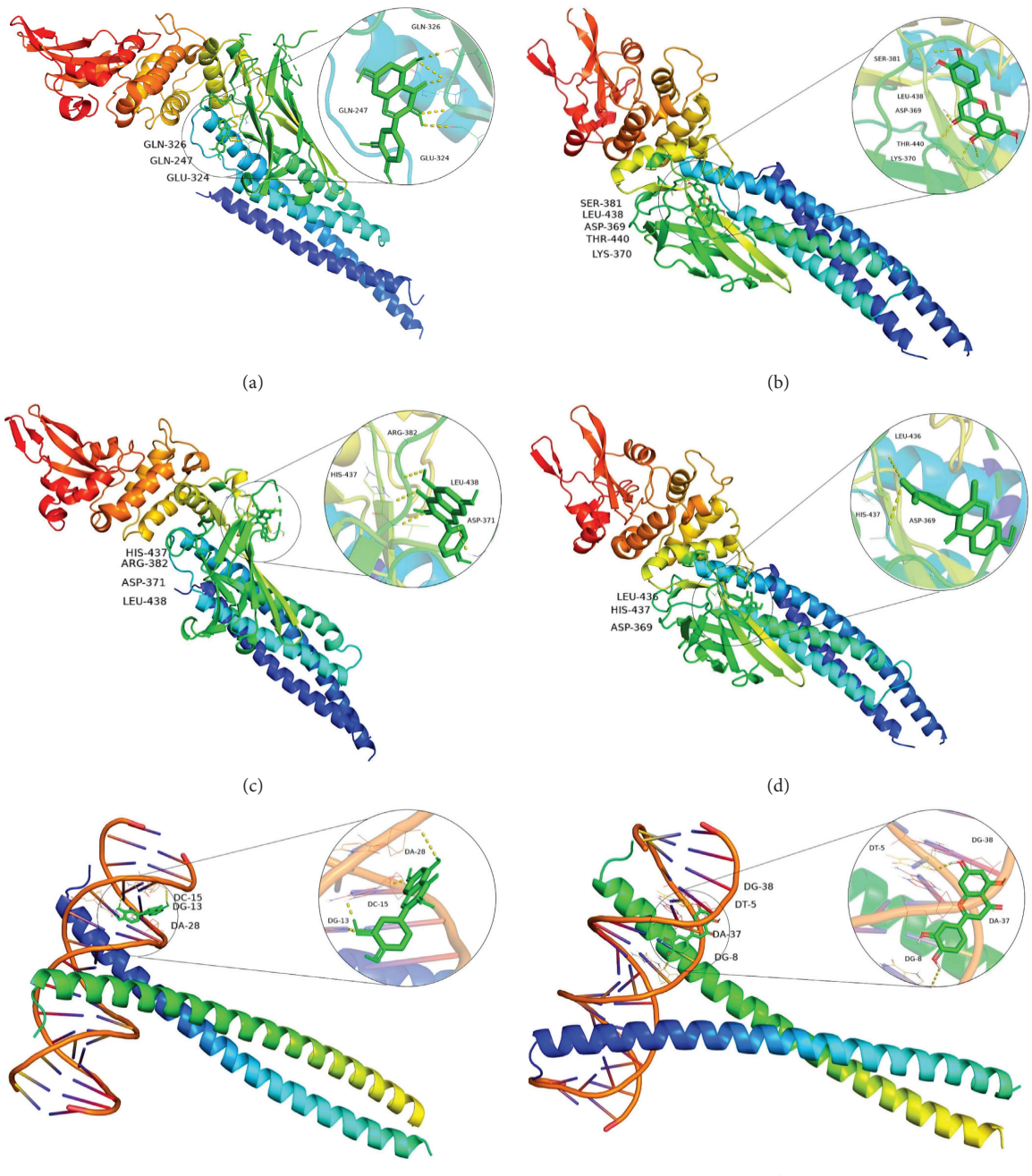

(a) (b) (c) (d) (e) (f)

Figure 7: Continued.

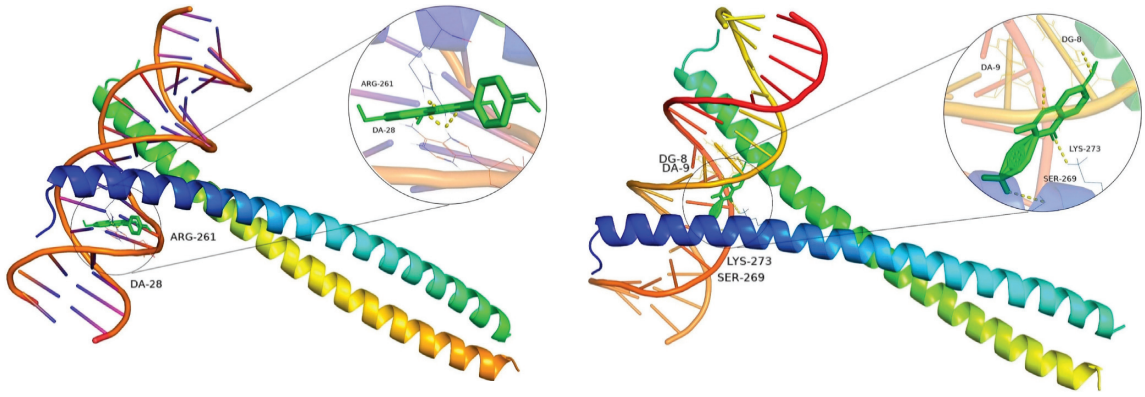

(g) (h)

Figure 7: The docking complex consisting of two targets and four components. The colored irregular lines represent proteins, the green rod-like structures represent compounds, and each image shows the details of the docked parts. (a) STAT3-quercetin, (b) STAT3-luteolin, (c) STAT3-kaempferol, (d) STAT3-7-methoxy-2-methyl isoflavone, (e) JUN-quercetin, (f) JUN-luteolin, (g) JUN-kaempferol, and (h) JUN-7-methoxy-2-methyl isoflavone.

conversion and thus produces antidepressant effects. It is thought that the biological function of estrogen is largely mediated by the intracellular activation of its primary receptors, estrogen receptor alpha (ESR1), and estrogen receptor beta (ESR2). Thus, genetic variation in ESR plays an important role in the susceptibility of women to depression [45, 46]. STAT3 is expressed in both hippocampal neurons and glial cells and is closely related to neurodegenerative diseases. It has been demonstrated that the pharmacological treatment of PSD and an improvement in the depressive state may be related to the inhibition of JAK2/STAT3 signaling pathway-related gene and protein expression, which promotes neural remodelling in the hippocampus [47].

Among the 20 pathways screened by KEGG enrichment analysis, some are closely related to PSD, including the TNF and toll-like receptor signaling pathways. The immune-inflammatory response is an important pathogenic mechanism of PSD. Elevated levels of various inflammatory biomarkers, such as IL-6 and TNF-α, and increased high-sensitivity C-reactive protein (CRP) concentrations were found to be present in patients with mild to moderate depression six months following stroke [48, 49]. It has also been shown that an improvement in depression in rats under acupuncture intervention may be closely related to the significant downregulation of differentially expressed genes involved in the toll-like receptor pathway and TNF signaling pathway in the hippocampus, frontal lobes, and pituitary gland [50]. Additionally, pathological mechanisms, such as neuronal apoptosis and nerve growth disorders, are involved in some pathways that also play an important role in the development of PSD. The efficacy of current antidepressants has been linked to the Ras signaling pathway, which may be involved in the onset and development of depression-related disorders by indirectly affecting neurotrophic factors or directly affecting neuroplasticity [51]. Furthermore, antidepressants not only upregulate cAMP levels in receptor cells but also activate protein kinase A (PKA) to phosphorylate PKA, which then activates the cAMP-response element-binding protein (CREB) signaling pathway, altering functional protein activity and gene expression patterns to form new synapses, thus exerting antidepressant effects [52].

5. Conclusions

In summary, network pharmacological analysis showed that there are as many as 203 possible targets of GMDZD in the treatment of PSD. Several pathways may be very closely related to the treatment of PSD, including the TNF and toll-like receptor signaling pathways, and the 19 core gene targets screened from the PPI network are also enriched in these important pathways. Therefore, the results of this study provide evidence for follow-up research and a basis for the clinical application of GMDZD in the treatment of PSD [53].

Abbreviations

PSD:	Poststroke depression
GMDZD:	*Gan-Mai-Da-Zao* decoction
TCAs:	Tricyclic antidepressants
SSRIs:	Selective serotonin reuptake inhibitors
TCM:	Traditional Chinese medicine
HAM-D:	Hamilton Depression Rating Scale
TCMSP:	Traditional Chinese Medicine Systems Pharmacology Database and Analysis Platform
OB:	Oral bioavailability
DL:	Drug-likeness
ADME:	Absorption, distribution, metabolism, and excretion
UniPort database:	The Universal Protein Resource
PPI:	Protein-protein interaction
STRING:	Search Tool for the Retrieval of Interacting Genes
BC:	Betweenness centrality
CC:	Closeness centrality
DC:	Degree centrality
GO:	Gene Ontology

KEGG: Kyoto Encyclopedia of Genes and Genomes
D-H-C-T: Disease-herb-component-target
PDB: Protein Data Bank
CRP: C-reactive protein.

Data Availability

All data are available in the manuscript, and they are exhibited in figures and tables.

Consent

No consent was required for this study.

Disclosure

This manuscript was published as a preprint on May 17, 2021, in *Research Square*.

Conflicts of Interest

The authors declare no conflicts of interest in relation to this work.

Authors' Contributions

DZC, XFF, and SQD were responsible for study design; acquisition of data; and analysis of data. DZC and XFF wrote the manuscript. CJW, LB, and LNX were involved in acquisition of data and critical revision of the manuscript. YSZ was involved in revision of the manuscript and study supervision. All the authors read and approved the final manuscript.

Acknowledgments

The authors would like to thank the authors of all references. This work was financially supported by the Research Fund of Traditional Chinese Science and Technology Projects in the field of healthcare in Jiangmen City, Guangdong Province (2021YL03021).

Supplementary Materials

Supplementary Table S1: active compounds of iujube-licorice-wheat. Table S2: network topology parameters of gene targets in PPI. Table S3: details in GO and KEGG pathway enrichment analysis. Table S4: the specific targets information in the top 20 pathways. Table S5: the value of the network topology parameters of the active ingredient. (*Supplementary Materials*)

References

[1] Y. Shi, D. Yang, Y. Zeng, and W. Wu, "Risk factors for post-stroke depression: a meta-analysis," *Frontiers in Aging Neuroscience*, vol. 9, p. 218, 2017.

[2] T. R. Martin, M. Oyiza, A. Luis, J. J. Evans, D. J. Stott, and T. J. Quinn, "Prevalence of pre-stroke depression and its association with post-stroke depression: a systematic review and meta-analysis," *Psychological Medicine*, vol. 49, no. 4, pp. 685–696, 2019.

[3] T. Zhang, "Stroke rehabilitation treatment guidelines in China," *Chinese Journal of the Frontiers of Medical Science (Electronic Version)*, vol. 4, pp. 55–76, 2012.

[4] E. J. Benjamin, P. Muntner, A. Alonso et al., "Heart disease and stroke statistics-2019 update: a report from the American heart association," *Circulation*, vol. 139, pp. e56–e528, 2019.

[5] L. Ayerbe, S. Ayis, C. D. A. Wolfe, and A. G. Rudd, "Natural history, predictors and outcomes of depression after stroke: systematic review and meta-analysis," *British Journal of Psychiatry*, vol. 202, no. 1, pp. 14–21, 2013.

[6] M. L. Hackett and K. Pickles, "Part I: frequency of depression after stroke: an updated systematic review and meta-analysis of observational studies," *International Journal of Stroke*, vol. 9, no. 8, pp. 1017–1025, 2014.

[7] T. S. Jørgensen, I. K. Wium-Andersen, M. K. Wium-Andersen et al., "Incidence of depression after stroke, and associated risk factors and mortality outcomes, in a large cohort of danish patients," *JAMA Psychiatry*, vol. 73, pp. 1032–1040, 2016.

[8] A. J. Mitchell, B. Sheth, J. Gill et al., "Prevalence and predictors of post-stroke mood disorders: a meta-analysis and meta-regression of depression, anxiety and adjustment disorder," *General Hospital Psychiatry*, vol. 47, pp. 48–60, 2017.

[9] M. L. Hackett, C. S. Anderson, A. House, and J Xia, "Interventions for treating depression after stroke," *Cochrane Database of Systematic Reviews*, Article ID Cd003437, 2008.

[10] C. Coupland, P. Dhiman, R. Morriss, A. Arthur, G. Barton, and J. Hippisley-Cox, "Antidepressant use and risk of adverse outcomes in older people: population based cohort study," *BMJ*, vol. 343, no. 1, p. d4551, 2011.

[11] S. Liu, Z. H. Yang, X. N. Zhu et al., "Research progress of TCM therapies in treating post-stroke depression," *Acta Chinese Medicine and Pharmacology*, vol. 49, pp. 83–87, 2021.

[12] D. Y. Jiang, P. P. Ren, W. H. Li et al., "Study and analysis of hysteria," *Jilin Journal of Chinese Medicine*, vol. 40, pp. 880–884, 2020.

[13] Y. Shao, "The effect of adding and subtracting Gan-Mai-Da-Zao decoction on postpartum women's sleep disorder and depressive state," *Chinese Journal of Clinical Rational Drug Use*, vol. 9, pp. 38-39, 2016.

[14] B. M. Xia, H. L. Zhang, W. D. Xue et al., "Postpartum depression animal model in mice and effect of Yuejuganmaidazaotang on PPD model," *Chinese Pharmacological Bulletin*, vol. 31, pp. 1324–1327, 2015.

[15] Y. Xiang, P. Meng, X. L. Zhang et al., "Research on central excitatory pharmacological effects of Ganmaidazao decoction," *Asia-Pacific Traditional Medicine*, vol. 12, pp. 22-23, 2016.

[16] D. D. Feng, T. Tang, X. P. Lin et al., "Nine traditional Chinese herbal formulas for the treatment of depression: an ethnopharmacology, phytochemistry, and pharmacology review," *Neuropsychiatric Disease and Treatment*, vol. 12, pp. 2387–2402, 2016.

[17] H. B. Chen, H. G. Zhou, W. T. Li et al., "Network pharmacology: a new perspective of mechanism research of traditional Chinese medicine formula," *China Journal of Traditional Chinese Medicine and Pharmacy*, vol. 34, pp. 2873–2876, 2019.

[18] J. Ru, P. Li, J. Wang et al., "TCMSP: a database of systems pharmacology for drug discovery from herbal medicines," *Journal of Cheminformatics*, vol. 6, no. 1, p. 13, 2014.

[19] Y. Shan, X. Feng, and Y. F. Dong, "The research of chemical constituents and pharmacological activities of *Triticum* L." in

Proceedings of the The Fourth National Symposium on Medicinal Botany and Phycology, pp. 376–384, Nanjing China, October 2004.

[20] Y. Zhang, Y. Li, J. Wang, Y.-L. Yang, and L.-J. Yuan, "Advance in studies on effective components in wheat bran and their pharmacological activities," *China Journal of Chinese Materia Medica*, vol. 39, no. 2, pp. 175–180, 2014.

[21] M. A. Alam, F. I. Al-Jenoobi, A. M. Al-Mohizea, and R. Ali, "Understanding and managing oral bioavailability: physiological concepts and patents," *Recent Patents on Anti-Cancer Drug Discovery*, vol. 10, pp. 87–96, 2015.

[22] S. Tian, J. Wang, Y. Li, D. Li, L. Xu, and T. Hou, "The application of in silico drug-likeness predictions in pharmaceutical research," *Advanced Drug Delivery Reviews*, vol. 86, pp. 2–10, 2015.

[23] Q. Cui, Y.-l. Zhang, Y.-h. Ma et al., "A network pharmacology approach to investigate the mechanism of Shuxuening injection in the treatment of ischemic stroke," *Journal of Ethnopharmacology*, vol. 257, Article ID 112891, 2020.

[24] S. Fishilevich, S. Zimmerman, A. Kohn et al., "Genic insights from integrated human proteomics in GeneCards," *Database*, vol. 2016, Article ID baw030, 2016.

[25] D. Szklarczyk, A. L. Gable, D. Lyon et al., "STRING v11: protein-protein association networks with increased coverage, supporting functional discovery in genome-wide experimental datasets," *Nucleic Acids Research*, vol. 47, no. D1, pp. D607–d613, 2019.

[26] Y. Tang, M. Li, J. Wang, Y. Pan, and F.-X. Wu, "CytoNCA: a cytoscape plugin for centrality analysis and evaluation of protein interaction networks," *Biosystems*, vol. 127, pp. 67–72, 2015.

[27] M. Kohl, S. Wiese, and B. Warscheid, "Cytoscape: software for visualization and analysis of biological networks," *Methods in Molecular Biology*, vol. 696, pp. 291–303, 2011.

[28] K.-Y. Hsin, Y. Matsuoka, Y. Asai et al., "systemsDock: a web server for network pharmacology-based prediction and analysis," *Nucleic Acids Research*, vol. 44, no. W1, pp. W507–W513, 2016.

[29] D. Seeliger and B. L. de Groot, "Ligand docking and binding site analysis with PyMOL and autodock/vina," *Journal of Computer-Aided Molecular Design*, vol. 24, no. 5, pp. 417–422, 2010.

[30] O. Trott, A. J. Olson, and A.D. Vina, "Improving the speed and accuracy of docking with a new scoring function, efficient optimization, and multithreading," *Journal of Computational Chemistry*, vol. 31, pp. 455–461, 2010.

[31] W. Stevens, D. Peneva, J. Z. Li et al., "Estimating the future burden of cardiovascular disease and the value of lipid and blood pressure control therapies in China," *BMC Health Services Research*, vol. 16, no. 1, p. 175, 2016.

[32] J. Y. Gong, X. Q. Wu, J. W. Mao et al., "Advanced in studies on antidepressant effect of flavonoids," *Chinese Traditional and Herbal Drugs*, vol. 42, pp. 195–200, 2011.

[33] N. Samad, A. Saleem, F. Yasmin, and M. A. Shehzad, "Quercetin protects against stress-induced anxiety-and depression-like behavior and improves memory in male mice," *Physiological Research*, vol. 67, pp. 795–808, 2018.

[34] N. Ma, Y. J. Li, and J. P. Fan, "Research progress on pharmacological action of quercetin," *Journal of Liaoning University of Traditional Chinese Medicine*, vol. 20, pp. 221–224, 2018.

[35] M. Ishisaka, K. Kakefuda, M. Yamauchi et al., "Luteolin shows an antidepressant-like effect via suppressing endoplasmic reticulum stress," *Biological and Pharmaceutical Bulletin*, vol. 34, no. 9, pp. 1481–1486, 2011.

[36] S. Zhu, S. Lei, S. Zhou et al., "Luteolin shows antidepressant-like effect by inhibiting and downregulating plasma membrane monoamine transporter (PMAT, Slc29a4)," *Journal of Functional Foods*, vol. 54, pp. 440–448, 2019.

[37] M. D. Burton, J. L. Rytych, R. Amin, and R. W. Johnson, "Dietary luteolin reduces proinflammatory microglia in the brain of senescent mice," *Rejuvenation Research*, vol. 19, no. 4, pp. 286–292, 2016.

[38] Y. D. Liang, Y. G. Tan, S. Zhang et al., "Effect and mechanism of kaempferol on depression-like behavior in elderly rats with chronic stress depression," *The Chinese Journal of Clinical Pharmacology*, vol. 36, no. 326, pp. 62–64, 2020.

[39] B. Ben-Azu, E. E. Nwoke, A. O. Aderibigbe et al., "Possible neuroprotective mechanisms of action involved in the neurobehavioral property of naringin in mice," *Biomedicine & Pharmacotherapy*, vol. 109, pp. 536–546, 2019.

[40] S. L. Xu, R. C. Choi, K. Y. Zhu et al., "Isorhamnetin, A flavonol aglycone from *Ginkgo biloba* L., induces neuronal differentiation of cultured PC12 cells: potentiating the effect of nerve growth factor," *Evidence-based Complementary and Alternative Medicine: ECAM*, vol. 2012, Article ID 278273, 11 pages, 2012.

[41] B. Bortolato, T. N. Hyphantis, S. Valpione et al., "Depression in cancer: the many biobehavioral pathways driving tumor progression," *Cancer Treatment Reviews*, vol. 52, pp. 58–70, 2017.

[42] A. Szelei and P. Döme, "Daganatos megbetegedések és a depresszió: rövid irodalmi áttekintés," *Orvosi Hetilap*, vol. 161, no. 22, pp. 908–916, 2020.

[43] D. C. McFarland, D. R. Jutagir, B. Rosenfeld et al., "Depression and inflammation among epidermal growth factor receptor (EGFR) mutant nonsmall cell lung cancer patients," *Psycho-Oncology*, vol. 28, no. 7, pp. 1461–1469, 2019.

[44] S. D. Iñiguez, L. F. Parise, M. K. Lobo et al., "Upregulation of hippocampal extracellular signal-regulated kinase (ERK)-2 induces antidepressant-like behavior in the rat forced swim test," *Behavioral Neuroscience*, vol. 133, no. 2, pp. 225–231, 2019.

[45] A. Różycka, R. Słopień, A. Słopień et al., "The MAOA, COMT, MTHFR and ESR1 gene polymorphisms are associated with the risk of depression in menopausal women," *Maturitas*, vol. 84, pp. 42–54, 2016.

[46] E.-C. Tan, H.-W. Lim, T.-E. Chua, H.-S. Tan, T. Lee, and H. Chen, "Investigation of variants in estrogen receptor genes and perinatal depression," *Neuropsychiatric Disease and Treatment*, vol. 14, pp. 919–925, 2018.

[47] H. P. Liu, "The effect of YinaoJieyu prescription on the intervention of JAK2 and STAT3 proteins in the hippocampus of post-stroke depressed rats," Master Thesis, Beijing University of Chinese Medicine, Beijing, China, 2020.

[48] D. Shinar, C. R. Gross, T. R. Price, M. Banko, P. L. Bolduc, and R. G. Robinson, "Screening for depression in stroke patients: the reliability and validity of the center for epidemiologic studies depression scale," *Stroke*, vol. 17, no. 2, pp. 241–245, 1986.

[49] W. Zhang and X.-A. Zhang, "A novel urinary metabolite signature for non-invasive post-stroke depression diagnosis," *Cell Biochemistry and Biophysics*, vol. 72, no. 3, pp. 661–667, 2015.

[50] Y. Wang, *Study on the antidepressant mechanism of acupuncture based on whole-transcriptome sequencing*, PhD

Thesis, Beijing University of Chinese Medicine, Beijing, China, 2017.

[51] F. Wang, C. Zhang, and Y. R. Fang, "Ras signaling pathway and neural plasticity mechanism of depression," *Journal of Shanghai Jiaotong University*, vol. 35, p. 1556, 2015.

[52] J. M. Wang, Y. Yang, X. Y. Liu, and C. L. Chen, "Research progress on mechanism and signaling pathway regulation of Chinese materia medica on depression," *Chinese Archives of Traditional Chinese Medicine*, vol. 39, pp. 115–118, 2021.

[53] Z. C. Ding, F. F. Xu, Q. D. Sun et al., "Exploring the mechanism of action of herbal medicine (Gan-Mai-Da-Zao decoction) for post-stroke depression based on network pharmacology and molecular docking," 2021, https://www.researchsquare.com/article/rs-508953/v1.

Hindawi
Evidence-Based Complementary and Alternative Medicine
Volume 2021, Article ID 9990020, 8 pages
https://doi.org/10.1155/2021/9990020

Review Article

The Combination of Tradition and Future: Data-Driven Natural-Product-Based Treatments for Parkinson's Disease

Zhijun Miao,[1,2] Jinwei Bai,[3] Li Shen ,[1] and Rajeev K. Singla [1,4]

[1]*Institutes for Systems Genetics, Frontiers Science Center for Disease-related Molecular Network, West China Hospital, Sichuan University, Chengdu 610041, Sichuan, China*
[2]*Department of Urology, Suzhou Dushu Lake Hospital, Suzhou, China*
[3]*Library of West-China Hospital, Sichuan University, Chengdu 610041, China*
[4]*iGlobal Research and Publishing Foundation, New Delhi 110059, India*

Correspondence should be addressed to Rajeev K. Singla; rajeevsingla26@gmail.com

Received 26 March 2021; Revised 29 June 2021; Accepted 6 July 2021; Published 14 July 2021

Academic Editor: Xue-Rui Wang

Copyright © 2021 Zhijun Miao et al. This is an open access article distributed under the Creative Commons Attribution License, which permits unrestricted use, distribution, and reproduction in any medium, provided the original work is properly cited.

Parkinson's disease (PD) is a neurodegenerative disorder in elderly people. The personalized diagnosis and treatment remain challenges all over the world. In recent years, natural products are becoming potential therapies for many complex diseases due to their stability and low drug resistance. With the development of informatics technologies, data-driven natural product discovery and healthcare is becoming reality. For PD, however, the relevant research and tools for natural products are quite limited. Here in this review, we summarize current available databases, tools, and models for general natural product discovery and synthesis. These useful resources could be used and integrated for future PD-specific natural product investigations. At the same time, the challenges and opportunities for future natural-product-based PD care will also be discussed.

1. Introduction

Parkinson's disease (PD) is a neurodegenerative disorder (NDD) commonly seen in the elderly. The prevalence of PD is increasing with age, of which the lifespan risk is 2% for men and 1.3% for women [1]. Many factors have been revealed to tightly relate to PD, including genes, gut microbes, the living environment, and lifestyle [2–4]. In the past decades, efforts have been made both in mechanism investigations and clinical treatments. A large number of molecules have been reported for their therapeutic potential against Parkinson's disease, such as levodopa [5], ubiquinone [6], and creatine [7]. The efficacy, however, is rather limited along with uncontrolled side effects [8]. Since several years ago, natural products have drawn more and more attention, which are considered as potential breakthroughs for PD treatments.

Natural products are a class of chemical compounds or substances produced by living organisms, the sources of which can be plants, animals, fungi, and bacteria [9]. Compared to synthetic drugs, natural products tend to have unique structures that are rather difficult to be synthesized in the lab. Nevertheless, the stabilities and efficacies sometimes are better [10]. Meanwhile, components in natural products are usually in the form of a mixture. Interactions among them result in weaker toxicity, side effects, and drug resistance [11,12]. Considering these advantages, an increasing number of research has been focusing on improving PD treatments with natural products. In a recent study, for example, gardenin A has shown its role in neuroprotection against environmental-toxin-induced Parkinson's disease pathogenesis [13]. Another study by Haruka et al. pointed out that sesaminol may increase Nrf2 expression and then activate the Nrf2-ARE signaling pathway and decrease the expression level of α-synuclein, indicating its preventative effect on PD [14]. Besides, Liu et al. also found that a fumarate salt form of dimethylaminomicheliolide called ACT001 derived from parthenolide can prevent the overexpression of α-synuclein induced by 1-methyl-4-phenyl-1, 2, 3, 6-tetrahydropyridine, which could serve as a good concomitant drug for L-3, 4-dihydroxyphenylalanine (L-DOPA) to lower the intake dose and its side effects [15].

These gathering evidence show a great therapeutic potential of natural products in PD treatments.

Traditional drug discovery is mainly based on two approaches: ligand-based drug design and structure-based drug design [16]. Computational technologies are frequently applied during this period, which is usually known as Computer-Aided Drug Discovery (CADD). Over the past decades, the innovations in chemistry, biomedical science, and engineering, as well as high-throughput screening, have rapidly improved the efficiency of a huge number of compounds' screening for 1–3 specific targets. Numerous tools, databases, and models are constructed with accumulating data [17], bringing current drug discovery into the "big data era." There are five intrinsic characteristics for big data, including volume, variety, value, velocity, and veracity [18], as shown in Figure 1. Compared to traditional CADD methods, a successful big-data-based CADD strategy firstly needs a standard for integration of multilevel data. At the same time, high-speed algorithms are required for data mining, structuring, and analysis in order to ensure the efficiency and accuracy for drug-target interaction simulation. Finally, the main roles for most previous databases are storage and reference. The density of data value is pretty low. How to utilize updated technologies and algorithms to figure out the real value of data will be very essential for novel drug discovery. In summary, it is necessary to develop novel approaches that systematically address the high-volume, multidimensional, and highly sparse data sources needed for drug efficacy and adverse effect prediction and evaluation.

In recent years, some studies have already employed computational methods on natural product identification and characterization. These resources could be quite valuable for PD-related natural product discovery. In this review, we will summarize available data sources, databases, computational tools, and models and, last but not the least, the future challenges and chances for data-driven natural product discovery for PD treatments.

2. Natural Product Databases for Data Sharing and References

Biomedical studies have made great advances with the development of omics and informatics technologies. Accumulating scientific data, including omics data, clinical data, and other biological data, are extremely valuable research resources. Thus, data standardization, annotation, sharing, and integration are becoming quite essential. The well-structured databases can not only store and manage existing data but also can be utilized for data sharing and integrated analysis. Good examples for such databases in PD research include NDDVD [19], Gene4PD [20], and PDmethDB [21]. Natural products have a broad range of compounds, and a large number of diseases can be treated by them. The establishment of relevant databases can greatly facilitate our understanding towards the mechanisms by which a certain natural product works on its target diseases, and clinicians can also get advised for precision treatments [22]. To date, there are already quite a few published natural-product-specific databases. Although Sorokina et al. have constructed a database named COCONUT (https://coconut.naturalproducts.net) where they collected a part of free available databases for natural products [23], we will make up and summarize some nonincluded databases for reference, the list of which is shown in Table 1.

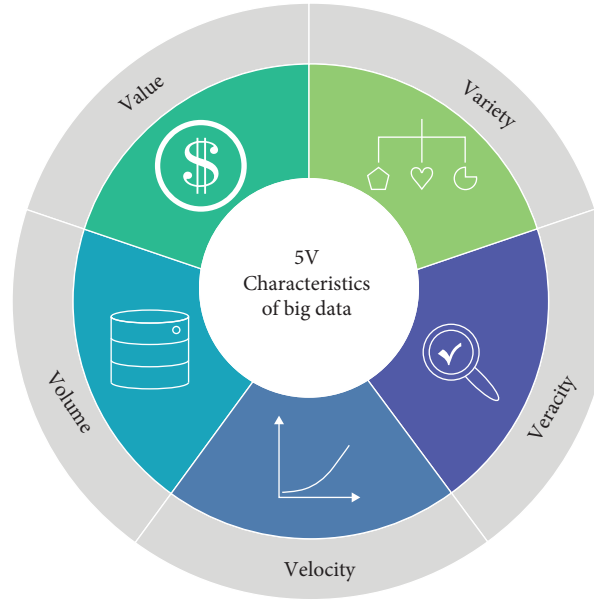

Figure 1: "5V" characteristics of big data.

2.1. Databases of Different Traditional Medicine Systems. Traditional medicine can be divided into several medical systems according to the regions, such as traditional Chinese medicine (TCM), traditional Indian medicine (also known as Ayurveda), and traditional Islamic medicine. Although there are overlaps between different traditional medical systems, they also have their own unique features. From a systemic view, databases and knowledge bases to share and annotate these medical systems is the first step for integrated analysis and natural products screening. Efforts have been made in the past decades. For example, Fang et al. built a comprehensive database for traditional Chinese medicine called HERB, in which the basic herb information, effective targets, and gene-gene interactions are provided [24]. Another TCM-related database is SymMap, which could be a good support for HERB as it contains not only prescriptions but also symptom mappings for users [32]. The Indian Medical Plants, Phytochemistry And Therapeutics (IMPPAT) is a curated database for Indian traditional medicine that shares the standardized names and usages of some traditional Indian herbs [33], and for Irian traditional medicine, there is also a similar database called Universal Natural Product Resource (UNaProd) [29]. A direct evidence among these databases is Atropa acuminata, which was reported to be a potential natural product medicine for PD. The effective compound named atropine is demonstrated to remarkably reduce raclopride-induced muscle rigidity through the activation of the ventral region of the striatum [39]. Meanwhile, there are also some indirect clues.

Table 1: A summary on natural product databases which are not included in COCONUT.

Name	Description	Url	Pmid	References
HERB	A traditional Chinese medicine database providing basic herb information, effective targets, expression profiling, and interaction networks	https://herb.ac.cn	33264402	[24]
PSC-db	A 3D database for plant secondary compounds	https://pscdb.appsbio.utalca.cl	33672700	[25]
NPBS	A database containing relationships between natural products and biological sources	https://www.organchem.csdb.cn/scdb/NPBS	33306802	[26]
BiG-FAM	A biosynthetic gene cluster families database	https://bigfam.bioinformatics.nl	33010170	[27]
CMNPD	A database of marine natural products	https://www.cmnpd.org	32986829	[28]
UNaProd	A natural products data resource for Iranian traditional medicine	https://jafarilab.com/unaprod	32454857	[29]
TeroKit	A database for terpenome academic research	https://terokit.qmclab.com	32286817	[30]
MedPServer	A database for therapeutic targets screening of natural products	https://bif.uohyd.ac.in/medserver	30381914	[31]
SymMap	A database for Chinese traditional medicine with symptom mapping	https://www.symmap.org	30380087	[32]
IMPPAT	An Indian medical plants, phytochemistry, and therapeutics database	https://cb.imsc.res.in/imppat	29531263	[33]
PAMDB	A database of *Pseudomonas aeruginosa* metabolome	https://pseudomonas.umaryland.edu	29106626	[34]
TriForC	A database for plant triterpene biosynthesis	https://bioinformatics.psb.ugent.be/triforc	29045755	[35]
DEREP-NP	A database for rapid dereplication of known natural products	https://github.com/clzani/DEREP-NP	28616931	[36]
TMDB	A database for small-molecule compounds from tea	https://pcsb.ahau.edu.cn:8080/TCDB/index.jsp	25224438	[37]
3DMET	A database for 3D structures of natural metabolites	https://www.3dmet.dna.affrc.go.jp	23293959	[38]

For instance, isorhynchophylline, which is the compound of *Uncaria sessilifructus, Uncaria tomentosa,* and *Semen Cavaliae*, can significantly promote autophagy of neuronal cells and avoid the accumulation of α-synuclein by targeting SCNA [40]. Curcumin derived from *Acorus calamus* and *Radix Angelicae sinensis* can notably inhibit the activity of LRRK2 kinase and suppress PD-like phenotypes [41]. Taken together, these databases are mainly from a clinical view, data from which may provide us with potential traditional medicine prescripts for PD treatments. At the same time, integrated analysis of them may give novel insights to researchers and clinicians from different regions. Real-time update, thus, is quite essential.

2.2. Databases of Different Natural Product Sources. Natural products have multiple sources. An unfractionated extract from these sources may contain a range of structurally diverse and often novel chemical compounds [42]. The biological diversity contributes to the chemical diversity in the nature; in other words, researchers have to collect samples all over the world for natural product screening and novel drug discovery [43]. During this period, databases for such data collection are highly demanded. There are two main roles for these databases. First, they are data containers. Second, they can serve as references. Once potential natural products are identified, a comparison could be conducted with known products in the databases between their compounds, structures, and so on [44]. Also, advanced molecular-level analysis can be performed for further mechanism investigation and target screening. In the past decades, several such databases have been already constructed, including NPASS [44], NANPDB [45], and Super Natural II [46], most of which were included or introduced in COCONUT. Recently, there are several newly published resources which are good supplementary for natural product source databases. For example, Xu et al. built a relationship database called Natural Products & Biological Sources (NPBS), which is an online resource that contains relationships between natural products and biological sources [26]. Compared to previous natural product databases, NPBS not only provides molecular properties and biological sources of natural products but also shows properties of biological sources. There are some other databases which focus on specific classes of natural products. For instance, the Comprehensive Marine Natural Products Database (CMNPD) is a database for marine-sourced natural products, whereas the *Pseudomonas aeruginosa* Metabolome Database (PAMDB) is a resource for *Pseudomonas aeruginosa* metabolome [28,34]. Network analysis and ontology analysis are inserted. These databases could serve as good references when we do novel natural product screenings for PD treatments.

3. Computational Models and Tools for PD Natural Product Investigation

Computational modeling is a powerful method for PD diagnosis, treatments, and drug discovery. Statistical tests,

such as *t*-test, Wilcoxon signed-rank test, and eBayes, are commonly used for dysfunctional molecule identification [47]. Combined with network-based analysis, these significantly dysfunctional molecules can be further investigated for their potential as biomarkers or therapeutic targets for PD [22]. In recent years, with the assistance of deep learning, the drug target screening has entered into a new era. AlphaFold, for example, is a deep-learning-based prediction tool for protein folding, which remarkably increased the target discovery efficiency [48]. How to integrate and utilize these resources well will be the key for future natural product investigation and PD care [49].

3.1. Models for Natural Product Synthesis. The production of natural products via extraction from biological organisms is often limited several factors, including slow growth, low yield, extraction and purification efficiencies, and weather and climate change. Laborious synthesis could be a quite accessible way for high-volume natural product production. However, it is always a challenge for computer-aided organic synthesis. Although there are already some tools and algorithms which are capable of completely autonomous planning, these programs can only execute one step at a time. In most cases, the computer-aided drug design and target screening are limited to relatively simple targets. Chematica, which was designed by Mikulak-Klucznik et al., is a tool for complex natural product syntheses route design [50]. With the input of reactants, steps, and target products, a highly efficient synthesis route can be designed in seconds. Compared to the reported synthesis routes, the steps taken in newly designed routes are less and the efficiency is higher, and the cost is lower as well [51]. Another route design tool developed by Waller et al. is in a different way [52]. Monte Carlo tree search was applied in this system for retrosynthetic route discovery, as shown in Figure 2. With the assistance of symbolic artificial intelligence, this new AI tool does not require chemists to input any rules, but learns the rules of chemical transformation on its own and then performs fast and efficient inverse synthesis analyses based on reported one-step reactions. When asked to design a synthetic route for a target molecule, this AI system can make selections and judgements by itself and select the most promising precursor molecule based on the design rules. Feasibility of the synthesis will be further evaluated until a best route is found. This is a sensational innovation as it can create new strategies to find the best way for target molecule syntheses, totally without relying on any existing experience or strategies. Taken together, these tools discussed above could serve as strong tools for natural product laborious synthesis design.

3.2. Models for Precise Natural Product Medication. Network is an important physics theory which has been applied into many fields [53]. The application of that in biomedicine enables us to measure different molecule interactions at the systemic level [54]. Previous biomedical studies tended to utilize biological networks to investigate the consequences to the whole systems brought by dysfunctional

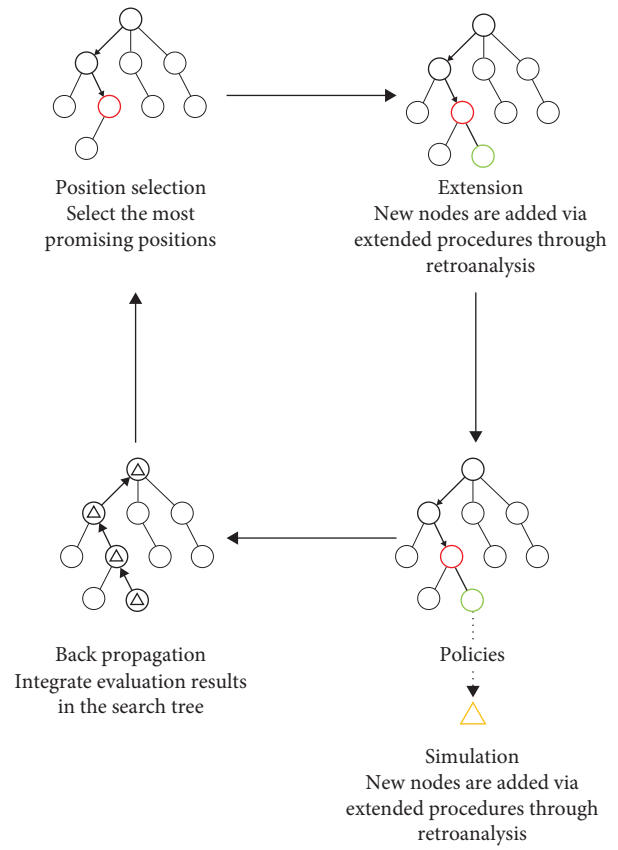

Figure 2: The Monte Carlo tree search algorithm for synthesis route design.

molecules [55]. A more functional application is to use protein-protein interaction, gene-gene interaction, or coexpression network for complex disease biomarker discovery and drug target screening [56–59]. In the "Genomic Era," DNA/RNA sequencing has enabled rapid identification of new targets and reuse of approved drugs to treat heterogeneous diseases by "precise" targeting of personalized disease modules [60]. The network-based approach makes it possible for drug retargeting and combination therapy by measuring the proximity of disease proteins in the human protein interaction group. Cheng et al. developed a genome-wide position system named Genome-wide Positioning Systems network (GPSnet), which can reuse drugs via specific disease module targets derived from an individual patient's DNA and RNA sequencing profiles mapped to the human protein-protein interactome network [61]. Two main functions are included in GPSnet: cancer specific disease module identification and computational drug repurposing. Random walk with restart process was applied for cancer-specific disease model identification, after which network distance between node *s* and nearest disease protein *t* was measured through the following formula:

$$d(S, T) = \frac{1}{\|T\|} \sum_{t \in T} \min_{s \in S} d(s, t). \quad (1)$$

Here, S is the set of disease proteins, and *T* is the set of drug targets. The significance of the network distance

between a drug and a given disease was further evaluated by setting a reference distance distribution. GPSnet may be a promising tool for natural product discovery, synthesis, and precise usage in PD treatments. Besides, there are also studies which applied network theory for natural products' potential in human health. Cao et al. employed a metabolome- and metagenome-wide association network to distinguish microbial natural products and microbial biotransformation products in human microbiota [62]. Chamberlin et al. analyzed a natural product-target interaction network and claimed that natural products show target family groupings both distinct from and in common with cancer drugs, showing tremendous potential of natural products in cancer therapy [63]. Another study by Gogoi et al. also provides similar evidence via pharmacology network analysis [64]. Although there are still no studies which applied network analysis to PD-specific natural product investigation, with the help of could computing and the evidence above, there could be great chances in the future.

4. Perspectives on Big-Data-Based PD Natural Product Medicine

In the big data era, PD care barely depends on clinical treatments. The involvement of informatics technologies has tightly combined basic research and advanced technologies in hardware development and clinical medicine, together promoting PD care into the "precision medical care era" [65]. In the last decade, technologies such as virtual reality and augmented reality, robot, and wearable devices have developed numerous strategies for PD prevention, diagnosis, and treatment [66], which has become an indispensable part for big-data-based PD medicine. Figure 3 shows a blueprint for future informatics-assisted PD care. First, huge databases for multilevel data storage, including omics data, clinical data, lifestyle data, environment data, and natural product data, are demanded. These data resources may provide references and knowledge for AI training. A well-trained AI system based on them will then play 2 main roles. On one hand, the system can be utilized for novel natural product screening and precise drug recommendation, which is slightly similar to GPSnet. On the other hand, with real-time physiological data as references, the system can monitor patients' health status and work as an alarming system. Meanwhile, daily analysis on the cloud platform can also provide PD care suggestions for PD patients. To realize such health care scheme, however, there are still several challenges need to be solved.

4.1. Databases and Knowledge Bases for PD-Specific Natural Products. Current natural product databases only stored very limited candidates for PD treatments. As the relevant research data accumulate, however, a PD-specific natural product database is urgently needed for future therapeutic compound screening. Since PD is a complex disease, a systematic analysis should be integrated into the database as well. As data are gathered from a different level, such as effective compounds in natural products, supportive molecules, targets, environments, and other PD-associated factors, a knowledge base could be further constructed, which will draw a multilayered landscape for PD care. Based on the constructed knowledge bases, a knowledge graph, which is a resource that integrates one or more expert-derived sources of information into a graph where nodes represent biomedical entities and edges represent relationships between two entities, will be a good support, giving novel and clear insights for both clinical decision and basic research [67].

4.2. AI-Based Systematic Modeling for Highly Efficient Natural Product Screening. Since PD is the product of a dynamic interaction between the patient's genetics, modeling for the evolution of PD and dynamic simulation of the effects of natural products on PD patients is the key for the AI system. To identify the key factors for PD development and figure out highly efficient natural products will be a challenge [68]. Meanwhile, as data accumulate, how to improve the accuracy and efficiency of AI systems for natural product screening and precise medication is another challenge. Under this situation, training data quality, feature extraction, algorithm selection and optimization, and validation are the most important parts for improvements. A standard for data collection and data clear is essential as well.

4.3. Integration of Cross-Level Data to Assist Precision PD Treatments. PD research and medication covers a broad range of data types, which are from molecular phenotypes to clinical phenotypes. The connections between them tend to be quite complex. At present, studies usually focus on only few parts and the data generated are isolated. The linkage between molecular phenotype and clinical phenotype are important for disease systemic modeling. An example is that a certain natural product is utilized and positive changes are noticed in the molecular level but nothing happened on patients' clinical phenotypes. Thus, if molecular-clinical paired data are collected over time, the progression of PD can be, therefore, simulated and modeled. There are already several mature paradigms such as The *Cancer* Genome Atlas (TCGA) and International *Cancer* Genome Consortium (ICGC), which could be excellent references for PD data integration.

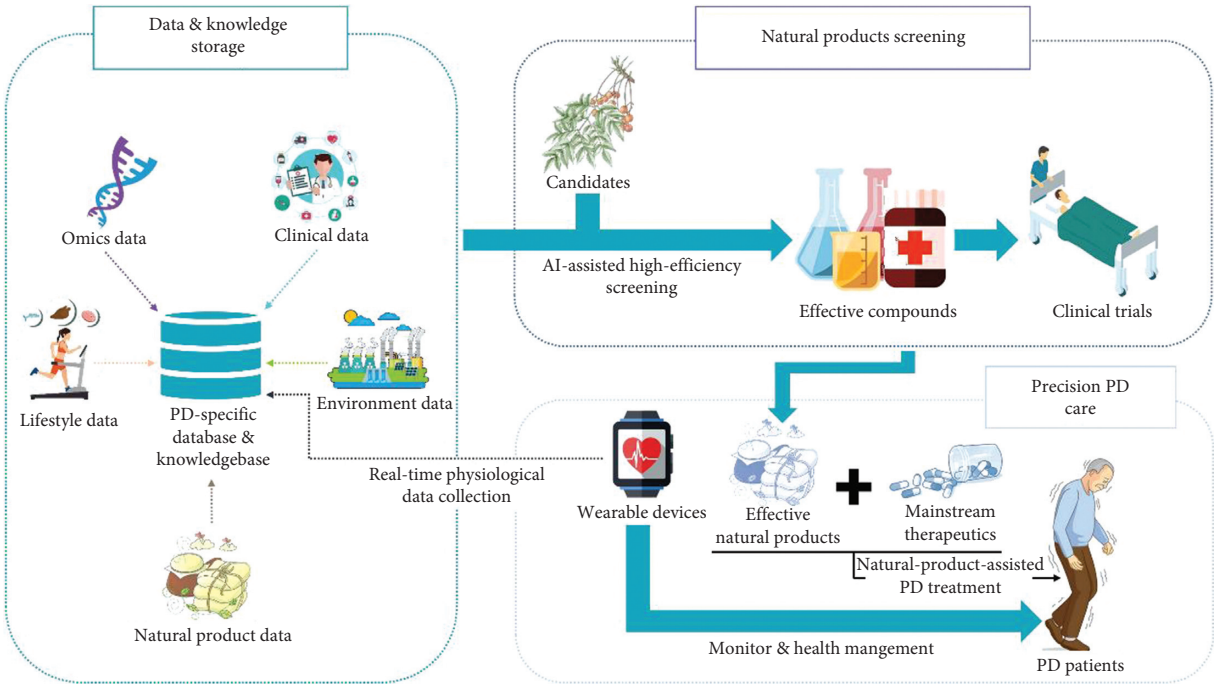

Figure 3: A systemic structure of data-driven PD care.

Data Availability

The literature used to prepare this review article is already available publicly.

Conflicts of Interest

The authors declare no conflicts of interest.

Acknowledgments

This work was supported by the National Key Research and Development Program of China (2016YFC1306605), the National Natural Science Foundation of China (32070671), and the Regional Innovation Cooperation between Sichuan and Guangxi Provinces (2020YFQ0019).

References

[1] R. B. Schneider, J. Iourinets, and I. H. Richard, "Parkinson's disease psychosis: presentation, diagnosis and management," *Neurodegenerative Disease Management*, vol. 7, no. 6, pp. 365–376, 2017.

[2] E. M. Kline, M. C. Houser, M. K. Herrick et al., "Genetic and environmental factors in Parkinson's disease converge on immune function and inflammation," *Movement Disorders*, vol. 36, no. 1, pp. 25–36, 2021.

[3] M. Elfil, S. Kamel, M. Kandil, B. B. Koo, and S. M. Schaefer, "Implications of the gut microbiome in Parkinson's disease," *Movement Disorders*, vol. 35, no. 6, pp. 921–933, 2020.

[4] C. Marras, C. G. Canning, and S. M. Goldman, "Environment, lifestyle, and Parkinson's disease: implications for prevention in the next decade," *Movement Disorders*, vol. 34, no. 6, pp. 801–811, 2019.

[5] C. Spanaki, I. Boura, A. Avgoustaki et al., "Buried bumper syndrome: a common complication of levodopa intestinal infusion for Parkinson disease," *Parkinsonism & Related Disorders*, vol. 85, pp. 59–62, 2021.

[6] D. Athauda and T. Foltynie, "The ongoing pursuit of neuroprotective therapies in Parkinson disease," *Nature Reviews Neurology*, vol. 11, no. 1, pp. 25–40, 2015.

[7] A. Bender, W. Koch, M. Elstner et al., "Creatine supplementation in Parkinson disease: a placebo-controlled randomized pilot trial," *Neurology*, vol. 67, no. 7, pp. 1262–1264, 2006.

[8] S. Duty and P. Jenner, "Animal models of Parkinson's disease: a source of novel treatments and clues to the cause of the disease," *British Journal of Pharmacology*, vol. 164, no. 4, pp. 1357–1391, 2011.

[9] R. J. Krueger, *Drugs of Natural Origin. A Textbook of Pharmacognosy*, G. Samuelson, Ed., vol. 620Swedish Pharmaceutical Press, Stockholm, Sweden, 5th edition, ISBN 91-9743-184-2, 2005.

[10] A. G. Atanasov, B. Waltenberger, E.-M. Pferschy-Wenzig et al., "Discovery and resupply of pharmacologically active plant-derived natural products: A review," *Biotechnology Advances*, vol. 33, no. 8, pp. 1582–1614, 2015.

[11] B. S. Moore, G. T. Carter, and M. Brönstrup, "Editorial: Are natural products the solution to antimicrobial resistance?" *Natural Product Reports*, vol. 34, no. 7, pp. 685-686, 2017.

[12] S. R. M. Ibrahim, A. Sirwi, B. G. Eid, S. G. A. Mohamed, and G. A. Mohamed, "Summary of natural products ameliorate concanavalin a-induced liver injury: structures, sources, pharmacological effects, and mechanisms of action," *Plants (Basel, Switzerland)*, vol. 10, no. 2, 2021.

[13] U. Maitra, T. Harding, Q. Liang, and L. Ciesla, "GardeninA confers neuroprotection against environmental toxin in a Drosophila model of Parkinson's disease," *Communications Biology*, vol. 4, no. 1, p. 162, 2021.

[14] H. Kaji, I. Matsui-Yuasa, K. Matsumoto, A. Omura, K. Kiyomoto, and A. Kojima-Yuasa, "Sesaminol prevents Parkinson's disease by activating the Nrf2-ARE signaling pathway," *Heliyon*, vol. 6, no. 11, Article ID e05342, 2020.

[15] Q. Liu, S. Zhang, D. Zhu, X. Tang, Y. Che, and X. Feng, "The parthenolide derivative ACT001 synergizes with low doses of L-DOPA to improve MPTP-induced Parkinson's disease in mice," *Behavioural Brain Research*, vol. 379, Article ID 112337, 2020.

[16] K. M. Merz, D. Ringe, and C. H. Reynolds, *Drug Design: Structure- and Ligand-Based Approaches*, Cambridge University Press, Cambridge, UK, 2010.

[17] L. Zhao, H. L. Ciallella, L. M. Aleksunes, and H. Zhu, "Advancing computer-aided drug discovery (CADD) by big data and data-driven machine learning modeling," *Drug Discovery Today*, vol. 25, no. 9, pp. 1624–1638, 2020.

[18] Y. Demchenko, P. Grosso, and C. D. L. P. Membrey, "Addressing big data issues in scientific data infrastructure," in *Proceedings of the 2013 International Conference on Collaboration Technologies and Systems (CTS)*, San Diego, CA, USA, May 2013.

[19] Y. Yang, *NDDVD: An Integrated and Manually Curated Neurodegenerative Diseases Variation Database*, Database, Oxford, UK, 2018.

[20] B. Li, G. Zhao, Q. Zhou et al., "Gene4PD: a comprehensive genetic database of Parkinson's disease," *Frontiers in Neuroscience*, vol. 15, Article ID 679568, 2021.

[21] C. Wang, L. Chen, M. Zhang, Y. Yang, and G. Wong, "PDmethDB: A curated Parkinson's disease associated methylation information database," *Computational and Structural Biotechnology Journal*, vol. 18, pp. 3745–3749, 2020.

[22] B. Shen, Y. Lin, C. Bi et al., "Translational informatics for Parkinson's disease: from big biomedical data to small actionable alterations," *Genomics, Proteomics & Bioinformatics*, vol. 17, no. 4, pp. 415–429, 2019.

[23] M. Sorokina, P. Merseburger, K. Rajan, M. A. Yirik, and C. Steinbeck, "Coconut online: collection of open natural products database," *Journal of Cheminformatics*, vol. 13, no. 1, p. 2, 2021.

[24] S. Fang, L. Dong, L. Liu et al., "HERB: a high-throughput experiment- and reference-guided database of traditional Chinese medicine," *Nucleic Acids Research*, vol. 49, no. D1, pp. D1197–D1206, 2021.

[25] A. Valdes-Jimenez, C. Peña-Varas, P. Borrego-Muñoz et al., "PSC-db: a structured and searchable 3D-database for plant secondary compounds," *Molecules*, vol. 26, no. 4, 2021.

[26] T. Xu, W. Chen, J. Zhou et al., *NPBS Database: A Chemical Data Resource with Relational Data between Natural Products and Biological Sources*, p. 2020, Database, Oxford, UK, 2020.

[27] S. A. Kautsar, K. Blin, S. Shaw, T. Weber, and M. H. Medema, "BiG-FAM: the biosynthetic gene cluster families database," *Nucleic Acids Research*, vol. 49, no. D1, pp. D490–D497, 2021.

[28] C. Lyu, T. Chen, B. Qiang et al., "CMNPD: a comprehensive marine natural products database towards facilitating drug discovery from the ocean," *Nucleic Acids Research*, vol. 49, no. D1, pp. D509–D515, 2021.

[29] A. Naghizadeh, D. Hamzeheian, S. Akbari et al., "UNaProd: a universal natural product database for materia medica of Iranian traditional medicine," *Evidence-based Complementary and Alternative Medicine: eCAM*, vol. 2020, Article ID 3690781, 2020.

[30] T. Zeng, Z. Liu, J. Zhuang et al., "TeroKit: a database-driven web server for terpenome research," *Journal of Chemical Information and Modeling*, vol. 60, no. 4, pp. 2082–2090, 2020.

[31] A. M. Potshangbam, R. Polavarapu, R. S. Rathore et al., "Med PS erver: A database for identification of therapeutic targets and novel leads pertaining to natural products," *Chemical Biology & Drug Design*, vol. 93, no. 4, pp. 438–446, 2019.

[32] Y. Wu, F. Zhang, K. Yang et al., "SymMap: an integrative database of traditional Chinese medicine enhanced by symptom mapping," *Nucleic Acids Research*, vol. 47, no. D1, pp. D1110–D1117, 2019.

[33] K. Mohanraj, B. S. Karthikeyan, R. P. Vivek-Ananth et al., "IMPPAT: A curated database of Indian medicinal plants, phytochemistry and therapeutics," *Scientific Reports*, vol. 8, no. 1, p. 4329, 2018.

[34] W. Huang, L. K. Brewer, J. W. Jones et al., "PAMDB: a comprehensive *Pseudomonas aeruginosa* metabolome database," *Nucleic Acids Research*, vol. 46, no. D1, pp. D575–D580, 2018.

[35] K. Miettinen, S. Iñigo, L. Kreft et al., "The TriForC database: a comprehensive up-to-date resource of plant triterpene biosynthesis," *Nucleic Acids Research*, vol. 46, no. D1, pp. D586–D594, 2018.

[36] C. L. Zani and A. R. Carroll, "Database for rapid dereplication of known natural products using data from MS and fast NMR experiments," *Journal of Natural Products*, vol. 80, no. 6, pp. 1758–1766, 2017.

[37] Y. Yue, G.-X. Chu, X.-S. Liu et al., "TMDB: a literature-curated database for small molecular compounds found from tea," *BMC Plant Biology*, vol. 14, no. 1, p. 243, 2014.

[38] M. H. Maeda and K. Kondo, "Three-dimensional structure database of natural metabolites (3DMET): a novel database of curated 3D structures," *Journal of Chemical Information and Modeling*, vol. 53, no. 3, pp. 527–533, 2013.

[39] K. M. Hemsley and A. D. Crocker, "Atropine reduces raclopride-induced muscle rigidity by acting in the ventral region of the striatum," *European Journal of Pharmacology*, vol. 434, no. 3, pp. 117–123, 2002.

[40] J.-H. Lu, J.-Q. Tan, S. S. K. Durairajan et al., "Isorhynchophylline, a natural alkaloid, promotes the degradation of alpha-synuclein in neuronal cells via inducing autophagy," *Autophagy*, vol. 8, no. 1, pp. 98–108, 2012.

[41] D. Yang, T. Li, Z. Liu et al., "LRRK2 kinase activity mediates toxic interactions between genetic mutation and oxidative stress in a Drosophila model: suppression by curcumin," *Neurobiology of Disease*, vol. 47, no. 3, pp. 385–392, 2012.

[42] T. P. T. Cushnie, B. Cushnie, J. Echeverría et al., "Bioprospecting for antibacterial drugs: a multidisciplinary perspective on natural product source material, bioassay selection and avoidable pitfalls," *Pharmaceutical Research*, vol. 37, no. 7, p. 125, 2020.

[43] M. S. Butler, "The role of natural product chemistry in drug discovery†," *Journal of Natural Products*, vol. 67, no. 12, pp. 2141–2153, 2004.

[44] X. Zeng, P. Zhang, W. He et al., "NPASS: natural product activity and species source database for natural product research, discovery and tool development," *Nucleic Acids Research*, vol. 46, no. D1, pp. D1217–D1222, 2018.

[45] F. Ntie-Kang, K. K. Telukunta, K. Döring et al., "NANPDB: a resource for natural products from northern African sources," *Journal of Natural Products*, vol. 80, no. 7, pp. 2067–2076, 2017.

[46] P. Banerjee, J. Erehman, B. O. Gohlke, T. Wilhelm, R. Preissner, and M. Dunkel, "Super Natural II--a database of natural products," *Nucleic Acids Research*, vol. 43, pp. D935–D939, 2015.

[47] Y. Lin, F. Qian, L. Shen, F. Chen, J. Chen, and B. Shen, "Computer-aided biomarker discovery for precision medicine: data resources, models and applications," *Briefings in Bioinformatics*, vol. 20, no. 3, pp. 952–975, 2019.

[48] A. W. Senior, R. Evans, J. Jumper et al., "Improved protein structure prediction using potentials from deep learning," *Nature*, vol. 577, no. 7792, pp. 706–710, 2020.

[49] S. Woo and R. A. Shenvi, "Natural product synthesis through the lens of informatics," *Accounts of Chemical Research*, vol. 54, no. 5, pp. 1157–1167, 2021.

[50] B. Mikulak-Klucznik, P. Gołębiowska, A. A. Bayly et al., "Computational planning of the synthesis of complex natural products," *Nature*, vol. 588, no. 7836, pp. 83–88, 2020.

[51] T. Klucznik, B. Mikulak-Klucznik, M. P. McCormack et al., "Efficient syntheses of diverse, medicinally relevant targets planned by computer and executed in the laboratory," *Chem*, vol. 4, no. 3, pp. 522–532, 2018.

[52] M. H. S. Segler, M. Preuss, and M. P. Waller, "Planning chemical syntheses with deep neural networks and symbolic AI," *Nature*, vol. 555, no. 7698, pp. 604–610, 2018.

[53] A. L. Barabási and J. Frangos, *Linked: How Everything is Connected to Everything Else and what it Means for Business, Science, and Everyday Life*, Basic Books, New York, NY, USA, 2014.

[54] A.-L. Barabási, N. Gulbahce, and J. Loscalzo, "Network medicine: a network-based approach to human disease," *Nature Reviews Genetics*, vol. 12, no. 1, pp. 56–68, 2011.

[55] J. X. Hu, C. E. Thomas, and S. Brunak, "Network biology concepts in complex disease comorbidities," *Nature Reviews Genetics*, vol. 17, no. 10, pp. 615–629, 2016.

[56] L. Shen, Y. Lin, Z. Sun, X. Yuan, L. Chen, and B. Shen, "Knowledge-guided bioinformatics model for identifying autism spectrum disorder diagnostic microRNA biomarkers," *Scientific Reports*, vol. 6, Article ID 39663, 2016.

[57] J. Montaner, L. Ramiro, A. Simats et al., "Multilevel omics for the discovery of biomarkers and therapeutic targets for stroke," *Nature Reviews Neurology*, vol. 16, no. 5, pp. 247–264, 2020.

[58] R. Zoraghi and N. E. Reiner, "Protein interaction networks as starting points to identify novel antimicrobial drug targets," *Current Opinion in Microbiology*, vol. 16, no. 5, pp. 566–572, 2013.

[59] R. V. Atreya, J. Sun, and Z. Zhao, "Exploring drug-target interaction networks of illicit drugs," *BMC Genomics*, vol. 14, no. 4, p. S1, 2013.

[60] S. A. Dugger, A. Platt, and D. B. Goldstein, "Drug development in the era of precision medicine," *Nature Reviews Drug Discovery*, vol. 17, no. 3, pp. 183–196, 2018.

[61] F. Cheng, W. Lu, C. Liu et al., "A genome-wide positioning systems network algorithm for in silico drug repurposing," *Nature Communications*, vol. 10, no. 1, p. 3476, 2019.

[62] L. Cao, E. Shcherbin, and H. Mohimani, "A metabolome- and metagenome-wide association network reveals microbial natural products and microbial biotransformation products from the human microbiota," *mSystems*, vol. 4, no. 4, 2019.

[63] S. R. Chamberlin, A. Blucher, G. Wu et al., "Natural product target network reveals potential for cancer combination therapies," *Frontiers in Pharmacology*, vol. 10, p. 557, 2019.

[64] B. Gogoi, D. Gogoi, Y. Silla, B. B. Kakoti, and B. S. Bhau, "Network pharmacology-based virtual screening of natural products from clerodendrum species for identification of novel anti-cancer therapeutics," *Molecular BioSystems*, vol. 13, no. 2, pp. 406–416, 2017.

[65] R. Luis-Martinez, M. H. G. Monje, A. Antonini, Á. Sánchez-Ferro, and T. A. Mestre, "Technology-enabled care: integrating multidisciplinary care in Parkinson's disease through digital technology," *Frontiers in Neurology*, vol. 11, Article ID 575975, 2020.

[66] T. Asakawa, K. Sugiyama, T. Nozaki et al., "Can the latest computerized technologies revolutionize conventional assessment tools and therapies for a neurological disease? the example of Parkinson's disease," *Neurologia Medico-Chirurgica*, vol. 59, no. 3, pp. 69–78, 2019.

[67] D. N. Nicholson and C. S. Greene, "Constructing knowledge graphs and their biomedical applications," *Computational and Structural Biotechnology Journal*, vol. 18, pp. 1414–1428, 2020.

[68] X. Yu, J. Zhang, S. Sun, X. Zhou, T. Zeng, and L. Chen, "Individual-specific edge-network analysis for disease prediction," *Nucleic Acids Research*, vol. 45, no. 20, p. e170, 2017.

Hindawi
Evidence-Based Complementary and Alternative Medicine
Volume 2021, Article ID 9995614, 14 pages
https://doi.org/10.1155/2021/9995614

Research Article

Anticholinesterase Activity of Eight Medicinal Plant Species: *In Vitro* and *In Silico* Studies in the Search for Therapeutic Agents against Alzheimer's Disease

Md Josim Uddin[1], **Daniela Russo**[2,3], **Md Mahbubur Rahman**[4], **Shaikh Bokhtear Uddin**[5], **Mohammad A. Halim**[6], **Christian Zidorn**[1] and **Luigi Milella**[2]

[1]*Pharmazeutisches Institut, Abteilung Pharmazeutische Biologie, Christian-Albrechts-Universität Zu Kiel, Gutenbergstraße 76, Kiel 24118, Germany*
[2]*Department of Science, University of Basilicata, Viale Dell'Ateneo Lucano 10, Potenza 85100, Italy*
[3]*Spinoff BioActiPlant s.r.l., Department of Science, University of Basilicata, Potenza, Italy*
[4]*Division of Infectious Diseases and Division of Computer-Aided Drug Design, The Red-Green Research Centre, BICCB, Tejgaon, Dhaka, Bangladesh*
[5]*Department of Botany, University of Chittagong, Chattogram 4331, Bangladesh*
[6]*Department of Physical Sciences, University of Arkansas-Fort Smith, Fort Smith, AR, USA*

Correspondence should be addressed to Luigi Milella; luigi.milella@unibas.it

Received 22 March 2021; Revised 29 May 2021; Accepted 8 June 2021; Published 25 June 2021

Academic Editor: Ghulam Ashraf

Copyright © 2021 Md Josim Uddin et al. This is an open access article distributed under the Creative Commons Attribution License, which permits unrestricted use, distribution, and reproduction in any medium, provided the original work is properly cited.

Many Bangladeshi medicinal plants have been used to treat Alzheimer's disease and other neurodegenerative diseases. In the present study, the anticholinesterase effects of eight selected Bangladeshi medicinal plant species were investigated. Species were selected based on the traditional uses against CNS-related diseases. Extracts were prepared using a gentle cold extraction method. *In vitro* cholinesterase inhibitory effects were measured by Ellman's method in 96-well microplates. *Blumea lacera* (Compositae) and *Cyclea barbata* (Menispermaceae) were found to have the highest acetylcholinesterase inhibitory ($IC_{50,}$ 150 ± 11 and $176 \pm 14\,\mu g/mL$, respectively) and butyrylcholinesterase inhibitory effect (IC_{50}, 297 ± 13 and $124 \pm 2\,\mu g/mL$, respectively). *Cyclea barbata* demonstrated competitive inhibition, where *Blumea lacera* showed an uncompetitive inhibition mode for acetylcholinesterase. *Smilax guianensis* (Smilacaceae) and *Byttneria pilosa* (Malvaceae) were also found to show moderate AChE inhibition ($IC_{50,}$ 205 ± 31 and $221 \pm 2\,\mu g/mL$, respectively), although no significant BChE inhibitory effect was observed for extracts from these plant species. Among others, *Thunbergia grandiflora* (Acanthaceae) and *Mikania micrantha* (Compositae) were found to display noticeable AChE (IC_{50}, $252 \pm 22\,\mu g/mL$) and BChE (IC_{50}, $314 \pm 15\,\mu g/mL$) inhibitory effects, respectively. Molecular docking experiment suggested that compounds 5-hydroxy-3,6,7,3′,4′-pentamethoxyflavone (BL4) and kaempferol-3-*O*-*α*-L-rhamnopyranosyl-(1⟶6)-*β*-D-glucopyranoside (BL5) from *Blumea lacera* bound stably to the binding groove of the AChE and BChE by hydrogen-bond interactions, respectively. Therefore, these compounds could be candidates for cholinesterase inhibitors. The present findings demonstrated that *Blumea lacera* and *Cyclea barbata* are interesting objects for further studies aiming at future therapeutics for Alzheimer's disease.

1. Introduction

Alzheimer's disease (AD) is a devastating neurodegenerative disorder linked with the two most common symptoms, memory dysfunction and cognition impairment. In the neuropathological symptoms of AD, cognitive deficit is consistent with the presence of cholinergic deficit, due to the degeneration or atrophy of cholinergic neurons in the basal forebrain, including senile plaques and neurofibrillary tangles [1]. Acetylcholine (ACh), the brain's important

natural neurotransmitter, plays a critical role in forming memories, verbal and logical reasoning, and the ability to concentrate. However, ACh's activity is greatly hindered by both acetylcholinesterase (AChE) and butyrylcholinesterase (BChE) enzymes.

Inhibition of the cholinesterase enzymes (AChE and BChE) can boost ACh levels in several parts of the brain and symptoms associated with the progressive loss of cholinergic function in AD improve [2]. Studies also showed that increased ACh concentration in the brain increases the expression of nicotinic ACh receptors related to cognitive function [3, 4]. This phenomenon might help AD patients generating new memories and remembering the older ones. Thus, AChE and BChE inhibition has been established as a primary therapeutic target based on this "cholinergic hypothesis."

Pharmacological treatment of AD is largely based on treating symptoms and severity with advanced stages rather than targeting the etiological mechanisms. The currently approved medications for AD are mostly cholinesterase inhibitors, including donepezil, rivastigmine, galantamine, and NMDA antagonist memantine [5]. Among the commonly prescribed AChE inhibitors, only donepezil was approved for the treatment of all stages of AD. However, this drug has some severe side effects, including gastrointestinal disturbance, liver-associated problems, and GIT-related abnormalities [6]. Considering all these limitations, it is worthy to find new lead compounds from different sources, including plant-derived natural products.

Natural products have already proven to be promising sources of useful acetylcholinesterase (AChE) inhibitors [7]. The currently approved drugs for AD, galantamine and rivastigmine, are plant-derived alkaloids, which offer symptomatic relief from AD [8]. In addition to these approved natural products, many potent cholinesterase inhibitors have been reported in literature [7]. Some reported potent cholinesterase inhibitors are nevertheless presented in Figure 1.

Our study is an attempt to identify and compare potential candidates from the following eight selected plant species (family affiliations of all species in Table 1) *Blumea lacera* (Burm.f.) DC., *Byttneria pilosa* Roxb., *Clerodendrum infortunatum* L., *Cyclea barbata* Miers, *Mikania micrantha* Kunth, *Smilax guianensis* Vitman, *Spermacoce articularis* L.f., and *Thunbergia grandiflora* Roxb. for anticholinesterase activity in rejuvenating and improving the memory and cognitive function. A study of ethnopharmacological background of the selected species is presented in Table 1.

2. Materials and Methods

2.1. Chemicals. Acetylcholinesterase (AChE) from electric eel (*Electrophorus electricus*) (type VI-s, lyophilized powder), acetylthiocholine iodide (ATCI), butyrylcholinesterase (BChE) from equine serum (lyophilized powder), butyrylthiocholine iodide (BTCI), and 5,5′-dithio-bis-(2-nitrobenzoic acid) (DTNB) were purchased from Sigma-Aldrich (St. Louis, MO, USA). Trizma hydrochloride (Tris-HCl) and bovine serum albumin (BSA) were obtained from Sigma-Aldrich (Steinheim, Germany). Deionized water was produced using a Milli-Q water purification system (Millipore, Bedford, MA, USA).

2.2. Plant Materials. All samples, except *Clerodendrum infortunatum*, were collected from Chittagong Hill Tracts, Bangladesh. The plant materials were certified by one of the authors, Taxonomist Prof. Dr. Sheikh Bokhtear Uddin. All voucher specimens have been deposited in the Department of Botany, University of Chittagong (Supplementary Material, Figure S1). The leaves of *Clerodendrum infortunatum* were collected from Pabna, Bangladesh, and authenticated by Prof. Dr. A.H.M. Mahbubur Rahman, Department of Botany, University of Rajshahi. Botanical names along with accession numbers are presented in Table 1 (Supplementary Material, Figure S1).

2.3. Extraction of Plant Materials. Freshly collected plant leaves were dried in the shade and then pulverized. To prepare the extract, 10 g of each plant part was extracted in 50 mL solvent employing the cold extraction method as described in Table 1, at room temperature. Solvent polarity has been selected on the nature of phytochemicals present in the plant species [17]. Filtered extracts were dried in a rotary evaporator under reduced pressure at 35°C temperature.

2.4. Determination of Cholinesterase (AChE/BChE) Inhibitory Activities. ChE inhibitory activity was measured based on Ellman's method [18] as reported in a previous study [19]. In the inhibition of AChE activity, the enzyme hydrolyzes the substrate acetylthiocholine resulting in the product thiocholine, which reacts with Ellman's reagent (DTNB) to produce 2-nitrobenzoate-5-mercapto-thiocholine and 5-thio-2-nitrobenzoate, detectable at 405 nm. In this assay, 25 μL of acetylthiocholine iodide (5 mM), 125 μL of DTNB (3 mM), 50 μL of buffer B (50 mM Tris-HCl, pH 8 containing 0.1% BSA), and 25 μL of each test extract solution at the different concentrations or negative control (25% DMSO in MeOH) were mixed and incubated for 10 min at 37°C. The reaction was started by adding 25 μL of 0.05 U/mL AChE. The absorbance was measured at 405 nm, and the reaction rates were calculated by MARS Data analysis software (SPECTROStar NANO, BMG Labtech, Germany). Estimation of BChE inhibition was performed in a similar way described above using 25 μL of 5 mM butyrylthiocholine iodide as substrate and 0.05 U/mL of BChE as an enzyme. Galantamine was used as a positive control for both enzymes. Three independent assays were performed in triplicate at different concentrations.

2.5. Mode of Inhibition and Kinetic Parameters. To investigate the type of inhibition of the effective extracts, the enzyme activity was determined in the presence of increasing concentrations of substrate ATCI (0.16–20 mM) and the absence or presence of two/three concentrations of each extract. The analysis of the type of inhibition of AChE

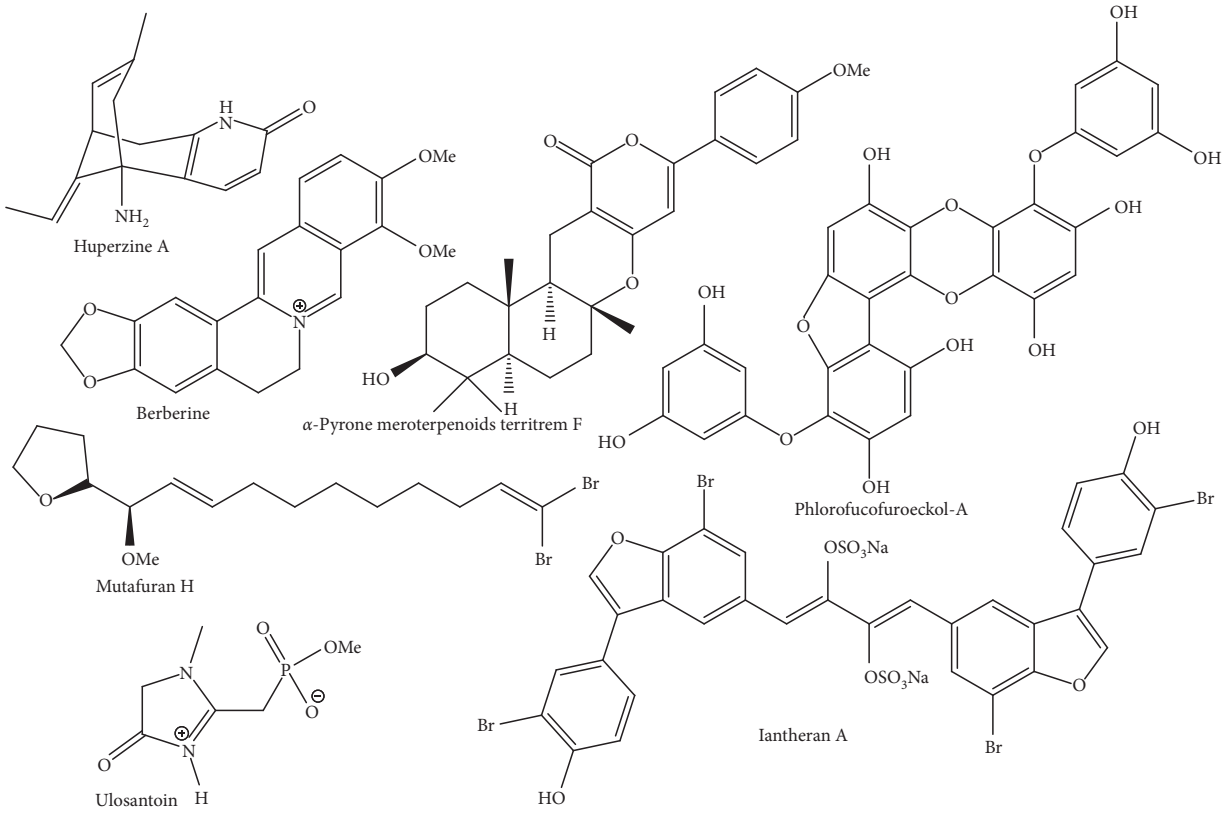

Figure 1: Structures of some representative lead inhibitors against AChE and BChE based on their IC_{50} values (<1 μM).

activity was determined by the Lineweaver-Burk (LB) plot, whereas the kinetic parameters km and Vmax were obtained by curve fitting according to the classical Michaelis-Menten equation by using GraphPad Prism version 6.

2.6. Molecular Docking Protocol. The crystal structure of cholinesterase enzymes has been collected from RCSB PDB (rcsb.org) [20]. PDB ID 4EY7 [21] and 4AQD [22] were assigned for AChE and BChE, respectively. The proteins were prepared in Swiss PDB Viewer [23] and PyMOL.

Nine compounds (Figure 2) from *Blumea lacera* [24–29] were selected for molecular docking study considering their chemical nature and action on cholinesterase [30, 31]. The structures were drawn in ChemDraw and Chem3D. The geometry optimization of all structures was carried out by the semiempirical PM6 method in Gaussian 09 [32]. The optimized structures were collected in PDB format suitable for molecular docking. The molecular docking of all compounds against AChE and BChE was performed in PyRx Virtual Screening Tool (Version 0.8) [33]. The compounds were saved in AutoDock ligand format (PDBQT) before docking. The grid box center and dimensions were set accordingly to cover the substrate-binding sites of the protein. For AChE, the grid box center was reserved at $X = -2.0303$, $Y = 38.0503$, and $Z = 29.9752$, and the dimension (angstrom) was $X = 42.2467$, $Y = 50.5623$, and $Z = 41.3235$. In case of BChE, the grid box center was fixed at $X = 1.6818$, $Y = -1.3768$, and $Z = -10.0914$ and the dimension (angstrom) was $X = 39.1883$, $Y = 39.4042$, and $Z = 33.0087$. The docking process was performed in triplicate for every ligand and the average of the binding affinities has been presented. Furthermore, the extracted ligand from the crystal structure was docked with the optimized protein following the same protocol, which validated our docking protocol [34]. The docked ligand-protein complexes were visualized in BIOVIA Discovery Studio (Version 4.5) to detect the noncovalent interactions.

2.7. Statistical Analysis. Data are given as the mean ± SD ($n = 3$). IC_{50} values were calculated via nonlinear regression analysis using GraphPad Prism v. 6.0 (GraphPad Software Inc., USA). One-way analysis of variance (ANOVA) and Tukey test were used to compare means among extracts; an observation was considered statistically significant if the p value is less than 0.05 ($p < 0.05$).

3. Results and Discussion

The extracts of eight plant species used as herbal medicine in different disorders were tested for AChE and BChE inhibitory activity using Ellman's method. The results are shown in Table 2, representing the IC_{50} values for the eight extracts prepared. The lowest IC_{50} AChE inhibitory activity was found for *Blumea lacera* followed by *Cyclea barbata*, *Smilax guianensis*, *Byttneria pilosa*, and *Thunbergia grandiflora* displayed values of 150 ± 11, 176 ± 14, 205 ± 30, 221 ± 2, and 252 ± 22 μg/mL, respectively. Figure 3 displays the activity of extracts at various concentrations, where AChE inhibition

Table 1: Details of the plant species used in this study along with its traditional uses.

Botanical name	Family	Common name	Local name (tribal name)	Parts used	Habitat	Solvent used for extraction	Traditional uses	Accession number
Blumea lacera (Burm.f.) DC.	Compositae	Lettuce-Leaf Blumea	Kukursunga, shialmutra	Leaves	Herb	Acetone	Neurological disorder [10], inflammation [11], stimulant, spasm, fever, bronchitis, burning sensation, and dysentery [9]	BL-07052016-7842
Byttneria pilosa Roxb.	Malvaceae	Not known	Harjora	Leaves	Climber	Methanol	Antidote of snake poisoning [12], bone fracture, scabies, and elephantiasis [13]	BP-10122013-10578
Clerodendrum infortunatum L. (syn.: *Clerodendrum viscosum*)	Lamiaceae	Glory bower	Bhat	Leaves	Undershrub	Acetone	Paralysis [14], snakebite [12], tonic, pain, tumor, skin diseases, cough, and jaundice [9]	CV-20180321-04
Cyclea barbata Miers	Menispermaceae	Green grass jelly plant	Patalpur (Chakma, Tanchangya)	Leaves	Shrub	Acetone-water (70 : 30)	Headache, epilepsy, allergy, asthma, lipoma, tetanus, and throat sore [9]	CB-07052015-4974
Mikania micrantha Kunth	Compositae	Bitter vine	Assam lata	Leaves	Climber	Methanol	Snakebite [12], ulcer, hemorrhage, and wound [9]	MM-03102016-4985
Smilax guianensis Vitman (*Smilax macrophylla* Roxb.)	Smilacaceae	Indian sarsaparilla	Kumarilata, Kumarika	Leaves	Climber	Methanol	Memory loss [15], pain, venereal diseases, sores, abscess, rheumatism, and gonorrhea [9]	SQ-04092016-5610
Spermacoce articularis L.f. (*Borreria articularis* F.N. Will.)	Rubiaceae	Shaggy buttonweed	Madnabata kadu	Leaves	Herb	Methanol	Headache [16], inflammation, blindness, earache, and spleen complaints [9]	SA-04092016-5632
Thunbergia grandiflora Roxb.	Acanthaceae	Bengal clockvine	Nillata	Leaves	Climber	Acetone-water (70 : 30)	Hysteria, dysentery, cataract, diabetes, gout, hydrocele, and rheumatism [14]	TG-04092016-5608

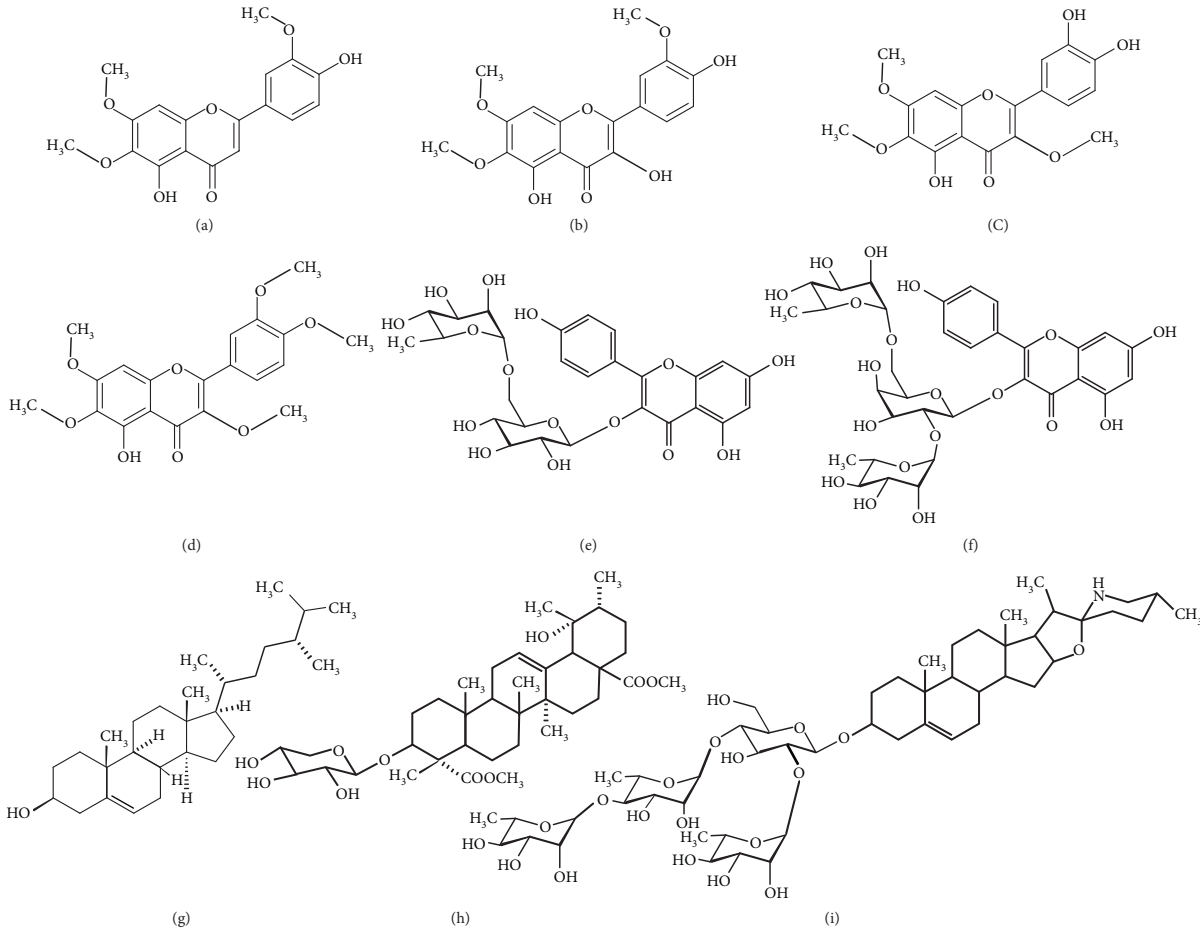

Figure 2: The selected compounds isolated from leaves of *Blumea lacera* for molecular docking with AChE and BChE. (a) 5,4′-dihydroxy 6,7,3′-trimethoxyflavone (**BL1**), (b) 3,5,4′-trihydroxy 6,7,3′-trimethoxyflavone (**BL2**), (c) 5,3′,4′-trihydroxy 3,6,7-trimethoxyflavone (**BL3**), (d) 5-hydroxy 3,6,7,3′,4′-pentamethoxyflavone (**BL4**), (e) Kaempferol-3-*O*-*α*-L-rhamnopyranosyl-(1⟶6)-*β*-D-glucopyranoside (**BL5**), (f) Kaempferol-3-*O*-(2″,6″-di-*O*-*α*-L-rhamnopyranosyl)-*β*-D-glucopyranoside (**BL6**), (g) Campesterol (**BL7**), (h) 19*α*-hydroxyurs-12-ene-24,28-dioate 3-*O*-*β*-D- xylopyranoside (**BL8**), (i) 25*R*)-3*β*-{*O*-*β*-D-glucopyranosyl-(1⟶ 4)-*O*-*α*-L-rhamnopyranosyl-(1⟶ 4)-[*O*-*α*-L-rhamnopyranosyl-(1⟶ 2)]-*α*-L-rhamnopyranosyl}-22*α*N-spirosol-5-ene (**BL9**).

Table 2: Anticholinesterase inhibition (IC_{50}, μg/mL) of eight plant extracts and galantamine (positive control).

Species name	AChE inhibition assay IC_{50} (μg/mL)	BChE inhibition assay IC_{50} (μg/mL)
Blumea lacera (Burm.f.) DC.	150 ± 11^{a}	297 ± 13^{c}
Byttneria pilosa Roxb.	$221 \pm 2^{a,b}$	536 ± 23^{d}
Clerodendrum infortunatum L.	598 ± 50^{d}	971 ± 77^{e}
Cyclea barbata Miers	176 ± 14^{a}	124 ± 2^{a}
Mikania micrantha Kunth	314 ± 15^{b}	216 ± 25^{b}
Smilax guianensis Vitman	205 ± 31^{a}	$>1000^{f}$
Spermacoce articularis L.f.	460 ± 126^{c}	$>1000^{f}$
Thunbergia grandiflora Roxb.	$252 \pm 22^{a,b}$	576 ± 64^{d}
Galantamine	0.92 ± 0.02 (2.49 ± 0.05 μM)	5.97 ± 0.97 (16.2 ± 2.6 μM)

Values are expressed as mean ± SD (n = 3). Different letters indicate statistically significant differences ($p < 0.05$, Tukey test). IC50 represents the half-maximal inhibitory concentration; AChE, acetylcholinesterase; BChE, butyrylcholinesterase.

increases in a dose-dependent manner. Galantamine was used as a standard AChE inhibitor showing IC_{50} of 0.92 ± 0.02 μg/mL (2.49 ± 0.05 μM).

In the BChE inhibitory activity, *Cyclea barbata* extract showed the highest inhibition against BChE followed by *Mikania micrantha*, *Blumea lacera*, and *Byttneria pilosa* with their IC_{50} values of 124 ± 2, 216 ± 24, 297 ± 13, 358 ± 32, and 536 ± 23 μg/mL, respectively (Table 2). The IC_{50} value of reference standard galantamine for BChE assay was 5.97 ± 0.97 μg/mL (16.2 ± 2.6 μM). The inhibition of BChE is also increasing corresponding to the concentration of extracts (Figure 4). Our results demonstrated a dual activity of

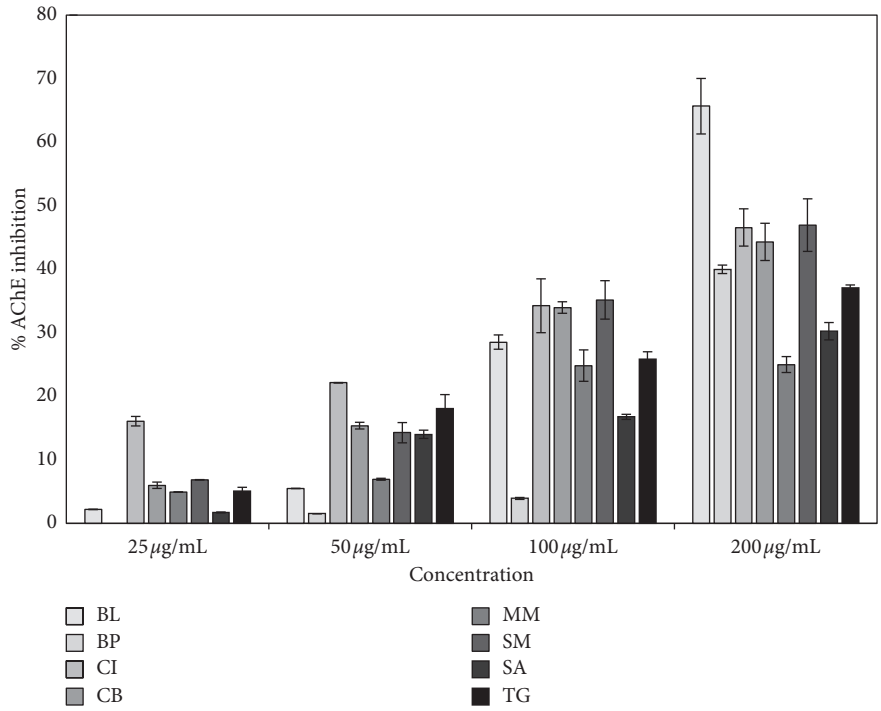

Figure 3: Inhibition of AChE activity of plant extracts. Column represents the inhibition percentage obtained with *Blumea lacera* (BL), *Byttneria pilosa* (BP), *Clerodendrum infortunatum* (CI), *Cyclea barbata* (CB), *Mikania micrantha* (MM), *Smilax macrophylla* (SM), *Spermacoce articularis* (SA), and *Thunbergia grandiflora* (TG). IC_{50} (μg/mL) of positive control galantamine for AChE inhibition assay was 0.92 ± 0.02 μg/mL. Mean values of three independent experiments have been plotted.

Blumea lacera, *Cyclea barbata*, and *Byttneria pilosa* extracts. Since AChE is mainly located in the central nervous system (CNS) and BChE is more abundant in the peripheral system, the potency toward both ChE found in the extracts is of paramount importance. These findings could activate mostly the central as well as peripheral cholinergic transmission to improve the mental abilities of AD patients. Among the eight screened extracts, *Blumea lacera*, *Cyclea barbata*, *Smilax guianensis*, and *Byttneria pilosa* were selected as efficacious candidates as sources of strong ChE (AChE and BChE) inhibitors. Due to the multifactorial pathogenesis of AD, multitargeted drugs will be preferred as the effective therapeutic strategy against AD.

Blumea lacera, a widely distributed herb in Bangladesh, is locally known as Kukursunga or Shimura. *B. lacera* is used to cure spasms, fever, and bronchitis and alleviate burning sensation [9]. Leaves of the plant are astringent, stimulant, anthelmintic, antiscorbutic, and diuretic [9, 27] and they are also used as antidysenteric and anti-inflammatory remedies [9]. Acetone extract of leaves of *B. lacera* showed an IC_{50} value of 150 ± 11 and 297 ± 13 μg/mL for AChE and BChE inhibition, respectively; efficacy of these leaves on enhancing cognitive functions might be due to the presence of terpenoids [35]. Acetone-water (70 : 30) extract of *B. lacera* displayed lower activity (IC_{50} value of 197 and 1040 μg/mL for AChE and BChE inhibition, respectively) compared with acetone extract.

Cyclea barbata is a tropical indigenous plant widely distributed in Asia, especially in Bangladesh. This climber is traditionally used against various diseases such as headache, epilepsy, allergy, asthma, lipoma, tetanus, and throat sore [9]. Acetone-water (70 : 30) extract of *Cyclea barbata* exhibited IC_{50} value of 176 ± 14 and 124 ± 2 μg/mL for AChE and BChE inhibition, respectively, which might be owing to its high alkaloid contents [36].

Smilax guianensis, locally known as Kumarika, is believed to possess CNS-modulating properties and is used in many herbal formulations. *S. guianensis* is also used in the treatment of epilepsy, venereal and skin diseases, fever, swellings, sores, and abscesses [9, 37]. Young stem is used to improve memory loss. The root is used for the management of rheumatism and pain in the lower extremities [15, 38]. Dried leaves of *S. guianensis* methanolic extract inhibited AChE with an IC_{50} value of 205 ± 31 μg/mL which might be due to the presence of steroidal saponin glycosides [39], while no significant inhibition on BChE was observed.

Byttneria pilosa, a large woody climber, is widely distributed in Chittagong, Bangladesh. Leaves and stems of this species are usually used to treat snakebite by the traditional healers and indigenous people in Chittagong hill tracts, Bangladesh. It is also used to cure scabies, bone fracture, and elephantiasis [9, 12, 13]. Methanolic extract of *B. pilosa* leaves revealed its AChE and BChE inhibitory potentials with an IC_{50} value of 221 ± 2 and 536 ± 23 μg/mL, respectively, because of the presence of favorable anticholinesterase natural products such as alkaloid, saponin, and terpenoid [13].

Both acetylcholinesterase and butyrylcholinesterase are the key enzymes in the cholinergic nervous system. Therapies designed to reverse the cholinergic deficit in AD are

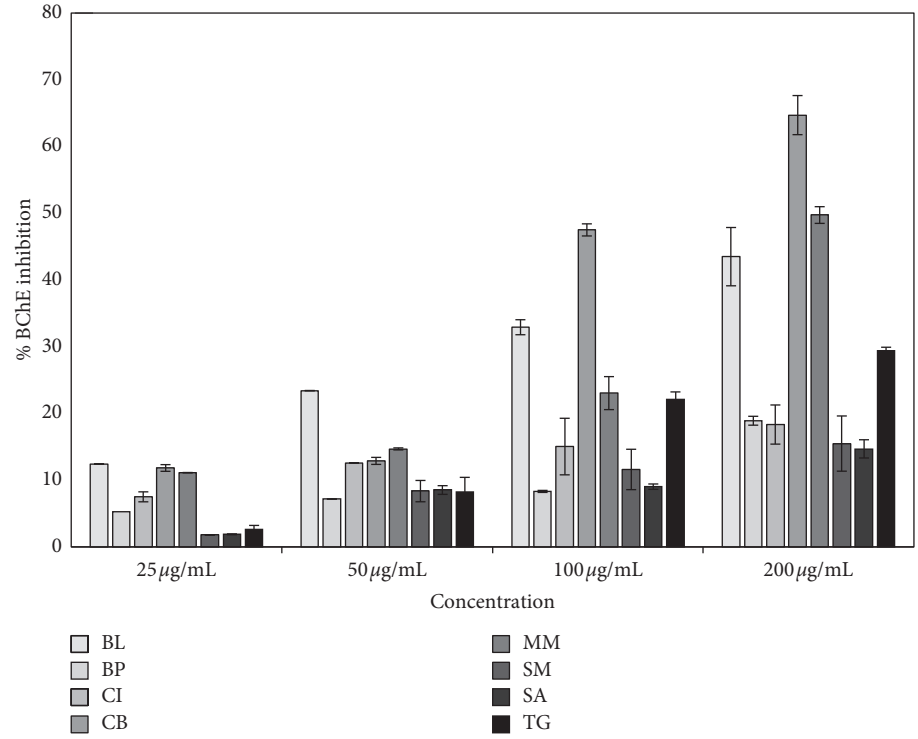

Figure 4: BChE inhibition activity of plant extracts. Column represents the inhibition percentage obtained with *Blumea lacera* (BL), *Byttneria pilosa* (BP), *Clerodendrum infortunatum* (CI), *Cyclea barbata* (CB), *Mikania micrantha* (MM), *Smilax guianensis* (SG), *Spermacoce articularis* (SA), and *Thunbergia grandiflora* (TG). IC_{50} (μg/mL) of positive control galantamine for BChE inhibition assay was 5.97 ± 0.97 μg/mL. Mean values of three independent experiments have been plotted.

mostly based on inhibitors of AChE. Several studies revealed that cholinesterase inhibitors could act on multiple therapeutic targets such as preventing the formation of β-amyloid plaques, antioxidant activity, and modulation of APP processing [40]. Moreover, AChE inhibition is also considered a promising therapeutic strategy for other types of dementia, myasthenia gravis, glaucoma, and Parkinson's disease [41]. Nonetheless, there is still a need to explore the nature of newer potent and long-lasting ChE inhibitors with minimal side effects. Natural products have already been proven to be promising sources of useful ChE inhibitors [7, 42]. Bioassay-guided approaches have studied many plants for the search of new AChE inhibitors with lower toxicity and higher CNS penetration.

The kinetic study revealed the potential mechanism of enzyme inhibition. The relationship between substrate concentration and reaction velocity was in good agreement with Michaelis-Menten kinetics. In absence of inhibitors, the km value of the substrate ATCI was 10.4 ± 1.8 mM, and the Vmax was 12.4 ± 1.1 mM/min for the electric eel acetylcholinesterase. Galantamine was used as positive control showing a competitive inhibition. The extracts *Blumea lacera*, *Byttneria pilosa,* and *Smilax guianensis* showed uncompetitive inhibition in which inhibitor only binds to enzyme-substrate complex (Table 3). Figure 5 represents the enzyme kinetics of *Blumea lacera*. In the uncompetitive pattern, both Vmax and km decrease, and the kinetic pattern produced parallel lines with increasing extract concentration. The mode of inhibition of *Cyclea barbata* seemed to be ambiguous at lower concentration while Vmax and km both increased, whereas at higher concentration, it reflected competitive inhibition (km increased and Vmax remained unchanged) (Figure 6). These types of inhibition could be due to the presence of various phytochemicals typical in medicinal plants. The kinetic study against BChE demonstrated an ambiguous inhibition mode.

In silico molecular docking is an efficient tool in recent structure-based drug design. In this anticholinesterase screening study, *Blumea lacera* exhibited the highest inhibition among the eight plant species. Here, the docking study was conducted to identify the responsible compounds from *Blumea lacera* on anticholinesterase potential. However, the binding affinity and binding pose of selected compounds (Figure 2) with the AChE and BChE could be considered as proof of our claimed biological outcome. All the ligands showed good binding affinity where some of them interacted with the catalytic site of proteins (Table 4). BL1, BL2, and BL7 demonstrated the highest binding affinity (kcal/mol) with AChE, whereas BL5, BL6, and BL8 reflected the highest binding affinity with BChE.

Ligands' interaction with the catalytic triad residues of acetylcholinesterase is essential to inhibit enzymatic activity. We analyzed all the ligands binding poses to investigate the interaction of the ligands with the AChE. The majority of the ligands did not interact with the catalytic triad residues of AChE that validated the uncompetitive inhibition mode in the experimental result (Figure 5; Supplementary Material, Figure S2) of *Blumea lacera*. Three out of nine compounds

Table 3: Enzyme kinetics of the extracts on AChE activity.

Samples	Concentration	Vmax (mM/min)	km (mM)	Mode of inhibition
Control	—	12.4 ± 1	10.4 ± 2	—
Galantamine	0.01 mg/mL	12.6 ± 2	16.2 ± 5	Competitive
Blumea lacera	0.50 mg/mL	8.35 ± 4	8.7 ± 4	Uncompetitive
	0.25 mg/mL	10.4 ± 1	8.0 ± 2	Uncompetitive
	0.10 mg/mL	10.1 ± 1	5.27 ± 1	Uncompetitive
Byttneria pilosa	1.00 mg/mL	5.23 ± 1	2.57 ± 1	Uncompetitive
	0.25 mg/mL	8.52 ± 2	5.54 ± 3	Uncompetitive
Cyclea barbata	0.50 mg/mL	14.6 ± 4	14.7 ± 7	Competitive
	0.10 mg/mL	16.3 ± 4	17.8 ± 8	Ambiguous
Smilax guianensis	0.50 mg/mL	6.22 ± 1	3.75 ± 2	Uncompetitive
	0.25 mg/mL	9.77 ± 1	6.70 ± 2	Uncompetitive

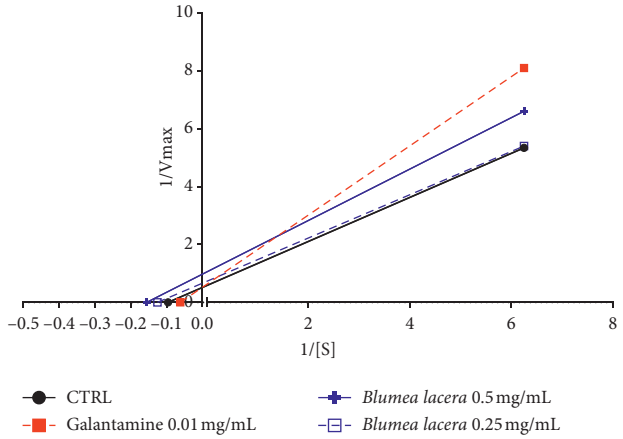

Figure 5: Lineweaver-Burk plot in the absence (control) and presence of inhibitors (galantamine and acetone extract of *Blumea lacera*).

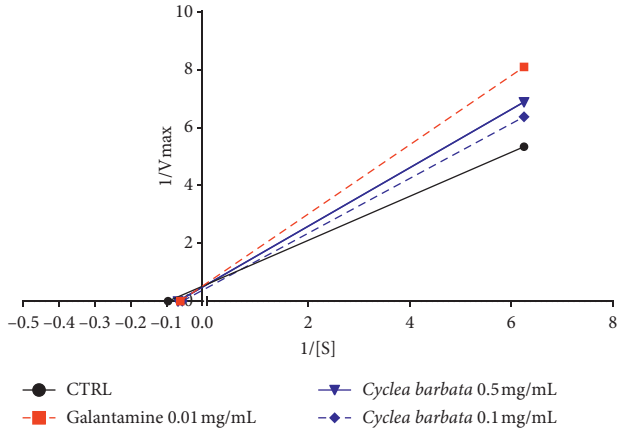

Figure 6: Lineweaver-Burk plot in the absence (control) and presence of inhibitors (galantamine and *Cyclea barbata*).

interact with both catalytic and peripheral anionic site (PAS) residues of AChE (Figure 7). All ligands except BL9 interact with the catalytic site residues of BChE (Figure 8; Supplementary Material, Figure S3).

The active site of both AChE and BChE consists of two subsites [43, 44]. The esteratic site (also called catalytic triad) of human AChE consists of three essential amino acids Ser203, Glu334 and, His447, while the PAS is composed of five residues Tyr72, Asp74, Tyr124, Trp286, and Tyr341. The catalytic triad of human BChE is comprised of Ser198, His438, and Glu325, whereas the PAS contains Asp70, Phe329, Trp82, Tyr128, and Tyr332 [45–48]. The binding of a ligand highly regulates the cholinesterase enzyme inhibition at the catalytic site. The aromatic ring in the ligand forms a few pi-alkyl, pi-pi, pi-pi T-shaped interactions with the amino acid residues of the protein. The 5,4′-dihydroxy-6,7,3′-trimethoxyflavone (BL1), 5-hydroxy-3,6,7,3′,4′-pentamethoxyflavone (BL4), and campesterol (BL7) interact

Table 4: Binding affinity of the selected isolates of *Blumea lacera* with AChE (PDB ID: 4EY7) and BChE (PDB ID: 4AQD) enzymes.

Compound name	Molecular formula	Molecular weight	Binding energy (kcal/mol)	
			AChE	BChE
5,4′-dihydroxy 6,7,3′-trimethoxyflavone (BL1)	$C_{18}H_{16}O_7$	344.31	−9.4	−8.5
3,5,4′-trihydroxy 6,7,3′-trimethoxyflavone (BL2)	$C_{18}H_{16}O_8$	360.31	−9.4	−8.8
5,3′,4′-trihydroxy 3,6,7-trimethoxyflavone (BL3)	$C_{18}H_{16}O_8$	360.31	−6.8	−8.3
5-hydroxy 3,6,7,3′,4′-pentamethoxyflavone (BL4)	$C_{20}H_{20}O_8$	388.36	−8.7	−7.7
Kaempferol-3-*O*-*α*-L-rhamnopyranosyl-(1→6)-*β*-D-glucopyranoside (BL5)	$C_{27}H_{30}O_{15}$	594.51	−8.7	−10.4
Kaempferol-3-*O*-(2″,6″-di-*O*-*α*-L-rhamnopyranosyl)-*β*-D-glucopyranoside (BL6)	$C_{33}H_{40}O_{19}$	740.65	−8.3	−10.7
Campesterol (BL7)	$C_{28}H_{48}O$	400.68	−10.9	−8.8
19*α*-Hydroxyurs-12-ene-24,28-dioate 3-*O*-*β*-D-xylopyranoside (BL8)	$C_{37}H_{58}O_{10}$	662.85	−8.7	−10.4
(25R)-3*β*-{*O*-*β*-D-Glucopyranosyl-(1→4)-*O*-*α*-L-rhamnopyranosyl-(1→4)-[*O*-*α*-L-rhamnopyranosyl-(1→2)]-*α*-L-rhamnopyranosyl}-22*α*N-spirosol-5-ene (BL9)	$C_{51}H_{83}NO_{19}$	1014.20	−8.7	−9.9
Galantamine	$C_{17}H_{21}NO_3$	287.35	−9.4	−8.5

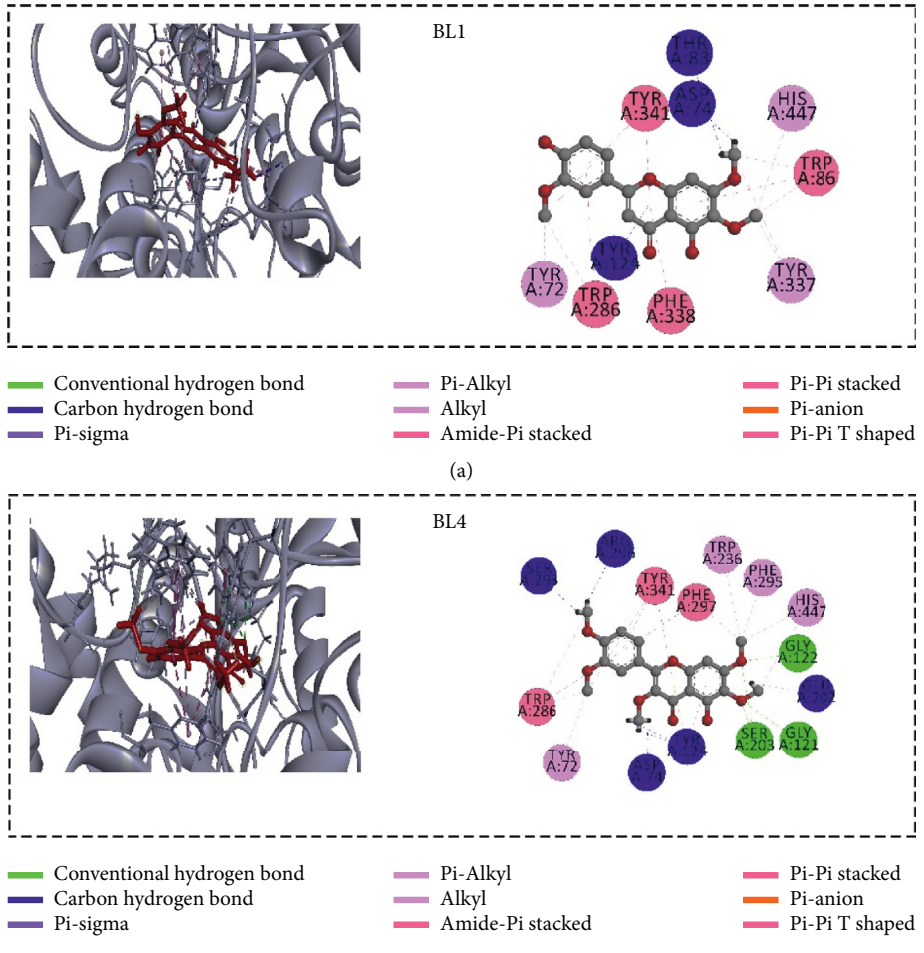

Figure 7: Continued.

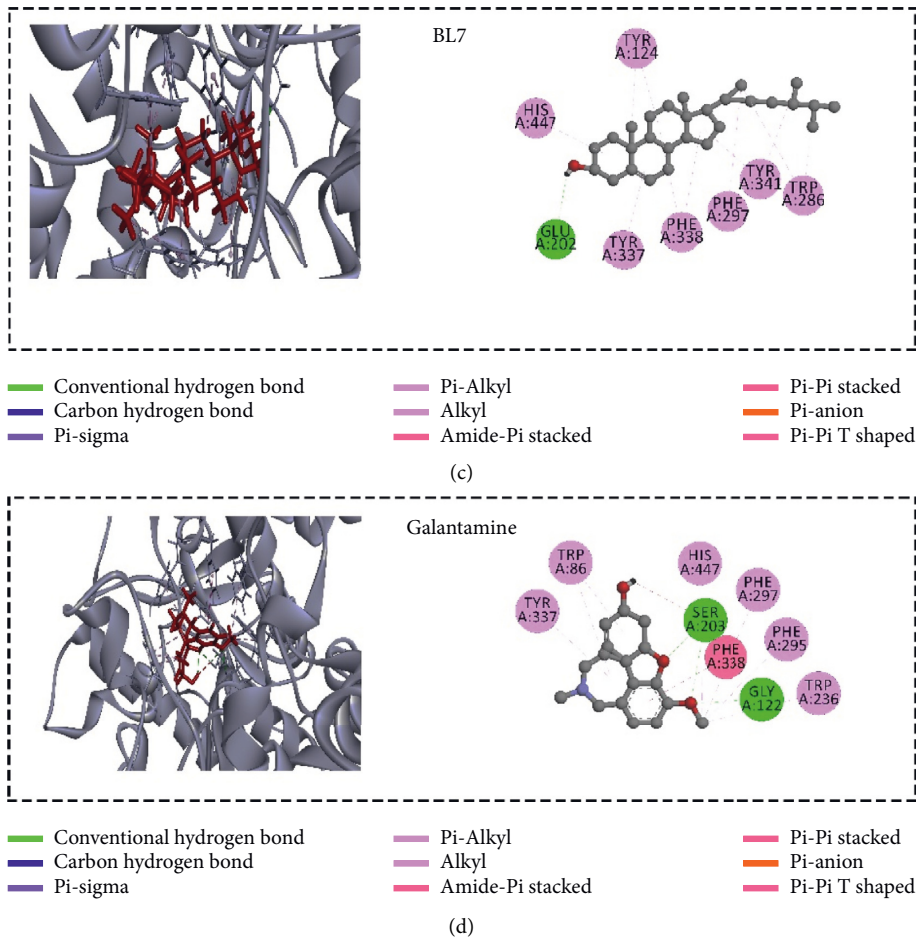

Figure 7: Noncovalent interactions (2D and 3D) of the top three ligands from *Blumea lacera* with AChE (PDB ID 4EY7). In the 3D figure, ligand molecule is represented as red and protein is dark silver (pose predicted by AutoDock Vina). The redocked structure of the native ligand (donepezil) binds to the protein with an RMSD of 0.004 Å. This lower RMSD value validates the docking protocol.

with the catalytic residues Ser203 and His447 of AChE reflecting the competitive inhibition (Figure 7). BL1 and BL4 interact with most of the peripheral site residues of AChE, while BL7 interacts only with Tyr124 and Tyr341. Despite having a high binding affinity, 19α-hydroxyurs-12-ene-24,28-dioate 3-*O*-β-D-xylopyranoside (BL2) does not interact with the PAS and catalytic triad residues. BL1, BL4, and BL7 displayed 16, 16, and 12 hydrophobic interactions as well as three, ten, and one hydrogen bonds with AChE, respectively (Table S1). Many agents could prevent the formation of amyloidogenic protein through blocking the peripheral binding site of AChE and offers additional therapeutic benefits besides the inhibitory activity [49]. BL1 and BL4 acted as a dual-binding agent, blocking both the peripheral and the catalytic binding sites of AChE simultaneously, and could offer additional benefits in AD management.

All compounds, except BL9, exhibited a hydrogen bond with the catalytic site of BChE. The hydroxyl groups in the ligands' side chain have a crucial role in ligand-protein interactions by forming a hydrogen bond with the protein residues. Kaempferol 3-*O*-α-L-rhamnopyranosyl-(1⟶6)-β-D-glucopyranoside (BL5) formed a hydrogen bond with Ser198 and His438 with side-chain oxygen of BChE. Kaempferol 3-*O*-(2″,6″-di-*O*-α-L-rhamnopyranosyl)-β-D-glucopyranoside (BL6) interacted with the catalytic residues and PAS residues with side-chain oxygen and hydrogen atoms, forming hydrogen bonds with Asp70, Tyr332, Ser198, and His438 (mixed inhibition). BL8 forms hydrogen bonds with Ala277, Asn289, Ser287, Ala328, and Thr284. BL5, BL6, and BL8 formed 9, 7, and 6 hydrogen bonds with BChE, respectively (Table S2). The methyl groups in the side chain of the ligands play a pivotal role in developing pi-alkyl interaction with the amino residues of the protein. Moreover, BChE has the ability to accommodate bulkier compounds compared to AChE because the active site of BChE has many aromatic residues replaced by residues with aliphatic side chains, such as leucine (Leu) and valine (Val) [49]. Due to space availability, BL5, BL6, and BL8 were able to accommodate and docked completely into the base of the active site and held in place by the hydrogen bond with Ser198 and His438. BL9 might not reach the peripheral site or the catalytic site due to its large molecular structure.

The chemical structure of natural compounds reflects their binding affinity as well as biological activity. It is

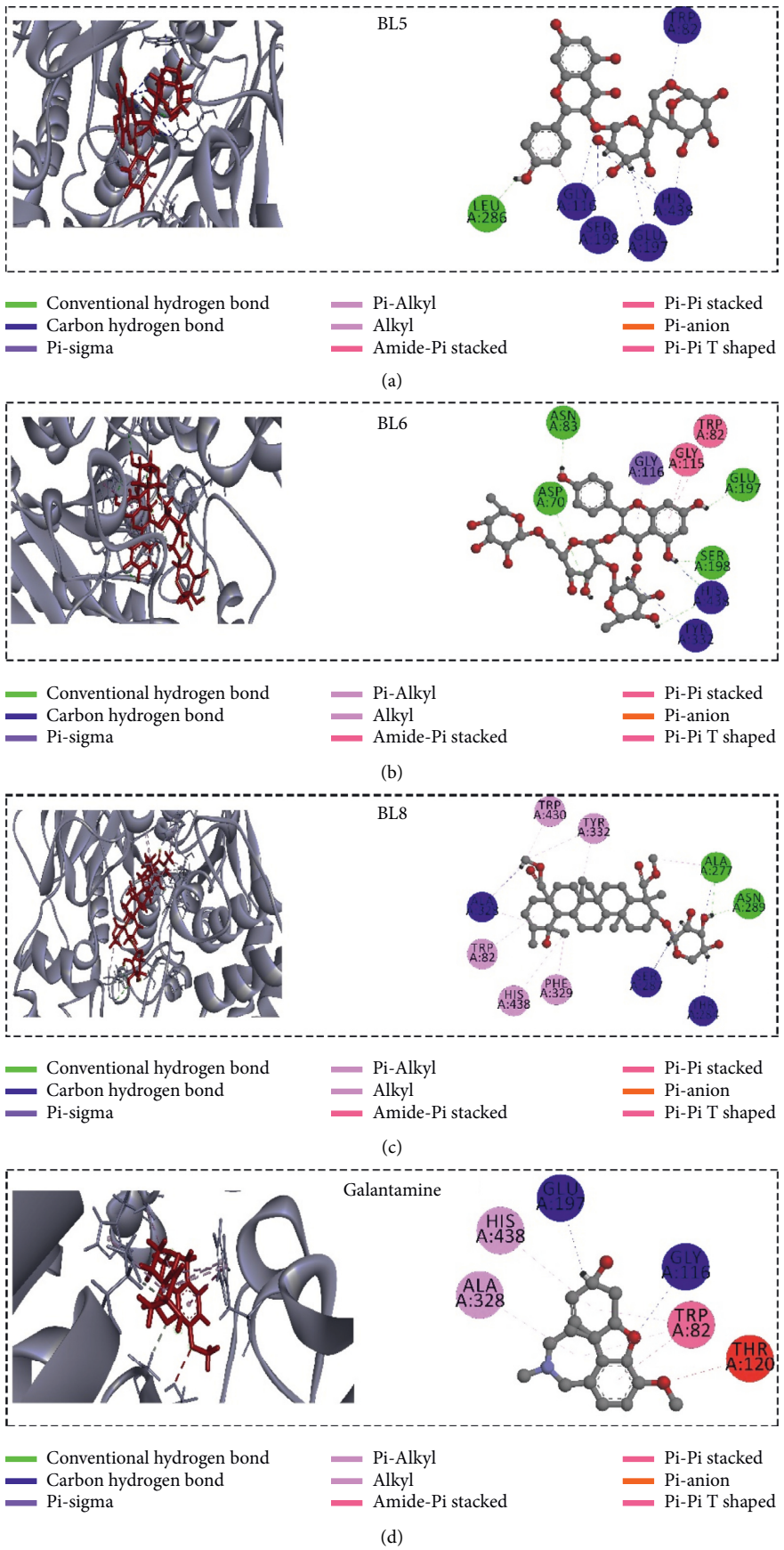

Figure 8: Noncovalent interactions (2D and 3D) of the top three ligands from *Blumea lacera* with BChE (PDB ID 4AQD). In the 3D figure, the ligand molecule and protein are shown in red and dark silver, respectively (pose predicted by AutoDock Vina). The redocked structure of the native ligand (donepezil) binds to the protein with an RMSD of 0.004 Å. This lower RMSD value validates the docking protocol.

noted that hydroxylation improves the inhibitory activities of flavonoids against ChE, while methoxylation may decrease or increase these activities [50]. In docking study, it has been observed that the methoxylation of flavonols decreased the binding affinity for ChE; on the other hand, glucose substitution decreased the binding affinity toward AChE but enhanced the affinity for BChE. In case of triterpenoids, glucosylation attenuated the binding affinity for AChE, while binding affinity has been increased against BChE.

4. Conclusion

The various traditionally used plant extracts were screened for cholinesterase (AChE and BChE) inhibition assay. The currently approved therapies for AD are based on improving cholinergic transmission via the inhibition of ChE which only provide fair improvement in memory and cognitive functions. This study shows that, out of eight tested species, the leaves of *Blumea lacera, Cyclea barbata*, *Smilax guianensis*, and *Byttneria pilosa* can be selected as promising sources of effective ChE inhibitors. The cholinesterase inhibitory potential of *Blumea lacera* has also been established by molecular docking studies. Since *Blumea lacera* and *Cyclea barbata* extracts can act on both *in vitro* AChE and BChE at a bit higher dose compared to galantamine, further evaluation is required to identify the active ingredients and assess their safety and bioavailability in animal models. With AD being a multifaceted neurodegenerative disease, other targets must be considered for future investigations on these extracts or single compounds along with pharmacokinetic, toxicity, and compound stability studies to establish dose-activity/toxicity relationship and any side effects for potential clinical application.

Abbreviations

AD: Alzheimer's disease
AChE: Acetylcholinesterase
APP: Amyloid precursor protein
ATCI: Acetylthiocholine iodide
BChE: Butyrylcholinesterase
BSA: Bovine serum albumin
BTCI: Butyrylthiocholine iodide
CNS: Central nervous system
DTNB: 5, 5′-Dithio-bis-(2-nitrobenzoic acid).

Data Availability

The data used to support the findings of this study are available from the corresponding author upon request.

Conflicts of Interest

The authors declare that they have no conflicts of interest.

Acknowledgments

Christian Zidorn and Md Josim Uddin acknowledge support from the German Academic Exchange Service (DAAD-91649878). The authors are grateful to A. S. M. Ali Reza from International Islamic University Chittagong for his support in plant collection.

Supplementary Materials

Figure S1-1 shows details of collection and identification of *Blumea lacera* (Burm.f.) DC.; Figure S1-2 shows details of collection and identification of *Byttneria pilosa* Roxb.; Figure S1-3 shows details of collection and identification of *Clerodendrum infortunatum* L.; Figure S1-4 shows details of collection and identification of *Cyclea barbata* Miers; Figure S1-5 shows details of collection and identification of *Mikania micrantha* Kunth; Figure S1-6 shows details of collection and identification of *Smilax guianensis* Vitman; Figure S1-7 shows details of collection and identification of *Spermacoce articularis* L.f.; Figure S1-8 shows details of collection and identification of *Thunbergia grandiflora* Roxb.; Figure S2-1 shows the best rank pose (2D and 3D) of noncovalent interactions between ligand and AChE; Figure S2-2 shows the best rank pose (2D and 3D) of noncovalent interactions between ligand and AChE; Figure S3-1 shows the best rank pose (2D and 3D) of noncovalent interactions between ligand and BChE; Figure S3-2 shows the best rank pose (2D and 3D) of noncovalent interactions between ligand and BChE; Table S1 shows noncovalent interactions of BL-1, BL-4, and BL-7 with AChE; Table S2 shows noncovalent interactions of BL-5, BL-6, and BL-8 with BChE. (*Supplementary Materials*)

References

[1] X.-Q. Chen and W. C. Mobley, "Exploring the pathogenesis of alzheimer disease in basal forebrain cholinergic neurons: converging insights from alternative hypotheses," *Frontiers in Neuroscience*, vol. 13, p. 446, 2019.

[2] M. F. Beal, "Oxidative damage as an early marker of alzheimer's disease and mild cognitive impairment," *Neurobiology of Aging*, vol. 26, no. 5, pp. 585-586, 2005.

[3] E. Giacobini, "Cholinergic function and alzheimer's disease," *International Journal of Geriatric Psychiatry*, vol. 18, no. S1, pp. S1–S5, 2003.

[4] J. Birks, "Cholinesterase inhibitors for alzheimer's disease," *Cochrane Database of Systematic Reviews*, no. 1, , 2006.

[5] F. Mangialasche, A. Solomon, B. Winblad, P. Mecocci, and M. Kivipelto, "Alzheimer's disease: clinical trials and drug development," *The Lancet Neurology*, vol. 9, no. 7, pp. 702–716, 2010.

[6] T. Tanaka, H. Kazui, T. Morihara, G. Sadik, T. Kudo, and M. Takeda, "Post-marketing survey of donepezil hydrochloride in Japanese patients with alzheimer's disease with behavioral and psychological symptoms of dementia (BPSD)," *Psychogeriatrics*, vol. 8, no. 3, pp. 114–123, 2008.

[7] L. W. K. Moodie, K. Sepčić, T. Turk, R. Frangež, and J. Svenson, "Natural cholinesterase inhibitors from marine organisms," *Natural Product Reports*, vol. 36, no. 8, pp. 1053–1092, 2019.

[8] A. Nordberg and A.-L. Svensson, "Cholinesterase inhibitors in the treatment of alzheimer's disease," *Drug Safety*, vol. 19, no. 6, pp. 465–480, 1998.

[9] M. S. Uddin, "Traditional knowledge of medicinal plants in Bangladesh," *Nature Info. Electronic Database*, https://www.natureinfo.com.bd/category/flora/medicinal-palnts/, 2019.

[10] N. Yadav, "Herbal compositions comprising *Blumea Lacera*, *Celosia Cristata*, and *Aristolochia Indica* for treatment or prevention of neurological disorders," *International Application Published under the Patent Cooperation Treaty*, 2012.

[11] S. J. Uddin, I. D. Grice, and E. Tiralongo, "Cytotoxic effects of Bangladeshi medicinal plant extracts," *Evidence-Based Complementary and Alternative Medicine*, vol. 2011, Article ID 578092, 7 pages, 2011.

[12] M. F. Kadir, J. R. Karmoker, M. Alam, S. R. Jahan, S. Mahbub, and M. M. K. Mia, "Ethnopharmacological survey of medicinal plants used by traditional healers and indigenous people in chittagong hill tracts, Bangladesh, for the treatment of snakebite," *Evidence-Based Complementary And Alternative Medicine*, vol. 2015, Article ID 871675, 23 pages, 2015.

[13] R. Zaman, M. Parvez, S. Ali, and M. Islam, "Possible anti-obesity activity of methanol extract of *Byttneria Pilosa Roxb*. leaves," *Middle-East Journal of Scietific Research*, vol. 23, no. 8, pp. 1585–1589, 2015.

[14] S. N. Uddin, *Traditional Uses of Ethnomedicinal Plants of the Chittagong Hill Tracts*, Bangladesh National Herbarium, Dhaka, Bangladesh, 2006.

[15] R. Afroz, N. Islam, K. R. Biswas et al., "Medicinal plants used by folk medicinal practitioners in three randomly surveyed villages of Rajbari district, Bangladesh," *American-eurasian Journal of Sustainable Agriculture*, vol. 5, pp. 226–232, 2011.

[16] A. Biswas, M. A. Bari, M. Roy, and S. K. Bhadra, "Inherited folk pharmaceutical knowledge of tribal people in the chittagong hill tracts, Bangladesh," *Indian Journal of Traditional Knowledge*, vol. 9, no. 1, pp. 77–89, 2010.

[17] 2018 https://mpbd.cu.ac.bd.

[18] G. L. Ellman, K. D. Courtney, V. Andres, and R. M. Featherstone, "A new and rapidcolorimetric determination of acetylcholinesterase activity," *Biochemical Pharmacology*, vol. 7, no. 2, pp. 88–95, 1961.

[19] I. Faraone, D. K. Rai, D. Russo et al., "Antioxidant, antidiabetic, and anticholinesterase activities and phytochemical profile of *Azorella glabra* Wedd," *Plants*, vol. 8, no. 8, p. 265, 2019.

[20] H. M. Berman, J. Westbrook, Z. Feng et al., "The protein data bank," *Nucleic Acids Research*, vol. 28, no. 1, pp. 235–242, 2000.

[21] J. Cheung, M. J. Rudolph, F. Burshteyn et al., "Structures of human acetylcholinesterase in complex with pharmacologically important ligands," *Journal of Medicinal Chemistry*, vol. 55, no. 22, pp. 10282–10286, 2012.

[22] X. Brazzolotto, M. Wandhammer, C. Ronco et al., "Human butyrylcholinesterase produced in insect cells: huprine-based affinity purification and crystal structure," *The FEBS Journal*, vol. 279, no. 16, pp. 2905–2916, 2012.

[23] N. Guex and M. C. Peitsch, "SWISS-MODEL and the swiss-Pdb viewer: an environment for comparative protein modeling," *Electrophoresis*, vol. 18, no. 15, pp. 2714–2723, 1997.

[24] R. Pal, S. K. Moitra, N. N. Chakravarti, and R. N. Adhya, "Campesterol from *Blumea lacera*," *Phytochemistry*, vol. 11, pp. 1855–1857, 1972.

[25] C. B. Rao, T. N. Rao, and B. Muralikrishna, "Flavonoids from *Blumea lacera*," *Planta Medica*, vol. 31, no. 3, pp. 235–237, 1977.

[26] R. Agarwal, R. Singh, I. R. Siddiqui, and J. Singh, "Triterpenoid and prenylated phenol glycosides from *Blumea lacera*," *Phytochemistry*, vol. 38, no. 4, pp. 935–938, 1995.

[27] C. Y. Ragasa, J. Wong, and J. A. Rideout, "Monoterpene glycoside and flavonoids from *Blumea lacera*," *Journal of Natural Medicines*, vol. 61, no. 4, pp. 474-475, 2007.

[28] R. Akter, S. J. Uddin, J. Tiralongo, I. D. Grice, and E. Tiralongo, "A new cytotoxic steroidal glycoalkaloid from the methanol extract of *Blumea lacera* leaves," *Journal of Pharmacy & Pharmaceutical Sciences*, vol. 18, no. 4, pp. 616–633, 2015.

[29] R. Akter, S. J. Uddin, J. Tiralongo, I. D. Grice, and E. Tiralongo, "A new cytotoxic diterpenoid glycoside from the leaves of *Blumea lacera* and its effects on apoptosis and cell cycle," *Natural Product Research*, vol. 30, no. 23, pp. 2688–2693, 2016.

[30] A. N. Panche, A. D. Diwan, and S. R. Chandra, "Flavonoids: an overview," *Journal of Nutritional Science*, vol. 5, pp. 1–15, Article ID e47, 2016.

[31] C. P. Yao, J. Li, J. F. Liu et al., "C27 steroidal glycosides with cholinesterase inhibitory activities from *Selaginella delicatula*," *Phytochemistry*, vol. 180, Article ID 112514, 2020.

[32] M. J. Frisch, G. W. Trucks, H. B. Schlegel et al., "Gaussian 09," *Expanding the Limits of Computational Chemistry*, 2009.

[33] S. Dallakyan and A. J. Olson, "Small-molecule library screening by docking with PyRx," *Methods in Molecular Biology*, vol. 1263, pp. 243–250, 2015.

[34] C. Shivanika, D. Kumar, V. Ragunathan, P. Tiwari, A. Sumitha, and P. B. Devi, "Molecular docking, validation, dynamics simulations, and pharmacokinetic prediction of natural compounds against the SARS-CoV-2 main-protease," *Journal of Biomolecular Structure & Dynamics*, vol. 38, pp. 1–27. In press, 2020.

[35] A. Manayi, S. M. Nabavi, M. Daglia, and S. Jafari, "Natural terpenoids as a promising source for modulation of GABAergic system and treatment of neurological diseases," *Pharmacological Reports*, vol. 68, no. 4, pp. 671–679, 216.

[36] A. Arkarapanthu, V. Chavasit, P. Sungpuag, and L. Phuphathanaphong, "Gel extracted from khruea-ma-noi (*Cyclea Barbata* miers) leaves: chemical composition and gelation properties," *Journal of the Science of Food and Agriculture*, vol. 85, no. 10, pp. 1741–1749, 2005.

[37] P. V. Sharma, *Classical Uses of Medicinal Plants*, Chaukamba Bharathi Academy, Varanasi, India, First ed. edition, 1996.

[38] S. P. Ambasta, *The Useful Plants of India*, Council of Scientific & Industrial Research, New Delhi, India, 1986.

[39] A. Sun, X. Xu, J. Lin, X. Cui, and R. Xu, "Neuroprotection by saponins," *Phytotherapy Research*, vol. 29, no. 2, pp. 187–200, 2015.

[40] M. L. Bolognesi, R. Matera, A. Minarini, M. Rosini, and C. Melchiorre, "Alzheimer's disease: new approaches to drug discovery," *Current Opinion in Chemical Biology*, vol. 13, no. 3, pp. 303–308, 2009.

[41] M. Mehta, A. Adem, and M. Sabbagh, "New acetylcholinesterase inhibitors for alzheimer's disease," *International Journal of Alzheimer's Disease*, vol. 2021, Article ID 728983, 8 pages, 2012.

[42] P. K. Mukherjee, V. Kumar, M. Mal, and P. J. Houghton, "Acetylcholinesterase inhibitors from plants," *Phytomedicine*, vol. 14, no. 4, pp. 289–300, 2007.

[43] Y. Zhou, S. Wang, and Y. Zhang, "Catalytic reaction mechanism of acetylcholinesterase determined by born-oppenheimer Ab initio QM/MM molecular dynamics simulations," *The Journal of Physical Chemistry B*, vol. 114, no. 26, pp. 8817–8825, 2010.

[44] J. Cheung, E. N. S. K. Gary, and T. L. Rosenberry, "Structures of human acetylcholinesterase bound to dihydrotanshinone I

and territrem B show peripheral site flexibility," *ACS Medicinal Chemistry Letters*, vol. 4, no. 11, pp. 1091–1096, 2013.

[45] S. Darvesh, D. A. Hopkins, and C. Geula, "Neurobiology of butyrylcholinesterase," *Nature Reviews Neuroscience*, vol. 4, no. 2, pp. 131–138, 2003.

[46] G. Johnson and S. W. Moore, "The peripheral anionic site of acetylcholinesterase: structure, functions and potential role in rational drug design," *Current Pharmaceutical Design*, vol. 12, no. 2, pp. 217–225, 2006.

[47] M. Bajda, A. Więckowska, M. Hebda, N. Guzior, C. A. Sotriffer, and B. Malawska, "Structure-based search for new inhibitors of cholinesterases," *International Journal of Molecular Sciences*, vol. 14, no. 3, pp. 5608–5632, 2013.

[48] N. Atatreh, S. Al Rawashdah, S. S. Al Neyadi, S. M. Abuhamdah, and M. A. Ghattas, "Discovery of new butyrylcholinesterase inhibitors via structure-based virtual screening," *Journal of Enzyme Inhibition and Medicinal Chemistry*, vol. 34, no. 1, pp. 1373–1379, 2019.

[49] N. Jamila, M. Khairuddean, K. K. Yeong, H. Osman, and V. Murugaiyah, "Cholinesterase inhibitory triterpenoids from the bark of *Garcinia hombroniana*," *Journal of Enzyme Inhibition and Medicinal Chemistry*, vol. 30, no. 1, pp. 133–139, 2015.

[50] Y. Xie, W. Yang, X. Chen, and J. Xiao, "Inhibition of flavonoids on acetylcholine esterase: binding and structure–activity relationship," *Food & Function*, vol. 5, no. 10, pp. 2582–2589, 2014.

Hindawi
Evidence-Based Complementary and Alternative Medicine
Volume 2021, Article ID 9940169, 20 pages
https://doi.org/10.1155/2021/9940169

Review Article

Therapeutic Potential of Polyphenols in the Management of Diabetic Neuropathy

Md. Tanvir Kabir,[1] Nuzhat Tabassum,[2] Md. Sahab Uddin,[3,4] Faissal Aziz,[5,6] Tapan Behl,[7] Bijo Mathew,[8] Md. Habibur Rahman,[3] Raushanara Akter,[1] Abdur Rauf,[9] and Lotfi Aleya[10]

[1]*Department of Pharmacy, Brac University, Dhaka, Bangladesh*
[2]*Department of Pharmacy, East West University, Dhaka, Bangladesh*
[3]*Department of Pharmacy, Southeast University, Dhaka, Bangladesh*
[4]*Pharmakon Neuroscience Research Network, Dhaka, Bangladesh*
[5]*Laboratory of Water, Biodiversity & Climate Change, Cadi Ayyad University, Marrakech, Morocco*
[6]*National Centre for Studies and Research on Water and Energy (CNEREE), Cadi Ayyad University, Marrakech, Morocco*
[7]*Chitkara College of Pharmacy, Chitkara University, Rajpura, Punjab, India*
[8]*Department of Pharmaceutical Chemistry, Amrita School of Pharmacy, Amrita Vishwa Vidyapeetham, AIMS Health Sciences Campus, Kochi 682041, India*
[9]*Department of Chemistry, University of Swabi, Anbar, Swabi, Khyber Pakhtunkhwa, Pakistan*
[10]*Chrono-Environnement Laboratory, UMR CNRS 6249, Bourgogne Franche-Comté University, Besançon, France*

Correspondence should be addressed to Md. Sahab Uddin; msu-neuropharma@hotmail.com

Received 22 March 2021; Accepted 27 April 2021; Published 13 May 2021

Academic Editor: Rajeev K Singla

Copyright © 2021 Md. Tanvir Kabir et al. This is an open access article distributed under the Creative Commons Attribution License, which permits unrestricted use, distribution, and reproduction in any medium, provided the original work is properly cited.

Diabetic neuropathy (DN) is a common and serious diabetes-associated complication that primarily takes place because of neuronal dysfunction in patients with diabetes. Use of current therapeutic agents in DN treatment is quite challenging because of their severe adverse effects. Therefore, there is an increased need of identifying new safe and effective therapeutic agents. DN complications are associated with poor glycemic control and metabolic imbalances, primarily oxidative stress (OS) and inflammation. Various mediators and signaling pathways such as glutamate pathway, activation of channels, trophic factors, inflammation, OS, advanced glycation end products, and polyol pathway have a significant contribution to the progression and pathogenesis of DN. It has been indicated that polyphenols have the potential to affect DN pathogenesis and could be used as potential alternative therapy. Several polyphenols including kolaviron, resveratrol, naringenin, quercetin, kaempferol, and curcumin have been administered in patients with DN. Furthermore, chlorogenic acid can provide protection against glutamate neurotoxicity via its hydrolysate, caffeoyl acid group, and caffeic acid through regulating the entry of calcium into neurons. Epigallocatechin-3-gallate treatment can protect motor neurons by regulating the glutamate level. It has been demonstrated that these polyphenols can be promising in combating DN-associated damaging pathways. In this article, we have summarized DN-associated metabolic pathways and clinical manifestations. Finally, we have also focused on the roles of polyphenols in the treatment of DN.

1. Introduction

Diabetic neuropathy (DN) is a common disorder and a microvascular complication of diabetes. Diabetic peripheral neuropathy (DPN) is linked with significant morbidity, mortality, and decreased quality of life [1]. The occurrence of neuropathy in diabetic individuals is around 30%, while up to 50% of diabetic individuals will develop neuropathy [2]. It has been estimated that around 472 million people will be affected by diabetes by 2030, while DPN will affect around 236 million individuals globally [3]. In general, DPN can be classified into focal/multifocal varieties and generalized

polyneuropathies [4, 5]. Furthermore, this generalized form of DPN can also be divided into atypical and typical forms, depending on the alteration in onset, duration, pathophysiology, clinical manifestations, and associations. Indeed, typical DPN is a progressive and symmetrical length-dependent sensorimotor polyneuropathy.

In addition, typical DPN is the most common symptom of diabetes-related injury of the peripheral nervous system [6]. Since there is an increased rate of DN occurrence, it is important to study DN pathophysiology and therapeutic approaches in detail. DN can be developed on a hyperglycemia background and related metabolic imbalances, primarily oxidative stress (OS). Further complications can take place due to the hyperglycemia-mediated overgeneration of free radicals. Various studies have detected main pathways that are associated with DN, including the induced level of polyol, advanced generation of glycation end products, and other cascades of stress responses [7]. It has been identified that OS plays a crucial role in DN development.

Despite advances in the therapy of diabetes complications including DN, still, there is a deficiency of effective therapeutic agents. Furthermore, current drugs that are available to treat DN involve various common and serious adverse effects (Table 1). There is an increased need of developing novel multitarget therapeutic agents to control more destructive signaling mechanisms in patients with DN. It has been reported that polyphenols [8] are multitarget agents that exert effective antioxidant and anti-inflammatory properties. It has been confirmed by various *in vitro* and *in vivo* studies that natural phenolic compounds play important roles in the management of type 2 diabetes via insulin-dependent mechanisms (Table 2). Besides, polyphenols have the efficacy to fight against various diseases including diabetes and diabetes-associated complications [8–10]. Polyphenols have been reported to exert potent neuroprotective activities in case of diabetes [11].

In order to develop polyphenols as therapeutic agents to treat DN, it is essential to understand the signaling mechanisms that are associated with the advancement of DN and the mechanisms by which polyphenols avert the advancement of these destructive mechanisms. In this article, we have summarized metabolic pathways and clinical manifestations that are associated with DN. Moreover, we have also focused on the roles of polyphenols in the treatment of DN.

2. Diabetic Neuropathy Pathogenesis-Associated Metabolic Pathways

It has been revealed that various mechanisms are associated with the development of DN pathogenesis including imbalances in the blood supply to peripheral nerves, gene expression of calcium and sodium channels, vascular system of the thalamic gland, and autoimmune disorders characterized via glial cell activation [71]. The main mediators and signaling mechanisms that are linked with DN include glutamate pathway, activation of channels, trophic factors, inflammation, OS, advanced glycation end products (AGEs), and polyol pathway [72–76].

2.1. Glutamate Pathway. Glutamate is important for various processes including cell migration, cell death, cell differentiation, and synapse plasticity [77]. In the central nervous system (CNS), glutamate also has a significant contribution to the peripheral transduction of sensory inputs [78]. Multiple studies have revealed that glutamate-induced toxicity is present in case of both chronic and acute neurodegenerative disorders of the CNS and peripheral nervous system (PNS) [79]. It has been reported that glutamatergic ligands can induce nociceptive behaviors, which indicates that glutamate is associated with peripheral sensory transduction and nociceptive pathways. In a mouse model of type I diabetes, hyperglycemia markedly elevated the expression of N-methyl-D-aspartate (NMDA) receptors [80]. In addition, activities of spinal NMDARs have been confirmed in nerve injury-mediated pain [81]. Interestingly, spinal NMDAR subunit 2B (NR2B) level was increased in both protein and mRNA levels of STZ-mediated DN, which further resulted in hyperactivity of spinal cord dorsal horn neurons [82]. It has been observed that glutamate (particularly NR2B) induces various DN-associated pathways including apoptosis, inflammation, and OS [83]. In order to combat DN, targeting the glutamate pathway and NR2B as upstream factors of apoptotic, inflammatory, and oxidative mechanisms via phytochemicals is highly promising.

2.2. Activation of Channels. Transient receptor potential vanilloid 1 (TRPV1) channel is associated with multiple modalities of nociceptive stimuli. In a streptozotocin- (STZ-) mediated DN model, the expression of TRPV1 was markedly elevated in individuals with hyperalgesic skin in comparison with the individuals with hypoalgesic and normoalgesic skin [84, 85]. Various studies have revealed that early stages of DN take place because of the TRPV1 upregulation via protein kinase C (PKC) and protein kinase A (PKA) [86], which further indicates the contribution of TRPV1 channels in hyperalgesia expression [86]. In case of DN, other TRPV receptors are yet to be properly investigated [87]. TRPV may be generally considered as an auspicious therapeutic target to develop new therapeutic agents for DN. TRPV1 activation-induced $[Ca^{2+}]$ transients and found to be commonly altered in hyperalgesia [86]. Therefore, voltage-gated calcium channels (CaVs) are supposed to be associated with painful DN [88]. It has been reported that the $\alpha 2\delta$ subunits elevated the trafficking and expression of these channels, however might have a contribution to synaptogenesis within the CNS and PNS [89]. Along with CaVs, an increased level of voltage-gated sodium channels (Nav) was detected at the site of neuronal injury in DN [90]. Furthermore, an increased level of methylglyoxal has been identified in the serum of patients with painful DN. Methylglyoxal resulted in mechanical and thermal hyperalgesia when injected into the diabetic mouse models (but not in Nav1.8 knockout mouse models) [91]. Collectively, all these findings suggest the significance of CaVs, Nav, and TRPV1 via multitarget phytochemicals in the DN development (Figure 1). Besides, TRPV1 was found to be coexpressed with glutamate receptors [92].

Table 1: Common and serious adverse effects of currently available drugs that are used in the treatment of diabetic neuropathy.

Drug	Common adverse effects	Serious adverse effects	References
Amitriptyline	Nausea, insomnia, headache, blurred vision, dizziness, sedation, dry mouth, orthostatic hypotension, urinary retention	Hyponatraemia, serotonin syndrome, suicidal thoughts, hepatotoxicity, seizures, cardiac arrhythmias, interstitial lung disease	[12–14]
Gabapentin	Dry mouth, peripheral oedema, somnolence, gait disturbance, weight gain, headache, dizziness	Suicidal thoughts and behavior, Stevens–Johnson syndrome, seizures, hepatitis, withdrawal reactions, confusion	[15]
Tramadol	Nausea, headache, dizziness, sweating, constipation, somnolence	Hallucinations, seizures, opioid abuse/misuse, serotonin syndrome	[16]
Duloxetine	Dizziness, nausea, headache, dry mouth, diarrhoea, somnolence, sweating, insomnia, constipation, tremor	Hepatic failure, serotonin syndrome, hypertensive crisis, urinary retention, interstitial lung disease, hyponatraemia, Stevens–Johnson syndrome, seizures	[17–19]
Venlafaxine	Nausea, headache, insomnia, vomiting, diarrhoea, sweating, dry mouth, anorexia, somnolence		[20]
Pregabalin	Dry mouth, dizziness, somnolence, weight gain, weakness, headache, peripheral oedema	Seizures, angioedema, hepatotoxicity, rhabdomyolysis, Stevens–Johnson syndrome, suicidal thoughts, cardiac arrhythmia, pulmonary oedema, thrombocytopenia	[21, 22]
Tapentadol extended release (ER)	Nausea, headache, somnolence, dizziness, sweating, constipation	Same as tramadol and angioedema	[23–26]

2.3. Polyol Pathway. Polyol pathway exists in various tissues including blood vessels and peripheral nerve and plays significant roles in DN development [93]. There are two major enzymes that are associated with the polyol pathway including sorbitol dehydrogenase and aldose reductase (AR). These enzymes are found in several tissues including vascular cells, glomerulus, retina, lens, and nerve [94]. Increased levels of blood glucose can result in AR activation that generates sorbitol from glucose. Indeed, this reaction utilizes nicotinic acid adenine dinucleotide phosphate (NADPH) and generates $NADP^+$. Increased NADPH utilization can decrease the concentration of a decreased level of glutathione (GSH) and elevates its oxidized form GSH disulfide. Since sorbitol is unable to cross the cell membrane, sorbitol accumulation increases blood osmolality which further results in the loss of electrolytes [74, 95]. Increased level of osmosis can lead to injury of cells that are located adjacent to peripheral neurons (Schwann cells) and results in a schwannopathy-associated phenotype of DN [95, 96]. It has been reported that sorbitol dehydrogenase can trigger the conversion of accrued sorbitol into fructose through oxidation and generation of nicotinic acid adenine dinucleotide. Nonetheless, increased levels of fructose and sorbitol exert harmful actions in nerve cells because of various causes including the reduced level of the osmolality regulator (taurine), regulator of insulin sensitivity (myoinositol), suppression of the Na^+/K^+ ATPase pump, intracellular Na^+ accumulation, ionic homoeostasis through reducing the PKC effect which results in swelling of the axon and axon-glia dysfunction, and decreased level of nerve conduction velocity (NCV) [72].

It has been revealed that accumulated glucose can enter into the hexosamine biosynthesis pathway and generates fructose-6-phosphate, which gets eventually converted into uridine diphosphate-N-acetylglucosamine (GlcNAc). In addition, GlcNAc is a sugar moiety that is utilized in O- or N-glycosylation of such translated proteins (posttranslational modification) since SP-1 transcription factor results in plasminogen activator inhibitor-1 overexpression and growth factor-β1 transformation. Therefore, these factors result in nerve injury by generating mitochondrial superoxides [97]. In animal models, inhibitors of AR were found to be very effective in reducing DN [98]. However, these inhibitors were not that much effective in clinical studies [99], which was partial because of the introduction of lower doses as compared to *in vivo* studies. Thus, inadequate levels were available to avert the flux through the polyol pathway [98].

2.4. Oxidative Stress and Advanced Glycation End Products. In case of OS, oxidation surpasses antioxidant ability in cells because of the imbalance in the level of enzymatic antioxidant catalase (CAT) and superoxide dismutase (SOD) or nonenzymatic factor GSH [100]. In the polyol pathway, NADPH consumption results in negative action in a decreased level of GSH. Increased level of reactive oxygen species (ROS) including hydrogen peroxide (H_2O_2), hydroxyl radical ($^{\bullet}OH$), and superoxide ($O_2^{\bullet-}$) was found to damage the proteins and lipid of cells. Furthermore, ROS can result in injury of lipids in the myelin sheath [101]. In a study, Edwards et al. [102] revealed that increased concentration of nitrosative products including nitrotyrosine (NT) and peroxynitrite ($ONOO^-$) in diabetic individuals is positively associated with DPN. Therefore, the increased lipid peroxidation, and damage rate of DNA and protein. It has been reported that nonenzymatic reactions between the damaged lipids, DNA, or proteins and aldehyde groups of reducing sugars lead to AGEs, which further stimulate ROS generation both during their formation and interaction with the AGE receptor (RAGE) [103, 104]. In addition, advanced lipoxidation end products are generated via an elevated level

Table 2: Antidiabetic properties of naturally occurring phenolic compounds.

Naturally occurring phenolic compounds	Effects	References
Flavonoids	(i) Intestinal microbiota ↑ (ii) Digestive enzymes ↓ (iii) Glucose absorption ↓ (iv) Formation of advanced glycation end products (AGEs) ↓	[27–31]
Catechins	(i) Insulin sensitivity ↑ (ii) Fecal excretion of bile acids and cholesterol ↑ (iii) Activation of AMPK ↑ (iv) White fat depots ↓ (v) Blood lipid ↓ (vi) Glycaemia ↓ (vii) Pancreatic α-glucosidase and also α-amylase and maltase ↓ (viii) Generation of reactive oxygen species ↓ (ix) Na^+-dependent glucose transporter ↓	[32–38]
Caffeoylquinic acids	(i) Insulin response ↑ (ii) Hepatic glucose-6-phosphatase ↓ (iii) Human pancreatic and salivary α-amylase ↓	[39–43]
Isoflavones	(i) Hypoglycemic effects through ameliorating insulin resistance and sensitivity ↑ (ii) Exerting anti-inflammation property ↑ (iii) Digestion of carbohydrate and uptake of glucose in the small intestine ↓ (iv) Protecting pancreatic β-cells ↑ (v) The mechanism of renal interstitial fibrosis in diabetic nephropathic rat models ↓ (vi) Oxidative damage ↓ (vii) Maillard reaction and formation of AGEs ↓	[44–46]
Hydroxycinnamic acids	(i) Insulin resistance and glucose intolerance ↑ (ii) Glucokinase activity ↑ (iii) β-Cell activity ↑ (iv) Antioxidant properties and anti-inflammatory activities ↑ (v) Activation of AMP-activated protein kinase ↑ (vi) Phosphoenolpyruvate carboxykinase and glucose-6-phosphatase effects in the liver ↓ (vii) Gluconeogenesis and adipogenesis ↓	[47–50]
Stilbenoids	(i) Metabolic control ↑ (ii) Pancreatic β-cell and hepatoprotective activity ↑ (iii) Insulin sensitivity ↑ (iv) DNA integrity ↑ (v) Level of digestive enzymes ↓ (vi) Oxidative stress and inflammation ↓	[51–57]
Tannins	(i) Uptake of glucose in adipose tissue through phosphorylation of IRS-1 ↑ (ii) Phosphorylation of AMPK ↑ (iii) Formation of AGEs and enzymatic action of sucrose, lactase, and maltase ↓ (iv) Activities of α-amylase and α-glucosidase ↓	[35, 58, 59]
Procyanidins	(i) Target digestive enzymes ↓ (ii) AMPK and insulin signaling pathways ↑ (iii) Cellular expression of NAD^+ and SIRT1 levels ↑ (iv) Proinflammatory cytokine expression ↓	[60–63]
Anthocyanins and anthocyanidins	(i) Antioxidant ↑ (ii) Blood glucose regulation ↑ (iii) Anti-inflammatory activity ↑ (iv) Oxidative damage ↓ (v) Concentrations of cholesterol, low-density cholesterol, and triglycerides ↓	[64–67]
Curcumin	(i) Protecting pancreatic β-cells ↑ (ii) Diabetic cardiomyopathy ↓ (iii) Insulin resistance ↓ (iv) Oxidative damage ↓	[44, 68–70]

Note: ↑ = induction; ↓ = inhibition.

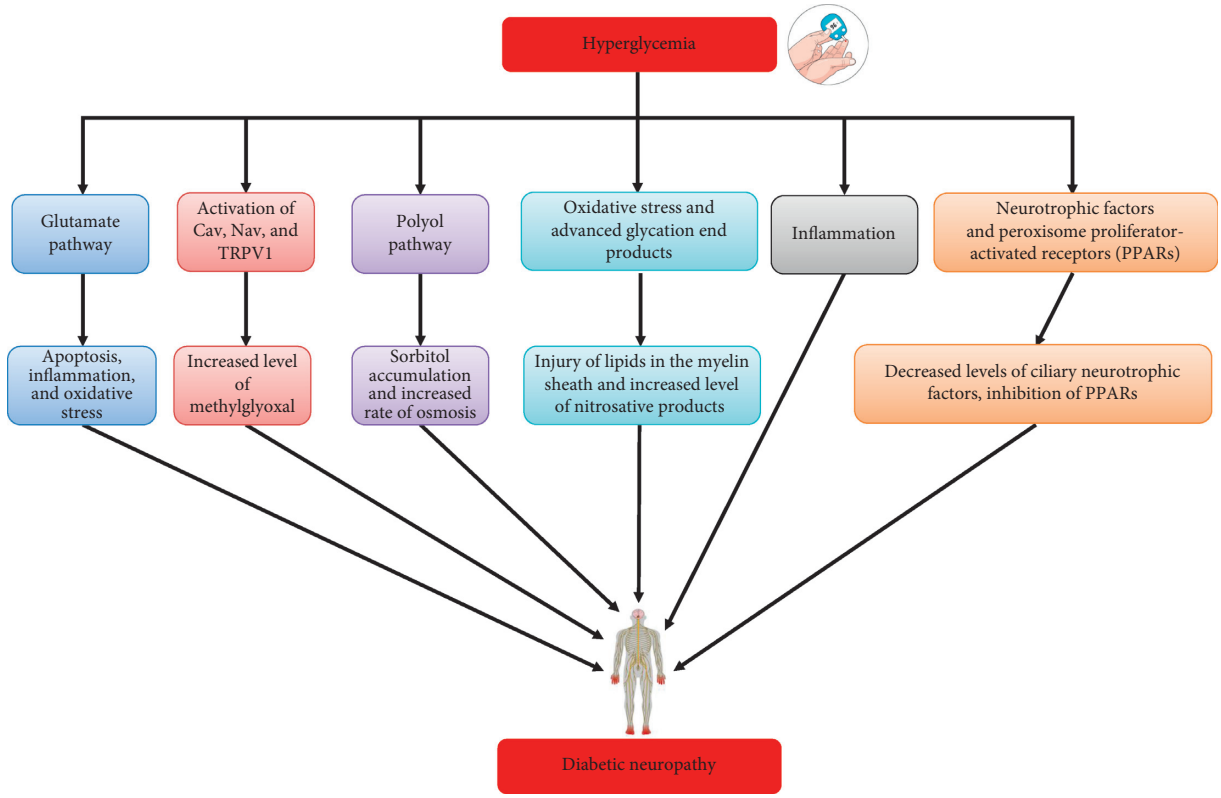

Figure 1: Diabetic neuropathy pathogenesis-associated metabolic pathways.

of OS-stimulated lipid peroxidation along with altered lipid metabolism [105].

Other enzymes including PKC-β, 12/15-lipoxygenase, Na^+/H^+ exchanger, and NADPH oxidase are also associated with ROS generation in DN individuals [106, 107]. Indeed, PKC-β has a contribution to nerve activity and DN pathogenesis [108]. Interestingly, streptozotocin- (STZ-) induced diabetic rat models revealed the positive outcomes of the PKC-β inhibitor on DN in decreasing free radicals [109]. In case of hyperglycemia, the mitochondrial membrane's potential is disturbed, and it secretes cytochrome c which then causes activation of procaspase-9 along with apoptotic protease activating factor-1 (Apaf-1) resulting in the caspase-3 activation in neurons [110, 111]. In a STZ-induced rat model of diabetes, Zherebitskaya et al. [112] revealed that an increased level of glucose reduced manganese-containing superoxide dismutase (MnSOD) and elevated level of ROS in axons which predominantly resulted in the injury of dystrophic structures and axon outgrowth. Collectively, these findings regarding OS indicate that regulating the level of ROS in patients with diabetes might be a possible way of preventing DN.

2.5. Inflammation. Inflammation is the response which is activated via damage in the dorsal root ganglion (DRG), spinal cord, skin, or nerve, which eventually leads to painful sensation. Furthermore, it is linked with diabetes and increased concentrations of inflammatory cytokines including tumor necrosis factor-α (TNF-α) and C-reactive protein in individuals with DN [113]. In a study, Conti et al. [114] observed that STZ-induced diabetes resulted in the infiltration of immune cells including monocytes and macrophages, the neuronal overexpression of interleukin-1 beta (IL-1β), and the expression of neurotrophin receptor p75 [114]. Moreover, the association of inflammation in DN was demonstrated in a STZ-induced diabetic animal model. It was observed that pioglitazone reduced the level of phosphorylated extracellular signal-regulated kinases (ERKs), changed the protein kinase C-alpha expression level, and reduced the number of accumulated macrophages in Schwann cells [115]. Since a transcriptional factor comprises 2 subunits including p50 and p65, nuclear factor kappa B (NF-κB) is located in the cytoplasm in an inhibitory state bound to the inhibitor of nuclear factor-κB (IκB).

After the simulation, IκB is tagged through ubiquitin for proteasomal degradation leaving active NF-κB. In the active state, NF-κB is translocated to the nucleus, where it induces the expression of various survival and inflammatory genes. It has been revealed that the level of NF-κB's p65 subunit is increased in the myelin sheath of neurons in case of demyelinating polyneuropathies [116]. In a different study, Ha et al. [117] revealed that hyperglycemia in glial cells induced NF-κB activation, which further resulted in increased concentration of various cell adhesion genes and inflammatory genes (TNF-α, cyclooxygenase-2 (COX-2), inducible nitric oxide synthase, IL-1β, and interleukin 6 (IL-6)). In another study, Bierhaus et al. [118] detected IL-6, receptor for AGEs, and p65 subunit of NF-κB in sural nerve biopsies obtained from people with diabetes. Collectively, these

results confirmed that inflammatory signaling pathways have a significant contribution in DN pathogenesis which makes them important pharmacological targets via phytochemicals (Figure 1).

2.6. Neurotrophic Factors and Peroxisome Proliferator-Activated Receptors. Neurotrophic factors induce nerve regeneration, mediate normal physiological activities of surviving neurons, and also elevate their resistance to damage. These activities ameliorate the clinical conditions of patients with DN [119]. It has been observed that deficiency of neurotrophin plays a role in DN pathogenesis. Interestingly, the levels of ciliary neurotrophic factor, insulin-like growth factors, neurotrophin-3/4/5, and brain-derived neurotrophic factor (BDNF) were decreased in the muscles of patients with DN [120]. Indeed, nerve growth factor (NGF) can decrease these neurotrophin imbalances [119]. Preclinical experiments supported the idea that influencing neurotrophic factors via phytochemicals may be a potent therapeutic strategy for various types of peripheral nerve disease.

It is known that peroxisome proliferator-activated receptors (PPARs) are a group of nuclear receptor proteins. By binding with the lipophilic stimulant, PPAR mediates the expression of proximal genes that are associated with hepatocarcinogenesis, lipid hemostasis, proximal proliferation, and beta-oxidation of fatty acids [121–123]. There are 3 major subtypes of PPARs including α, β/δ, and γ that have a significant contribution in regulating inflammatory processes, morphogenesis, glucose, mobilization of lipids, storage, and metabolism [122, 124, 125]. PPARs work together with various cellular transcription factors including activated protein-1 (AP-1), signal transducer/activator of transcription-1, and NF-κB [125]. Furthermore, PPARs suppress the expressions of chemokines and proinflammatory genes (interleukin 1 beta (IL-1β) and TNF-α) and decrease the sensation of pain [126]. Agonists of PPAR gamma (PPAR-γ) including rosiglitazone and pioglitazone are commonly suggested to treat insulin resistance and hyperglycemia [127] and to reduce the activation of spinal nociceptive neurons in type II diabetic rat models [128]. Furthermore, PPAR agonists have the future potential to be used as novel analgesics in treating various chronic pain conditions including DN. Nevertheless, their possible adverse effects need to be carefully considered during targeting PPAR signaling pathway as analgesics [129]. Thus, there is a growing research interest regarding the use of PPAR agonists to decrease DN.

3. Clinical Manifestations of Diabetic Neuropathy

DPN might present with various clinical signs and symptoms. In some cases, patients might be completely asymptomatic; however, foot ulcer might be the first presentation. Nevertheless, other individuals might exhibit one or multiple different symptoms including numbness, paresthesia, and neuropathic pain (frequently stated as aching, shooting, lancinating, or burning) which may range from mild to severe, which can lead to severe suffering [130]. In addition, these symptoms might be constant or sporadic. Interestingly, sensory symptoms might persist for a short duration before they vanish completely, or they might become chronic.

Sensory signs and symptoms first appear in the distal foot/toes. Pinprick and light touch of the distal foot is normally impaired on first physical examination and then more advanced motor (particularly loss of muscle bulk, loss of ankle reflex, clawing of the toes, and weakness) and sensory (specifically proprioception loss and vibration) abnormalities. It spreads proximally up the leg before affecting the upper limbs and fingertips as the disease advances. Physical examination for individuals with painful DPN is typically unclear as compared to those without neuropathic pain. Nonetheless, certain people might contain pure small fiber neuropathy, which can lead to a loss of small fiber modalities (particularly pinprick and loss of temperature sensation) with normal large fiber activity [6]. It was observed that a small number of individuals possess the so-called "irritable nociceptor" phenotype with "positive" sensory signs including hyperalgesia and allodynia [131, 132].

4. Polyphenols in the Treatment of Diabetic Neuropathy

It has been reported that around 800 plants might contain antidiabetic properties. So far, various phytochemicals including kolaviron, resveratrol, naringenin, quercetin, kaempferol, and curcumin (Figure 2) have been administered in patients with DN. However, it is essential to detect the phytochemicals that can be used in the treatment of DN. In the following sections, we have summarized the cellular signaling pathways and pharmacological targets that are associated with the therapeutic effect of polyphenols in DN.

4.1. Nonenzymatic and Enzymatic Antioxidant Performance. In diabetic animals, hyperglycemia decreases the effect of antioxidant enzymes with nonenzymatic glycosylation and results in OS [133]. In DN development, stimulation of some negative effects including generation of free radicals by OS, lower GSH levels, Cu/Zn SOD, glutathione S-transferase, decreased glutathione peroxidase (GPx), oxidations of leukocytes and catecholamines, elevated mitochondrial leak, perglycemia, and ischemia play a major destructive role [133–136]. Various antioxidants, particularly polyphenols, have exerted some promising activities in the experimental DN treatment. In experimental DN, α-lipoic acid treatment averted neurovascular irregularities. In diabetic rat models, this treatment also attenuated GSH levels, digital nerve conduction velocity, and nerve blood flow via increasing free radical scavenging activity [137, 138]. Probucol is a strong free radical scavenger and an inhibitor of low-density lipoprotein oxidation that normalizes both electrophysiology and nerve blood flow [139]. In a study, Al-Rejaie et al. [140] revealed that naringenin contains antioxidant properties.

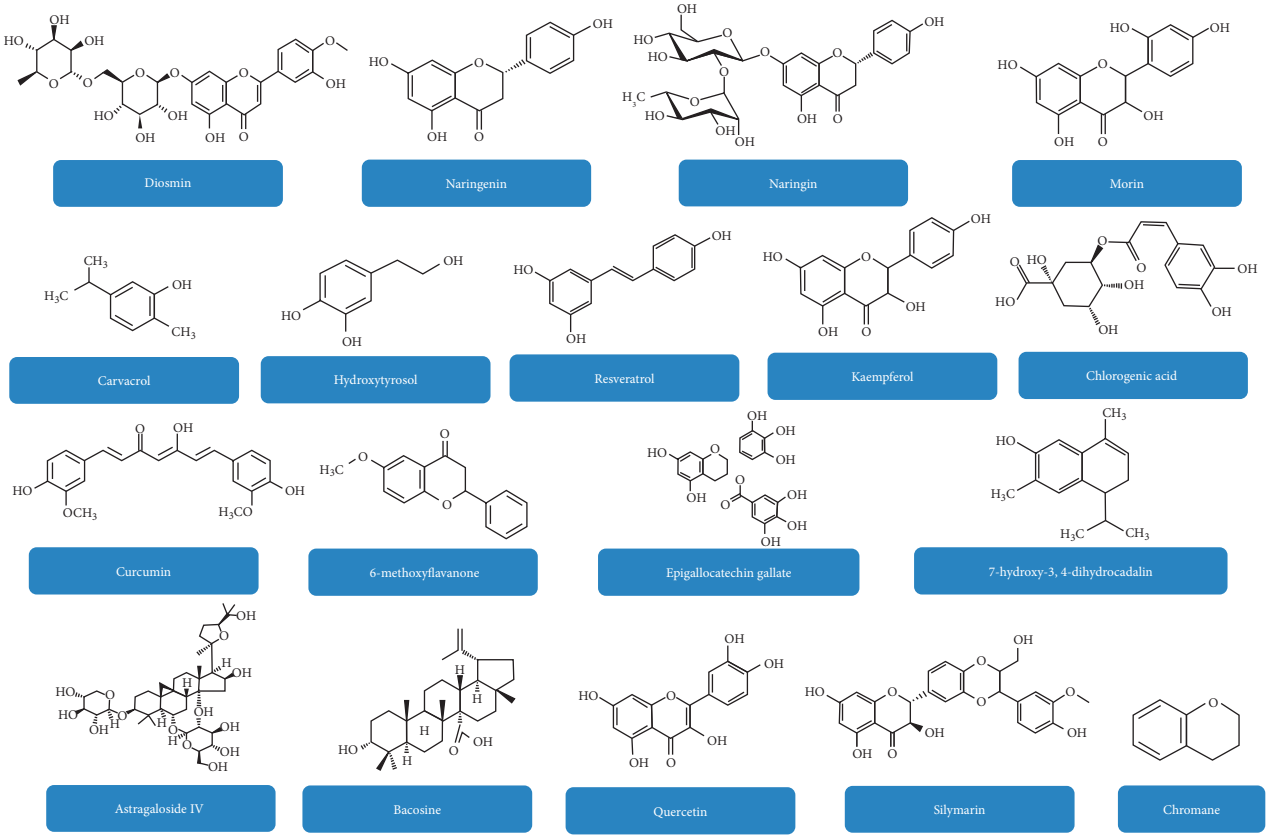

Figure 2: Chemical structures of various polyphenolic compounds that can be effective in the treatment of diabetic neuropathy.

Moreover, it inhibited the levels of nitric oxide (NO) and thiobarbituric acid reactive substances (TBARS) and attenuated the decreased concentrations of GPx and CAT in STZ-induced diabetic rat models [140, 141].

Resveratrol (a polyphenolic compound) (Figure 2) protected neural tissues from diabetes-mediated OS via decreasing the levels of malondialdehyde (MDA), xanthine oxidase (XO), and NO in the brain stem, spinal cord, cortex, hippocampus, and cerebellum via increasing the level of GSH in diabetic rat models [142]. In addition, apocynin and curcumin attenuated the elevated spinal H_2O_2 level and level of MDA and increased the level of SOD in STZ-induced diabetic rat models. It has been confirmed that curcumin suppressed the activation of spinal NADPH oxidases, the major enzymes that generate ROS via reversing the upregulation of phagocyte NADPH oxidase subunits ($gp91^{phox}$ and $p47^{phox}$) [143]. More related cellular signaling pathways and pharmacological targets that are associated with the antioxidant property of polyphenols have been summarized in Table 3.

4.2. Prevention of the Inflammatory Response and Proinflammatory Cytokines. Proinflammatory alterations that are seen in diabetes have a significant contribution to the pathogenesis of retinopathy, nephropathy, neuropathy, and atherosclerosis [175]. Production of hyperglycemia-mediated ROS is directly associated with the DN pathogenesis. Indeed, these ROS might trigger the generation of IL-1β and TNF-α. In the CNS, insulin resistance and hyperglycemia are linked with the TNF-α signaling pathway, which might trigger pain and hyperalgesia in DN [176–178]. Various studies have revealed that suppression of TNF-α decreased hyperalgesia in models of painful DN [179]. It has been confirmed that TNF-α intraplantar injection is linked with thermal hyperalgesia and mechanical allodynia in rat models [74, 176, 180]. IL-1β can be obtained from various cell types including Schwann cells, endothelial cells, mononuclear cells, synoviocytes, and fibroblasts and has a significant contribution in triggering mechanical hyperalgesia. In the mouse model of experimental neuropathy, it neutralized the IL-1 receptors that further resulted in the reduction of pain-related behavior [181, 182].

Increased lipid level and hyperglycemia resulted in activation of NF-κB that has a significant contribution to the generation of ROS and TNF-α, which further induces inflammatory demyelination. NF-κB might increase metabolic disorders including diabetes and trigger inflammation [183]. Inhibitor of NF-κB (IκB-α) and p65 are the subunits of NF-κB that are overexpressed in sural nerve macrophages in chronic and acute inflammatory demyelinating polyneuropathies [116, 184]. In STZ-induced DN rat models, it has been confirmed that resveratrol exerts anti-inflammatory property via reducing the expression of IκB-α and p65 and ameliorating the increased concentrations of NF-κB, IL-6, COX-2, and TNF-α [169]. Furthermore, resveratrol

Table 3: Polyphenols in the treatment of diabetic neuropathy.

Polyphenols	Animal models	Duration	Dosage	Effects	References
Diosmin	STZ-induced diabetic rats	4 weeks	50 and 100 mg/kg/day	Increased tail-flick latency; decreased traveling duration; increased concentration of SOD and GSH; decreased levels of MDA and NO	[144]
Hydroxytyrosol	STZ-induced diabetic rats	6 weeks	10 and 100 mg/kg/day	Reduced thermal nociception; elevated paw withdrawal threshold and Na^+/K^+ ATPase activity; increased MNCV level	[145]
Kolaviron	STZ-induced diabetic rats	6 weeks	100 and 200 mg/kg/day	Reduced level of OS, IL-1β, TNF-α, MDA, and TBARS; elevated concentrations of GSH, CAT, and GPx	[146]
Carvacrol	STZ-induced diabetic rats	7 weeks	25, 50, and 100 mg/kg/day	Increased SOD level; decreased concentrations of IL-1β, MDA, and TNF-α	[147]
Naringenin	STZ-induced diabetic rats	5 weeks	25 and 50 mg/kg/day	Increased tail-flick latency and paw withdrawal; elevated NGF and IGF-1 in sciatic nerves; decreased IL-1β and TNF-α levels; increased concentrations of CAT, GSH, and GPx	[140]
Naringin	STZ-induced diabetic rats	4 weeks	40 and 80 mg/kg/day	Reduced mechanotactile allodynia, oxidative-nitrosative stress, and TNF-α level; increased tail-flick latency and nociceptive threshold; increased concentrations of MNCV and SOD	[141]
Curcumin	STZ-induced diabetic rats	6 weeks	100 mg/kg/day	Decreased thermal nociception, levels of TNF-α and IL-10; increased tail-flick latency and paw withdrawal threshold	[148]
	STZ-induced diabetic rats	3 weeks	200 mg/kg/day	Decreased mechanical allodynia and thermal hyperalgesia; increased paw withdrawal threshold; decreased AR, prostaglandin peroxidase, and COX levels	[149]
	STZ-induced diabetic rats	14 days	200 mg/kg/day	Increased paw withdrawal threshold and SOD level; decreased levels of MDA and H_2O_2 in the spinal cord	[143]
Curcumin and gliclazide	STZ-induced diabetic rats	5 weeks	100 mg/kg/day	Increased mechanical hyperalgesia threshold, hot-plate, and tail-flick latencies; decreased levels of peroxynitrite, LPO, and TNF-α	[150]
Curcumin and resveratrol	STZ-induced diabetic rats	4 weeks	Curcumin = 60 mg/kg/day; resveratrol = 20 mg/kg/day	Increased nociceptive threshold; decreased levels of brain nitrite and TNF-α	[151]
Astragaloside IV	STZ-induced diabetic rats	12 weeks	3, 6, and 12 mg/kg/day	Increased myelinated fiber density, myelinated fiber area, and segmental demyelination; decreased levels of HbA1C; increased levels of MNCV and GPx; decreased AR level in erythrocytes; increased activity of Na^+/K^+ ATPase in nerves and erythrocytes	[152]
Epigallocatechin gallate	STZ-induced diabetic rats	10 weeks	2 g/L/day	Decreased mechanical allodynia and thermal hyperalgesia; elevated paw withdrawal pressure; decreased 8-OHdG immunoreaction, numbers of Fos-immunoreacted neurons, and colocalization of 8-OHdG and Fos in laminae I–III	[153]
	STZ-induced diabetic rats	7 weeks	20 and 40 mg/kg/day	Increased nociceptive threshold and tail-flick latency; reduced formalin-mediated nociceptive behavior; decreased concentrations of nitrite, TBARS, and MDA; elevated SOD level	[154]

Table 3: Continued.

Polyphenols	Animal models	Duration	Dosage	Effects	References
Grape seed proanthocyanidins	STZ-induced diabetic rats	16 weeks	125, 250, and 500 mg/kg/day	Increased hot-plate latency and nerve conduction velocity; decreased level of free Ca^{2+}; elevated activities of ATPase in sciatic nerves	[155]
Bacosine	STZ-induced diabetic rats	30 days	5 and 10 mg/kg/day	Diabetes-linked cognitive impairment; decreased hyperalgesia; increased levels of MNCV and SOD; decreased levels of AGEs, ROS, MDA, TNF-α, and IL-1β	[156]
6-Methoxyflavanone	STZ-induced diabetic rats	—	10 and 30 mg/kg/day	Elevated paw withdrawal threshold and latency; reduced thermal nociception; involvement of GABA receptors; increased flinching response threshold and latency by a preference for the δ- and κ-opioid receptors	[157]
Chlorogenic acid	STZ-induced diabetic rats	14 days	100 mg/kg/day	Increased threshold of mechanical hyperalgesia; decreased formalin-mediated nociceptive behavior	[158]
7-Hydroxy-3,4-dihydrocadalin	STZ-induced diabetic rats and mice	—	0.3–30 and 30–300 mg/kg/day	Decreased mechanical hyperalgesia and allodynia and formalin-evoked hyperalgesia; increased withdrawal threshold; reduced level of MDA	[159]
Mulberry flavonoids	ALX-induced diabetic rats	8 weeks	0.3 and 0.1 g/kg/day	Reduced myelin breakdown and myelinated fiber cross-sectional area; decreased peripheral nerve injury and numbers of extramedullary fiber of sciatic nerves	[160]
Chromane	STZ-induced diabetic rats	30 days	5 and 10 mg/kg/day	Decreased mechanical allodynia and thermal hyperalgesia; increased paw withdrawal threshold and MNCV level; decreased levels of AGEs and ROS	[161]
Kaempferol	STZ-induced diabetic mice	3 weeks	25, 50, and 100 mg/kg/day	Decreased formalin-mediated nociceptive behavior in phases 1 and 2 and oedema size; reduced hyperalgesia; elevated thermal pain threshold; decreased levels of IL-1β, TNF-α, LPO, and nitrite	[162]
Oryzanol	STZ-induced diabetic rats	—	50 and 100 mg/kg/day	Increased pain threshold, hot-plate latency, and GSH; decreased flinching in diabetic rats during both quiescent phase and phase 2 but not in phase 1; reduced nitrite and MDA levels; attenuated activity of Na^+-K^+ ATPase	[163]
Pepino polyphenolic extract	STZ-induced diabetic mice	12 weeks	—	Decreased concentrations of IL-6, TNF-α, AGEs, and ROS; increased GSH and GPx levels; elevated fascicle with numerous small myelinated fibers	[164]
Quercetin	STZ-induced diabetic rats	2 weeks	40 mg/kg/day	Increased hot-plate, tail-withdrawal latency, and cold allodynia latency; reduced number of foot slips	[165]
	STZ-induced diabetic rats	8 weeks	10, 20, and 40 mg/kg/day	Reduced thermal hyperalgesia and mechanical allodynia; increased concentrations of MNCV, SOD, and GPx; decreased levels of TNF-α and IL-1β	[166]
	STZ-induced diabetic rats	4 weeks	10 mg/kg/day	Increased tail-flick latencies and nociceptive threshold in both diabetic and nondiabetic mice	[167]
	STZ-induced diabetic rats	4 weeks	10 mg/kg/day	Decreased thermal nociception; elevated tail withdrawal latencies and nociceptive threshold	[168]

Table 3: Continued.

Polyphenols	Animal models	Duration	Dosage	Effects	References
Resveratrol	STZ-induced diabetic rats	2 weeks	10 and 20 mg/kg/day	Increased tail-flick latency and paw withdrawal pressure; elevated concentrations of MNCV and CAT; reduced MDA level	[169]
	STZ-induced diabetic rats	2 weeks	10 and 20 mg/kg/day	Increased MNCV level; decreased concentrations of p65, MDA, NF-κB, IκB-α, TNF-α, IL-6, and COX-2	[170]
	STZ-induced diabetic rats	6 weeks	20 mg/kg/day	Decreased cerebral MDA and COX-2; increased cerebral level of IL-4 and GSH	[171]
	STZ-induced diabetic rats	>6 weeks	10 mg/kg/day	Decreased concentrations of MDA, XO, and NO; increased level of GSH in the cortex, hippocampus, brain stem, cerebellum, and spinal cord	[142]
	STZ-induced diabetic rats	2 weeks	20 mg/kg/day	Elevated tail withdrawal threshold and latencies	[172]
Silymarin	STZ-induced diabetic rats	8 weeks	100 and 200 mg/kg/day	Elevated tail-flick latency; decreased nociceptive scores in both phases of the formalin test	[173]
Morin	STZ-induced diabetic rats	3 weeks	15 and 30 mg/kg/day	Increased paw withdrawal and tail-flick latency; elevated NGF and IGF-1 in sciatic nerves; decreased levels of IL-1β, TNF-α, and LPO	[174]

8-OHdG: 8-hydroxy-2′-deoxyguanosine; AGEs: advanced glycation end products; ALX: alloxan; AR: aldose reductase; CAT: catalase; COX: cyclooxygenase; DNP: diabetic neuropathy; GABA: gamma-aminobutyric acid; GPx: glutathione peroxidase; GSH: glutathione; HbA1C: hemoglobin A1c; IGF-1: insulin-like growth factor; IL-10: interleukin-10; IL-1β: interleukin 1 beta; LPO: lipid peroxidation; MDA: malondialdehyde; MNCV: motor nerve conduction velocity; NGF: nerve growth factor; NO: nitric oxide; NOS: nitric oxide synthase; OS: oxidative stress; ROS: reactive oxygen species; SOD: superoxide dismutase; STZ: streptozotocin; TBARS: thiobarbituric acid reactive substances; TNF-α: tumor necrosis factor-α; XO: xanthine oxidase.

markedly reduced the atherogenic index, serum glucose level, and expression of cerebral COX-2 and MDA [171]. In a study, Deng et al. [147] revealed that carvacrol reduced STZ-mediated DN by reducing the level of NF-κB p65 subunit, TNF-α, caspase-3, and IL-1β [147]. Kaempferia (a polyphenol) decreased STZ-induced DN via reducing the levels of TNF-α and IL-1β and inhibiting the formalin-triggered nociceptive behavior (Figure 3). Moreover, it improved lipopolysaccharide-mediated inflammatory mediators (such as ROS, IL-1β, TNF-α, phagocytosis, prostaglandins, and NO) in microglial cells [162, 185].

4.3. Antinociceptive Activities. Hyperglycemia-induced ROS generation and lipid peroxidation in sciatic nerves decreased endoneurial blood flow and induced sciatic nerve dysfunctions in case of DN. Indeed, neuropathic pain is a common diabetes-associated complication that takes place due to the induction of the abnormal activity of the CNS or PNS, which further leads to central sensitization, alterations of primary afferent nerves, and sensory abnormalities. Various studies have already confirmed the efficacy of tramadol, dextromethorphan, lamotrigine, phenytoin, pregabalin, gabapentin, tricyclic antidepressants (TCAs), gamma-aminobutyric acid (GABA), and opioids in the treatment of painful sensory neuropathy. Even though these therapeutic agents may relieve the pain by 30 to 50%, their uses are often limited because of marked side effects [175]. Thus, there is an increased need of using polyphenols as alternative therapies. In a plantar heat hyperalgesia test, quercetin (Figure 2) significantly suppressed the increase of paw withdrawal threshold (PWT) in STZ-induced diabetic rat models which was assessed through Hargreaves' test. On a Randall–Selitto paw pressure device, quercetin also markedly elevated mechanical PWT as compared to STZ-induced diabetic control rats [141]. In addition to this, quercetin elevated the tail withdrawal latency in both nondiabetic and diabetic mouse models [167]. In a dose-dependent manner, it also has markedly elevated the paw and tail withdrawal latency and reduced the number of foot slips of STZ-induced diabetic rat models in comparison with the normal control [154, 165, 186].

As compared to the control group, Kaur et al. [161] revealed that chromane markedly corrected the reduced PWT of STZ-induced diabetic rat models in hot-plate and tail immersion tests [161]. In diabetic rat models, 6-methoxyflavanones and chlorogenic acid elevated mechanical and thermal PWT, respectively [157, 158]. In a different study, in STZ-induced diabetic rat models, Attia et al. [150] showed that combined administration of gabapentin and curcumin resulted in a marked rise in mechanical PWT along with tail-flick and hot-plate latencies. Interestingly, curcumin significantly elevated the pain threshold, reaction times, and tail-flick latencies [148]. As compared to untreated diabetic rat models, curcumin treatment increased the antinociceptive effect in hot-plate and allodynia tests in STZ-induced DN by elevating the pain threshold [149]. It has been reported that diosmin and oryzanol markedly elevated the tail-flick latency in the tail immersion test and decreased thermal hyperalgesia in STZ-induced diabetes

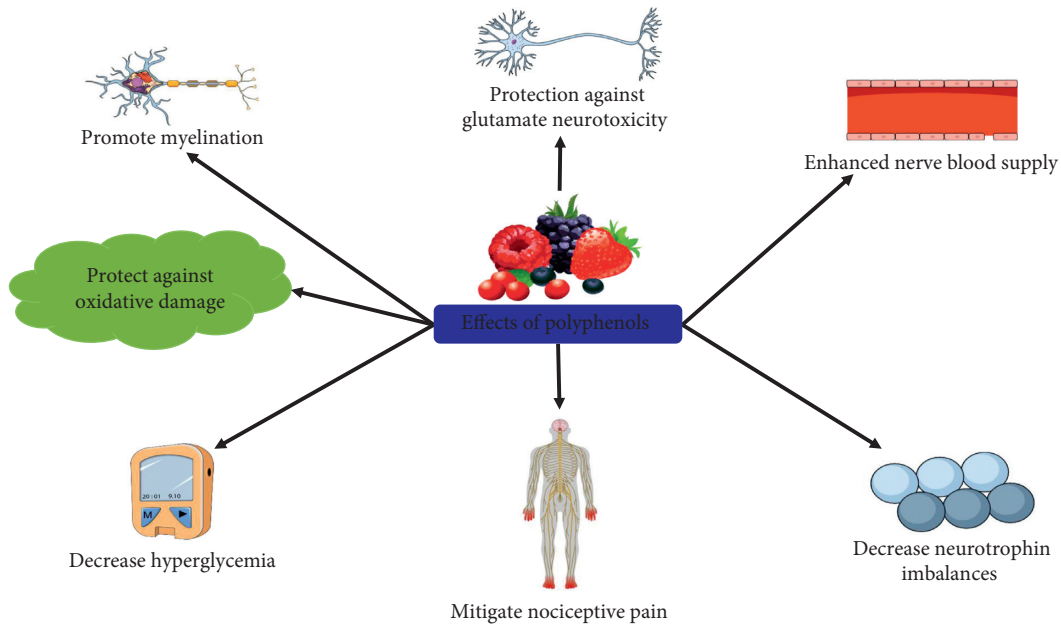

Figure 3: Possible effects of polyphenols in the management of diabetic neuropathy.

[163]. In diabetic rat models, treatment with diosmin also markedly ameliorated the shortening of time on walking function tests [144]. In a study, Kumar et al. [169] confirmed that resveratrol treatment significantly corrected the reduction of PWT and tail-flick latency in hot and cold immersion performance [169]. In addition, two polyphenols including 7-hydroxy-3,4-dihydrocadalin and silymarin resulted in a marked reduction of pain scores of the formalin test [159, 173].

4.4. Enhancement of Nerve Growth Factors. Multiple complex processes are associated with DN including various molecular changes and sensory modalities. In the nervous system, various neurotrophic factors (especially NGF) affect the population of certain neurons [118]. DN might be regulated via neurotrophins including transient receptor potential ion channels, such as vanilloid receptor 1 and NGF, including its receptors p75 and tyrosine kinase A (TrkA) and their downstream signaling pathways. NGF exerts significant neuroprotective activity, and it causes axonal growth. Indeed, pathological conditions that change NGF levels can induce neurons to lose their activity and die. Following nerve injury and inflammation, NGF level elevates in the nervous system and mediates pain and hyperalgesia that can be decreased via anti-NGF therapy. Interestingly, the complex of TrkA and NGF sensitizes VR1 thereby elevating pain. After the binding of NGF with TrkA, several processes including cell survival, nerve regeneration, and neurite growth pathways will start [187]. IGF-1 is structurally similar to insulin, and it has a significant contribution to cellular growth and proliferation. IGF-1 is also a potent apoptosis inhibitor. In addition, it regulates the development and growth of DNA synthesis and nerve cells [174]. In morin-treated diabetic animals, levels of IGF-1 and NGF in sciatic nerves significantly increased as compared to the negative control group [174].

In diabetic rat models, Methycobal and mulberry flavonoids lessened the inhibition of the average optical density of the myelin sheath and myelinated extramedullary fiber cross-sectional area. Interestingly, animals pretreated with 0.3 g/kg mulberry flavonoids exhibited ultrastructural properties of myelin, significantly decreased the level of myelin breakdown, and also caused significant axonal improvement [160]. In diabetic rat models, astragaloside IV (a polyphenol) inhibited a reduction in the myelinated fiber area and density and segmental demyelination via reducing the levels of AR and hemoglobin A1c (HbA1C) in erythrocytes, which further increased the plasma insulin concentrations and GPx function in nerves. In STZ-induced diabetic rat models, astragaloside IV increased Na^+/K^+-ATPase activity in both erythrocytes and nerves [152]. Treatment with grape seed proanthocyanidins ameliorated the abnormal activity of the peripheral nerve and impaired nerve tissues. It also decreased the level of nerve conduction velocity (NCV) and the level of free Ca^{2+}, which further increased the activity of Ca^{2+}-ATPase in sciatic nerves [155]. In diabetic rat models, curcumin treatment gradually recovered cyclooxygenase function in the sciatic nerve [149].

4.5. Glutamate Pathway and NMDA Receptors. In experimental DN models, glutamate receptors and ligands are supposed to be associated with nociceptive behaviors. Besides, it is regarded that glutamate and N-methyl-D-aspartate (NMDA) receptors are associated with peripheral sensory transduction and nociceptive pathways [188]. NMDA receptors also couple with mitogen-activated protein kinase (MAPK) and extracellular signal-regulated kinase (ERK) phosphorylation and activation in the superficial

laminae of the spinal cord that could be inhibited via treatment with NMDA receptor antagonists [83, 189, 190]. NMDA receptor ion channel-induced entry of calcium has a significant contribution to the activation of extracellular signal-regulated kinase (ERK) and MAPK pathways in painful DN [188]. It has been reported that resveratrol prevented glutamate injuries via blocking the NMDA receptor and inhibited glutamatergic neurotransmission [191, 192]. It also markedly reduced glutamine expression, transportation, synthetase to avert diabetic retinopathy [193]. Resveratrol also suppressed impairments in Na^+/K^+-ATPase, intracellular ROS generation, mitochondrial dysfunction, and activation of microglia [194, 195]. Furthermore, it decreased the level of glutamate-induced tissue plasminogen activator through ERK and AMPK/mammalian target of rapamycin signaling pathways and reduced the activation of MAPK, which eventually inhibited the activity of the voltage-dependent Ca^{2+} channel and suppressed induced release of glutamate [196, 197]. Like resveratrol, piceatannol stimulated the expression of nuclear factor erythroid 2-related factor 2-dependent and heme oxygenase-1 and thus protected HT22 neuronal cells from glutamate-mediated cell death [198].

Chlorogenic acid (a polyphenol) protected against glutamate neurotoxicity via its hydrolysate, caffeoyl acid group, and caffeic acid via controlling the entry of calcium into neurons [199, 200]. Epigallocatechin-3-gallate mediated protection of motor neurons which was found to be linked with the regulation of glutamate concentration [201]. Furthermore, it suppressed glutamate dehydrogenase in pancreatic β-cells and activated adenosine monophosphate-activated protein kinase to positively influence diabetes [202]. Like quercetin, epigallocatechin-3-gallate also decreased glutamate-mediated raised level of calcium via attenuating PKC and influx of ionotropic Ca^{2+} [203–205]. In diabetic rat models, curcumin prevented intracellular elevation of calcium [206], improved both NR2B gene expression and glutamate level [207, 208], and attenuated excitotoxicity mediated by the NMDA receptor [209]. It also influenced the PI3K/AKT signaling pathway and downstream signaling pathways via BDNF and Trkβ, perhaps via reducing the activation of MAPK/ERK [210, 211]. It was revealed that naringin, chlorogenic acid, and apigenin 8-C-glucoside control glutamate pathways [212, 213]. Kaempferol and astragaloside IV attenuated OS and glutamate-induced toxicity [214, 215]. Therefore, these polyphenols might be good options in preventing complications related to DN (Figure 2).

5. Future Research Directions

DN is one of the most distressing diabetes-associated complications that affects over 30% of diabetic people worldwide. In addition, there are increasing types of diabetes-mediated peripheral nerve damages including mononeuritis multiplex, mononeuropathy, radiculopathy, diabetic amyotrophy, and autonomic and small fiber neuropathy. DN pathogenesis is multifactorial, and its main categories include ischemic and metabolic. In the treatment of neuropathic pain, even though opioid therapy and neuromodulating drugs, including anticonvulsants and TCAs, are effective treatments, these treatments are expensive. Because of the lack of safe and consistently effective therapies for DN, there is an increased need to develop novel herbal therapies to ameliorate the quality of life of DN individuals [216]. Various findings suggested that polyphenols exert protective activities by anti-inflammatory and antioxidant pathways. Indeed, polyphenols have the potential to fight against various chronic diseases including diabetes and diabetes-associated complications with less toxic effects in *in vitro* and animal models [9, 10]. In nutrition, these aforementioned properties have made polyphenols a promising area of research interest [217, 218].

6. Conclusion

Polyphenols are potent natural compounds that can be useful to combat DN via influencing various signaling mechanisms with fewer side effects. It has been confirmed that herbal therapies with various polyphenols can exert a positive effect on DN management. Further research regarding novel pathogenicity signaling mechanisms of DN, safety, and efficacy of polyphenols in humans may reveal more effective applications of polyphenols in the management, prevention, and treatment of DN. Nonetheless, more studies are required to develop more effective therapeutic agents for DN.

Conflicts of Interest

The authors declare that they have no conflicts of interest.

Authors' Contributions

MSU conceived the original idea and designed the outlines of the study. MTK, NT, and MSU wrote the draft of the manuscript. MTK prepared the figures and tables of the manuscript. FA, TB, BM, MHR, RA, AR, and LA performed the literature review and aided in revising the manuscript. All the authors read and approved the final manuscript.

Acknowledgments

The authors are grateful to the Pharmakon Neuroscience Research Network, Dhaka, Bangladesh.

References

[1] V. Bril, "Treatments for diabetic neuropathy," *Journal of the Peripheral Nervous System*, vol. 17, no. 2, pp. 22–27, 2012.

[2] B. C. Callaghan, H. T. Cheng, C. L. Stables, A. L. Smith, and E. L. Feldman, "Diabetic neuropathy: clinical manifestations and current treatments," *The Lancet Neurology*, vol. 11, no. 6, pp. 521–534, 2012.

[3] S. Tesfaye and D. Selvarajah, "Advances in the epidemiology, pathogenesis and management of diabetic peripheral neuropathy," *Diabetes/Metabolism Research and Reviews*, vol. 28, no. 1, pp. 8–14, 2012.

[4] P. Thomas, "Classification, differential diagnosis, and staging of diabetic peripheral neuropathy," *Diabetes*, vol. 46, no. 2, pp. S54–S57, 1997.

[5] A. J. M. Boulton, A. I. Vinik, J. C. Arezzo et al., "Diabetic neuropathies: a statement by the American diabetes association," *Diabetes Care*, vol. 28, no. 4, pp. 956–962, 2005.

[6] S. Tesfaye, A. J. M. Boulton, P. J. Dyck et al., "Diabetic neuropathies: update on definitions, diagnostic criteria, estimation of severity, and treatments," *Diabetes Care*, vol. 33, no. 10, pp. 2285–2293, 2010.

[7] V. P. Singh, A. Bali, N. Singh, and A. S. Jaggi, "Advanced glycation end products and diabetic complications," *The Korean Journal of Physiology & Pharmacology*, vol. 18, no. 1, pp. 1–14, 2014.

[8] K. Hanhineva, R. Törrönen, I. Bondia-Pons et al., "Impact of dietary polyphenols on carbohydrate metabolism," *International Journal of Molecular Sciences*, vol. 11, no. 4, pp. 1365–1402, 2010.

[9] K. B. Pandey and S. I. Rizvi, "Plant polyphenols as dietary antioxidants in human health and disease," *Oxidative Medicine and Cellular Longevity*, vol. 2, no. 5, pp. 270–278, 2009.

[10] A. Scalbert, C. Manach, C. Morand, C. Rémésy, and L. Jiménez, "Dietary polyphenols and the prevention of diseases," *Critical Reviews in Food Science and Nutrition*, vol. 45, no. 4, pp. 287–306, 2005.

[11] G. Cásedas, F. Les, E. González-Burgos, M. P. Gómez-Serranillos, C. Smith, and V. López, "Cyanidin-3-O-glucoside inhibits different enzymes involved in central nervous system pathologies and type-2 diabetes," *South African Journal of Botany*, vol. 120, pp. 241–246, 2019.

[12] M. Vrethem, J. Boivie, H. Arnqvist, H. Holmgren, T. Lindström, and L.-H. Thorell, "A comparison of amitriptyline and maprotiline in the treatment of painful polyneuropathy in diabetics and nondiabetics," *The Clinical Journal of Pain*, vol. 13, no. 4, pp. 313–323, 1997.

[13] R. Biesbroeck, V. Bril, P. Hollander et al., "A double-blind comparison of topical capsaicin and oral amitriptyline in painful diabetic neuropathy," *Advances in Therapy*, vol. 12, no. 2, pp. 111–120, 1995.

[14] D. Bansal, A. Bhansali, D. Hota, A. Chakrabarti, and P. Dutta, "Amitriptyline vs. pregabalin in painful diabetic neuropathy: a randomized double blind clinical trial," *Diabetic Medicine*, vol. 26, no. 10, pp. 1019–1026, 2009.

[15] P. J. Wiffen, S. Derry, R. F. Bell et al., "Gabapentin for chronic neuropathic pain in adults," *Cochrane Database of Systematic Reviews*, vol. 2017, no. 6, Article ID CD007938, 2017.

[16] R. M. Duehmke, S. Derry, P. J. Wiffen, R. F. Bell, D. Aldington, and R. A. Moore, "Tramadol for neuropathic pain in adults," *Cochrane Database of Systematic Reviews*, vol. 2017, no. 6, Article ID CD003726, 2017.

[17] M. P. Lunn, R. A. Hughes, and P. J. Wiffen, "Duloxetine for treating painful neuropathy, chronic pain or fibromyalgia," *Cochrane Database of Systematic Reviews*, vol. 2014, no. 1, Article ID CD007115, 2014.

[18] S. Brunton, F. Wang, S. B. Edwards et al., "Profile of adverse events with duloxetine treatment," *Drug Safety*, vol. 33, no. 5, pp. 393–407, 2010.

[19] J. Gahimer, J. Wernicke, I. Yalcin, M. J. Ossanna, M. Wulster-Radcliffe, and L. Viktrup, "A retrospective pooled analysis of duloxetine safety in 23 983 subjects," *Current Medical Research and Opinion*, vol. 23, no. 1, pp. 175–184, 2007.

[20] H. C. Gallagher, R. M. Gallagher, M. Butler, D. J. Buggy, and M. C. Henman, "Venlafaxine for neuropathic pain in adults," *Cochrane Database of Systematic Reviews*, vol. 2015, no. 8, Article ID CD011091, 2015.

[21] R. Hurley, M. Lesley, M. Adams, C. Brummett, and C. Wu, "Pregabalin as a treatment for painful diabetic peripheral neuropathy: a meta-analysis," *Regional Anesthesia and Pain Medicine*, vol. 33, no. 5, pp. 389–394, 2008.

[22] S. Derry, R. F. Bell, S. Straube, P. J. Wiffen, D. Aldington, and R. A. Moore, "Pregabalin for neuropathic pain in adults," *Cochrane Database of Systematic Reviews*, vol. 2019, no. 1, 2019.

[23] A. I. Vinik, D. Y. Shapiro, C. Rauschkolb et al., "A randomized withdrawal, placebo-controlled study evaluating the efficacy and tolerability of tapentadol extended release in patients with chronic painful diabetic peripheral neuropathy," *Diabetes Care*, vol. 37, no. 8, pp. 2302–2309, 2014.

[24] M. Niesters, P. L. Proto, L. Aarts, E. Y. Sarton, A. M. Drewes, and A. Dahan, "Tapentadol potentiates descending pain inhibition in chronic pain patients with diabetic polyneuropathy," *British Journal of Anaesthesia*, vol. 113, no. 1, pp. 148–156, 2014.

[25] N. Vadivelu, B. Maslin, A. Kai, A. Legler, G. Kodumudi, and J. Berger, "Tapentadol extended release in the management of peripheral diabetic neuropathic pain," *Therapeutics and Clinical Risk Management*, vol. 11, pp. 95–105, 2015.

[26] N. Vadivelu, Y. Huang, B. Mirante et al., "Patient considerations in the use of tapentadol for moderate to severe pain," *Drug, Healthcare and Patient Safety*, vol. 5, pp. 151–159, 2013.

[27] G. Loureiro and F. Martel, "The effect of dietary polyphenols on intestinal absorption of glucose and fructose: relation with obesity and type 2 diabetes," *Food Reviews International*, vol. 35, no. 4, pp. 390–406, 2019.

[28] J. Xiao, X. Ni, G. Kai, and X. Chen, "A review on structure-activity relationship of dietary polyphenols inhibiting α-amylase," *Critical Reviews in Food Science and Nutrition*, vol. 53, no. 5, pp. 497–506, 2013.

[29] V. Gowd, N. Karim, M. R. I. Shishir, L. Xie, and W. Chen, "Dietary polyphenols to combat the metabolic diseases via altering gut microbiota," *Trends in Food Science & Technology*, vol. 93, pp. 81–93, 2019.

[30] Y. Xie and X. Chen, "Structures required of polyphenols for inhibiting advanced glycation end products formation," *Current Drug Metabolism*, vol. 14, no. 4, pp. 414–431, 2013.

[31] J. Xiao, G. Kai, K. Yamamoto, and X. Chen, "Advance in dietary polyphenols as α-glucosidases inhibitors: a review on structure-activity relationship aspect," *Critical Reviews in Food Science and Nutrition*, vol. 53, no. 8, pp. 818–836, 2013.

[32] F. Thielecke and M. Boschmann, "The potential role of green tea catechins in the prevention of the metabolic syndrome–a review," *Phytochemistry*, vol. 70, no. 1, pp. 11–24, 2009.

[33] R. Park, S.-Y. Kook, J.-C. Park, and I. Mook-Jung, "Aβ1-42 reduces P-glycoprotein in the blood-brain barrier through RAGE-NF-κB signaling," *Cell Death & Disease*, vol. 5, no. 6, p. e1299, 2014.

[34] Y. Kobayashi, M. Suzuki, H. Satsu et al., "Green tea polyphenols inhibit the sodium-dependent glucose transporter of intestinal epithelial cells by a competitive mechanism," *Journal of Agricultural and Food Chemistry*, vol. 48, no. 11, pp. 5618–5623, 2000.

[35] T. Matsui, T. Tanaka, S. Tamura et al., "α-Glucosidase inhibitory profile of catechins and theaflavins," *Journal of*

Agricultural and Food Chemistry, vol. 55, no. 1, pp. 99–105, 2007.

[36] M. Shimizu, Y. Kobayashi, M. Suzuki, H. Satsu, and Y. Miyamoto, "Regulation of intestinal glucose transport by tea catechins," *BioFactors*, vol. 13, no. 1–4, pp. 61–65, 2000.

[37] G. Solinas and B. Becattini, "JNK at the crossroad of obesity, insulin resistance, and cell stress response," *Molecular Metabolism*, vol. 6, no. 2, pp. 174–184, 2017.

[38] F. Li, C. Gao, P. Yan et al., "EGCG reduces obesity and white adipose tissue gain partly through AMPK activation in mice," *Frontiers in Pharmacology*, vol. 9, p. 1366, 2018.

[39] Y. Narita and K. Inouye, "Kinetic analysis and mechanism on the inhibition of chlorogenic acid and its components against porcine pancreas α-amylase isozymes I and II," *Journal of Agricultural and Food Chemistry*, vol. 57, no. 19, pp. 9218–9225, 2009.

[40] M. Nurul Islam, H. A. Jung, H. S. Sohn, H. M. Kim, and J. S. Choi, "Potent α-glucosidase and protein tyrosine phosphatase 1B inhibitors from *Artemisia capillaris*," *Archives of Pharmacal Research*, vol. 36, no. 5, pp. 542–552, 2013.

[41] W. J. Arion, W. K. Canfield, F. C. Ramos et al., "Chlorogenic acid and hydroxynitrobenzaldehyde: new inhibitors of hepatic glucose 6-phosphatase," *Archives of Biochemistry and Biophysics*, vol. 339, no. 2, pp. 315–322, 1997.

[42] C. Henry-Vitrac, A. Ibarra, M. Roller, J.-M. Mérillon, and X. Vitrac, "Contribution of chlorogenic acids to the inhibition of human hepatic glucose-6-phosphatase activity in vitro by svetol, a standardized decaffeinated green coffee extract," *Journal of Agricultural and Food Chemistry*, vol. 58, no. 7, pp. 4141–4144, 2010.

[43] C. E. G. Reis, J. G. Dórea, and T. H. M. da Costa, "Effects of coffee consumption on glucose metabolism: a systematic review of clinical trials," *Journal of Traditional and Complementary Medicine*, vol. 9, no. 3, pp. 184–191, 2019.

[44] M. Jin, M.-H. Shen, M.-H. Jin, A.-H. Jin, X.-Z. Yin, and J.-S. Quan, "Hypoglycemic property of soy isoflavones from hypocotyl in Goto-Kakizaki diabetic rats," *Journal of Clinical Biochemistry and Nutrition*, vol. 62, no. 2, pp. 148–154, 2018.

[45] C. L. Liu, L. Yan, K. R. Cai et al., "Effects of soybean isoflavones on Wnt/β-catenin and the TGF-β1 signaling pathway in renal tissue of type 2 diabetic rats," *Journal of Biological Regulators and Homeostatic Agents*, vol. 32, no. 3, pp. 455–464, 2018.

[46] X. Chen, J. Yu, and J. Shi, "Management of diabetes mellitus with puerarin, a natural isoflavone from *Pueraria lobata*," *The American Journal of Chinese Medicine*, vol. 46, no. 8, pp. 1771–1789, 2018.

[47] R. B. Kasetti, S. A. Nabi, S. Swapna, and C. Apparao, "Cinnamic acid as one of the antidiabetic active principle(s) from the seeds of *Syzygium alternifolium*," *Food and Chemical Toxicology*, vol. 50, no. 5, pp. 1425–1431, 2012.

[48] V. Cherezov, D. M. Rosenbaum, M. A. Hanson et al., "High-resolution crystal structure of an engineered human 2-adrenergic G protein-coupled receptor," *Science*, vol. 318, no. 5854, pp. 1258–1265, 2007.

[49] M. J. Son, C. W. Rico, S. H. Nam, and M. Y. Kang, "Effect of oryzanol and ferulic acid on the glucose metabolism of mice fed with a high-fat diet," *Journal of Food Science*, vol. 76, no. 1, pp. H7–H10, 2011.

[50] K. Pei, J. Ou, J. Huang, and S. Ou, "p-Coumaric acid and its conjugates: dietary sources, pharmacokinetic properties and biological activities," *Journal of the Science of Food and Agriculture*, vol. 96, no. 9, pp. 2952–2962, 2016.

[51] M. Bahmanzadeh, M. T. Goodarzi, A. Rezaei Farimani, N. Fathi, and Z. Alizadeh, "Resveratrol supplementation improves DNA integrity and sperm parameters in streptozotocin-nicotinamide-induced type 2 diabetic rats," *Andrologia*, vol. 51, no. 8, p. e13313, 2019.

[52] A. Rašković, V. Ćućuz, L. Torović et al., "Resveratrol supplementation improves metabolic control in rats with induced hyperlipidemia and type 2 diabetes," *Saudi Pharmaceutical Journal*, vol. 27, no. 7, pp. 1036–1043, 2019.

[53] G. Sadi, M. B. Pektaş, H. B. Koca, M. Tosun, and T. Koca, "Resveratrol improves hepatic insulin signaling and reduces the inflammatory response in streptozotocin-induced diabetes," *Gene*, vol. 570, no. 2, pp. 213–220, 2015.

[54] C. Zhao, C. Yang, S. T. C. Wai et al., "Regulation of glucose metabolism by bioactive phytochemicals for the management of type 2 diabetes mellitus," *Critical Reviews in Food Science and Nutrition*, vol. 59, no. 6, pp. 830–847, 2019.

[55] E. Bhakkiyalakshmi, D. Shalini, T. V. Sekar, P. Rajaguru, R. Paulmurugan, and K. M. Ramkumar, "Therapeutic potential of pterostilbene against pancreatic beta-cell apoptosis mediated through Nrf2," *British Journal of Pharmacology*, vol. 171, no. 7, pp. 1747–1757, 2014.

[56] E.-S. M. El-Sayed, A. M. Mansour, and M. E. Nady, "Protective effects of pterostilbene against acetaminophen-induced hepatotoxicity in rats," *Journal of Biochemical and Molecular Toxicology*, vol. 29, no. 1, pp. 35–42, 2015.

[57] F. Yan, X. Sun, and C. Xu, "Protective effects of resveratrol improve cardiovascular function in rats with diabetes," *Experimental and Therapeutic Medicine*, vol. 15, no. 2, pp. 1728–1734, 2018.

[58] H. Hosoyama, A. Sugimoto, Y. Suzuki, I. Sakane, and T. Kakuda, "Isolation and quantitative analysis of the α-amylase inhibitor in *Lagerstroemia speciosa* (L.) pers. (Banaba)," *Yakugaku Zasshi*, vol. 123, no. 7, pp. 599–605, 2003.

[59] T. F. d. Miranda Pedroso, T. R. Bonamigo, J. da Silva et al., "Chemical constituents of *Cochlospermum regium* (Schrank) Pilg. root and its antioxidant, antidiabetic, antiglycation, and anticholinesterase effects in Wistar rats," *Biomedicine & Pharmacotherapy*, vol. 111, pp. 1383–1392, 2019.

[60] K. Ogura, M. Ogura, T. Shoji et al., "Oral administration of apple procyanidins ameliorates insulin resistance via suppression of pro-inflammatory cytokine expression in liver of diabetic ob/ob mice," *Journal of Agricultural and Food Chemistry*, vol. 64, no. 46, pp. 8857–8865, 2016.

[61] Y. Yamashita, L. Wang, F. Nanba, C. Ito, T. Toda, and H. Ashida, "Procyanidin promotes translocation of glucose transporter 4 in muscle of mice through activation of insulin and AMPK signaling pathways," *PLoS One*, vol. 11, no. 9, Article ID e0161704, 2016.

[62] G. Aragonès, M. Suárez, A. Ardid-Ruiz et al., "Dietary proanthocyanidins boost hepatic NAD+ metabolism and SIRT1 expression and activity in a dose-dependent manner in healthy rats," *Scientific Reports*, vol. 6, no. 1, 2016.

[63] A. A. Vazquez-Flores, A. I. Martinez-Gonzalez, E. Alvarez-Parrilla et al., "Proanthocyanidins with a low degree of polymerization are good inhibitors of digestive enzymes because of their ability to form specific interactions: a hypothesis," *Journal of Food Science*, vol. 83, no. 12, pp. 2895–2902, 2018.

[64] W. Zhu, Q. Jia, Y. Wang, Y. Zhang, and M. Xia, "The anthocyanin cyanidin-3-O-β-glucoside, a flavonoid, increases hepatic glutathione synthesis and protects hepatocytes

against reactive oxygen species during hyperglycemia: involvement of a cAMP-PKA-dependent signaling pathway," *Free Radical Biology and Medicine*, vol. 52, no. 2, pp. 314–327, 2012.

[65] M. Roy, S. Sen, and A. S. Chakraborti, "Action of pelargonidin on hyperglycemia and oxidative damage in diabetic rats: implication for glycation-induced hemoglobin modification," *Life Sciences*, vol. 82, no. 21-22, pp. 1102–1110, 2008.

[66] T. Tsuda, F. Horio, and T. Osawa, "Absorption and metabolism of cyanidin 3-O-β-D-glucoside in rats," *FEBS Letters*, vol. 449, no. 2-3, pp. 179–182, 1999.

[67] M. Shi, H. Loftus, A. J. McAinch, and X. Q. Su, "Blueberry as a source of bioactive compounds for the treatment of obesity, type 2 diabetes and chronic inflammation," *Journal of Functional Foods*, vol. 30, pp. 16–29, 2017.

[68] F. Pivari, A. Mingione, C. Brasacchio, and L. Soldati, "Curcumin and type 2 diabetes mellitus: prevention and treatment," *Nutrients*, vol. 11, no. 8, p. 1837, 2019.

[69] K. Rashid, S. Chowdhury, S. Ghosh, and P. C. Sil, "Curcumin attenuates oxidative stress induced NFκB mediated inflammation and endoplasmic reticulum dependent apoptosis of splenocytes in diabetes," *Biochemical Pharmacology*, vol. 143, pp. 140–155, 2017.

[70] W. Zha, Y. Bai, L. Xu et al., "Curcumin attenuates testicular injury in rats with streptozotocin-induced diabetes," *BioMed Research International*, vol. 2018, Article ID 7468019, 10 pages, 2018.

[71] R. A. Kowluru, R. L. Engerman, and T. S. Kern, "Abnormalities of retinal metabolism in diabetes or experimental galactosemia. VI. Comparison of retinal and cerebral cortex metabolism, and effects of antioxidant therapy," *Free Radical Biology and Medicine*, vol. 26, no. 3-4, pp. 371–378, 1999.

[72] J. Zenker, D. Ziegler, and R. Chrast, "Novel pathogenic pathways in diabetic neuropathy," *Trends in Neurosciences*, vol. 36, no. 8, pp. 439–449, 2013.

[73] S. Dewanjee, S. Das, A. K. Das et al., "Molecular mechanism of diabetic neuropathy and its pharmacotherapeutic targets," *European Journal of Pharmacology*, vol. 833, pp. 472–523, 2018.

[74] M. Brownlee, "Biochemistry and molecular cell biology of diabetic complications," *Nature*, vol. 414, no. 6865, pp. 813–820, 2001.

[75] N. Bhattacharjee, S. Barma, N. Konwar, S. Dewanjee, and P. Manna, "Mechanistic insight of diabetic nephropathy and its pharmacotherapeutic targets: an update," *European Journal of Pharmacology*, vol. 791, pp. 8–24, 2016.

[76] E. H. Bayram, A. D. Sezer, and H. K. Elçioglu, "Diabetic neuropathy and treatment strategy—new challenges and applications," in *Smart Drug Delivery System*, A. D. Sezer, Ed., IntechOpen, London, UK, 2016.

[77] N. C. Danbolt, "Glutamate uptake," *Progress in Neurobiology*, vol. 65, no. 1, pp. 1–105, 2001.

[78] A. Rustioni, "Modulation of sensory input to the spinal cord by presynaptic ionotropic glutamate receptors," *Archives italiennes de biologie*, vol. 143, no. 2, pp. 103–112, 2005.

[79] B. A. Chizh, "Novel approaches to targeting glutamate receptors for the treatment of chronic pain: review article," *Amino Acids*, vol. 23, no. 1–3, pp. 169–176, 2002.

[80] H. Roshanravan, E. Y. Kim, and S. E. Dryer, "NMDA receptors as potential therapeutic targets in diabetic nephropathy: increased renal NMDA receptor subunit expression in akita mice and reduced nephropathy following sustained treatment with memantine or MK-801," *Diabetes*, vol. 65, no. 10, pp. 3139–3150, 2016.

[81] D.-H. Roh, H.-W. Kim, S.-Y. Yoon et al., "Depletion of capsaicin sensitive afferents prevents lamina-dependent increases in spinal N-methyl-d-aspartate receptor subunit 1 expression and phosphorylation associated with thermal hyperalgesia in neuropathic rats," *European Journal of Pain*, vol. 12, no. 5, pp. 552–563, 2008.

[82] H.-P. Bai, P. Liu, Y.-M. Wu, W.-Y. Guo, Y.-X. Guo, and X.-L. Wang, "Activation of spinal GABAB receptors normalizes N-methyl-D-aspartate receptor in diabetic neuropathy," *Journal of the Neurological Sciences*, vol. 341, no. 1-2, pp. 68–72, 2014.

[83] S. Fakhri, F. Abbaszadeh, L. Dargahi, and M. Jorjani, "Astaxanthin: a mechanistic review on its biological activities and health benefits," *Pharmacological Research*, vol. 136, pp. 1–20, 2018.

[84] R. M. Pabbidi, S.-Q. Yu, S. Peng, R. Khardori, M. E. Pauza, and L. S. Premkumar, "Influence of TRPV1 on diabetes-induced alterations in thermal pain sensitivity," *Molecular Pain*, vol. 4, pp. 1744–8069, 2008.

[85] E. V. Khomula, V. Y. Viatchenko-Karpinski, A. L. Borisyuk, D. E. Duzhyy, P. V. Belan, and N. V. Voitenko, "Specific functioning of Cav3.2 T-type calcium and TRPV1 channels under different types of STZ-diabetic neuropathy," *Biochimica et Biophysica Acta (BBA)—Molecular Basis of Disease*, vol. 1832, no. 5, pp. 636–649, 2013.

[86] M. R. Pabbidi and L. S. Premkumar, "Role of transient receptor potential channels Trpv1 and Trpm8 in diabetic peripheral neuropathy," *Journal of Diabetes and Treatment*, vol. 2017, no. 4, p. 29, 2017.

[87] L. S. Premkumar and M. Abooj, "TRP channels and analgesia," *Life Sciences*, vol. 92, no. 8-9, pp. 415–424, 2013.

[88] P. Fernyhough and N. A. Calcutt, "Abnormal calcium homeostasis in peripheral neuropathies," *Cell Calcium*, vol. 47, no. 2, pp. 130–139, 2010.

[89] A. C. Dolphin, "Calcium channel auxiliary $\alpha 2\delta$ and β subunits: trafficking and one step beyond," *Nature Reviews Neuroscience*, vol. 13, no. 8, pp. 542–555, 2012.

[90] M. J. Craner, J. P. Klein, M. Renganathan, J. A. Black, and S. G. Waxman, "Changes of sodium channel expression in experimental painful diabetic neuropathy," *Annals of Neurology*, vol. 52, no. 6, pp. 786–792, 2002.

[91] A. Bierhaus, T. Fleming, S. Stoyanov et al., "Methylglyoxal modification of Nav1.8 facilitates nociceptive neuron firing and causes hyperalgesia in diabetic neuropathy," *Nature Medicine*, vol. 18, no. 6, pp. 926–933, 2012.

[92] S. Carlton, "Peripheral excitatory amino acids," *Current Opinion in Pharmacology*, vol. 1, no. 1, pp. 52–56, 2001.

[93] S. Yagihashi, H. Mizukami, and K. Sugimoto, "Mechanism of diabetic neuropathy: where are we now and where to go?" *Journal of Diabetes Investigation*, vol. 2, no. 1, pp. 18–32, 2011.

[94] R. Ramasamy and I. J. Goldberg, "Aldose reductase and cardiovascular diseases, creating human-like diabetic complications in an experimental model," *Circulation Research*, vol. 106, no. 9, pp. 1449–1458, 2010.

[95] D. R. Tomlinson and N. J. Gardiner, "Glucose neurotoxicity," *Nature Reviews Neuroscience*, vol. 9, no. 1, pp. 36–45, 2008.

[96] D. W. Zochodne, "Diabetes mellitus and the peripheral nervous system: manifestations and mechanisms," *Muscle & Nerve*, vol. 36, no. 2, pp. 144–166, 2007.

[97] X.-L. Du, D. Edelstein, L. Rossetti et al., "Hyperglycemia-induced mitochondrial superoxide overproduction activates the hexosamine pathway and induces plasminogen activator inhibitor-1 expression by increasing Sp1 glycosylation," *Proceedings of the National Academy of Sciences*, vol. 97, no. 22, pp. 12222–12226, 2000.

[98] P. Oates, "Aldose reductase, still a compelling target for diabetic neuropathy," *Current Drug Targets*, vol. 9, no. 1, pp. 14–36, 2008.

[99] N. Hotta, R. Kawamori, M. Fukuda, and Y. Shigeta, "Long-term clinical effects of epalrestat, an aldose reductase inhibitor, on progression of diabetic neuropathy and other microvascular complications: multivariate epidemiological analysis based on patient background factors and severity of diabetic neuropathy," *Diabetic Medicine*, vol. 29, no. 12, pp. 1529–1533, 2012.

[100] M. S. Uddin and A. B. Upaganlawar, *Oxidative Stress and Antioxidant Defense: Biomedical Value in Health and Diseases*, Nova Science Publishers, Hauppauge, NY, USA, 2019.

[101] A. Vinik, J. Ullal, H. K. Parson, and C. M. Casellini, "Diabetic neuropathies: clinical manifestations and current treatment options," *Nature Clinical Practice Endocrinology & Metabolism*, vol. 2, no. 5, pp. 269–281, 2006.

[102] J. F. Edwards, C. M. Casellini, H. K. Parson, I. G. Obrosova, M. Yorek, and A. I. Vinik, "Role of peroxynitrite in the development of diabetic peripheral neuropathy," *Diabetes Care*, vol. 38, no. 7, pp. e100–e101, 2015.

[103] N. E. Cameron, T. M. Gibson, M. R. Nangle, and M. A. Cotter, "Inhibitors of advanced glycation end product formation and neurovascular dysfunction in experimental diabetes," *Annals of the New York Academy of Sciences*, vol. 1043, no. 1, pp. 784–792, 2005.

[104] S. Y. Rhee and Y. S. Kim, "The role of advanced glycation end products in diabetic vascular complications," *Diabetes & Metabolism Journal*, vol. 42, no. 3, pp. 188–195, 2018.

[105] P. S. Van Dam, M. A. Cotter, B. Bravenboer, and N. E. Cameron, "Pathogenesis of diabetic neuropathy: focus on neurovascular mechanisms," *European Journal of Pharmacology*, vol. 719, no. 1–3, pp. 180–186, 2013.

[106] I. G. Obrosova, R. Stavniichuk, V. R. Drel et al., "Different roles of 12/15-lipoxygenase in diabetic large and small fiber peripheral and autonomic neuropathies," *The American Journal of Pathology*, vol. 177, no. 3, pp. 1436–1447, 2010.

[107] J. Eichberg, "Protein kinase C changes in diabetes: is the concept relevant to neuropathy?" *International Review of Neurobiology*, vol. 50, pp. 61–82, 2002.

[108] P. Geraldes and G. L. King, "Activation of protein kinase C isoforms and its impact on diabetic complications," *Circulation Research*, vol. 106, no. 8, pp. 1319–1331, 2010.

[109] T. Sasase, H. Yamada, K. Sakoda et al., "Novel protein kinase C-β isoform selective inhibitor JTT-010 ameliorates both hyper- and hypoalgesia in streptozotocin- induced diabetic rats," *Diabetes, Obesity and Metabolism*, vol. 7, no. 5, pp. 586–594, 2005.

[110] J. L. Edwards, A. Quattrini, S. I. Lentz et al., "Diabetes regulates mitochondrial biogenesis and fission in mouse neurons," *Diabetologia*, vol. 53, no. 1, pp. 160–169, 2010.

[111] A. M. Vincent, L. L. Mclean, C. Backus, and E. L. Feldman, "Short-term hyperglycemia produces oxidative damage and apoptosis in neurons," *The FASEB Journal*, vol. 19, no. 6, pp. 1–24, 2005.

[112] E. Zherebitskaya, E. Akude, D. R. Smith, and P. Fernyhough, "Development of selective axonopathy in adult sensory neurons isolated from diabetic rats: role of glucose-induced oxidative stress," *Diabetes*, vol. 58, no. 6, pp. 1356–1364, 2009.

[113] J. Doupis, T. E. Lyons, S. Wu, C. Gnardellis, T. Dinh, and A. Veves, "Microvascular reactivity and inflammatory cytokines in painful and painless peripheral diabetic neuropathy," *The Journal of Clinical Endocrinology & Metabolism*, vol. 94, no. 6, pp. 2157–2163, 2009.

[114] G. Conti, E. Scarpini, P. Baron et al., "Macrophage infiltration and death in the nerve during the early phases of experimental diabetic neuropathy: a process concomitant with endoneurial induction of IL-1β and p75NTR," *Journal of the Neurological Sciences*, vol. 195, no. 1, pp. 35–40, 2002.

[115] S. I. Yamagishi, S. Ogasawara, H. Mizukami et al., "Correction of protein kinase C activity and macrophage migration in peripheral nerve by pioglitazone, peroxisome proliferator activated-γ- ligand, in insulin-deficient diabetic rats," *Journal of Neurochemistry*, vol. 104, no. 2, pp. 491–499, 2008.

[116] B. Andorfer, B. C. Kieseier, E. Mathey et al., "Expression and distribution of transcription factor NF-κB and inhibitor IκB in the inflamed peripheral nervous system," *Journal of Neuroimmunology*, vol. 116, no. 2, pp. 226–232, 2001.

[117] H. C. Ha, L. D. Hester, and S. H. Snyder, "Poly(ADP-ribose) polymerase-1 dependence of stress-induced transcription factors and associated gene expression in glia," *Proceedings of the National Academy of Sciences*, vol. 99, no. 5, pp. 3270–3275, 2002.

[118] A. Bierhaus, K.-M. Haslbeck, P. M. Humpert et al., "Loss of pain perception in diabetes is dependent on a receptor of the immunoglobulin superfamily," *Journal of Clinical Investigation*, vol. 114, no. 12, pp. 1741–1751, 2004.

[119] S. C. Apfel, "Neurotrophic factors in the therapy of diabetic neuropathy," *The American Journal of Medicine*, vol. 107, no. 2, pp. 34–42, 1999.

[120] J.-O. Jeong, M.-O. Kim, H. Kim et al., "Dual angiogenic and neurotrophic effects of bone marrow-derived endothelial progenitor cells on diabetic neuropathy," *Circulation*, vol. 119, no. 5, pp. 699–708, 2009.

[121] S. Tyagi, S. Sharma, P. Gupta, A. Saini, and C. Kaushal, "The peroxisome proliferator-activated receptor: a family of nuclear receptors role in various diseases," *Journal of Advanced Pharmaceutical Technology & Research*, vol. 2, no. 4, pp. 236–240, 2011.

[122] L. Michalik and W. Wahli, "Involvement of PPAR nuclear receptors in tissue injury and wound repair," *Journal of Clinical Investigation*, vol. 116, no. 3, pp. 598–606, 2006.

[123] M. S. Uddin, M. T. Kabir, M. Jakaria et al., "Endothelial PPARγ is crucial for averting age-related vascular dysfunction by stalling oxidative stress and ROCK," *Neurotoxicity Research*, vol. 36, no. 3, pp. 583–601, 2019.

[124] C. Janani and B. D. Ranjitha Kumari, "PPAR gamma gene—a review," *Diabetes & Metabolic Syndrome: Clinical Research & Reviews*, vol. 9, no. 1, pp. 46–50, 2015.

[125] A. C. P. Oliveira, C. M. Bertollo, L. T. S. Rocha, E. B. Nascimento, K. A. Costa, and M. M. Coelho, "Antinociceptive and antiedematogenic activities of fenofibrate, an agonist of PPAR alpha, and pioglitazone, an agonist of PPAR gamma," *European Journal of Pharmacology*, vol. 561, no. 1–3, pp. 194–201, 2007.

[126] C. M. Freitag and R. J. Miller, "Peroxisome proliferator-activated receptor agonists modulate neuropathic pain: a link to chemokines?" *Frontiers in Cellular Neuroscience*, vol. 8, p. 238, 2014.

[127] A. D. Mooradian, J. Chehade, and J. E. Thurman, "The role of thiazolidinediones in the treatment of patients with type 2 diabetes mellitus," *Treatments in Endocrinology*, vol. 1, no. 1, pp. 13–20, 2002.

[128] R. B. Griggs, R. R. Donahue, B. G. Adkins, K. L. Anderson, O. Thibault, and B. K. Taylor, "Pioglitazone inhibits the development of hyperalgesia and sensitization of spinal nociresponsive neurons in type 2 diabetes," *The Journal of Pain*, vol. 17, no. 3, pp. 359–373, 2016.

[129] B. N. Okine, J. C. Gaspar, and D. P. Finn, "PPARs and pain," *British Journal of Pharmacology*, vol. 176, no. 10, pp. 1421–1442, 2019.

[130] B. S. Galer, A. Gianas, and M. P. Jensen, "Painful diabetic polyneuropathy: epidemiology, pain description, and quality of life," *Diabetes Research and Clinical Practice*, vol. 47, no. 2, pp. 123–128, 2000.

[131] A. C. Themistocleous, J. D. Ramirez, P. R. Shillo et al., "The Pain in Neuropathy Study (PiNS): a cross-sectional observational study determining the somatosensory phenotype of painful and painless diabetic neuropathy," *Pain*, vol. 157, no. 5, pp. 1132–1145, 2016.

[132] J. Raputova, I. Srotova, E. Vlckova et al., "Sensory phenotype and risk factors for painful diabetic neuropathy: a cross-sectional observational study," *Pain*, vol. 158, no. 12, pp. 2340–2353, 2017.

[133] P. A. Low, K. K. Nickander, and H. J. Tritschler, "The roles of oxidative stress and antioxidant treatment in experimental diabetic neuropathy," *Diabetes*, vol. 46, no. 2, pp. S38–S42, 1997.

[134] F. J. Romero, "Antioxidants in peripheral nerve," *Free Radical Biology and Medicine*, vol. 20, no. 7, pp. 925–932, 1996.

[135] D. K. Sahoo, A. Roy, and G. B. N. Chainy, "Protective effects of vitamin E and curcumin on l-thyroxine-induced rat testicular oxidative stress," *Chemico-Biological Interactions*, vol. 176, no. 2-3, pp. 121–128, 2008.

[136] L. Packer, E. H. Witt, and H. J. Tritschler, "Alpha-lipoic acid as a biological antioxidant," *Free Radical Biology and Medicine*, vol. 19, no. 2, pp. 227–250, 1995.

[137] D. Ziegler, M. Hanefeld, K. J. Ruhnau et al., "Treatment of symptomatic diabetic polyneuropathy with the antioxidant alpha-lipoic acid: a 7-month multicenter randomized controlled trial (ALADIN III Study). ALADIN III study group. Alpha-lipoic acid in diabetic neuropathy," *Diabetes Care*, vol. 22, no. 8, pp. 1296–1301, 1999.

[138] M. Nagamatsu, K. K. Nickander, J. D. Schmelzer et al., "Lipoic acid improves nerve blood flow, reduces oxidative stress, and improves distal nerve conduction in experimental diabetic neuropathy," *Diabetes Care*, vol. 18, no. 8, pp. 1160–1167, 1995.

[139] N. E. Cameron, M. A. Cotter, V. Archibald, K. C. Dines, and E. K. Maxfield, "Anti-oxidant and pro-oxidant effects on nerve conduction velocity, endoneurial blood flow and oxygen tension in non-diabetic and streptozotocin-diabetic rats," *Diabetologia*, vol. 37, no. 5, pp. 449–459, 1994.

[140] S. S. Al-Rejaie, A. M. Aleisa, H. M. Abuohashish et al., "Naringenin neutralises oxidative stress and nerve growth factor discrepancy in experimental diabetic neuropathy," *Neurological Research*, vol. 37, no. 10, pp. 924–933, 2015.

[141] A. D. Kandhare, K. S. Raygude, P. Ghosh, A. E. Ghule, and S. L. Bodhankar, "Neuroprotective effect of naringin by modulation of endogenous biomarkers in streptozotocin induced painful diabetic neuropathy," *Fitoterapia*, vol. 83, no. 4, pp. 650–659, 2012.

[142] O. Ates, S. R. Cayli, N. Yucel et al., "Central nervous system protection by resveratrol in streptozotocin-induced diabetic rats," *Journal of Clinical Neuroscience*, vol. 14, no. 3, pp. 256–260, 2007.

[143] W.-C. Zhao, B. Zhang, M.-J. Liao et al., "Curcumin ameliorated diabetic neuropathy partially by inhibition of NADPH oxidase mediating oxidative stress in the spinal cord," *Neuroscience Letters*, vol. 560, pp. 81–85, 2014.

[144] D. Jain, M. K. Bansal, R. Dalvi, A. Upganlawar, and R. Somani, "Protective effect of diosmin against diabetic neuropathy in experimental rats," *Journal of Integrative Medicine*, vol. 12, no. 1, pp. 35–41, 2014.

[145] G. Ristagno, F. Fumagalli, C. Porretta-Serapiglia et al., "Hydroxytyrosol attenuates peripheral neuropathy in streptozotocin-induced diabetes in rats," *Journal of Agricultural and Food Chemistry*, vol. 60, no. 23, pp. 5859–5865, 2012.

[146] O. R. Ayepola, M. E. Cerf, N. L. Brooks, and O. O. Oguntibeju, "Kolaviron, a biflavonoid complex of Garcinia kola seeds modulates apoptosis by suppressing oxidative stress and inflammation in diabetes-induced nephrotoxic rats," *Phytomedicine*, vol. 21, no. 14, pp. 1785–1793, 2014.

[147] W. Deng, H. Lu, and J. Teng, "Carvacrol attenuates diabetes-associated cognitive deficits in rats," *Journal of Molecular Neuroscience*, vol. 51, no. 3, pp. 813–819, 2013.

[148] E. S. H. Abd Allah and A. M. S. Gomaa, "Effects of curcumin and captopril on the functions of kidney and nerve in streptozotocin-induced diabetic rats: role of angiotensin converting enzyme 1," *Applied Physiology, Nutrition, and Metabolism*, vol. 40, no. 10, pp. 1061–1067, 2015.

[149] B. Nagilla and K. P. Reddy, "Neuroprotective and anti-nociceptive effect of curcumin in diabetic neuropathy in rats," *International Journal of Pharmacy and Pharmaceutical Sciences*, vol. 6, no. 5, pp. 131–138, 2014.

[150] H. N. Attia, N. M. Al-Rasheed, N. M. Al-Rasheed, Y. A. Maklad, A. A. E. Ahmed, and S. A. B. Kenawy, "Protective effects of combined therapy of gliclazide with curcumin in experimental diabetic neuropathy in rats," *Behavioural Pharmacology*, vol. 23, no. 2, pp. 153–161, 2012.

[151] S. Sharma, K. Chopra, and S. K. Kulkarni, "Effect of insulin and its combination with resveratrol or curcumin in attenuation of diabetic neuropathic pain: participation of nitric oxide and TNF-alpha," *Phytotherapy Research*, vol. 21, no. 3, pp. 278–283, 2007.

[152] J. Yu, Y. Zhang, S. Sun et al., "Inhibitory effects of astragaloside IV on diabetic peripheral neuropathy in rats," *Canadian Journal of Physiology and Pharmacology*, vol. 84, no. 6, pp. 579–587, 2006.

[153] D. Raposo, C. Morgado, P. Pereira-Terra, and I. Tavares, "Nociceptive spinal cord neurons of laminae I-III exhibit oxidative stress damage during diabetic neuropathy which is prevented by early antioxidant treatment with epigallocatechin-gallate (EGCG)," *Brain Research Bulletin*, vol. 110, pp. 68–75, 2015.

[154] T. Baluchnejadmojarad and M. Roghani, "Chronic oral epigallocatechin-gallate alleviates streptozotocin-induced diabetic neuropathic hyperalgesia in rat: involvement of oxidative stress," *Iranian Journal of Pharmaceutical Research: IJPR*, vol. 11, no. 4, pp. 1243–1253, 2012.

[155] Y. Ding, X. Dai, Y. Jiang, Z. Zhang, and Y. Li, "Functional and morphological effects of grape seed proanthocyanidins on peripheral neuropathy in rats with type 2 diabetes

mellitus," *Phytotherapy Research*, vol. 28, no. 7, pp. 1082–1087, 2014.

[156] L. Kishore, N. Kaur, and R. Singh, "Bacosine isolated from aerial parts of Bacopa monnieri improves the neuronal dysfunction in streptozotocin-induced diabetic neuropathy," *Journal of Functional Foods*, vol. 34, pp. 237–247, 2017.

[157] S. Akbar, F. Subhan, N. Karim et al., "6-Methoxyflavanone attenuates mechanical allodynia and vulvodynia in the streptozotocin-induced diabetic neuropathic pain," *Biomedicine & Pharmacotherapy*, vol. 84, pp. 962–971, 2016.

[158] D. Bagdas, H. Y. Ozboluk, N. Cinkilic, and M. S. Gurun, "Antinociceptive effect of chlorogenic acid in rats with painful diabetic neuropathy," *Journal of Medicinal Food*, vol. 17, no. 6, pp. 730–732, 2014.

[159] H. I. Rocha-González, M. Ramírez-Aguilar, V. Granados-Soto et al., "Antineuropathic effect of 7-hydroxy-3,4-dihydrocadalin in streptozotocin-induced diabetic rodents," *BMC Complementary and Alternative Medicine*, vol. 14, no. 1, 2014.

[160] S. T. Ma, D. L. Liu, J. J. Deng, and Y. J. Peng, "Protective effect of mulberry flavonoids on sciatic nerve in alloxan-induced diabetic rats," *Brazilian Journal of Pharmaceutical Sciences*, vol. 50, no. 4, pp. 765–772, 2014.

[161] N. Kaur, L. Kishore, and R. Singh, "Chromane isolated from leaves of dillenia indica improves the neuronal dysfunction in STZ-induced diabetic neuropathy," *Journal of Ethnopharmacology*, vol. 206, pp. 19–30, 2017.

[162] O. M. Abo-Salem, "Kaempferol attenuates the development of diabetic neuropathic pain in mice: possible anti-inflammatory and anti-oxidant mechanisms," *Open Access Macedonian Journal of Medical Sciences*, vol. 2, no. 3, pp. 424–430, 2014.

[163] S. B. Ghatak and S. S. Panchal, "Protective effect of oryzanol isolated from crude rice bran oil in experimental model of diabetic neuropathy," *Revista Brasileira de Farmacognosia*, vol. 22, no. 5, pp. 1092–1103, 2012.

[164] C.-T. Ma, C.-C. Chyau, C.-C. Hsu et al., "Pepino polyphenolic extract improved oxidative, inflammatory and glycative stress in the sciatic nerves of diabetic mice," *Food & Function*, vol. 7, no. 2, pp. 1111–1121, 2016.

[165] K. Dureshahwar, M. Mubashir, and H. Une, "Quantification of quercetin obtained from *Allium cepa* Lam. leaves and its effects on streptozotocin-induced diabetic neuropathy," *Pharmacognosy Research*, vol. 9, no. 3, pp. 287–293, 2017.

[166] A. D. Kandhare, K. S. Raygude, V. Shiva Kumar et al., "Ameliorative effects quercetin against impaired motor nerve function, inflammatory mediators and apoptosis in neonatal streptozotocin-induced diabetic neuropathy in rats," *Biomedicine & Aging Pathology*, vol. 2, no. 4, pp. 173–186, 2012.

[167] M. Anjaneyulu and K. Chopra, "Quercetin, a bioflavonoid, attenuates thermal hyperalgesia in a mouse model of diabetic neuropathic pain," *Progress in Neuro-Psychopharmacology and Biological Psychiatry*, vol. 27, no. 6, pp. 1001–1005, 2003.

[168] M. Anjaneyulu and K. Chopra, "Quercetin attenuates thermal hyperalgesia and cold allodynia in STZ-induced diabetic rats," *Indian Journal of Experimental Biology*, vol. 42, no. 8, pp. 766–769, 2004.

[169] A. Kumar, R. K. Kaundal, S. Iyer, and S. S. Sharma, "Effects of resveratrol on nerve functions, oxidative stress and DNA fragmentation in experimental diabetic neuropathy," *Life Sciences*, vol. 80, no. 13, pp. 1236–1244, 2007.

[170] A. Kumar and S. S. Sharma, "NF-κB inhibitory action of resveratrol: a probable mechanism of neuroprotection in experimental diabetic neuropathy," *Biochemical and Biophysical Research Communications*, vol. 394, no. 2, pp. 360–365, 2010.

[171] H. E. Mohamed, S. E. El-Swefy, R. A. Hasan, and A. A. Hasan, "Neuroprotective effect of resveratrol in diabetic cerebral ischemic-reperfused rats through regulation of inflammatory and apoptotic events," *Diabetology & Metabolic Syndrome*, vol. 6, no. 1, p. 88, 2014.

[172] S. Sharma, M. Anjaneyulu, S. K. Kulkarni, and K. Chopra, "Resveratrol, a polyphenolic phytoalexin, attenuates diabetic nephropathy in rats," *Pharmacology*, vol. 76, no. 2, pp. 69–75, 2006.

[173] T. Baluchnejadmojarad, M. Roghani, and M. Mafakheri, "Neuroprotective effect of silymarin in 6-hydroxydopamine hemi-parkinsonian rat: involvement of estrogen receptors and oxidative stress," *Neuroscience Letters*, vol. 480, no. 3, pp. 206–210, 2010.

[174] S. Alsharari, S. Al-Rejaie, H. Abuohashish, A. Aleisa, M. Parmar, and M. Ahmed, "Ameliorative potential of morin in streptozotocin-induced neuropathic pain in rats," *Tropical Journal of Pharmaceutical Research*, vol. 13, no. 9, pp. 1429–1436, 2014.

[175] C. Sommer and M. Kress, "Recent findings on how proinflammatory cytokines cause pain: peripheral mechanisms in inflammatory and neuropathic hyperalgesia," *Neuroscience Letters*, vol. 361, no. 1–3, pp. 184–187, 2004.

[176] M. Schäfers, C. I. Svensson, C. Sommer, and L. S. Sorkin, "Tumor necrosis factor-α induces mechanical allodynia after spinal nerve ligation by activation of p38 MAPK in primary sensory neurons," *The Journal of Neuroscience*, vol. 23, no. 7, pp. 2517–2521, 2003.

[177] J. M. González-Clemente, D. Mauricio, C. Richart et al., "Diabetic neuropathy is associated with activation of the TNF-α system in subjects with type 1 diabetes mellitus," *Clinical Endocrinology*, vol. 63, no. 5, pp. 525–529, 2005.

[178] D. M. Shafer, L. Assael, L. B. White, and E. F. Rossomando, "Tumor necrosis factor-α as a biochemical marker of pain and outcome in temporomandibular joints with internal derangements," *Journal of Oral and Maxillofacial Surgery*, vol. 52, no. 8, pp. 786–791, 1994.

[179] J. Satoh, S. Yagihashi, and T. Toyota, "The possible role of tumor necrosis factor-α in diabetic polyneuropathy," *Experimental Diabesity Research*, vol. 4, no. 2, pp. 65–71, 2003.

[180] N. Cameron and M. Cotter, "Pro-inflammatory mechanisms in diabetic neuropathy: focus on the nuclear factor kappa B pathway," *Current Drug Targets*, vol. 9, no. 1, pp. 60–67, 2008.

[181] J. Copray, I. Mantingh, N. Brouwer et al., "Expression of interleukin-1 beta in rat dorsal root ganglia," *Journal of Neuroimmunology*, vol. 118, no. 2, pp. 203–211, 2001.

[182] J. M. Cunha, F. Q. Cunha, S. Poole, and S. H. Ferreira, "Cytokine-mediated inflammatory hyperalgesia limited by interleukin-1 receptor antagonist," *British Journal of Pharmacology*, vol. 130, no. 6, pp. 1418–1424, 2000.

[183] M. Bujalska, J. Tatarkiewicz, A. de Cordé, and S. W. Gumułka, "Effect of cyclooxygenase and nitric oxide synthase inhibitors on streptozotocin-induced hyperalgesia in rats," *Pharmacology*, vol. 81, no. 2, pp. 151–157, 2008.

[184] A. P. Kellogg, T. D. Wiggin, D. D. Larkin, J. M. Hayes, M. J. Stevens, and R. Pop-Busui, "Protective effects of cyclooxygenase-2 gene inactivation against peripheral nerve dysfunction and intraepidermal nerve fiber loss in experimental diabetes," *Diabetes*, vol. 56, no. 12, pp. 2997–3005, 2007.

[185] S. Park, K. Sapkota, S. Kim, H. Kim, and S. Kim, "Kaempferol acts through mitogen-activated protein kinases and protein kinase B/AKT to elicit protection in a model of neuroinflammation in BV2 microglial cells," *British Journal of Pharmacology*, vol. 164, no. 3, pp. 1008–1025, 2011.

[186] T. Baluchnejadmojarad, M. Roghani, and Z. Khastehkhodaie, "Chronic treatment of silymarin improves hyperalgesia and motor nerve conduction velocity in diabetic neuropathic rat," *Phytotherapy Research*, vol. 24, no. 8, pp. 1120–1125, 2010.

[187] K. R. Shieh, C. H. Yi, T. T. Liu et al., "Evidence for neurotrophic factors associating with TRPV1 gene expression in the inflamed human esophagus," *Neurogastroenterology & Motility*, vol. 22, no. 9, pp. 971–e252, 2010.

[188] V. A. Carozzi and C. Ceresa, "The role of glutamate in diabetic and in chemotherapy induced peripheral neuropathies and its regulation by glutamate carboxypeptidase II," *Current Medicinal Chemistry*, vol. 19, no. 9, pp. 1261–1268, 2012.

[189] L. Daulhac, C. Mallet, C. Courteix et al., "Diabetes-induced mechanical hyperalgesia involves spinal mitogen-activated protein kinase activation in neurons and microglia via N-Methyl-D-aspartate-dependent mechanisms," *Molecular Pharmacology*, vol. 70, no. 4, pp. 1246–1254, 2006.

[190] S. Fakhri, L. Dargahi, F. Abbaszadeh, and M. Jorjani, "Effects of astaxanthin on sensory-motor function in a compression model of spinal cord injury: involvement of ERK and AKT signalling pathway," *European Journal of Pain*, vol. 23, no. 4, pp. 750–764, 2019.

[191] S. Takehana, Y. Kubota, N. Uotsu et al., "The dietary constituent resveratrol suppresses nociceptive neurotransmission via the NMDA receptor," *Molecular Pain*, vol. 13, Article ID 174480691769701, 2017.

[192] R. Moldzio, K. Radad, C. Krewenka, B. Kranner, J. C. Duvigneau, and W.-D. Rausch, "Protective effects of resveratrol on glutamate-induced damages in murine brain cultures," *Journal of Neural Transmission*, vol. 120, no. 9, pp. 1271–1280, 2013.

[193] K. Zeng, N. Yang, D. Wang et al., "Resveratrol prevents retinal dysfunction by regulating glutamate transporters, glutamine synthetase expression and activity in diabetic retina," *Neurochemical Research*, vol. 41, no. 5, pp. 1050–1064, 2016.

[194] C. Girbovan and H. Plamondon, "Resveratrol downregulates type-1 glutamate transporter expression and microglia activation in the hippocampus following cerebral ischemia reperfusion in rats," *Brain Research*, vol. 1608, pp. 203–214, 2015.

[195] A. Quincozes-Santos, L. D. Bobermin, A. C. Tramontina et al., "Oxidative stress mediated by NMDA, AMPA/KA channels in acute hippocampal slices: neuroprotective effect of resveratrol," *Toxicology in Vitro*, vol. 28, no. 4, pp. 544–551, 2014.

[196] K. S. Cho, E. J. Lee, K. J. Kwon et al., "Resveratrol downregulates a glutamate-induced tissue plasminogen activator via Erk and AMPK/mTOR pathways in rat primary cortical neurons," *Food & Function*, vol. 5, no. 5, pp. 951–960, 2014.

[197] Y. Chang and S.-J. Wang, "Inhibitory effect of glutamate release from rat cerebrocortical nerve terminals by resveratrol," *Neurochemistry International*, vol. 54, no. 2, pp. 135–141, 2009.

[198] Y. Son, S. J. Byun, and H.-O. Pae, "Involvement of heme oxygenase-1 expression in neuroprotection by piceatannol, a natural analog and a metabolite of resveratrol, against glutamate-mediated oxidative injury in HT22 neuronal cells," *Amino Acids*, vol. 45, no. 2, pp. 393–401, 2013.

[199] Y. Mikami and T. Yamazawa, "Chlorogenic acid, a polyphenol in coffee, protects neurons against glutamate neurotoxicity," *Life Sciences*, vol. 139, pp. 69–74, 2015.

[200] O. Rebai, M. Belkhir, M. V. Sanchez-Gomez, C. Matute, S. Fattouch, and M. Amri, "Differential molecular targets for neuroprotective effect of chlorogenic acid and its related compounds against glutamate induced excitotoxicity and oxidative stress in rat cortical neurons," *Neurochemical Research*, vol. 42, no. 12, pp. 3559–3572, 2017.

[201] J. Yu, Y. Jia, Y. Guo et al., "Epigallocatechin-3-gallate protects motor neurons and regulates glutamate level," *FEBS Letters*, vol. 584, no. 13, pp. 2921–2925, 2010.

[202] S. Pournourmohammadi, M. Grimaldi, M. H. Stridh et al., "Epigallocatechin-3-gallate (EGCG) activates AMPK through the inhibition of glutamate dehydrogenase in muscle and pancreatic β-cells: a potential beneficial effect in the pre-diabetic state?" *The International Journal of Biochemistry & Cell Biology*, vol. 88, pp. 220–225, 2017.

[203] C.-W. Chou, W.-J. Huang, L.-T. Tien, and S.-J. Wang, "(−)-Epigallocatechin gallate, the most active polyphenolic catechin in green tea, presynaptically facilitates Ca^{2+}-dependent glutamate release via activation of protein kinase C in rat cerebral cortex," *Synapse*, vol. 61, no. 11, pp. 889–902, 2007.

[204] J.-H. Lee, D.-K. Song, C.-H. Jung et al., "(−)-Epigallocatechin gallate attenuates glutamate-induced cytotoxicity via intracellular Ca^{2+} modulation in PC12 cells," *Clinical and Experimental Pharmacology and Physiology*, vol. 31, no. 8, pp. 530–536, 2004.

[205] C.-W. Lu, T.-Y. Lin, and S.-J. Wang, "Quercetin inhibits depolarization-evoked glutamate release in nerve terminals from rat cerebral cortex," *Neurotoxicology*, vol. 39, pp. 1–9, 2013.

[206] H.-C. Huang, P. Chang, S.-Y. Lu, B.-W. Zheng, and Z.-F. Jiang, "Protection of curcumin against amyloid-β-induced cell damage and death involves the prevention from NMDA receptor-mediated intracellular Ca^{2+} elevation," *Journal of Receptors and Signal Transduction*, vol. 35, no. 5, pp. 450–457, 2015.

[207] R. M. Khalil and N. F. Khedr, "Curcumin protects against monosodium glutamate neurotoxicity and decreasing NMDA2B and mGluR5 expression in rat hippocampus," *NeuroSignals*, vol. 24, no. 1, pp. 81–87, 2016.

[208] L. Zhang, T. Xu, S. Wang et al., "NMDA GluN2B receptors involved in the antidepressant effects of curcumin in the forced swim test," *Progress in Neuro-Psychopharmacology and Biological Psychiatry*, vol. 40, pp. 12–17, 2013.

[209] S. Jayanarayanan, S. Smijin, K. T. Peeyush, T. R. Anju, and C. S. Paulose, "NMDA and AMPA receptor mediated excitotoxicity in cerebral cortex of streptozotocin induced diabetic rat: ameliorating effects of curcumin," *Chemico-Biological Interactions*, vol. 201, no. 1–3, pp. 39–48, 2013.

[210] T. Y. Lin, C. W. Lu, S. K. Huang, and S. J. Wang, "Curcumin inhibits glutamate release from rat prefrontal nerve endings by affecting vesicle mobilization," *International Journal of Molecular Sciences*, vol. 13, no. 7, pp. 9097–9109, 2012.

[211] P. Srivastava, Y. K. Dhuriya, V. Kumar et al., "PI3K/Akt/GSK3β induced CREB activation ameliorates arsenic mediated alterations in NMDA receptors and associated signaling in rat hippocampus: neuroprotective role of curcumin," *Neurotoxicology*, vol. 67, pp. 190–205, 2018.

[212] G. S. B. Aseervatham, U. Suryakala, Doulethunisha, S. Sundaram, P. C. Bose, and T. Sivasudha, "Expression pattern of NMDA receptors reveals antiepileptic potential of apigenin 8-C-glucoside and chlorogenic acid in pilocarpine induced epileptic mice," *Biomedicine & Pharmacotherapy*, vol. 82, pp. 54–64, 2016.

[213] A. Ramakrishnan, N. Vijayakumar, and M. Renuka, "Naringin regulates glutamate-nitric oxide cGMP pathway in ammonium chloride induced neurotoxicity," *Biomedicine & Pharmacotherapy*, vol. 84, pp. 1717–1726, 2016.

[214] R. Yue, X. Li, B. Chen et al., "Astragaloside IV attenuates glutamate-induced neurotoxicity in PC12 cells through Raf-MEK-ERK pathway," *PLoS One*, vol. 10, no. 5, Article ID e0126603, 2015.

[215] E.-J. Yang, G.-S. Kim, M. Jun, and K.-S. Song, "Kaempferol attenuates the glutamate-induced oxidative stress in mouse-derived hippocampal neuronal HT22 cells," *Food & Function*, vol. 5, no. 7, pp. 1395–1402, 2014.

[216] E. Eisenberg, E. D. McNicol, and D. B. Carr, "Opioids for neuropathic pain," *Cochrane Database of Systematic Reviews*, vol. 19, no. 2, Article ID CD006146, 2006.

[217] H. Cory, S. Passarelli, J. Szeto, M. Tamez, and J. Mattei, "The role of polyphenols in human health and food systems: a mini-review," *Frontiers in Nutrition*, vol. 5, p. 87, 2018.

[218] S. Lecour and K. T. Lamont, "Natural polyphenols and cardioprotection," *Mini-Reviews in Medicinal Chemistry*, vol. 11, no. 14, pp. 1191–1199, 2011.

Hindawi
Evidence-Based Complementary and Alternative Medicine
Volume 2021, Article ID 9921534, 20 pages
https://doi.org/10.1155/2021/9921534

Research Article

Deciphering Pharmacological Mechanism of Buyang Huanwu Decoction for Spinal Cord Injury by Network Pharmacology Approach

Zhencheng Xiong,[1] **Feng Yang**,[1] **Wenhao Li**,[1,2] **Xiangsheng Tang**,[1] **Haoni Ma**,[1] **and Ping Yi**[1]

[1]*Department of Spine Surgery, China-Japan Friendship Hospital, Beijing 100029, China*
[2]*Beijing University of Chinese Medicine, Beijing 100029, China*

Correspondence should be addressed to Ping Yi; 13811758985@139.com

Received 12 March 2021; Revised 1 April 2021; Accepted 8 April 2021; Published 23 April 2021

Academic Editor: Rajeev K Singla

Copyright © 2021 Zhencheng Xiong et al. This is an open access article distributed under the Creative Commons Attribution License, which permits unrestricted use, distribution, and reproduction in any medium, provided the original work is properly cited.

Objective. The purpose of this study was to investigate the mechanism of action of the Chinese herbal formula Buyang Huanwu Decoction (BYHWD), which is commonly used to treat nerve injuries, in the treatment of spinal cord injury (SCI) using a network pharmacology method. *Methods*. BYHWD-related targets were obtained by mining the TCMSP and BATMAN-TCM databases, and SCI-related targets were obtained by mining the DisGeNET, TTD, CTD, GeneCards, and MalaCards databases. The overlapping targets of the abovementioned targets may be potential therapeutic targets for BYHWD anti-SCI. Subsequently, we performed protein-protein interaction (PPI) analysis, screened the hub genes using Cytoscape software, performed Gene Ontology (GO) annotation and KEGG pathway enrichment analysis, and finally achieved molecular docking between the hub proteins and key active compounds. *Results*. The 189 potential therapeutic targets for BYHWD anti-SCI were overlapping targets of 744 BYHWD-related targets and 923 SCI-related targets. The top 10 genes obtained subsequently included AKT1, IL6, MAPK1, TNF, TP53, VEGFA, CASP3, ALB, MAPK8, and JUN. Fifteen signaling pathways were also screened out after enrichment analysis and literature search. The results of molecular docking of key active compounds and hub target proteins showed a good binding affinity for both. *Conclusion*. This study shows that BYHWD anti-SCI is characterized by a multicomponent, multitarget, and multipathway synergy and provides new insights to explore the specific mechanisms of BYHWD against SCI.

1. Introduction

Spinal cord injury (SCI) is a group of disorders in which the integrity and continuity of the spinal cord are disrupted by trauma, tumor, hypoxia, inflammation, and other factors [1]. According to the World Health Organization (WHO) report, about 250,000 to 500,000 people worldwide suffer from SCI every year, and the population is mainly under 30 years old [2]. The Beijing SCI Epidemiology Survey Group reported in 2002 that the incidence of SCI in Beijing was about $60/10^6$, an increase of nearly 10 times compared to the late 1980s, and that the per capita hospitalization cost was 27819.3 CNY [3]. The high disability rate and high consumption of SCI have imposed a heavy burden on the families of patients and society, while how to protect and restore injured neurons after SCI has been considered a great challenge in clinical and experimental research [4]. There is still a lack of effective treatment for SCI, but it is known that traditional Chinese medicine (TCM) has a long history and rich practical experience, which may be explored for the treatment of SCI [2].

Modern Chinese medicine scholars classify SCI as "Ti Duo" and "Wei Zheng" based on the TCM classics "Ling Shu Jing-Han Re Bing" and "Su Wen-Wei Lun" [3]. Based on the analysis of the etiology and pathogenesis of SCI by TCM, as well as the pathological changes of the damaged Governor

Vessel and the symptoms corresponding to SCI, the main treatment of TCM is to unblock Governor Vessel and strengthen "Yang Qi," supplemented by tonifying the kidney and filling the essence, strengthening the tendons and bones, activating blood circulation and removing blood stasis, and warming the meridians [3]. Buyang Huanwu Decoction (BYHWD), recorded in "Yi Lin Gai Cuo" by Wang Qingren in the Qing Dynasty, has been used in China for hundreds of years to treat stroke-related disabilities and improve the recovery of neurological function [5]. The whole formula of BYHWD consists of seven herbs: Chishao (*Radix Paeoniae Rubra*), Chuanxiong (*Rhizoma Chuanxiong*), Danggui (*Radix Angelicae Sinensis*), Dilong (*Pheretima*), Huangqi (*Radix Astragali*), Honghua (*Flos Carthami*), and Taoren (*Semen Persicae*) [5]. Studies have shown that BYHWD may promote the repair of SCI by upregulating the expression of Notch1 gene [6], and BYHWD combined with bone marrow mesenchymal stem cells (BMSCs) transplantation can promote the recovery after SCI by saving axotomized red nucleus neurons in rats [4]. Although some progress has been made in the study of BYHWD for SCI, the complexity of herbal prescriptions with multiple components, targets, and pathways makes the study of the specific mechanism of action of BYHWD for SCI difficult to clarify.

In the last decade, with the development of modern multiomics theories such as genomics, proteomics, and metabolomics, the introduction of a systems biology perspective, and the application of bioinformatics, the concept of network pharmacology has emerged. According to the network basis of drug action, network pharmacology methods, including protein-protein interaction (PPI) network, Gene Ontology (GO) annotation, and Kyoto Encyclopedia of Genes and Genomes (KEGG) pathway enrichment analysis, are applied to infer the specific pathways of multimolecular drug action in the human body, which is consistent with the multicomponent, multitarget, and multipathway synergy of Chinese herbal medicine and helps to clarify the mechanism of action of BYHWD (Figure 1).

2. Materials and Methods

2.1. Acquisition of BYHWD-Related Targets and SCI-Related Targets. The compounds related to BYHWD were obtained by searching "Chishao or CHI SHAO or *Radix Paeoniae Rubra*," "Chuanxiong or CHUAN XIONG or *Rhizoma Chuanxiong*," "Danggui or DANG GUI or *Radix Angelicae Sinensis*," "Dilong or DI LONG or *Pheretima*," "Huangqi or HUANG QI or *Radix Astragali*," "Honghua or HONG HUA or *Flos Carthami*," and "Taoren or TAO REN or *Semen Persicae*" in Traditional Chinese Medicine Systems Pharmacology (TCMSP, version 2.3, https://tcmspw.com/tcmsp.php) database [7], and then the active compounds that met the criteria (oral bioavailability (OB) ≥ 30 and drug-likeness (DL) ≥ 0.18) were further screened by the absorption, distribution, metabolism, and excretion (ADME) principle [8, 9], and the corresponding target protein information of the active compounds was also obtained. Subsequently, by using the UniProt database (https://www.uniprot.org/) (species should be set to "*Homo sapiens*"), the target protein name is converted into the corresponding gene name and UniProt ID [10]. The compounds and targets related to BYHWD were also obtained directly by searching the above keywords in the BATMAN-TCM platform (http://bionet.ncpsb.org/batman-tcm/) according to the set criteria (score cutoff >25, adjusted P value < 0.05) [11]. Finally, the results of the two databases are summarized, integrated, and deduplicated to obtain BYHWD-related targets.

DisGeNet database (https://www.disgenet.org/, v7.0) (score ≥ 0.01) [12], GeneCards (https://www.genecards.org/) (relevance score ≥ 20) [13], MalaCards (https://www.malacards.org/) [14], Comparative Toxicogenomics Database (CTD) (http://ctdbase.org/, last update by June 2020) (inference score ≥ 20) [15], and Therapeutic Target Database (TTD) (http://db.idrblab.net/ttd/, last update by June 1, 2020) [16] were used to screen out potential targets related to SCI by searching for the keyword "Spinal cord injury or Spinal cord diseases." The results of the five databases are summarized, integrated, and deduplicated to obtain SCI-related targets.

2.2. Acquisition of Potential Therapeutic Targets for BYHWD Anti-SCI. Potential therapeutic targets of BYHWD in the treatment of SCI should be derived from the overlapping targets of BYHWD-related targets and SCI-related targets obtained from the Venn online tool (http://www.bioinformatics.com.cn/). Subsequently, we used Cytoscape software (version 3.7.2) to construct a network diagram of "BYHWD-active compounds-target genes-SCI" [17].

2.3. Construction of PPI Network and Acquisition of Hub Genes. PPI is composed of proteins that interact with each other to participate in various aspects of life processes such as biological signaling, regulation of gene expression, energy and material metabolism, and cell cycle regulation [18]. The potential therapeutic targets of BYHWD against SCI were analyzed by a PPI network using the STRING database (http://string-db.org/; version 11) with the species set to "*Homo sapiens*" and a confidence level greater than 0.4 [19]. Subsequently, the PPI network was visualized by Cytoscape software (version 3.7.2).

To obtain the hub genes for BYHWD anti-SCI, we use the CytoHubba plug-in in Cytoscape software, which provides 12 topological analysis methods, including Degree, Maximal Clique Centrality (MCC), BottleNeck, Betweenness, ClusteringCoefficient, Closeness, Density of Maximum Neighborhood Component (DMNC), EcCentricity, Edge Percolated Component (EPC), Maximum Neighborhood Component (MNC), Radiality, and Stress [20, 21].

2.4. GO and KEGG Pathway Enrichment Analysis of Potential Therapeutic Genes for BYHWD Anti-SCI. R is commonly used for statistical analysis and plotting software, and its open-source and free features have been favored by many programming enthusiasts, resulting in the birth of many convenient and efficient packages, such as the

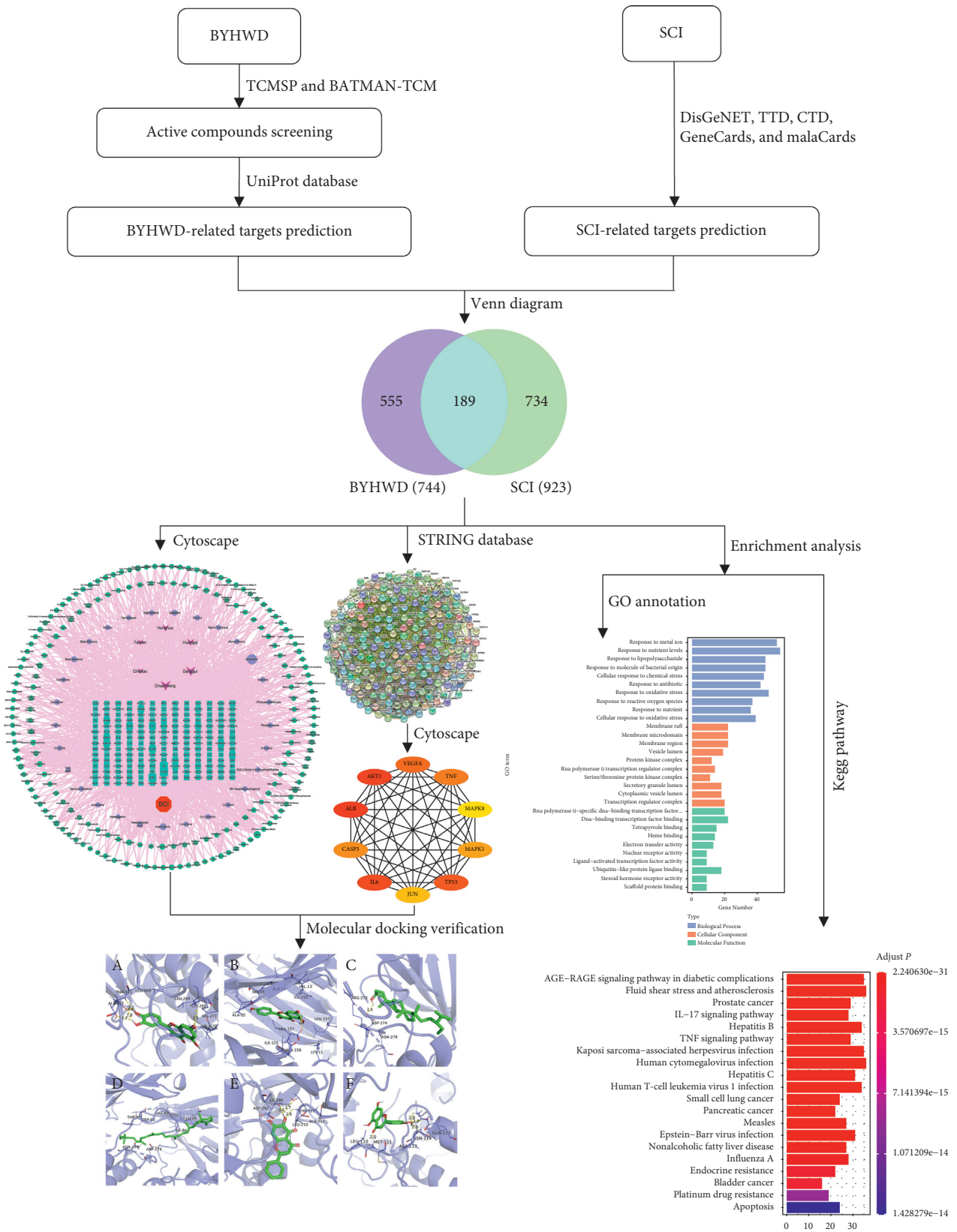

Figure 1: The overall flowchart of this study.

ClusterProfiler package for GO annotation and KEGG pathway enrichment analysis [22–24]. In this study, we used ClusterProfiler package (adjusted P value < 0.05) to explore the biological processes (BP), cellular components (CC), molecular functions (MF), and signaling pathways associated with BYHWD anti-SCI.

2.5. Molecular Docking of Hub Genes and Key Active Compounds. Based on the previously mined BYHWD-related targets and related active compounds, the active compounds and herbs corresponding to the top 10 hub genes need to be sorted out. The interrelationship between "herbs in BYHWD-active compounds-top 10 hub genes" was visualized by a Sankey diagram (http://sankeymatic.com/). In the following, we will select key active compounds as small molecule ligands and corresponding large molecule receptors (proteins encoded by the top 10 hub genes) for molecular docking analysis. The raw files of key active compounds (MOL2 format) can be downloaded from PubChem database (https://pubchem.ncbi.nlm.nih.gov/), and the raw files of the top 10 core genes (PDB format) can be downloaded from the RCSB protein data (http://www.rcsb.org/), and after corresponding processing by AutoDock Tool [25], they are finally converted to PDBQT format for molecular docking in Pymol software (https://pymol.org/2/; version 2.4.1) [26]. The molecular docking score reflects the binding affinity, with smaller values representing higher affinity for the binding of small molecule ligands and large molecule receptors [27].

3. Results

3.1. Acquisition Results of BYHWD-Related Targets and SCI-Related Targets. A total of 775 compounds (BATMAN-TCM: 219; after deduplication: 189) in BYHWD were preliminarily retrieved from the TCMSP database and BATMAN-TCM platform (score cutoff >25; adjusted P value < 0.05), of which 119 (BATMAN-TCM: 8) were from Chishao, 189 (87) were from Chuanxiong, 125 (77) were from Danggui, 87 (23) were from Huangqi, 189 (22) were from Honghua, and 66 (2) were from Taoren. Relevant compounds and targets' information for Dilong was not retrieved in either database. After setting the ADME criteria (OB ≥ 30% and DL ≥ 0.18), a total of 103 active compounds (after removing duplicates and nontarget compounds: 60) were screened from the TCMSP database, of which 29 (After removing nontarget compounds: 14) were from Chishao, 7 (6) were from Chuanxiong, 2 (2) were from Danggui, 20 (17) were from Huangqi, 22 (17) were from Honghua, and 23 (19) were from Taoren. The BATMAN-TCM platform provides the gene names directly, while the TCMSP database first provides the target protein names of the active compounds and therefore needs to be converted to gene names via the UniProt database. Finally, after integrating the results of the two databases, we obtained 244 BYHWD-related active compounds and 744 BYHWD-related targets.

After deduplication, a total of 923 SCI-related targets were obtained by mining the DisGeNET (number: 84), TTD (number: 5), CTD (number: 553), GeneCards (number: 432), and MalaCards (number: 19) databases.

3.2. Acquisition Results of Potential Therapeutic Targets for BYHWD Anti-SCI. The overlapping targets of BYHWD-related targets and SCI-related targets were considered as potential therapeutic targets for BYHWD anti-SCI. As shown in Figure 2, we screened the overlapping targets of both by constructing a Venn diagram, and a total of 189 targets were obtained. Through multiple databases mining and construction of the Venn diagram, we obtained BYHWD-related compounds and potential therapeutic targets for BYHWD anti-SCI and finally used Cytoscape software to construct a "BYHWD-active compounds-target genes-SCI" network (Figure 3). In Figure 3, the lines between two nodes represent the existence of mutual relationships, and the larger the node is, the more relationships exist.

3.3. Acquisition Results of Hub Genes for BYHWD Anti-SCI and PPI Network Construction. In the STRING database, we first set the species to "*Homo sapiens*" and then entered 189 potential therapeutic targets for BYHWD anti-SCI to obtain the PPI network (Figure 4(a)), which involved 189 nodes and 3717 edges. The obtained TSV files were then imported into Cytoscape software (version 3.7.2) for further analysis and visualization (Figure 4(b)). To obtain the hub genes for BYHWD anti-SCI, based on the above the PPI network, we used the CytoHubba plug-in of Cytoscape software, which currently contains 12 topological analysis methods. We targeted the top 10 hub genes for BYHWD anti-SCI, and the results of the 12 algorithms each contained 10 genes. We integrated and analyzed the results to obtain a total of 45 different genes, which were then sorted by the number of algorithms to which they were attributed. Table 1 shows the basic information on hub genes for BYHWD anti-SCI. The top 10 hub genes (AKT1, IL6, MAPK1, TNF, TP53, VEGFA, CASP3, ALB, MAPK8, and JUN) sorted are completely consistent with some algorithms (Degree, Closeness, and MNC) (Figure 4(c)).

3.4. Results of GO and KEGG Pathway Enrichment Analysis. GO and KEGG pathway enrichment analysis are important tools to explore the biological processes and signal pathways involved in clinical drug therapy for diseases, as well as key genes. Through the ClusterProfiler package in R, we performed GO enrichment analysis on the 189 potential therapeutic targets for BYHWD anti-SCI and obtained 2842 GO items (after adjustment, $P < 0.05$), including 2567 BP items, 99 CC items, and 176 MF items. We combined the top 10 enrichment results for each of GO-BP, GO-CC, and GO-MF by a bar graph (Figure 5). The basic information of the top 10 GO enrichment items is shown in Table 2.

In the same way, through the ClusterProfiler package in R, we performed KEGG pathway enrichment analysis on the 189 potential therapeutic targets for BYHWD anti-SCI and obtained 177 KEGG pathways (after adjustment, $P < 0.05$). The top 20 KEGG enrichment pathways are listed below, including AGE-RAGE signaling pathway in diabetic complications (hsa04933), Fluid shear stress and atherosclerosis (hsa05418), Prostate cancer (hsa05215), IL-17 signaling pathway (hsa04657), Hepatitis B (hsa05161), TNF signaling pathway (hsa04668), Kaposi sarcoma-associated herpesvirus infection (hsa05167), Human cytomegalovirus infection (hsa05163), Hepatitis C (hsa05160), Human T-cell leukemia virus 1 infection (hsa05166), Small cell lung cancer

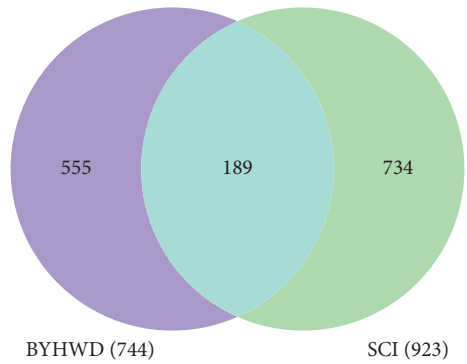

Figure 2: Venn diagram for BYHWD-related targets and SCI-related targets.

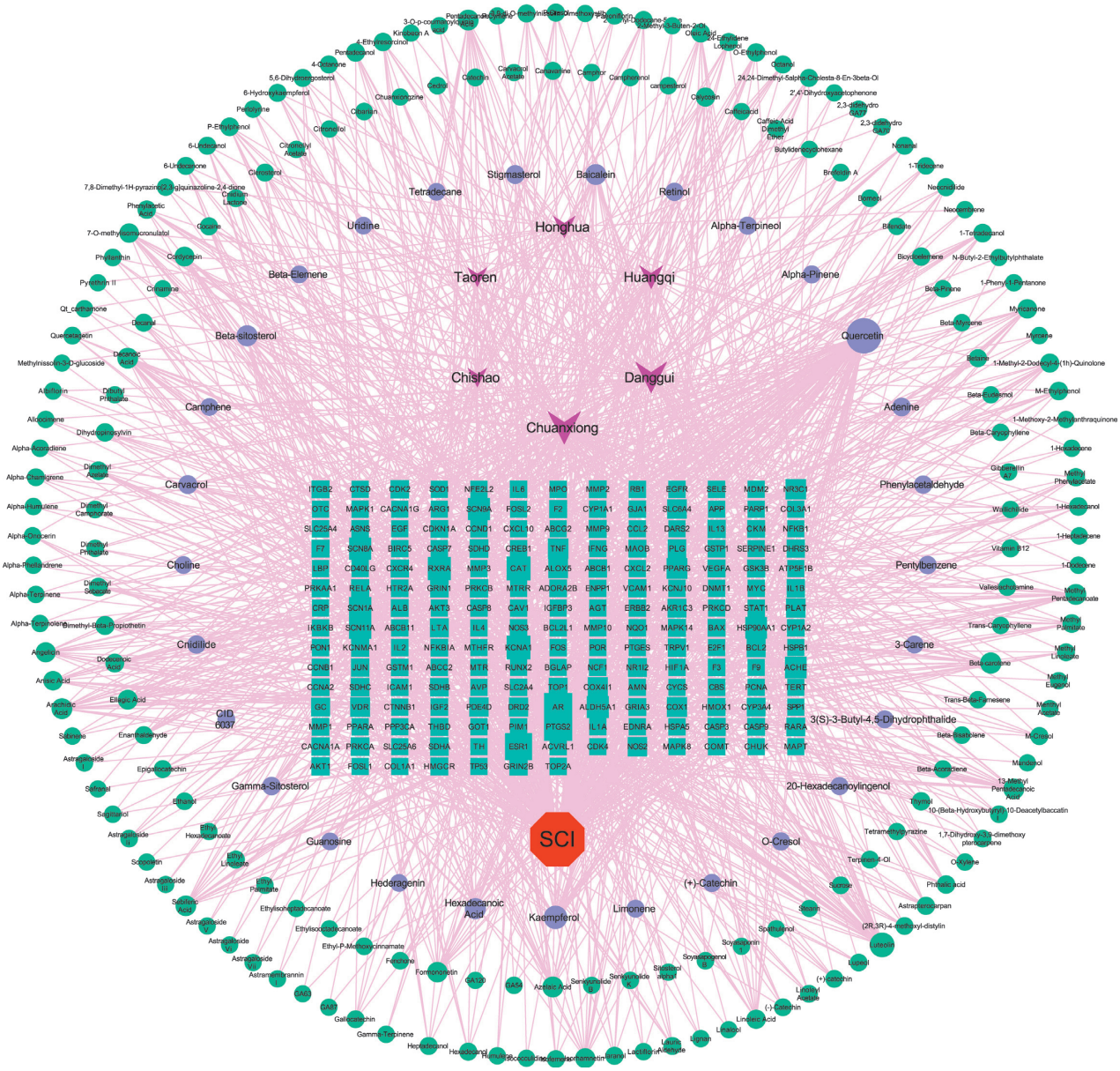

Figure 3: BYHWD-active compounds-target genes-SCI" network. The purple diamond represents the herbs contained in BYHWD; the red octagon represents SCI; the cyan rectangle represents the potential therapeutic targets for BYHWD anti-SCI; the light green ellipse represents the active compounds contained in BYHWD; the blue ellipse represents the common active compounds of the herb.

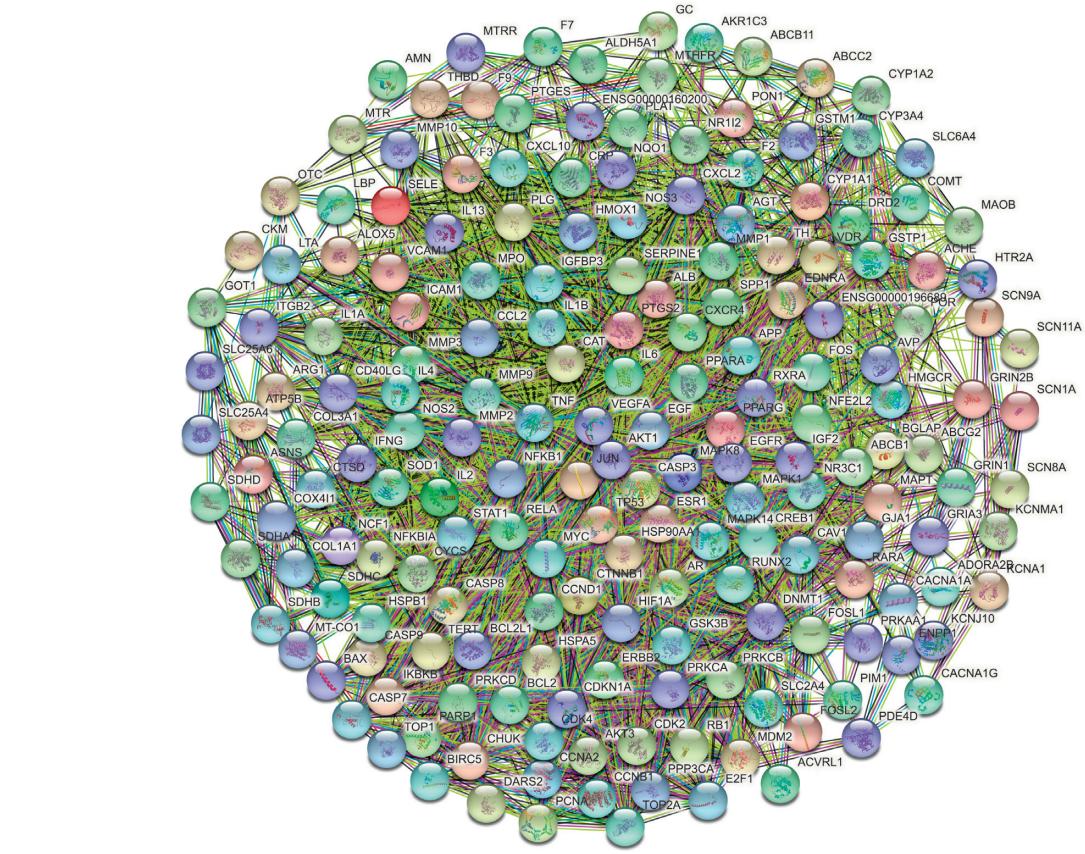

(a)

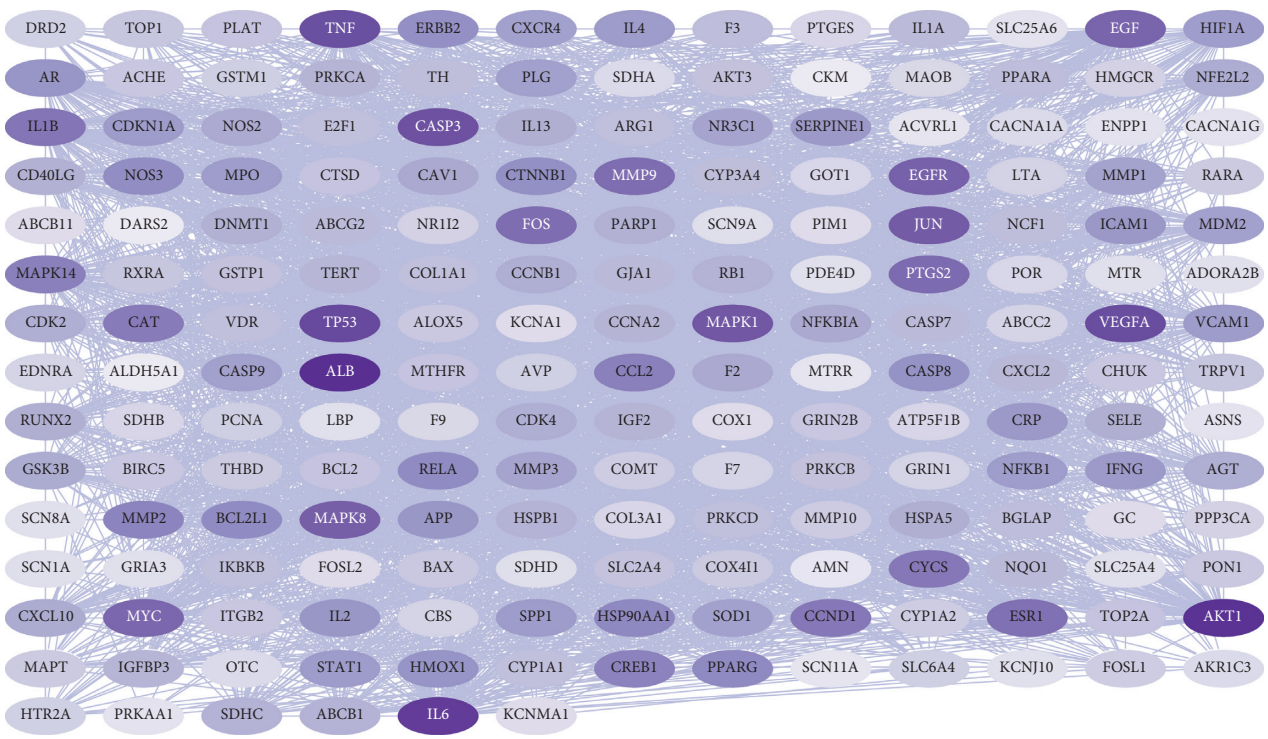

(b)

Figure 4: Continued.

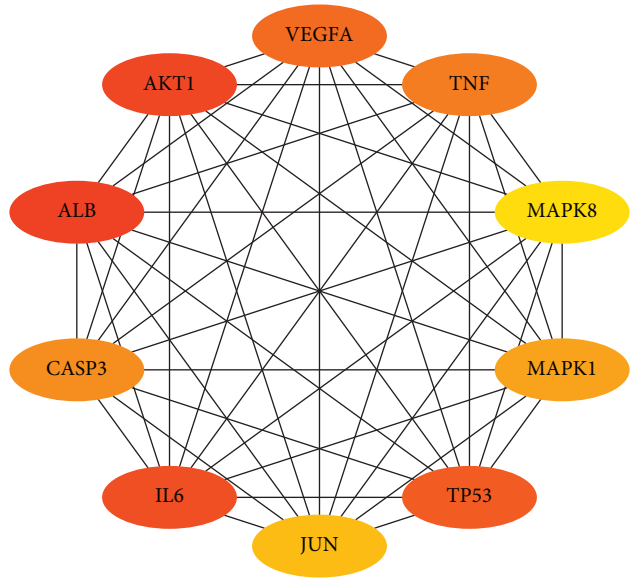

(c)

FIGURE 4: PPI network and top 10 hub genes for BYHWD anti-SCI. (a) PPI network constructed with STRING. (b) PPI network constructed with Cytoscape software (the darker the node color, the higher the number of connected proteins). (c) Top 10 hub genes for BYHWD anti-SCI were obtained by using the Degree algorithm.

(hsa05222), Pancreatic cancer (hsa05212), Measles (hsa05162), Epstein-Barr virus infection (hsa05169), Non-alcoholic fatty liver disease (hsa04932), Influenza A (hsa05164), Endocrine resistance (hsa01522), Bladder cancer (hsa05219), Platinum drug resistance (hsa01524), and Apoptosis (hsa04210). The visualization of the abovementioned KEGG enrichment pathway is realized in Figure 6. More KEGG pathways were enriched, and another fine screening of the pathways was required. Therefore, the SCI-related literature was searched in the PubMed database, and then the retrieved potentially relevant pathways were compared with the enriched 177 pathways, and finally, 15 relatively relevant pathways for SCI were obtained. Subsequently, we used Cytoscape software to visualize the network relationship between potential therapeutic targets for BYHWD anti-SCI and pathways (Figure 7). Table 3 shows the basic information of 15 pathways that may be relevant for SCI.

3.5. Results of Molecular Docking of Hub Genes and Key Active Compounds. Sankey diagram was used to establish one-to-one correspondence between the top 10 hub genes (AKT1, IL6, MAPK1, TNF, TP53, VEGFA, CASP3, ALB, MAPK8, and JUN) for BYHWD anti-SCI and BYHWD-related compounds, providing the basis for the next molecular docking analysis. Among them, the gene that targets the most active compounds is TNF, and the key active compounds that target the most hub genes are quercetin and luteolin (Figure 8). As seen in the Sankey diagram, 6 of the 33 active compounds (quercetin, luteolin, beta-carotene, kaempferol, baicalein, and beta-sitosterol) targeted more hub genes, so we decided to perform the molecular docking between these 6 active compounds and top 10 hub genes. The results of the molecular docking score are presented as a heat map (Figure 9), with a range of −6.4 to −10.9 kcal·mol^{-1}, representing the large molecule protein receptor (hub genes) that binds well to the small molecule ligand (key active compounds). As shown in Figure 10, the molecular docking process of each key active compound and its corresponding protein encoded by the hub gene with the best docking affinity was visualized using Pymol. Table 4 shows the basic information of active compounds targeting hub genes in BYHWD.

4. Discussion

According to the report of the National SCI Statistics Center, there are about 17,000 new cases of SCI in the United States each year, and the annual incidence of SCI is about 54 cases per million people [1]. Over the past century, advances in understanding the mechanisms of SCI have changed the clinical management strategies for SCI, including surgical procedures, supportive measures, and rehabilitative training that have improved neurological outcomes and reduced morbidity in SCI patients [1]. However, there is still a lack of effective treatments for SCI and thus has been stimulating the desire of researchers to explore and try to find effective treatments, including drugs, surgical methods, and rehabilitation programs. As we all know, TCM has a long history of being used to treat various diseases in China and other Asian countries [28]. Among them, BYHWD, Jisuikang, single herb, and Governor Vessel electroacupuncture have all been shown in relevant studies to be used in the treatment of SCI [4, 5, 28–30].

BYHWD, which comes from Qing Dynasty medical classics, consists of seven herbs: Chishao, Chuanxiong, Danggui, Dilong, Huangqi, Honghua, and Taoren [5]. Based on the theory of TCM, Huangqi is the main ingredient in this

Table 1: Basic information of hub genes based on 12 topological algorithms.

UniProt ID	Gene symbol	Protein names	Algorithms
P31749	AKT1	RAC-alpha serine/threonine-protein kinase	(1), (2), (3), (4), (5), (8), (10), (11), and (12)
P05231	IL6	Interleukin-6	(1), (2), (3), (4), (5), (8), (10), (11), and (12)
P28482	MAPK1	Mitogen-activated protein kinase 1	(1), (2), (3), (5), (8), (9), (10), (11), and (12)
P01375	TNF	Tumor necrosis factor	(1), (2), (3), (4), (5), (8), (10), (11), and (12)
P04637	TP53	Cellular tumor antigen p53	(1), (2), (3), (4), (5), (8), (10), (11), and (12)
P15692	VEGFA	Vascular endothelial growth factor A	(1), (2), (3), (4), (5), (8), (10), (11), and (12)
P42574	CASP3	Caspase-3	(1), (2), (3), (5), (8), (10), (11), and (12)
P02768	ALB	Albumin	(1), (3), (5), (8), (10), (11), and (12)
P45983	MAPK8	Mitogen-activated protein kinase 8	(1), (2), (4), (5), (8), and (10)
P05412	JUN	Transcription factor AP-1	(1), (2), (5), (10), and (11)
P04040	CAT	Catalase	(3), (4), and (12)
P99999	CYCS	Cytochrome c	(3) and (12)
P09238	MMP10	Stromelysin-2	(6) and (7)
P07101	TH	Tyrosine 3-monooxygenase	(4) and (9)
P37023	ACVRL1	Serine/threonine-protein kinase receptor R3	(6)
P01019	AGT	Angiotensinogen	(9)
P09917	ALOX5	Polyunsaturated fatty acid 5-lipoxygenase	(6)
P01185	AVP	Vasopressin-neurophysin 2-copeptin	(9)
Q07812	BAX	Apoptosis regulator BAX	(6)
O15392	BIRC5	Baculoviral IAP repeat-containing protein 5	(6)
P55211	CASP9	Caspase-9	(7)
P20248	CCNA2	Cyclin-A2	(7)
P14635	CCNB1	G2/mitotic-specific cyclin-B1	(7)
P13073	COX4I1	Cytochrome c oxidase subunit 4 isoform 1, mitochondrial	(9)
P02741	CRP	C-reactive protein	(4)
P02778	CXCL10	C-X-C motif chemokine 10	(7)
P00533	EGFR	Epidermal growth factor receptor	(11)
P15407	FOSL1	Fos-related antigen 1	(6)
P15408	FOSL2	Fos-related antigen 2	(6)
Q13224	GRIN2B	Glutamate receptor ionotropic, NMDA 2B	(9)
Q16665	HIF1A	Hypoxia-inducible factor 1-alpha	(9)
P04792	HSPB1	Heat shock protein beta-1	(7)
P05362	ICAM1	Intercellular adhesion molecule 1	(7)
P35225	IL13	Interleukin-13	(7)
P05112	IL4	Interleukin-4	(7)
P01374	LTA	Lymphotoxin-alpha	(6)
P01106	MYC	Myc proto-oncogene protein	(8)
P29474	NOS3	Nitric oxide synthase, endothelial	(9)
O14684	PTGES	Prostaglandin E synthase	(6)
P35354	PTGS2	Prostaglandin G/H synthase 2	(2)
Q15858	SCN9A	Sodium channel protein type 9 subunit alpha	(4)
P16581	SELE	E-selectin	(7)
P07204	THBD	Thrombomodulin	(6)
Q8NER1	TRPV1	Transient receptor potential cation channel subfamily V member 1	(9)
P11473	VDR	Vitamin D3 receptor	(9)

(1): Degree, (2): Maximal Clique Centrality (MCC), (3): Betweenness, (4): BottleNeck, (5): Closeness, (6): ClusteringCoefficient, (7): Density of Maximum Neighborhood Component (DMNC), (8): Edge Percolated Component (EPC), (9): EcCentricity, (10): Maximum Neighborhood Component (MNC), (11): Radiality, and (12): Stress

formula, which has the function of tonifying Qi and nourishing blood, eliminating blood stasis without harming the proper function; Danggui is the secondary herb, which has the effect of invigorating blood and harmonizing blood; Chishao, Chuanxiong, Dilong, Honghua, and Taoren are the adjuvant herbs in this formula; all the five herbs have the function of activating blood circulation and removing blood stasis, promoting the flow of Qi and blood circulation; the combination of the five herbs not only activates blood circulation and removes blood stasis but also helps the Qi and blood that the main herbs benefit to reach the whole body [3, 31]. Studies have shown that BYHWD in combination with neural stem cells (NSCs) attenuates the process of demyelination or improves the recovery of myelin and exerts a synergistic effect on the neurological function recovery [5]. It has been shown that BYHWD restores hindlimb motor function in rats with SCI, and the neuroprotective effect is associated with the regulation of apoptosis-related protein expression [32]. BYHWD rescues axotomized neurons and promotes functional recovery after

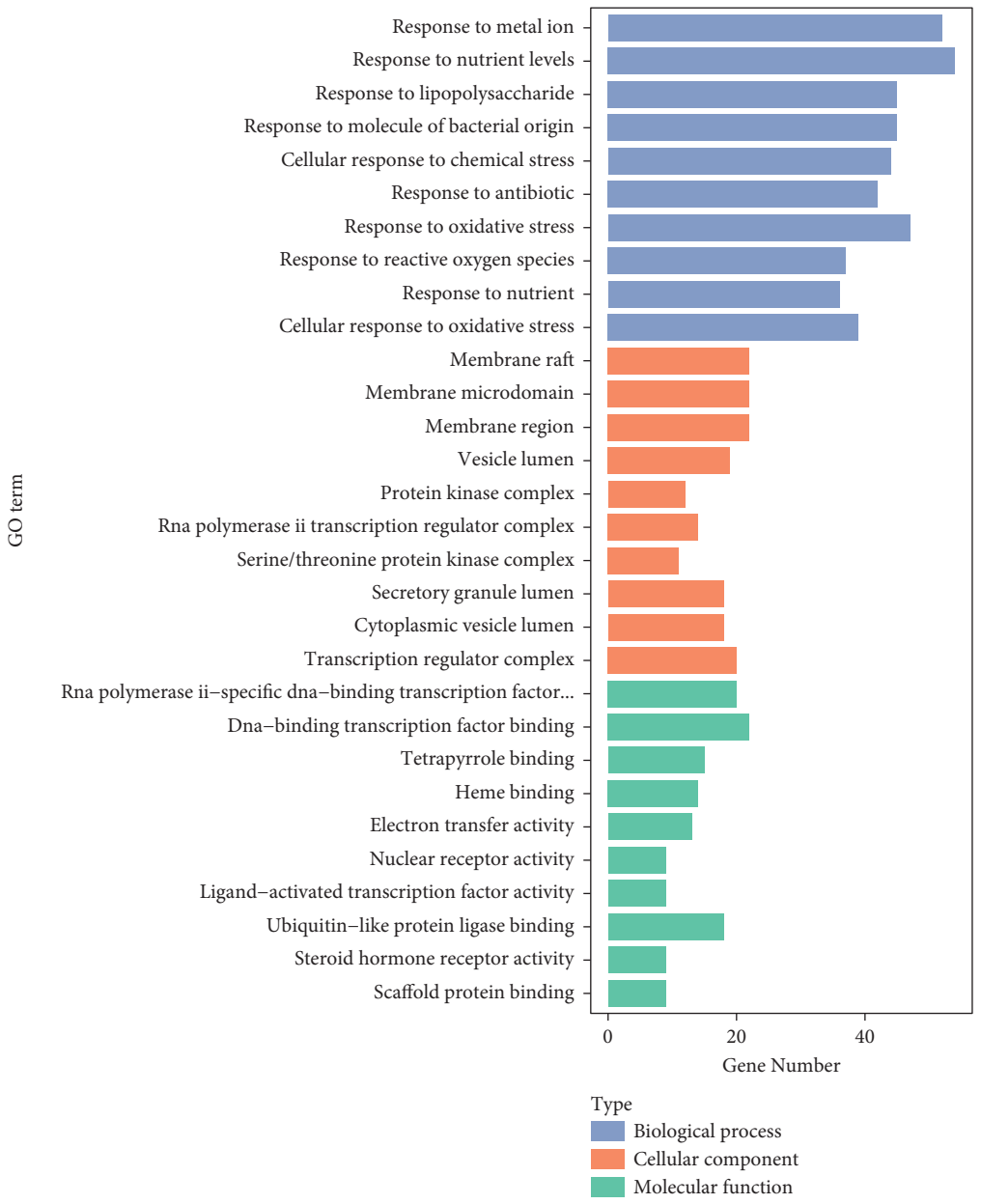

Figure 5: The bar chart of top 10 GO (BP, CC, and MF) enriched items.

spinal cord injury in rats. A study published in 2008 showed that BYHWD protected the injured neurons and promoted functional recovery after SCI in rats [33]. However, since the specific mechanism of BYHWD for the treatment of SCI is still unclear due to its complex composition and wide range of effects, we decided to use a network pharmacology approach to investigate in this study and to lay the foundation for the next in-depth study.

In the first step, BYHWD-related compounds and related targets were obtained. We obtained relevant compounds and targets by mining two herbal-related databases, TCMSP and BATMAN-TCM. The mining methods of these two databases are different: TCMSP database (ADME principle: OB $\geq$ 30 and DL $\geq$ 0.18) first obtains BYHWD-related compounds, then obtains related target proteins, and finally needs to be converted into standard gene names by UniProt database; BATMAN-TCM platform (score cutoff >25, adjusted P value <0.05) directly obtains BYHWD-related compounds and target genes. The screening process of TCMSP database is divided into five steps: (1) the relevant compounds of each component of BYHWD are directly obtained (Chishao: 119, Chuanxiong: 189, Danggui: 125, Huangqi: 87, Honghua: 189, Taoren: 66, and Dilong: 0); (2) the relevant compounds of each component are screened by ADME criteria (Chishao: 29, Chuanxiong: 7, Danggui: 2, Huangqi: 20, Honghua: 22, Taoren: 23, and Dilong: 0); (3) the above compounds are screened again by removing the null targets (Chishao: 14, Chuanxiong: 6, Danggui: 2, Huangqi: 17, Honghua: 17, Taoren: 19, and Dilong: 0); (4) the above compounds are finally screened by removing

Table 2: Top 10 items of Gene Ontology (GO) enrichment analysis.

GO items	ID	Description	P value	Adjusted P value	Gene number
Biological process	GO: 0010038	Response to metal ion	2.68739E−45	1.20529E−41	52
Biological process	GO: 0031667	Response to nutrient levels	2.05974E−40	4.61896E−37	54
Biological process	GO: 0032496	Response to lipopolysaccharide	5.34106E−38	7.98488E−35	45
Biological process	GO: 0002237	Response to molecule of bacterial origin	3.1151E−37	3.4928E−34	45
Biological process	GO: 0062197	Cellular response to chemical stress	1.44121E−35	1.29277E−32	44
Biological process	GO: 0046677	Response to antibiotic	2.54411E−34	1.90172E−31	42
Biological process	GO: 0006979	Response to oxidative stress	3.05284E−34	1.956E−31	47
Biological process	GO: 0000302	Response to reactive oxygen species	9.13447E−34	5.12101E−31	37
Biological process	GO: 0007584	Response to nutrient	2.40193E−33	1.19696E−30	36
Biological process	GO: 0034599	Cellular response to oxidative stress	6.07803E−32	2.726E−29	39
Cellular component	GO: 0045121	Membrane raft	3.92204E−13	7.60946E−11	22
Cellular component	GO: 0098857	Membrane microdomain	4.18102E−13	7.60946E−11	22
Cellular component	GO: 0098589	Membrane region	8.84519E−13	1.07322E−10	22
Cellular component	GO: 0031983	Vesicle lumen	4.00266E−10	3.64242E−08	19
Cellular component	GO: 1902911	Protein kinase complex	5.90811E−10	4.10759E−08	12
Cellular component	GO: 0090575	RNA polymerase II transcription regulator complex	7.53142E−10	4.10759E−08	14
Cellular component	GO: 1902554	Serine/threonine-protein kinase complex	7.89922E−10	4.10759E−08	11
Cellular component	GO: 0034774	Secretory granule lumen	2.08462E−09	9.48503E−08	18
Cellular component	GO: 0060205	Cytoplasmic vesicle lumen	2.53536E−09	1.02541E−07	18
Cellular component	GO: 0005667	Transcription regulator complex	3.48128E−09	1.26718E−07	20
Molecular function	GO: 0061629	RNA polymerase II-specific DNA-binding transcription factor binding	1.80793E−11	7.91763E−09	20
Molecular function	GO: 0140297	DNA-binding transcription factor binding	2.70226E−11	7.91763E−09	22
Molecular function	GO: 0046906	Tetrapyrrole binding	4.34881E−11	8.49468E−09	15
Molecular function	GO: 0020037	Heme binding	1.91194E−10	2.801E−08	14
Molecular function	GO: 0009055	Electron transfer activity	2.62858E−10	3.08069E−08	13
Molecular function	GO: 0004879	Nuclear receptor activity	1.43492E−09	1.20123E−07	9
Molecular function	GO: 0098531	Ligand-activated transcription factor activity	1.43492E−09	1.20123E−07	9
Molecular function	GO: 0044389	Ubiquitin-like protein ligase binding	5.74415E−09	4.20759E−07	18
Molecular function	GO: 0003707	Steroid hormone receptor activity	7.34487E−09	4.78232E−07	9
Molecular function	GO: 0097110	Scaffold protein binding	1.18514E−08	5.67261E−07	9

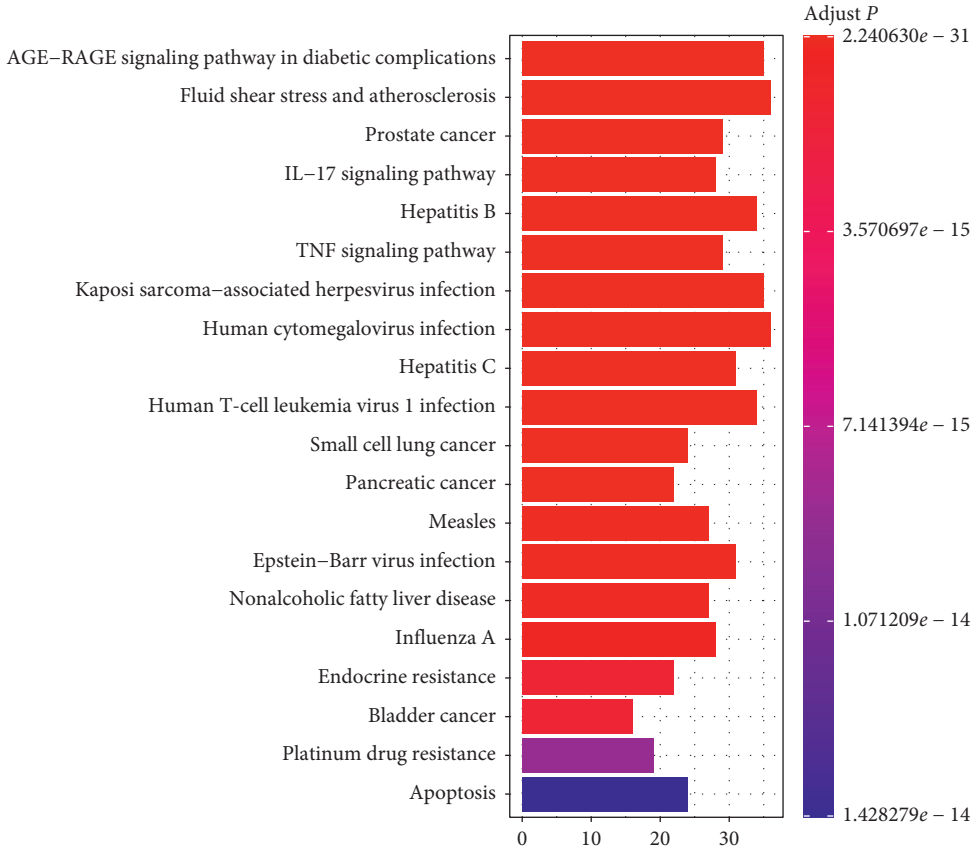

Figure 6: The bar chart of top 20 KEGG enriched pathways.

duplicates (total number of active compounds: 60); and (5) the target proteins corresponding to the obtained active compounds are converted into gene names (total number of targets: 227). And the screening process of BATMAN-TCM platform is divided into two steps: (1) the relevant compounds and targets of each component of BYHWD are directly obtained (Chishao: 8, Chuanxiong: 87, Danggui: 77, Huangqi: 23, Honghua: 22, Taoren: 2, and Dilong: 0), and (2) the relevant compounds of each component are screened after deduplication (total number of active compounds: 189; the total number of targets: 586). The results of the two databases were integrated and deduplicated to finally obtain 244 BYHWD-related active compounds and 744 BYHWD-related targets. In the second step, a total of 923 SCI-related targets were acquired by mining 5 disease databases, including DisGeNET (number: 84), TTD (number: 5), CTD (number: 553), GeneCards (number: 432), and MalaCards (number: 19). Next, the Venn diagram of BYHWD-related targets and SCI-related targets was plotted by the website online tool to obtain 189 potential therapeutic targets of BYHWD against SCI.

In total, Cytoscape software was used four times in this study: (1) the "BYHWD-active compounds-target genes-SCI" network was constructed, involving 410 nodes and 1571 interactions; (2) the PPI network obtained from the STRING database was reconstructed here, involving 189 nodes and 3717 interactions; (3) the top 10 hub genes (AKT1, IL6, MAPK1, TNF, TP53, VEGFA, CASP3, ALB, MAPK8, and JUN) of BYHWD against SCI were obtained based on 12 topological analysis methods (Degree, MCC, Stress, ClusteringCoefficient, EcCentricity, BottleNeck, Closeness, Radiality, Betweenness, EPC, DMNC, and MNC) contained in the CytoHubba plug-in; (4) the "potential therapeutic targets-pathways" network was constructed, involving 347 nodes and 2650 interactions. Studies have shown that the protein encoded by TP53 and other factors regulate the regeneration, germination, and functional recovery of axons after central nervous system injury [34]; the rapid upregulation of CASP3 mRNA seen after SCI in rats may be associated with cell death in the spinal cord [35]; inflammatory mediators such as TNF-α and IL6 mediate the recruitment of inflammatory cells to the site of injury and by targeting these cytokines may be a potential strategy to reduce secondary injury in SCI [36, 37]; by targeting MAPK1, the overexpression of miRNA-433-5p protects motor dysfunction and inflammation after SCI [38].

The Sankey diagram was used once, mainly to show the correspondence between the top 10 hub genes and the corresponding active compounds contained in BYHWD (quercetin, luteolin, beta-carotene, kaempferol, baicalein, beta-sitosterol, carvacrol, O-cresol, anisic acid, 1-methyl-2-dodecyl-4-(1h)-quinolone, 4-ethylresorcinol, angelicin, astragaloside I, astragaloside II, caffeic acid dimethyl ether, cibarian, cordycepin, dihydropinosylvin, dodecenoic acid, ellagic acid, ethyl-P-methoxycinnamate, formononetin, linoleic acid, M-cresol, M-ethylphenol, O-ethylphenol, oleic

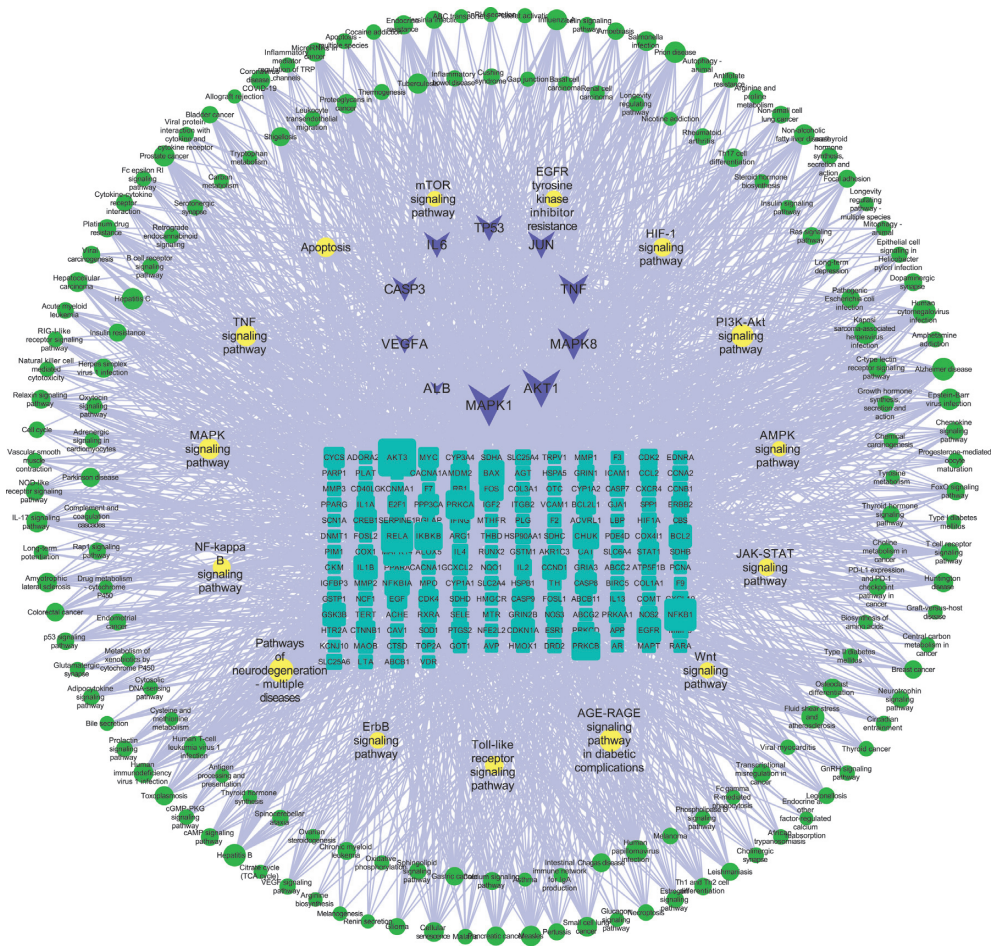

Figure 7: Potential therapeutic targets-pathways" network. The blue diamond represents the top 10 hub genes; the cyan rectangle represents the potential therapeutic targets for BYHWD anti-SCI; the yellow ellipse represents potential SCI-related pathways supported by literature; the green ellipse represents possible pathways related to SCI.

Table 3: The enriched 15 possible related pathways for SCI.

ID	Description	*P* value	Adjusted *P* value	Gene number
hsa04933	AGE-RAGE signaling pathway in diabetic complications	8.58479*E*−34	2.24063*E*−31	35
hsa04668	TNF signaling pathway	8.83261*E*−24	3.84219*E*−22	29
hsa04210	Apoptosis	1.13129*E*−15	1.42828*E*−14	24
hsa05022	Pathways of neurodegeneration - multiple diseases	1.12387*E*−14	1.0476*E*−13	41
hsa04620	Toll-like receptor signaling pathway	5.71758*E*−14	4.52208*E*−13	20
hsa04151	PI3K-Akt signaling pathway	1.43931*E*−13	1.00595*E*−12	34
hsa04066	HIF-1 signaling pathway	1.4646*E*−13	1.00595*E*−12	20
hsa04010	MAPK signaling pathway	5.84978*E*−12	3.39287*E*−11	29
hsa04064	NF-kappa B signaling pathway	7.32616*E*−12	4.1568*E*−11	18
hsa01521	EGFR tyrosine kinase inhibitor resistance	1.25843*E*−09	5.13202*E*−09	14
hsa04012	ErbB signaling pathway	3.21508*E*−08	1.0622*E*−07	13
hsa04630	JAK-STAT signaling pathway	4.40433*E*−07	1.27726*E*−06	16
hsa04310	Wnt signaling pathway	0.000748937	0.001515292	11
hsa04152	AMPK signaling pathway	0.001230137	0.002407294	9
hsa04150	mTOR signaling pathway	0.002091493	0.003927191	10

acid, paeoniflorin, P-cresol, P-ethylphenol, sebiferic acid, sucrose, and thymol). Among them, quercetin targeted six hub genes, luteolin targeted six hub genes, beta-carotene targeted five hub genes, kaempferol targeted four hub genes, baicalein targeted three hub genes, beta-sitosterol targeted two hub genes, anisic acid targeted two hub genes, and the others targeted one hub gene. The experimental results showed that quercetin exerts a protective effect on the spinal cord by inhibiting the activation of the p38MAPK/iNOS signaling pathway in SCI rats and subsequently regulating

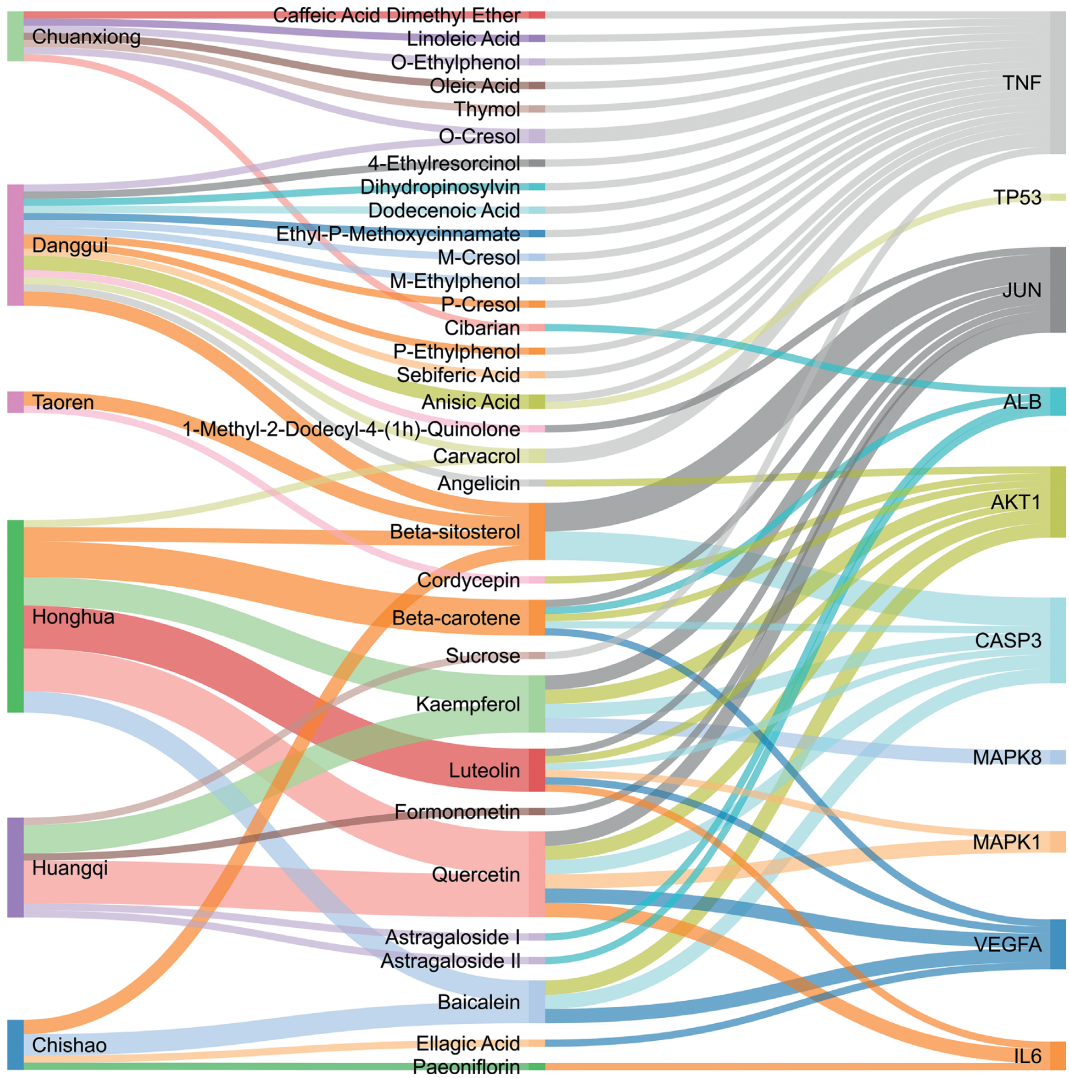

Figure 8: Sankey diagram of "herbs-active compounds-hub genes." The band between the two bars represents a targeting relationship.

secondary oxidative stress [39]; the combination of luteolin and palmitoylethanolamide reduced autophagy in SCI [40]; beta-carotene effectively reduced the course of secondary damage events after SCI by blocking NF-κB pathway activation [41]; baicalein may alleviate the harm caused by SCI by activating PI3K and inducing autophagy to reduce neuronal apoptosis [42].

Based on the results of the Sankey diagram, we performed molecular docking of the top 10 genes and the top 6 compounds in terms of the number of targeted genes (quercetin, luteolin, beta-carotene, kaempferol, baicalein, and beta-sitosterol). The results of molecular docking of 60 cohorts of hub target proteins and key active compounds showed a good binding affinity for both. We used R software twice, once to present the scores of the above molecular docking as a heat map, and another time to perform GO and KEGG pathway enrichment analysis using the ClusterProfiler package.

The top 10 results of the GO enrichment analysis of 189 potential therapeutic targets for BYHWD anti-SCI, based on the adjusted P value (from small to large), are as follows: response to metal ion (GO-BP:0010038), response to nutrient levels (GO-BP:0031667), response to lipopolysaccharide (GO-BP:0032496), response to molecule of bacterial origin (GO-BP:0002237), cellular response to chemical stress (GO-BP: 0062197), response to antibiotic (GO-BP:0046677), response to oxidative stress (GO-BP: 0006979), response to reactive oxygen species (GO-BP:0000302), response to nutrient (GO-BP:0007584), cellular response to oxidative stress (GO-BP: 0034599), membrane raft (GO-CC:0045121), membrane microdomain (GO-CC:0098857), membrane region (GO-CC:0098589), vesicle lumen (GO-CC: 0031983), protein kinase complex (GO-CC: 1902911), RNA polymerase II transcription regulator complex (GO-CC: 0090575), serine/threonine-protein kinase complex (GO-CC:1902554), secretory granule lumen (GO-CC: 0034774), cytoplasmic vesicle lumen (GO-CC: 0060205), transcription regulator complex (GO-CC: 0005667), RNA polymerase II-specific DNA-binding transcription factor binding (GO-MF: 0061629), DNA-binding transcription factor binding (GO-MF:0140297), tetrapyrrole binding (GO-MF:0046906), heme binding (GO-MF:0020037), electron transfer activity

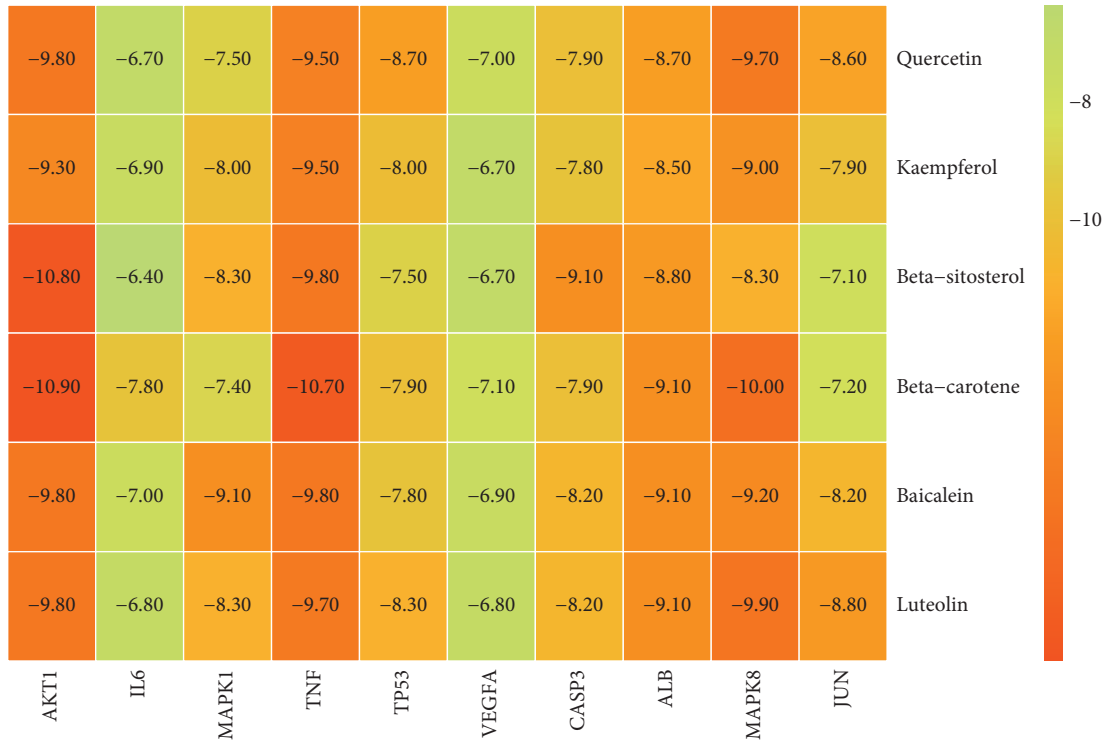

Figure 9: Heatmap of the scores of molecular docking in this study.

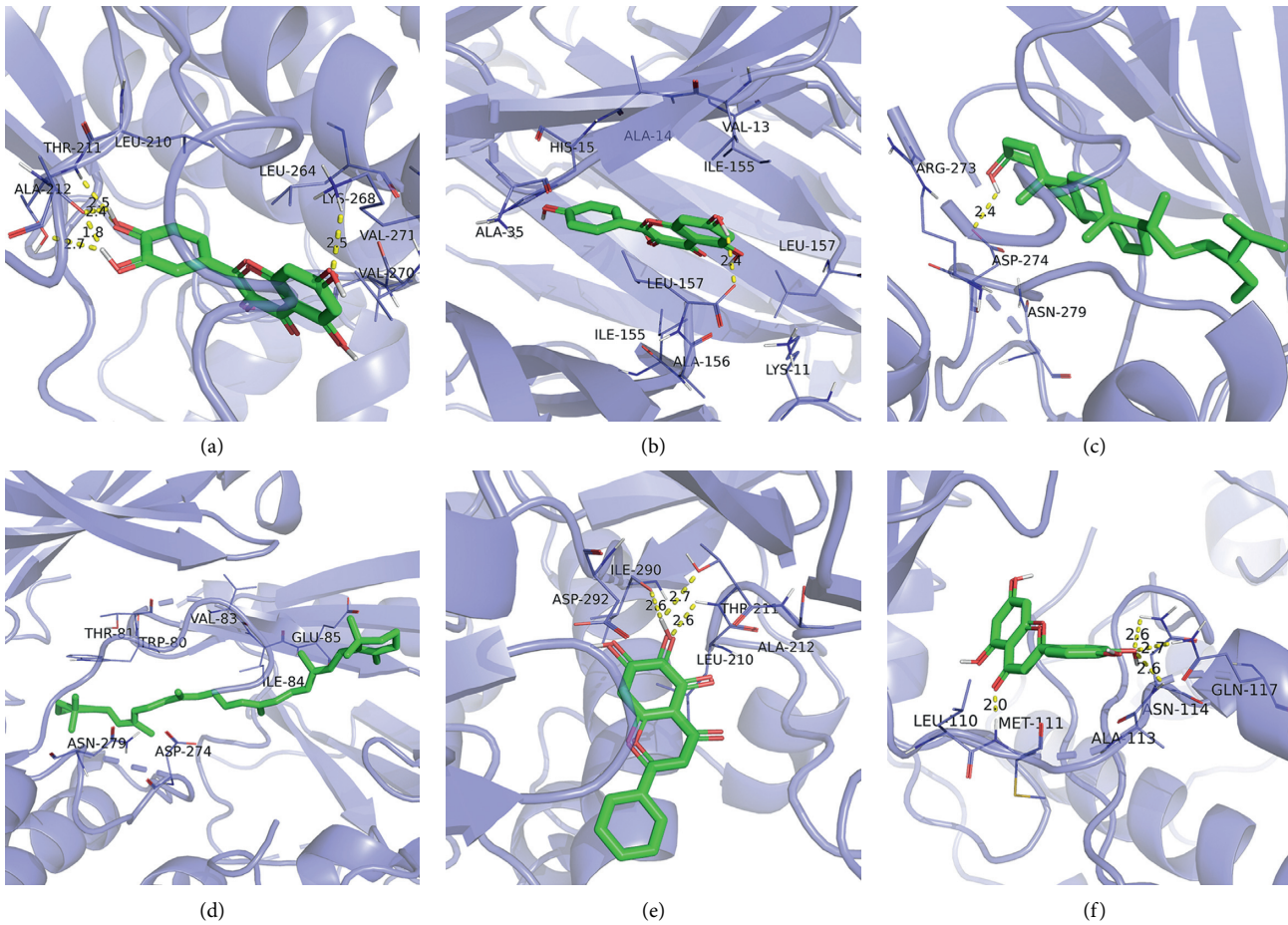

Figure 10: Results of molecular docking between hub genes and key active compounds. (a) Quercetin to AKT1. (b) Kaempferol to TNF. (c) Beta-sitosterol to AKT1. (d) Beta-carotene to AKT1. (e) Baicalein to AKT1. (f) Luteolin to MAPK8.

Table 4: Basic information of active compounds targeting hub genes in BYHWD.

Molecule ID	Molecule name	PubChem CID	OB (%)	DL	2D Structure	Source database	Source	Targeted hub genes
MOL000098	Quercetin	5280343	46.43	0.28	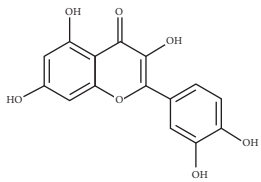	TCMSP	Honghua; Huangqi	AKT1, CASP3, IL6, JUN, MAPK1, and VEGFA
MOL000006	Luteolin	5280445	36.16	0.25	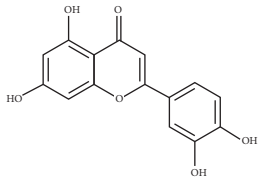	TCMSP	Honghua	AKT1, CASP3, IL6, JUN, MAPK1, and VEGFA
MOL002773	Beta-carotene	5280489	37.18	0.58	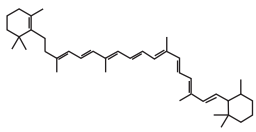	TCMSP	Honghua	AKT1, CASP3, ALB, JUN, and VEGFA
MOL000422	Kaempferol	5280863	41.88	0.24	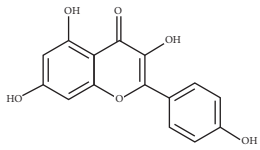	TCMSP	Honghua; Huangqi	AKT1, CASP3, JUN, and MAPK8
MOL002714	Baicalein	5281605	33.52	0.21	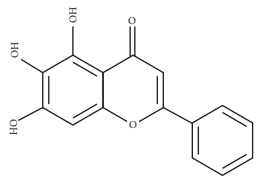	TCMSP	Chishao; Honghua	AKT1, CASP3, and VEGFA
MOL000358	Beta-sitosterol	222284	36.91	0.75	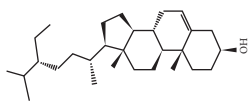	TCMSP	Chishao, Danggui, Honghua, and Taoren	CASP3 and JUN
MOL001002	Ellagic acid	5281855	43.06	0.43	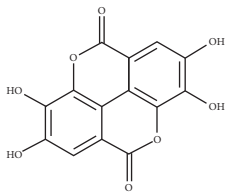	TCMSP	Chishao	VEGFA
MOL001924	Paeoniflorin	442534	53.87	0.79	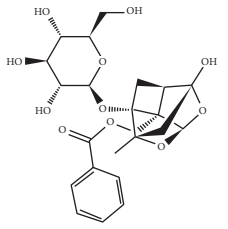	TCMSP	Chishao	IL6
MOL000392	Formononetin	5280378	69.67	0.21	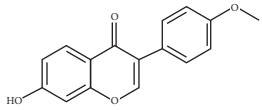	TCMSP	Huangqi	JUN
—	Anisic acid	7478	—	—	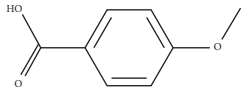	BATMAN-TCM	Danggui	TNF and TP53
—	Caffeic acid dimethyl ether	717531	—	—	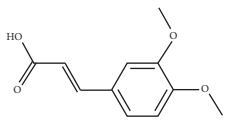	BATMAN-TCM	Chuanxiong	TNF

Table 4: Continued.

Molecule ID	Molecule name	PubChem CID	OB (%)	DL	2D Structure	Source database	Source	Targeted hub genes
—	Cibarian	100275	—	—	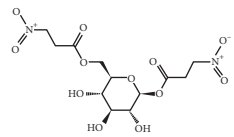	BATMAN-TCM	Chuanxiong	ALB
—	Linoleic acid	5280450	—	—	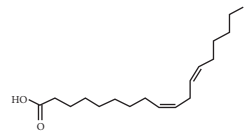	BATMAN-TCM	Chuanxiong	TNF
—	O-Cresol	335	—	—	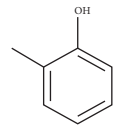	BATMAN-TCM	Chuanxiong	TNF
—	O-Ethylphenol	6997	—	—	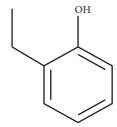	BATMAN-TCM	Chuanxiong	TNF
—	Oleic acid	445639	—	—	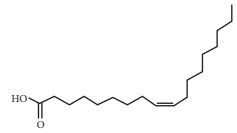	BATMAN-TCM	Chuanxiong	TNF
—	Thymol	6989	—	—	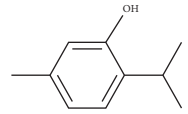	BATMAN-TCM	Chuanxiong	TNF
—	1-Methyl-2-dodecyl-4-(1h)-quinolone	5319601	—	—	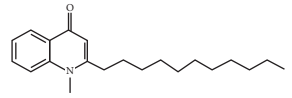	BATMAN-TCM	Danggui	JUN
—	4-Ethylresorcinol	17927	—	—	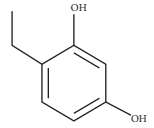	BATMAN-TCM	Danggui	TNF
—	Angelicin	10658	—	—	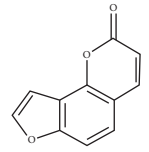	BATMAN-TCM	Danggui	AKT1
—	Carvacrol	10364	—	—	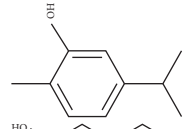	BATMAN-TCM	Danggui	TNF
—	Dihydropinosylvin	442700	—	—	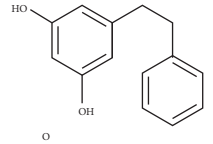	BATMAN-TCM	Danggui	TNF
—	Dodecenoic acid	96204	—	—	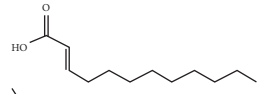	BATMAN-TCM	Danggui	TNF
—	Ethyl-P-methoxycinnamate	5281783	—	—	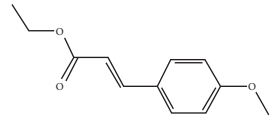	BATMAN-TCM	Danggui	TNF

Table 4: Continued.

Molecule ID	Molecule name	PubChem CID	OB (%)	DL	2D Structure	Source database	Source	Targeted hub genes
—	M-Cresol	342	—	—	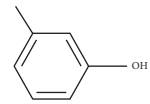	BATMAN-TCM	Danggui	TNF
—	M-Ethylphenol	12101	—	—	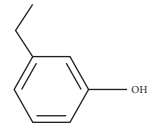	BATMAN-TCM	Danggui	TNF
—	P-Cresol	2879	—	—	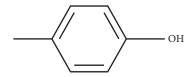	BATMAN-TCM	Danggui	TNF
—	P-Ethylphenol	31242	—	—	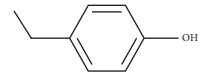	BATMAN-TCM	Danggui	TNF
—	Sebiferic acid	5321206	—	—	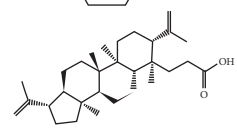	BATMAN-TCM	Danggui	TNF
—	Astragaloside I	13996685	—	—	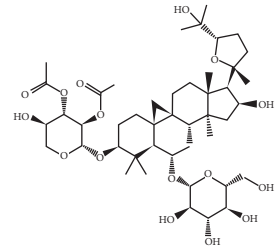	BATMAN-TCM	Huangqi	ALB
—	Astragaloside II	13996693	—	—	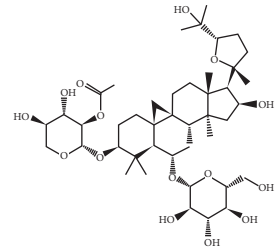	BATMAN-TCM	Huangqi	ALB
—	Sucrose	5988	—	—	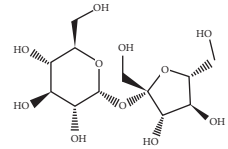	BATMAN-TCM	Huangqi	TNF
—	Cordycepin	6303	—	—	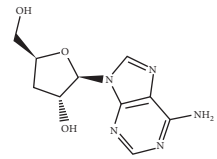	BATMAN-TCM	Taoren	AKT1

OB, oral bioavailability; DL, drug-likeness.

(GO-MF: 0009055), nuclear receptor activity (GO-MF: 0004879), ligand-activated transcription factor activity (GO-MF:0098531), ubiquitin-like protein ligase binding (GO-MF: 0044389), steroid hormone receptor activity (GO-MF: 0003707), and scaffold protein binding (GO-MF:0097110). The first 20 results of the (adjusted *P* value based) KEGG pathway enrichment analysis of 189 potential therapeutic targets of BYHWD against SCI have been presented, and we screened the enriched pathways again to find possible relevant pathways for SCI. By searching the relevant literature, we screened a total of 15 pathways with strong relevance, as follows: AGE-RAGE signaling pathway in diabetic complications (hsa04933) [43], TNF signaling pathway (hsa04668), Apoptosis (hsa04210) [44], Pathways of neurodegeneration-multiple diseases (hsa05022), Toll-like receptor signaling pathway (hsa04620) [45], PI3K-Akt signaling pathway (hsa04151) [46], HIF-1 signaling pathway (hsa04066) [47], MAPK signaling pathway (hsa04010) [48], NF-kappa B signaling pathway (hsa04064) [49], EGFR tyrosine kinase inhibitor resistance (hsa01521) [50], JAK-

STAT signaling pathway (hsa04630) [51], Wnt signaling pathway (hsa04310) [43], AMPK signaling pathway (hsa04152) [44], and mTOR signaling pathway (hsa04150) [46]. The above pathways and hub genes are not in a disconnected relationship; rather, many hub genes are important components of some of the pathways. Taking PI3K-Akt signaling pathway as an example, it contains AKT1, MAPK1, IL6, TP53, and VEGFA. Based on the results of the above network pharmacological analysis, we hypothesize that the key active compounds of BYHWD may exert anti-SCI effects through the above pathways and hub genes.

4.1. Limitations. This study still has some limitations. First, the corresponding experimental validation is lacking. Second, the compounds, targets, and pathways contained in these databases may not be exhaustive. Finally, compounds screened based on ADME principles may be missing other important compounds.

4.2. Future Perspectives. This study uncovered the multicompound, multitarget, and multipathway characteristics of BYHWD through a network pharmacology approach. Among them, the key compounds include quercetin, luteolin, beta-carotene, kaempferol, baicalein, and beta-sitosterol; the hub genes include AKT1, IL6, MAPK1, TNF, TP53, VEGFA, CASP3, ALB, MAPK8, and JUN; and the important pathways are the 15 related pathways mentioned above. These results clearly give a general direction for SCI-related researchers, and there is no doubt that the anti-SCI mechanism of BYHWD is much more than the above-mentioned research directions, and we will find more accurate targets and pathways while exploring them one by one.

5. Conclusion

Using a network pharmacology approach, we explored the potential mechanism of BYHWD as a classical herbal formula for treating nerve injury in the treatment of SCI. The top 10 core genes among the potential therapeutic targets for BYHWD anti-SCI include AKT1, IL6, MAPK1, TNF, TP53, VEGFA, CASP3, ALB, MAPK8, and JUN. Key active compounds of BYHWD against SCI include quercetin, luteolin, beta-carotene, kaempferol, baicalein, and beta-sitosterol. In addition, combining the KEGG pathway enrichment results and reviewing SCI-related literature, we obtained 15 SCI potentially relevant pathways, mainly including PI3K-Akt signaling pathway, MAPK signaling pathway, NF-kappa B signaling pathway, TNF signaling pathway, Apoptosis, Toll-like receptor signaling pathway, HIF-1 signaling pathway, JAK-STAT signaling pathway, Wnt signaling pathway, AMPK signaling pathway, and mTOR signaling pathway. The above analysis results demonstrated the multitarget, multicomponent, and multipathway characteristics of BYHWD in treating SCI, which laid the foundation for us to carry out specific experimental validation in the next step, and provided new ideas for researchers dedicated to the treatment of SCI with herbal extracts.

Data Availability

The data used to support the findings of this study are included within the article.

Disclosure

Zhencheng Xiong and Feng Yang are joint first authors.

Conflicts of Interest

The authors declare that there are no conflicts of interest regarding the publication of this article.

Acknowledgments

This work was supported by the National Natural Science Foundation of China (no. 81873141).

References

[1] G. Courtine and M. V. Sofroniew, "Spinal cord repair: advances in biology and technology," *Nature Medicine*, vol. 25, no. 6, p. 898, 2019.

[2] Y. Zheng, S. Qi, F. Wu et al., "Chinese herbal medicine in treatment of spinal cord injury: a systematic review and meta-analysis of randomized controlled trials," *The American Journal of Chinese Medicine*, vol. 48, no. 7, p. 1593, 2020.

[3] "Current status of traditional Chinese medicine research on spinal cord injury," *World Journal of Integrated Traditional and Western Medicine*, vol. 12, no. 3, p. 440, 2017.

[4] P. Yang, A. Chen, Y. Qin et al., "Buyang huanwu decoction combined with BMSCs transplantation promotes recovery after spinal cord injury by rescuing axotomized red nucleus neurons," *Journal of Ethnopharmacology*, vol. 228, p. 123, 2019.

[5] M. Zhang, Y. Chai, T. Liu, N. Xu, and C. Yang, "Synergistic effects of Buyang Huanwu decoction and embryonic neural stem cell transplantation on the recovery of neurological function in a rat model of spinal cord injury," *Experimental and Therapeutic Medicine*, vol. 9, no. 4, p. 1141, 2015.

[6] Z. P. Guo, M. N. Huang, A. Q. Liu, Y. J. Yuan, J. B. Zhao, and X. F. Mei, "Buyang Huanwu decoction up-regulates Notch1 gene expression in injured spinal cord," *Neural Regeneration Research*, vol. 10, no. 8, p. 1321, 2015.

[7] J. Ru, P. Li, J. Wang et al., "TCMSP: a database of systems pharmacology for drug discovery from herbal medicines," *Journal of Cheminformatics*, vol. 6, no. 13, 2014.

[8] K. Tsaioun, B. Blaauboer, and T. Hartung, "Evidence-based absorption, distribution, metabolism, excretion (ADME) and its interplay with alternative toxicity methods," *ALTEX*, vol. 33, no. 4, p. 343, 2016.

[9] S. Sheng, Z. Yang, F. Xu, and Y. Huang, "Network pharmacology-based exploration of synergistic mechanism of guanxin II formula (II) for coronary heart disease," *Chinese Journal of Integrative Medicine*, vol. 27, no. 2, pp. 106–114, 2021.

[10] T. UniProt Consortium, "UniProt: the universal protein knowledgebase," *Nucleic Acids Research*, vol. 46, no. 5, p. 2699, 2018.

[11] Z. Liu, F. Guo, Y. Wang et al., "BATMAN-TCM: a bioinformatics analysis tool for molecular mechANism of

traditional Chinese medicine," *Scientific Reports*, vol. 6, p. 21146, 2016.

[12] J. Piñero, J. M. Ramírez-Anguita, J. Saüch-Pitarch et al., "The DisGeNET knowledge platform for disease genomics: 2019 update," *Nucleic Acids Research*, vol. 48, no. D1, p. D845, 2020.

[13] G. Stelzer, N. Rosen, I. Plaschkes et al., "The GeneCards suite: from gene data mining to disease genome sequence analyses," *Current Protocols in Bioinformatics*, vol. 54, pp. 1–30, 2016.

[14] N. Rappaport, M. Twik, I. Plaschkes et al., "MalaCards: an amalgamated human disease compendium with diverse clinical and genetic annotation and structured search," *Nucleic Acids Research*, vol. 45, no. D1, p. D877, 2017.

[15] A. Davis, C. Grondin, R. Johnson et al., "Comparative Toxicogenomics database (CTD): update 2021," *Nucleic Acids Research*, vol. 49, no. D1, 2021.

[16] Y. Wang, S. Zhang, F. Li et al., "Therapeutic target database 2020: enriched resource for facilitating research and early development of targeted therapeutics," *Nucleic Acids Research*, vol. 48, no. D1, p. D1031, 2020.

[17] P. Shannon, A. Markiel, O. Ozier et al., "Cytoscape: a software environment for integrated models of biomolecular interaction networks," *Genome Research*, vol. 13, no. 11, p. 2498, 2003.

[18] K. Yang, L. Zeng, A. Ge et al., "Hedysarum multijugum MaximThe effect of .- compound on ischemic stroke: a research based on network and experimental pharmacology," *Oxidative Medicine and Cellular Longevity*, vol. 2020, Article ID 6072380, 2020.

[19] D. Szklarczyk, J. H. Morris, H. Cook et al., "The STRING database in 2017: quality-controlled protein-protein association networks, made broadly accessible," *Nucleic Acids Research*, vol. 45, no. D1, p. D362, 2017.

[20] C. Xu, R. Li, and J. Wu, "Effects of Yuanhu- Zhitong tablets on alcohol-induced conditioned place preference in mice," *Biomedicine & Pharmacotherapy = Biomedecine & Pharmacotherapie*, vol. 133, p. 110962, 2020.

[21] C. Chin, S. Chen, H. Wu, C. Ho, M. Ko, and C. Lin, "cytoHubba: identifying hub objects and sub-networks from complex interactome," *BMC Systems Biology*, vol. S11, 2014.

[22] T. G. O. Consortium, "Gene Ontology consortium: going forward," *Nucleic Acids Research*, vol. 43, p. D1049, 2015.

[23] M. Kanehisa, M. Araki, S. Goto et al., "KEGG for linking genomes to life and the environment," *Nucleic Acids Research*, vol. 36, p. D480, 2008.

[24] G. Yu, L.-G. Wang, Y. Han, and Q.-Y. He, "clusterProfiler: an R package for comparing biological themes among gene clusters," *OMICS: A Journal of Integrative Biology*, vol. 16, no. 5, p. 284, 2012.

[25] O. Trott and A. J. Olson, "AutoDock Vina: improving the speed and accuracy of docking with a new scoring function, efficient optimization, and multithreading," *Journal of Computational Chemistry*, vol. 31, no. 2, p. 455, 2010.

[26] N. Zhu and J. Hou, "Exploring the mechanism of action Xianlingubao Prescription in the treatment of osteoporosis by network pharmacology," *Computational Biology and Chemistry*, vol. 85, p. 107240, 2020.

[27] J. Chang, L. Liu, Y. Wang, Y. Sui, H. Li, and L. Feng, "Investigating the multitarget mechanism of traditional Chinese medicine prescription for cancer-related pain by using network pharmacology and molecular docking approach. Evidence-based complementary and alternative medicine," *eCAM*, vol. 7617261, p. 2020, 2020.

[28] Y. Lu, J. Yang, X. Wang et al., "Research progress in use of traditional Chinese medicine for treatment of spinal cord injury," *Biomedicine & Pharmacotherapy*, vol. 127, p. 110136, 2020.

[29] C. Wu, Y. Zhou, P. Tu et al., "Jisuikang promotes the repair of spinal cord injury in rats by regulating NgR/RhoA/ROCK signal pathway. Evidence-based complementary and alternative medicine," *eCAM*, vol. 9542359, p. 2020, 2020.

[30] H. Xu, Y. Yang, Q. Deng et al., "Governor Vessel electroacupuncture promotes the intrinsic growth ability of spinal neurons through activating calcitonin gene-related peptide/α-calcium/calmodulin-dependent protein kinase/neurotrophin-3 pathway after spinal cord injury," *Journal of Neurotrauma*, vol. 38, no. 6, pp. 734–745, 2020.

[31] Y.-S. Lee, S.-C. Woo, S.-Y. Kim, and J.-Y. Park, "Understanding the multi-herbal composition of Buyang Huanwu Decoction: a review for better clinical use," *Journal of Ethnopharmacology*, vol. 255, Article ID 112765, 2020.

[32] X. Dong, X. He, and W. Gao, "Neuroprotective effects of the Buyang Huanwu decoction on functional recovery in rats following spinal cord injury," *The Journal of Spinal Cord Medicine*, vol. 39, no. 1, p. 85, 2016.

[33] A. Chen, H. Wang, J. Zhang et al., "BYHWD rescues axotomized neurons and promotes functional recovery after spinal cord injury in rats," *Journal of Ethnopharmacology*, vol. 117, no. 3, p. 451, 2008.

[34] Y. Joshi, M. G. Sória, G. Quadrato et al., "The MDM4/MDM2-p53-IGF1 axis controls axonal regeneration, sprouting and functional recovery after CNS injury," *Brain*, vol. 138, no. 7, p. 1843, 2015.

[35] B. A. Citron, P. M. Arnold, C. Sebastian et al., "Rapid upregulation of caspase-3 in rat spinal cord after injury: mRNA, protein, and cellular localization correlates with apoptotic cell death," *Experimental Neurology*, vol. 166, no. 2, p. 213, 2000.

[36] E. Esposito and S. Cuzzocrea, "Anti-TNF therapy in the injured spinal cord," *Trends in Pharmacological Sciences*, vol. 32, no. 2, p. 107, 2011.

[37] J. Kim, H. P. Joshi, S. H. Sheen et al., "Resolvin D3 promotes inflammatory resolution, neuroprotection, and functional recovery after spinal cord injury," *Molecular Neurobiology*, vol. 58, no. 1, p. 424, 2021.

[38] C. L. Zhou, F. Li, X. W. Wu et al., "Overexpression of miRNA-433-5p protects acute spinal cord injury through activating MAPK1," *European Review for Medical and Pharmacological Sciences*, vol. 24, no. 6, p. 2829, 2020.

[39] Y. Song, J. Liu, F. Zhang, J. Zhang, T. Shi, and Z. Zeng, "Antioxidant effect of quercetin against acute spinal cord injury in rats and its correlation with the p38MAPK/iNOS signaling pathway," *Life Sciences*, vol. 92, no. 24-26, p. 1215, 2013.

[40] R. Siracusa, I. Paterniti, G. Bruschetta et al., "The association of palmitoylethanolamide with Luteolin decreases autophagy in spinal cord injury," *Molecular Neurobiology*, vol. 53, no. 6, p. 3783, 2016.

[41] L. Zhou, L. Ouyang, S. Lin et al., "Protective role of β-carotene against oxidative stress and neuroinflammation in a rat model of spinal cord injury," *International Immunopharmacology*, vol. 61, p. 92, 2018.

[42] Y. Li, S. Lin, C. Xu, P. Zhang, and X. Mei, "Triggering of autophagy by Baicalein in response to apoptosis after spinal cord injury: possible involvement of the PI3K activation," *Biological and Pharmaceutical Bulletin*, vol. 41, no. 4, p. 478, 2018.

[43] H. Wang, Z. Zhao, C. Liu et al., "Receptor for advanced glycation end-products (RAGE) blockade do damage to

neuronal survival via disrupting Wnt/β-catenin signaling in spinal cord injury," *Neurochemical Research*, vol. 43, no. 7, p. 1405, 2018.

[44] K. Gao, J. Niu, and X. Dang, "Neuroprotection of melatonin on spinal cord injury by activating autophagy and inhibiting apoptosis via SIRT1/AMPK signaling pathway," *Biotechnology Letters*, vol. 42, no. 10, p. 2059, 2020.

[45] S. Xu, J. Wang, J. Jiang et al., "TLR4 promotes microglial pyroptosis via lncRNA-F630028O10Rik by activating PI3K/AKT pathway after spinal cord injury," *Cell Death & Disease*, vol. 11, no. 8, p. 693, 2020.

[46] Z. Ding, C. Dai, L. Zhong et al., "Neuregulin-1 converts reactive astrocytes toward oligodendrocyte lineage cells via upregulating the PI3K-AKT-mTOR pathway to repair spinal cord injury," *Biomedicine & Pharmacotherapy*, vol. 134, p. 111168, 2021.

[47] H. Chen, J. Li, S. Liang et al., "Effect of hypoxia-inducible factor-1/vascular endothelial growth factor signaling pathway on spinal cord injury in rats," *Experimental and Therapeutic Medicine*, vol. 13, no. 3, p. 861, 2017.

[48] J. Ye, R. Xue, Z. Y. Ji et al., "Effect of NT-3 on repair of spinal cord injury through the MAPK signaling pathway," *European Review for Medical and Pharmacological Sciences*, vol. 24, no. 5, p. 2165, 2020.

[49] C. Wang, T. Xu, B. Lachance et al., "Critical roles of sphingosine kinase 1 in the regulation of neuroinflammation and neuronal injury after spinal cord injury," *Journal of Neuroinflammation*, vol. 18, no. 1, p. 50, 2021.

[50] W. Xue, Y. Zhao, Z. Xiao et al., "Epidermal growth factor receptor-extracellular-regulated kinase blockade upregulates TRIM32 signaling cascade and promotes neurogenesis after spinal cord injury," *Stem Cells*, vol. 38, no. 1, p. 118, 2020.

[51] K. Alexander, H. Tseng, W. Fleming et al., "Inhibition of JAK1/2 tyrosine kinases reduces neurogenic heterotopic ossification after spinal cord injury," *Frontiers in Immunology*, vol. 10, p. 377, 2019.

Hindawi
Evidence-Based Complementary and Alternative Medicine
Volume 2021, Article ID 6643950, 8 pages
https://doi.org/10.1155/2021/6643950

Review Article

Therapeutic Potential of Saffron (*Crocus sativus* L.) in Ischemia Stroke

Shakiba Azami,[1] Zahra Shahriari,[2] Samira Asgharzade,[3] Tahereh Farkhondeh,[4] Mahmood Sadeghi,[4] Fatemeh Ahmadi,[5] Mohammad Mahdi Vahedi,[6] and Fatemeh Forouzanfar [7,8]

[1]*Student Research Committee, Mashhad University of Medical Sciences, Mashhad, Iran*
[2]*Medical Toxicology Research Center, Faculty of Medicine, Mashhad University of Medical Sciences, Mashhad, Iran*
[3]*Cellular and Molecular Research Center, Basic Health Sciences Institute, Shahrekord University of Medical Sciences, Shahrekord, Iran*
[4]*Medical Toxicology and Drug Abuse Research Center (MTDRC), Birjand University of Medical Sciences, Birjand, Iran*
[5]*Department of Clinical Sciences, Faculty of Veterinary Medicine, Ferdowsi University of Mashhad, Mashhad, Iran*
[6]*Department of Pharmacology, Faculty of Medicine, Zahedan University of Medical Sciences, Zahedan, Iran*
[7]*Neuroscience Research Center, Mashhad University of Medical Sciences, Mashhad, Iran*
[8]*Department of Neuroscience, Faculty of Medicine, Mashhad University of Medical Sciences, Mashhad, Iran*

Correspondence should be addressed to Fatemeh Forouzanfar; forouzanfarff@gmail.com

Received 10 December 2020; Revised 4 February 2021; Accepted 17 February 2021; Published 2 March 2021

Academic Editor: Rajeev K Singla

Copyright © 2021 Shakiba Azami et al. This is an open access article distributed under the Creative Commons Attribution License, which permits unrestricted use, distribution, and reproduction in any medium, provided the original work is properly cited.

Stroke is the second leading cause of death and a main cause of disability worldwide. The majority (approximately 80%) of strokes are ischemic. Saffron (*Crocus sativus* L.) has been considered for medicinal purposes since ancient times. Pharmacological effects of saffron are attributed to the presence of crocin, crocetin, picrocrocin, and safranal. In the present review, we summarized the reported neuroprotective effects of saffron and its active constituents against cerebral ischemia stroke. Saffron and its components exert its beneficial effects as an antioxidant, anti-inflammatory, and antiapoptotic agent though inhibition of biochemical, inflammatory, and oxidative stress markers. Taken together, this review indicates that saffron and its ingredients could be a potent candidate in the process of new drug production for the treatment of ischemia stroke.

1. Introduction

Stroke is the second leading cause of death and a major cause of long-term disability worldwide [1]. Over recent decades, the burden of stroke has been highly increased in many regions of the world and, particularly, in developing countries [2]. Notably, as societies are getting older, the demand for long-term care for such illnesses is rising [1]. Ischemic stroke accounts for the highest percentage of all strokes, approximately 80%. The remaining 20% of strokes are hemorrhagic in nature [2, 3]. Cerebral ischemic stroke is the interruption of blood flow to the brain resulting from blood vessel blockage by vascular thrombus formation [4, 5]. Ischemic stroke contributes to tissue damage, neurological deficits, impairment of motor function, epilepsy, and poststroke dementia and may lead to death [6–8]. To date, the number of efficient curative treatments for ischemic stroke is limited. Currently, thrombolytic therapy with tissue plasminogen activator is the most effective treatment, which must be administered within 4.5 hours from ischemic stroke onset [9, 10]. Medicinal plants are invaluable source for the discovery of new therapeutic agents for a wide variety of human ailments [11–13]. The complex pathogenesis of stroke and multifactorial effect of herbal drugs and their active ingredients may indicate the promising future of herbal medicine for stroke treatment. Neuroprotective, anti-inflammatory, antioxidant, antiapoptotic, and vascular protective properties of herbal drugs are believed to be

efficacious in treating stroke [11, 14–16]. Saffron has been extensively used for many medicinal purposes such as a pain reliever and expectorant, as well as for treatment of inflammation, wounds, and abscesses in folk medicine [17, 18]. Recent studies showed the value of saffron and its components in ischemia stroke. Therefore, in the current study, we aimed to review the anti-ischemic activities of saffron. Table 1 shows experimental studies assessing the effect of saffron and its bioactive ingredients on cerebral ischemic stroke.

2. Research Methodology

A comprehensive search of Embase, PubMed, Scopus, and Google Scholar databases was carried out. Different relative keywords including *Crocus sativus*, safranal, stroke, neuroprotection, herbal medicine, and crocin were searched. The search included the papers published up to August 2020.

3. Saffron

Saffron is a valuable dietary spice derived from the flowers of *Crocus sativus* (Iridaceae). Saffron has been known since a long time as an herbal medicine [18, 19]. Saffron is now likely to be such an agent that has aroused physicians' interest [20]. At present, modern pharmacological investigations have demonstrated that saffron and its ingredients have a lot of therapeutic effects such as anticancer [21], antimicrobial [22], antineuropathic pain [23], hypolipidemic [24], antidiabetic [25], antianxiety [26], antitussive [27], antiobesity [28], antitremor [29], hypotensive [30], anticonvulsant [31], antidepressant [32], and antiarthritis effects [33]. Also, gastric ulcer healing [34], memory improvement [35], and management of metabolic syndrome [36] have been reported for this medicinal plant.

3.1. Bioactive Principles of Saffron. The main ingredients of saffron are water, nitrogenous matter, anthocyanins, glycosides, monoterpenes, aldehydes, flavonoids, vitamins (especially riboflavin: 56–138 μg/g and thiamine: 0.7–4 μg/g), volatile oil, proteins, amino acids, carbohydrates, minerals, raw fibers, and gums. Furthermore, picrocrocin (responsible for the bitter taste) and apocarotenoids ingredients such as crocetin, crocin (responsible for the color), and safranal (responsible for odor and aroma) are considered to be the main bioactive constituents [37, 38]. High-quality saffron has approximately 30% crocins, 5 to 15% picrocrocin, and 2.5% volatile compounds, including safranal [39].

4. Experimental Studies Conducted on the Effects of Saffron on Ischemia Stroke

Zhong et al. utilized the ischemic rat model to explore the neuroprotective effects of saffron on late cerebral ischemia injuries. Sprague-Dawley rats were subjected to focal cerebral ischemia induced by middle cerebral artery occlusion (MCAO). Rats were then assigned to six groups: sham, MCAO, Edaravone (as a positive control), and saffron extract (30, 100, and 300 mg/kg for 42 days). Saffron effectively reduced the levels of IL-6 and IL-1β and expressions of glial fibrillary acidic protein (GFAP), neurocan, and phosphocan, quantified by ELISA and Western blot, respectively. It also reduced neurological problems and spontaneous movements as well as anxiety-like behaviors and cognitive impairment, examined by elevated plus maze (EPM), marble burying test (MBT), and novel object recognition test (NORT). Besides, saffron showed anticerebral ischemia properties by reducing the infarct volume and glial scar formation [20].

Abdel-Rahman et al. designed a study to examine the role of vascular endothelial growth factor (VEGF) in the neuroprotective effect of saffron against cerebral ischemia/reperfusion injury (IR) in rats. Focal cerebral ischemia was induced by left MCAO. Wistar rats received only normal saline or saffron at doses of 100 and 200 mg/kg. Saffron was administrated intraperitoneally three weeks before surgery and then administered four times (60 min before surgery, during the surgery, and on 1 day and 2 days post-IR). A significant reduction in the latency to move their bodies and to fall in animals treated with saffron in relation to the control group was observed. According to the findings of this study, reducing oxidative stress and apoptotic proteins and exertion of vascular protection are among the main mechanisms mediating the neuroprotective effect of saffron. Also, the modulation of VEGF by saffron was considered as a pathway arbitrating its neuroprotective and antiapoptotic properties [40].

5. Experimental Studies Conducted on the Effects of Crocin on Ischemia Stroke

In one study, the anti-ischemic effect of crocin in male rats, which underwent a two-hour right MCAO, was investigated. Male rats were randomly divided into four groups: the sham-operated group, the MCAO group, and the crocin groups that were administrated 50 and 100 mg/kg of crocin orally. The treatments were applied for seven days, and rats were operated two h after the last administration. The results showed that the infarction areas and the neurological score decreased in crocin groups. Besides, crocin reduced the level of autophagy following cerebral ischemia by activating mTOR, which is a downregulator of autophagy processes. The results obtained from in vitro study showed that oxygen-glucose deprivation/reoxygenation significantly enhanced the proportion of apoptotic cells. Moreover, transmission electron microscope images demonstrate that the amount of autophagosome increased after oxygen-glucose deprivation/reoxygenation but decreased after treatment with 50 μM crocin [41].

Huang and Jia examined the neuroprotective effect of crocin in the mouse model of hypoxic-ischemic encephalopathy. C57BL/6J mice were subjected to left common carotid artery ligation, and, after one-hour recovery, mice were treated by either hypothermia, crocin (10 mg/kg), or combined treatment. Results displayed that crocin treatment alone decreased brain damage and inflammation after hypoxia-ischemia. Combined treatment of crocin and hypothermia demonstrated increased therapeutic effect

Table 1: Experimental studies assessing the effect of saffron and its bioactive ingredients on cerebral ischemic stroke.

Product	Animal type	Stroke model	Dose administration	Duration of administration	Major effects	References
Saffron hydroalcoholic extract	Male Sprague-Dawley rat	MCAO	30, 100, and 300 mg/kg/day orally	2 h at the first day and once daily from day 2 to day 42 after ischemia	(1) ↓Body weight loss, neurological deficit, spontaneous activity, infarct volume, and glial scar formation. (2) ↓GFAP, neurocan, and phosphocan in ischemic boundary zone. (3) ↓Contents of IL-6 and IL-1β in ischemic boundary zone. (4) ↑Content of IL-10 in ischemic boundary zone.	[20]
Saffron hydroalcoholic extract	Male Wistar rat	MCAO	100 and 200 mg/kg/day intraperitoneally	3 successive weeks before being subjected to left brain I/R and then administered four times (60 min before surgery, during the surgery, and 1 day and 2 days after the I/R)	(1) ↓Latency to move the body. (2) ↓MDA and NO in brain tissue. (3) ↑VEGF in brain tissue. (4) ↓BNP in brain tissue.	[40]
Crocin	Adult male SD rats of specific pathogen-free (SPF) grade	MCAO	50 and 100 mg/kg/day orally	7 days before MCAO induction	(1) ↓Neurological score, infarct volume. (2) ↓p-AMPK/AMPK, LC3-II/I, and ULK1 in brain tissues. (3) ↑p-mTOR/mTOR and p62 in brain tissues.	[41]
Crocin	C57BL/6J mice	Hypoxic-ischemic encephalopathy	5, 10, and 20 mg/kg	Every 12 h, starting immediately or at 2 h after hypoxia-ischemia.	(1) ↓Tissue loss and brain infarction. (2) ↓iNOS and COX-2 mRNA expression in the brain tissues-neurological function recovery.	[42]
Crocin	24-month-old male rat	MCAO	10, 20, 40, and 60 mg/kg, orally	Every two days for 2 months before induction of MCAO	(1) ↓Infarct volume. (2) ↑BBB integrity. (3) ↓Loss of tight junction proteins. (4) ↓Enhanced NADPH oxidase in brain tissues. (5) ↓MMP-2 and MMP-9 level in brain tissues.	[43]
Crocin	Adult female Sprague-Dawley rats	BCCAO	40 mg/kg/day orally	10 days before CCAO induction	(1) ↓Ischemic lesions. (2) ↓Hippocampal TUNEL-positive cells. (3) ↑TAS in brain tissues. (4) ↓OSI in brain tissues. (5) ↓Caspase-3 and HIF-1α in brain tissues	[44]

Table 1: Continued.

Product	Animal type	Stroke model	Dose administration	Duration of administration	Major effects	References
Crocin	Adult male Wistar rat	MCAO	15, 30, 60, and 120 mg/kg intraperitoneally	At the start and 1, 3, and 6 hours after MCAO induction	(1) ↓Neurological deficit and infarct volume. (2) ↑SOD, GPx, and TAC in the cortex of the brain tissue. (3) ↓Brain water content. (4) ↓MDA level in the cortex of the brain tissues.	[45]
Crocin	Adult male Wistar rat	MCAO	50 and 80 mg/kg intraperitoneally	At the start of ischemia	(1) ↓Neurological deficit and infarct volume. (2) ↓Axonal fragmentation, fiber demyelination, and prenecrotic neurons number.	[46]
Crocin	Male ddY mice	MCAO	10 mg/kg intravenously	Before and 3 hours after MCAO induction	↓Infarct volume.	[49]
Safranal	Adult male NMRI rat	Global cerebral ischemia was induced using the four-vessel occlusion method	727.5, 363.75, 145.5, and 72.75 mg/kg intraperitoneally	5 min prior to reperfusion and the administration was continued every 24 hours for 72 hours after the induction of ischemia	(1) ↓MDA level in brain tissues. (2) ↑Antioxidant capacity in brain tissues. (3) ↑Total thiol concentration in brain tissues.	[51]
Safranal	Adult male Wistar rat	MCAO	72.5 and 145 mg/kg intraperitoneally	0, 3, and 6 hours after induction of MCAO	(1) ↓Neurological score, infarct volume, and hippocampal cell loss. (2) ↓MDA level in brain tissue. (3) ↑Antioxidant capacity in brain tissue.	[50]

SD, Sprague-Dawley; MCAO, middle cerebral artery occlusion; BCCAO, bilateral common carotid artery occlusion; GFAP, glial fibrillary acidic protein; MDA, malondialdehyde; GPx, glutathione peroxidase; NO, nitric oxide; TAC, total antioxidant capacity; VEGF, vascular endothelial growth factor; BNP, brain natriuretic peptide; BBB, blood-brain barrier; ULK, Unc-51 like autophagy activating kinase; NADPH, nicotinamide adenine dinucleotide phosphate; MMP, matrix metallopeptidase; SOD, superoxide dismutase.

compared with single treatment, resulting in markedly less brain injury, decreased oxidative and inflammatory responses, and improved functional outcome. Their result demonstrated the beneficial effect of crocin as a part of combined therapy to enhance the neuroprotective effect of hypothermia and reduce hypoxia [42].

The therapeutic effect of crocin in improving the blood-brain barrier (BBB) disruption following MCAO was evaluated. 24-month-old rats randomly received either vehicle (controls) or crocin (10, 20, 40, or 60 mg/kg) every alternate day for two months before ischemia induction. In the presence of cerebral ischemia, crocin saved the BBB function. Besides, loss of tight junction complexes, the activity of matrix metallopeptidase (MMP), and increased NADPH oxidase were all attenuated in the crocin-treated group. These findings revealed that the antioxidant capacity of crocin could ameliorate the ischemia-induced damage [43].

Another study showed that crocin pretreatment (40 mg/kg for ten days) once daily attenuated apoptosis, probably mediated by decreasing oxidative stress index and increasing total antioxidant capacity (TAC) induced by reactive oxygen species (ROS) generation and inhibiting the protein expression of HIF-1α, TUNEL, and caspase-3 in a rat global cerebral IR induced by bilateral common carotid artery occlusion (BCCAO), followed by 30-minute reperfusion [44].

Crocin treatment (30, 60, and 120 mg/kg) markedly reduced infarct volume by 64%, 74%, and 73%, respectively, in a rat model of transient focal cerebral ischemia. Indeed,

the most effective dose of crocin was 60 mg/kg and suggested that higher doses do not have more protective effect. Administration of crocin (60 mg/kg) 1 hour before, at the start, or 1 hour after ischemia decreased brain edema by 48%, 52%, and 51%, respectively. Furthermore, crocin (60 mg/kg) markedly decreased the level of malondialdehyde (MDA) and enhanced activity of glutathione peroxidase (GPx) and superoxide dismutase (SOD) in the ischemic cortex [45].

Using an MCAO rat model, Sarshoori et al. explored the histopathological manifestations of transient focal cerebral ischemia in response to crocin intraperitoneal injection. Briefly, Wistar rats were treated by intraperitoneal injection of 50 and 80 mg/kg of crocin at the start of ischemia. A significant decrease in infarct volume was evident in the cortex and striatum at the right hemispheres of the crocin group 24 hours after ischemia. However, 80 mg/kg of crocin exerted a higher efficacy. Another histopathological finding was that crocin effectively reduced axonal fragmentation, fiber demyelination, and prenecrotic neurons number in the ischemic areas. This study concluded that crocin is sufficient to suppress ischemia-induced damage by preventing the alternations of histopathological parameters [46].

Transient global cerebral I/R markedly promoted the generation of nitric oxide (NO) and the activity of nitric oxide synthase (NOS). The reperfusion led to serious edema with mitochondrial injuries in the cortical microvascular endothelial cells, as well as increased membrane G protein-coupled receptor kinase 2 (GRK2) expression, and decreased cytosol GRK2 expression. Besides, increased phosphorylation of extracellular signal-regulated kinase1/2 (ERK1/2) and reduced expression of MMP-9 were detected in cortical microvessels after I/R (20 min/24 h). As well as the positive control crocin (20 mg/kg, 21 days), pretreatment with Weinaokang, which contains active compounds of Ginkgo, Ginseng, and saffron, on ischemic injuries (20, 10 mg/kg, 21 days) significantly inhibited nitrative injury and modulated the ultrastructure of cortical microvascular endothelial cells. Besides, Weinaokang inhibited GRK2 translocation from cytosol to the membrane (at 20 mg/kg) and decreased MMP-9 expression and ERK1/2 phosphorylation in cortical microvessels [47].

Zhang et al. [48] showed that oral administration of crocin had better effectiveness in cerebral protection than an intravenous injection. Crocin and its metabolite crocetin were not detected in the brain of cerebral I/R rats, indicating a target site of periphery. After oral administration of crocin instead of intravenous injection, abundant crocetin was found in plasma. Indeed, oral administration of crocetin displayed similar cerebral protection to that of crocin, but this effect was not clearly found by intravenous crocetin administration, representing the importance of crocetin in gut. Furthermore, orally administered crocin demonstrated less cerebral-protective effect in pseudo-germ-free MCAO rats.

Among saffron's ingredients, crocin was the most effective in promoting mRNA expression of gamma-glutamylcysteine synthase, which contributes to glutathione synthesis as the rate-limiting enzyme, and the carotenoid markedly decreased infarcted areas caused by MCAO in mice [49].

6. Experimental Studies Conducted on the Effects of Safranal on Ischemia Stroke

Sadeghnia et al. utilized the rat models of transient MCAO, which continued by 24 hours of reperfusion. Safranal (72.5 and 145 mg/kg) was administrated intraperitoneally by 0, 3, and 6 hours after reperfusion. Compared with the control animals, the level of MDA significantly decreased in safranal groups, while total sulfhydryl (SH) and antioxidant power showed a considerable increase. The percentages of degenerated hippocampal cells, mean infarct volume, and neurological deficits were reduced with both doses of safranal. Collectively, safranal exerted an explicit neuroprotective effect on transient focal cerebral ischemia [50]. One study showed that administration of safranal increased the total SH contents and antioxidant capacity in hippocampus of rats with transient global cerebral ischemia. Besides, administration of safranal reduced the MDA level in hippocampus of rats with transient global cerebral ischemia [51].

In a recent study by Forouzanfar et al. [52], oxygen-glucose deprivation exposure decreased the cell viability and enhanced intracellular ROS production, apoptosis, and oxidative DNA damage, in comparison with untreated control PC12 cells. Pretreatment with safranal (40 and 160 μM) markedly attenuated cell death, apoptosis, and oxidative damage induced by oxygen-glucose deprivation in PC12 cells. Additionally, safranal significantly decreased the overexpression of Bax/Bcl-2 ratio and active caspase-3 following oxygen-glucose deprivation.

7. Human Studies Conducted on the Effects of Saffron on Ischemia Stroke

Fifty ischemic stroke patients with specific severity of symptoms at admission (National Institute of Health Stroke Scale (NIHSS) score = 5–20) and less than 24 h since the onset of stroke were randomly assigned to receive either routine stroke care (control group) or routine care plus aqueous extract of saffron capsule (200 mg/day) (saffron group). Patients in both groups were monitored for the study days including four days of hospital stay and the following three months. In saffron group, the severity of stroke during the first four days was reduced compared to the control group. Compared to the concentrations on the first day, serum neuron specific enolase and s100 levels were markedly reduced and brain-derived neurotrophic factor (BDNF) level was enhanced in the saffron group on the fourth day. At the end of the three-month follow-up period, the mean Barthel index was markedly higher in the saffron group compared to the control group [53].

A recent study has been conducted to evaluate the role of aqueous extract of saffron in decreasing oxidative stress among patients with ischemic stroke. Forty ischemic stroke patients with NIHSS score = 5–20 less than 24 h since the onset of stroke were randomly divided into two groups: control group and saffron group. The patients in control group received routine stroke care and the patients in saffron group received routine care plus capsule of saffron 400 mg/

day (200 mg twice daily) over a period of four days. On the fourth day after the onset of ischemic stroke, the saffron-treated group had higher levels of antioxidant enzymes activities and GSH and TAC levels than the control group, while MDA concentration was lower. Furthermore, the severity of stroke was markedly decreased after 4 days in the saffron-treated group. The severity of stroke was negatively associated with the GSH and TAC concentrations and positively associated with the MDA concentration [54].

8. Possible Mechanism of Neuroprotective Potency of Saffron and Its Ingredients in Ischemia Stroke

Several investigations attempted to clarify the mechanisms underlying the neuroprotective function of saffron and its active derivatives in ischemia stroke. Oxidative stress is caused by an imbalance between prooxidants and antioxidants, resulting in overproduction of ROS. ROS are biphasic and are involved in natural physiological processes as well as in a number of disease processes, thereby mediating damage to cellular structures such as lipids, membranes, proteins, and DNA [55, 56]. The cerebral vasculature is a main target of oxidative stress which plays a major role in the pathogenesis of ischemic brain injury after cerebrovascular attack [55, 56]. Consequently, oxidative stress contributes directly to necrosis and apoptosis via a number of pathways in ischemic tissue [57, 58]. Previous studies showed that saffron exhibited a potential antioxidant and antiapoptotic property, which is attributed to the bioactive ingredients of saffron [40, 50, 59]. Brain edema, as a result of ischemic stroke, could be attributed to the elevated brain natriuretic peptide (BNP) level [60]. Saffron has exhibited a substantial effect on decreasing BNP in brain of I/R rats. It is suggested that saffron-induced BNP lowering may be due to its antioxidant properties [40].

Recently, it has been reported that saffron effectively enhanced the expression of VEGF in ischemic boundary zone, which plays a critical role in cerebral protection after I/R injuries [40]. Indeed, VEGF confers neuroprotection and promotes neurogenesis and cerebral angiogenesis [61]. Brain ischemia leads to an acute and prolonged inflammatory process, characterized by rapid activation of resident cells (mainly microglia), production of proinflammatory mediators, and infiltration of numerous types of inflammatory cells (including neutrophils, different subtypes of T cells, monocyte/macrophages, and other cells) into the ischemic brain tissue [62, 63]. Recent experiment has found that saffron could attenuate inflammation in the ischemic brain [20, 42].

9. Conclusion

Collectively, the data from the referred experiments provide insight into the beneficial effect of saffron and its derivatives, particularly safranal and crocin, against neural injuries in the cerebral ischemia. The studies indicated that administration of saffron or its ingredients could make a notable contribution to the prevention of histopathological alternation as well as improvement of neurological deficit. However, several investigations have noted that the downregulation of apoptosis, inflammation, and autophagy, alleviation of glial scar formation, prevention of oxidative stress, and reduction of brain edema are among the most mentioned mechanisms mediating the saffron efficacy. Thus, saffron and its active constituents can be a candidate as therapeutic agent, either alone or in a combined form, with current strategies for ischemia stroke treatment.

Data Availability

No data were used to support this study.

Conflicts of Interest

The authors declare that they have no conflicts of interest.

Supplementary Materials

Graphic abstract: saffron and its ingredients showed protective effect against ischemia stroke. (*Supplementary Materials*)

References

[1] M. Katan and A. Luft, "Global burden of stroke," *Seminars in Neurology*, vol. 38, no. 2, pp. 208–211, 2018.

[2] E. S. Donkor, "Stroke in the 21st century: a snapshot of the burden, epidemiology, and quality of life," *Stroke Research and Treatment*, vol. 2018, Article ID 3238165, 10 pages, 2018.

[3] A. K. Boehme, C. Esenwa, and M. S. V. Elkind, "Stroke risk factors, genetics, and prevention," *Circulation Research*, vol. 120, no. 3, pp. 472–495, 2017.

[4] Y. Huang and J. O. McNamara, "Ischemic stroke: "acidotoxicity" is a perpetrator," *Cell*, vol. 118, no. 6, pp. 665-666, 2004.

[5] R. H. C. Lee, M. H. H. Lee, C. Y. C Wu et al., "Cerebral ischemia and neuroregeneration," *Neural Regeneration Research*, vol. 13, no. 3, pp. 373–385, 2018.

[6] P. M. Rothwell, A. Algra, and P. Amarenco, "Medical treatment in acute and long-term secondary prevention after transient ischaemic attack and ischaemic stroke," *The Lancet*, vol. 377, no. 9778, pp. 1681–1692, 2011.

[7] O. B. C. Swayne, J. C. Rothwell, N. S. Ward, and R. J. Greenwood, "Stages of motor output reorganization after hemispheric stroke suggested by longitudinal studies of cortical physiology," *Cerebral Cortex*, vol. 18, no. 8, pp. 1909–1922, 2008.

[8] L. Lorente, M. M. Martín, A. Pérez-Cejas et al., "Association between total antioxidant capacity and mortality in ischemic stroke patients," *Annals of Intensive Care*, vol. 6, no. 1, p. 39, 2016.

[9] R. E. Hughes, P. Tadi, and P. C. Bollu, *TPA Therapy*StatPearls Publishing, Treasure Island, FL, USA, 2019.

[10] Y. Shi, R. K. Leak, R. F. Keep, and J. Chen, "Translational stroke research on blood-brain barrier damage: challenges, perspectives, and goals," *Translational Stroke Research*, vol. 7, no. 2, pp. 89–92, 2016.

[11] B. P. Gaire, "Herbal medicine in ischemic stroke: challenges and prospective," *Chinese Journal of Integrative Medicine*, vol. 24, no. 4, pp. 243–246, 2018.

[12] A. K. Shakya, "Medicinal plants: future source of new drugs," *International Journal of Herbal Medicine*, vol. 4, no. 4, pp. 59–64, 2016.

[13] A. E. Al-Snafi, T. A. Talab, and W. J. Majid, "Medicinal plants with central nervous activity-an overview (Part 1)," *IOSR Journal of Pharmacy*, vol. 9, no. 3, pp. 52–102, 2019.

[14] G. Deng, C. Ma, H. Zhao et al., "Anti-edema and antioxidant combination therapy for ischemic stroke via glyburide-loaded betulinic acid nanoparticles," *Theranostics*, vol. 9, no. 23, pp. 6991–7002, 2019.

[15] Z. Pan, M. Cui, G. Dai et al., "Protective effect of anthocyanin on neurovascular unit in cerebral ischemia/reperfusion injury in rats," *Frontiers in Neuroscience*, vol. 12, p. 947, 2018.

[16] S. Asgharzade, R. D. E. Sewell, Z. Rabiei, F. Forouzanfar, S. Kazemi Sheikhshabani, and M. Rafieian-Kopaei, "Hydro-alcoholic extract of *Anchusa italica* protects global cerebral ischemia-reperfusion injury via a nitrergic mechanism," *Basic and Clinical Neuroscience Journal*, vol. 11, no. 3, p. 323, 2020.

[17] T. Ziaee, B. M. Razavi, and H. Hosseinzadeh, "Saffron reduced toxic effects of its constituent, safranal, in acute and subacute toxicities in rats," *Jundishapur Journal of Natural Pharmaceutical Products*, vol. 9, no. 1, pp. 3–8, 2014.

[18] A. R. Khorasany and H. Hosseinzadeh, "Therapeutic effects of saffron (*Crocus sativus* L.) in digestive disorders: a review," *Iranian Journal of Basic Medical Sciences*, vol. 19, no. 5, pp. 455–469, 2016.

[19] S. Z. Mousavi and S. Z. Bathaie, "Historical uses of saffron: identifying potential new avenues for modern research," *Avicenna Journal of Phytomedicine*, vol. 1, no. 2, pp. 57–66, 2011.

[20] K. Zhong, R. X. Wang, X. D. Qian et al., "Neuroprotective effects of saffron on the late cerebral ischemia injury through inhibiting astrogliosis and glial scar formation in rats," *Biomedicine and Pharmacotherapy*, vol. 126, p. 110041, 2020.

[21] F. I. Abdullaev, "Cancer chemopreventive and tumoricidal properties of saffron (*Crocus sativus* L.)," *Experimental Biology and Medicine*, vol. 227, no. 1, pp. 20–25, 2002.

[22] H. Vahidi, M. Kamalinejad, and N. Sedaghati, "Antimicrobial properties of *Crocus sativus* L." *Iranian Journal of Pharmaceutical Research*, vol. 1, no. 1, pp. 33–35, 2010.

[23] H. A. Safakhah, T. Taghavi, A. Rashidy-Pour et al., "Effects of saffron (*Crocus sativus* L.) stigma extract and its active constituent crocin on neuropathic pain responses in a rat model of chronic constriction injury," *Iranian journal of pharmaceutical research: IJPR*, vol. 15, no. 1, pp. 253–261, 2016.

[24] S. M. B. Asdaq and M. N. Inamdar, "Potential of *Crocus sativus* (saffron) and its constituent, crocin, as hypolipidemic and antioxidant in rats," *Applied Biochemistry and Biotechnology*, vol. 162, no. 2, pp. 358–372, 2010.

[25] J. Bajerska, S. Mildner-Szkudlarz, T. Podgórski, and E. Oszmatek-Pruszyńska, "Saffron (*Crocus sativus* L.) powder as an ingredient of rye bread: an anti-diabetic evaluation," *Journal of Medicinal Food*, vol. 16, no. 9, pp. 847–856, 2013.

[26] N. Pitsikas, "Constituents of saffron (*Crocus sativus* L.) as potential candidates for the treatment of anxiety disorders and schizophrenia," *Molecules*, vol. 21, no. 3, p. 303, 2016.

[27] H. Hosseinzadeh and J. Ghenaati, "Evaluation of the anti-tussive effect of stigma and petals of saffron (*Crocus sativus*) and its components, safranal and crocin in Guinea pigs," *Fitoterapia*, vol. 77, no. 6, pp. 446–448, 2006.

[28] M. Mashmoul, A. Azlan, H. Khaza'ai, B. Yusof, and S. Noor, "Saffron: a natural potent antioxidant as a promising anti-obesity drug," *Antioxidants*, vol. 2, no. 4, pp. 293–308, 2013.

[29] B. Amin, M. Malekzadeh, M. R. Heidari, and H. Hosseinzadeh, "Effect of *Crocus sativus* extracts and its active constituent safranal on the harmaline-induced tremor in mice," *Iranian Journal of Basic Medical Sciences*, vol. 18, no. 5, pp. 449–458, 2015.

[30] M. Imenshahidi, H. Hosseinzadeh, and Y. Javadpour, "Hypotensive effect of aqueous saffron extract (*Crocus sativus* L.) and its constituents, safranal and crocin, in normotensive and hypertensive rats," *Phytotherapy Research*, vol. 24, no. 7, pp. 990–994, 2010.

[31] H. Hosseinzadeh and V. Khosravan, "Anticonvulsant effects of aqueous ana ethanolic extracts of *Crocus sativus* L stigmas in mice," *Archives of Iranian Medicine*, vol. 5, no. 1, pp. 44–47, 2002.

[32] A. L. Lopresti and P. D. Drummond, "Saffron (*Crocus sativus*) for depression: a systematic review of clinical studies and examination of underlying antidepressant mechanisms of action," *Human Psychopharmacology: Clinical and Experimental*, vol. 29, no. 6, pp. 517–527, 2014.

[33] W. Liu, Y. Sun, Z. Cheng, Y. Guo, P. Liu, and Y. Wen, "Crocin exerts anti-inflammatory and anti-arthritic effects on type II collagen-induced arthritis in rats," *Pharmaceutical Biology*, vol. 56, no. 1, pp. 209–216, 2018.

[34] E. Tamaddonfard, A. Erfanparast, A. A. Farshid et al., "Safranal, a constituent of saffron, exerts gastro-protective effects against indomethacin-induced gastric ulcer," *Life Sciences*, vol. 224, pp. 88–94, 2019.

[35] J. W. Finley and S. Gao, "A perspective on *Crocus sativus* L. (Saffron) constituent crocin: a potent water-soluble antioxidant and potential therapy for Alzheimer's disease," *Journal of Agricultural and Food Chemistry*, vol. 65, no. 5, pp. 1005–1020, 2017.

[36] B. M. Razavi and H. Hosseinzadeh, "Saffron: a promising natural medicine in the treatment of metabolic syndrome," *Journal of the Science of Food and Agriculture*, vol. 97, no. 6, pp. 1679–1685, 2017.

[37] H. B. Bostan, S. Mehri, and H. Hosseinzadeh, "Toxicology effects of saffron and its constituents: a review," *Iranian Journal of Basic Medical Sciences*, vol. 20, no. 2, pp. 110–121, 2017.

[38] S. Ghaffari and N. Roshanravan, "Saffron; an updated review on biological properties with special focus on cardiovascular effects," *Biomedicine & Pharmacotherapy*, vol. 109, pp. 21–27, 2019.

[39] M. Schmidt, G. Betti, and A. Hensel, "Saffron in phytotherapy: pharmacology and clinical uses," *Wiener Medizinische Wochenschrift*, vol. 157, no. 13-14, pp. 315–319, 2007.

[40] R. F. Abdel-Rahman, S. A. El Awdan, R. R. Hegazy, D. F. Mansour, H. A. Ogaly, and M. Abdelbaset, "Neuroprotective effect of *Crocus sativus* against cerebral ischemia in rats," *Metabolic Brain Disease*, vol. 35, no. 3, pp. 427–439, 2020.

[41] Z. Huang, J. Xu, X. Huang et al., "Crocin induces anti-ischemia in middle cerebral artery occlusion rats and inhibits autophagy by regulating the mammalian target of rapamycin," *European Journal of Pharmacology*, vol. 857, p. 172424, 2019.

[42] A. Huang and L. Jia, "Crocin enhances hypothermia therapy in hypoxic ischemia-induced brain injury in mice," *Acta Neurologica Belgica*, 2019.

[43] X. Zhang, Z. Fan, and T. Jin, "Crocin protects against cerebral-ischemia-induced damage in aged rats through maintaining the integrity of blood-brain barrier," *Restorative Neurology and Neuroscience*, vol. 35, no. 1, pp. 65–75, 2017.

[44] S. Oruc, Y. Gönül, K. Tunay et al., "The antioxidant and antiapoptotic effects of crocin pretreatment on global cerebral ischemia reperfusion injury induced by four vessels occlusion in rats," *Life Sciences*, vol. 154, pp. 79–86, 2016.

[45] A. Vakili, M. R. Einali, and A. R. Bandegi, "Protective effect of crocin against cerebral ischemia in a dose-dependent manner in a rat model of ischemic stroke," *Journal of Stroke and Cerebrovascular Diseases*, vol. 23, no. 1, pp. 106–113, 2014.

[46] J. R. Sarshoori, M. H. Asadi, and M. T. Mohammadi, "Neuroprotective effects of crocin on the histopathological alterations following brain ischemia-reperfusion injury in rat," *Iranian Journal of Basic Medical Sciences*, vol. 17, no. 11, pp. 895–902, 2014.

[47] Y.-Q. Zheng, J.-X. Liu, X.-Z. Li, and L. Xu, "Effects and mechanism of Weinaokang (维脑康) on reperfusioninduced vascular injury to cerebral microvessels after global cerebral ischemia," *Chinese Journal of Integrative Medicine*, vol. 16, no. 2, pp. 145–150, 2010.

[48] Y. Zhang, J. Geng, Y. Hong et al., "Orally administered crocin protects against cerebral ischemia/reperfusion injury through the metabolic transformation of crocetin by gut microbiota," *Frontiers in Pharmacology*, vol. 10, p. 440, 2019.

[49] T. Ochiai, H. Shimeno, K.-I. Mishima et al., "Protective effects of carotenoids from saffron on neuronal injury in vitro and in vivo," *Biochimica et Biophysica Acta (BBA)-General Subjects*, vol. 1770, no. 4, pp. 578–584, 2007.

[50] H. R. Sadeghnia, H. Shaterzadeh, F. Forouzanfar, and H. Hosseinzadeh, "Neuroprotective effect of safranal, an active ingredient of *Crocus sativus*, in a rat model of transient cerebral ischemia," *Folia Neuropathologica*, vol. 3, no. 3, pp. 206–213, 2017.

[51] H. Hosseinzadeh and H. R. Sadeghnia, "Safranal, a constituent of *Crocus sativus* (saffron), attenuated cerebral ischemia induced oxidative damage in rat hippocampus," *Journal of Pharmacy & Pharmaceutical Sciences*, vol. 8, no. 3, pp. 394–399, 2005.

[52] F. Forouzanfar, E. Asadpour, H. Hosseinzadeh et al., "Safranal protects against ischemia-induced PC12 cell injury through inhibiting oxidative stress and apoptosis," *Naunyn-Schmiedeberg's Archives of Pharmacology*, pp. 1–10, 2020.

[53] M. Asadollahi, P. Nikdokht, B. Hatef et al., "Protective properties of the aqueous extract of saffron (*Crocus sativus* L.) in ischemic stroke, randomized clinical trial," *Journal of Ethnopharmacology*, vol. 238, p. 111833, 2019.

[54] S. Gudarzi, M. Jafari, G. Pirzad Jahromi, R. Eshrati, M. Asadollahi, and P. Nikdokht, "Evaluation of modulatory effects of saffron (*Crocus sativus* L.) aqueous extract on oxidative stress in ischemic stroke patients: a randomized clinical trial," *Nutritional Neuroscience*, pp. 1–10, 2020.

[55] C. L. Allen and U. Bayraktutan, "Oxidative stress and its role in the pathogenesis of ischaemic stroke," *International Journal of Stroke*, vol. 4, no. 6, pp. 461–470, 2009.

[56] P. Li, R. A. Stetler, R. K. Leak et al., "Oxidative stress and DNA damage after cerebral ischemia: potential therapeutic targets to repair the genome and improve stroke recovery," *Neuropharmacology*, vol. 134, pp. 208–217, 2018.

[57] S. Manzanero, T. Santro, and T. V. Arumugam, "Neuronal oxidative stress in acute ischemic stroke: sources and contribution to cell injury," *Neurochemistry International*, vol. 62, no. 5, pp. 712–718, 2013.

[58] L. Wu, X. Xiong, X. Wu et al., "Targeting oxidative stress and inflammation to prevent ischemia-reperfusion injury," *Frontiers in Molecular Neuroscience*, vol. 13, p. 28, 2020.

[59] S. Rahaiee, S. Moini, M. Hashemi, and S. A. Shojaosadati, "Evaluation of antioxidant activities of bioactive compounds and various extracts obtained from saffron (*Crocus sativus* L.): a review," *Journal of Food Science and Technology*, vol. 52, no. 4, pp. 1881–1888, 2015.

[60] P. J. Modrego, B. Boned, J. J. Berlanga, and M. Serrano, "Plasmatic B-type natriuretic peptide and C-reactive protein in hyperacute stroke as markers of CT-evidence of brain edema," *International Journal of Medical Sciences*, vol. 5, no. 1, pp. 18–23, 2008.

[61] Y. Sun, K. Jin, L. Xie et al., "VEGF-induced neuroprotection, neurogenesis, and angiogenesis after focal cerebral ischemia," *Journal of Clinical Investigation*, vol. 111, no. 12, pp. 1843–1851, 2003.

[62] R. Jin, G. Yang, and G. Li, "Inflammatory mechanisms in ischemic stroke: role of inflammatory cells," *Journal of Leukocyte Biology*, vol. 87, no. 5, pp. 779–789, 2010.

[63] J. Anrather and C. Iadecola, "Inflammation and stroke: an overview," *Neurotherapeutics*, vol. 13, no. 4, pp. 661–670, 2016.